The Ion-Dipole Effect is a Force for Molecular Recognition and Biomimetic Catalysis

Thesis by

David Alan Stauffer

In Partial Fulfillment of the Requirements
for the Degree of
Doctor of Philosophy

California Institute of Technology
Pasadena, California

1989

(Submitted May 25, 1989)

Two Moms

Too Dads

Tu Holmes

To those who Burn

Acknowledgement

My experiences at Caltech have been enriched by many special friends. I wish I had time and space to put into words my appreciation for your support and affection. Here is a flavor of what I take with me. . . .

I thank Dennis Dougherty for his encouragement, enthusiasm, support, and advice about science and my career objectives. His patience and tolerance during difficult times are most appreciated. His relentless, often subtle, advocacy of scientific truth continues to grow with me. (There is one word to describe Dennis that cannot be found in this thesis; those who know him well know that this word is not unremarkable.)

I have been fortunate to stand upon the shoulders of two brilliant scientists. Drs. Michael Petti and Timothy Shepodd laid the foundation and put up most of the structural framework for the evolving work described in this thesis. I am grateful for Tim's "Ah!" contagious enthusiasm for our project in particular and for life in general; Mike's brainstorming ability during "rhea sessions" and "work with similar compounds" are part of the growing legend of The Babe. (I apologize for the exaggerated images I've helped to create for these two gentleman; however, I am both confident and fearful that future generations will make "Spud" filled with schmaltz.)

I am also grateful to Rich Barrans for his invaluable assistance with data reduction. "Mr. Metabolism's" computational and programming appetite can devour all the experimental results we feed him. I am happy to "pass the torch" into the increasingly capable hands of Rich, Pat, Alison, Laura, and Liz.

On the hardware side of things, I thank Dave Wheeler and Dom McGrath for helpful discussions and consideration for my countless time-consuming nmr experiments.

I had lots of fun apart from the lab, too. Summer smog was much easier to digest with the comical athleticism of the Chicken Boy Mutant Killer Pig Potato Smeggies. Whether it was football, softball, or basketball, I'm happy that Frank Coms was a late-afternoon co-conspirator. (I sometimes wonder if Dennis ever went outside when we *weren't* conspiring?) Thanks to Gary Snyder and his Uncle Roy for teaching Brian Masek and myself how to sail without a keel. Thanks to Josh The Boy and Dave Mack for letting me hack with them Brookside. Also thanks to Rakesh Jain, and expecially David Kaisaki, for helping me survive the Last Road Trip of Our Lives (yeah, right!).

I warmly thank Ernie Harrison and Phil DeShong for sparking my interest in chemistry a long time ago in a galaxy called Penn State.

I also thank the NSF for a Predoctoral Fellowship and BioDesign and Caltech Housing for financial assistance.

Finally, I acknowledge the incredible love and support of my mother, without whom I could not have come so far, and still have so far to go. . . .

Random thoughts I remember:

A nanogram is a ton of iron
This is what happens when God gives you infinite computer time--you stop thinking

This is an important point
It's kind of subtle
And it really doesn't matter

I have worked with similar compounds

Tuesday

Ah!!!

Speed bah

Please don't be a lazy boo-boo head

Never mind

This may be a stupid question, but. . .

12:13

Nothing ever lasts

I know anudder X word: Xcape

Get back to work!

SD40-2

Oh, definitely!!

My ahm!

Where's the beef?!

Br^{u}nie and Chl^{o}e. . .

Didn't anyone ever tell you. . . ?

The permutational approach to dynamic stereochemistry

Syncomposition

Well, how did I get here?

One step
And down the hall we fall. . .

To catch my breath. . .

Said the woman give him
Courage and
Strength

In the long run. . .

One pebble snatched
The fortune hunt continues

I'll be back

ibidibidi

"I think that enzymes are molecules that are complementary in structure to the activated complexes of the reactions they catalyse, that is, to the molecular configuration that is intermdeiate between the reacting substances and the products of reaction for these catalysed processes. The attraction of the enzyme moleucle for the activated complex would thus lead to a decrease in its energy, and hence to a decrease in the energy of activation of the reaction, and to an increase in the rate of the reaction. Although convincing evidence is not yet at hand, I believe that it will be found that the highly specific powers of self-duplication shown by genes and viruses are due to the same intermolecular forces, dependent upon atomic contact, and the same processes of replica formation through complementariness in structure as are operative in the formation of antibodies under the influence of an antigen. I believe that it is molecular size and shape, on the atomic scale, that are of primary importance in these phenomena, rather than the ordinary chemical properties of the substances, involving their power of entering into reactions in which ordinary chemical bonds are broken and formed."

Linus Pauling, 1948

Abstracts

Chapter 1

In aqueous and organic media, electron-rich synthetic macrocycles serve as hosts for positively-charged guests. Binding studies in different solvents have quantified hydrophobic, donor/acceptor, and ion-dipole interactions as forces for molecular recognition. We have found clear evidence for substantial host-guest donor/acceptor π-stacking interactions (ca. 1.5 kcal/mol) in aqueous media only. The ion-dipole effect is an appreciable driving force (worth up to 3.5 kcal/mol) for molecular recognition in *both* aqueous and organic media.

Chapter 2

Variable-temperature binding studies were performed to assess enthalpic ($\Delta H°$) and entropic ($\Delta S°$) contributions to free energies ($\Delta G°$) of host-guest complexation. The van't Hoff plots ($R\ln K_a$ vs T^{-1}), which are clearly non-linear, have revealed significant values for the heat capacities (ΔC_p) of complexation in both organic and aqueous media. The ΔC_p values reflect a phenomenon generally overlooked in molecular recognition studies: both $\Delta H°$ and $\Delta S°$ are strongly temperature-dependent.

Hydrophobic, donor/acceptor, and ion-dipole interactions are tentatively partitioned into $\Delta H°$ and $\Delta S°$ contributions *at 298K*. "Classic" hydrophobic binding is characterized by a large, positive $\Delta S°$ and a near-zero $\Delta H°$ term. Strong donor/acceptor π-stacking interactions are typically balanced between large, favorable enthalpic and unfavorable entropic contributions. The ion-dipole effect is primarily an enthalpically-driven binding force.

Chapter 3

Electron-rich synthetic macrocyclic host **1** accelerates a class of alkylation reactions in aqueous media. Specifically, host **1** catalyzes the reactions of pyridine-type nucleophiles with alkyl halides in an aqueous pD~9 borate buffer. The rate constants of catalyzed versus uncatalyzed reactions and the binding affinities for substrates and products demand that *host 1 binds transition states more tightly than ground states*. This extension of molecular recognition through ion-dipole interactions to biomimetic catalysis provides compelling evidence for transition-state stabilization via favorable dipole-dipole interactions in aqueous media.

Chapter 4

A new class of high-symmetry, water soluble, hydrophobic binding sites is described that feature 1,5-substituents on a rigid ethenoanthracene (DEA) framework. These new 1,5-hosts are compared to the analogous 2,6-hosts described in the Ph.D. theses of Petti and Shepodd. Because of more favorable solvation (by water) of amide linker groups that line the cavity, the 1,5-hosts exhibit significantly reduced affinities for all guests considered: only positively-charged guests are bound to any appreciable extent.

While the binding sites designed herein are composed of topographically well-defined, rigid units to give a chiral host (with a "greater sense of twist"), the disposition of the 1,5-substituents allows the collapse of hosts into a "bowl" conformation. We therefore suggest that the more successful high-symmetry, hydrophobic binding sites are to be found with 2,6-DEA-constructed hosts rather than with 1,5-DEA-constructed hosts.

One benefit of the synthetic approach taken here is the development of a series of DEA building blocks for the construction of hosts with even more pronounced hydrophobic character.

Table of Contents

List of Figures

page

List of Tables

page

Chapter 1

Ion-Dipole Effect as a Force for Molecular Recognition in Aqueous and Organic Media

Introduction

Molecular recognition studies in aqueous media using synthetic receptors of the cyclophane-type have revealed hydrophobic and electrostatic interactions as two major binding forces. Several researchers have taken advantage of the hydrophobic effect,[1] in which relatively water-insoluble guests replace the water in the cavity of the host.[2] There is a correlation between the water-insolubility of the guest and the binding affinity for guests that can fit into the host receptor site.[3] In combination with the hydrophobic effect often is an electrostatic effect in which one finds, for example, a favorable interaction wherein the cationic, water-solubilizing groups of the host come into close contact with the anionic substructures of the guest.[4]

For receptors featuring convergent functional groups in organic media, hydrogen-bonding and, to a lesser extent, π-stacking interactions have been dominant.[5] Also, crown ethers and related structures employ electrostatic and solvophobic interactions to selectively complex organic and inorganic ions.[6]

One of the primary goals of our group's research in synthetic host-guest chemistry continues to be the understanding of weak, non-bonded interactions as forces for molecular recognition. This thesis details more recent work to elucidate hydrophobic, donor/acceptor π-stacking,[5,7,8] and ion-dipole interactions. Particular emphasis is placed upon characterizing the ion-dipole effect as a force for complexation (Chapter 1) and biomimetic catalysis (Chapter 3). Also described are efforts to define further the nature of these forces for complexation by partitioning the binding free energies into enthalpic and entropic contributions (Chapter 2).

Ion-Dipole Effect in Aqueous Media

As reviewed at some length below, earlier research in the Dougherty group has demonstrated that, in addition to hydrophobic interactions, donor/acceptor π-stacking and ion-dipole interactions can contribute significantly to aqueous binding.[9] Evidence for such interactions is based upon the comparison of a pair of high-symmetry, chiral hosts that possess similar binding-site dimensions and comparable degrees of preorganization.[10] Water-soluble hosts **1** (*p*-xylyl linkers) and **2** (*trans*-1,4-dimethylenecyclohexyl linkers) each feature a rigid macrocyclic framework that describes a hydrophobic binding site in which charged, water-solubilizing groups are prevented from achieving close contacts with encapsulated guests.[11] Consequently, any differences between **1** and **2**

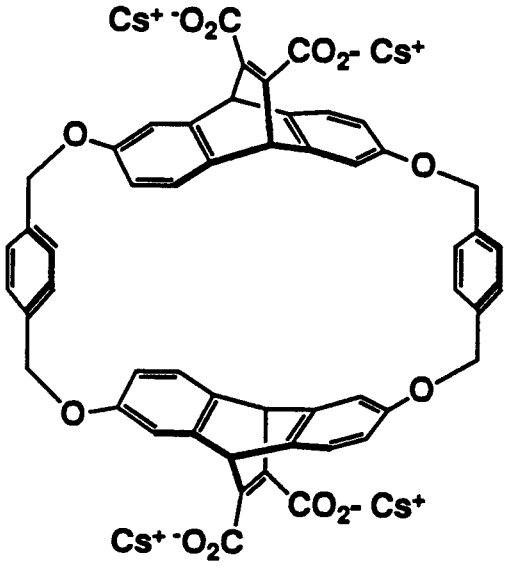

1

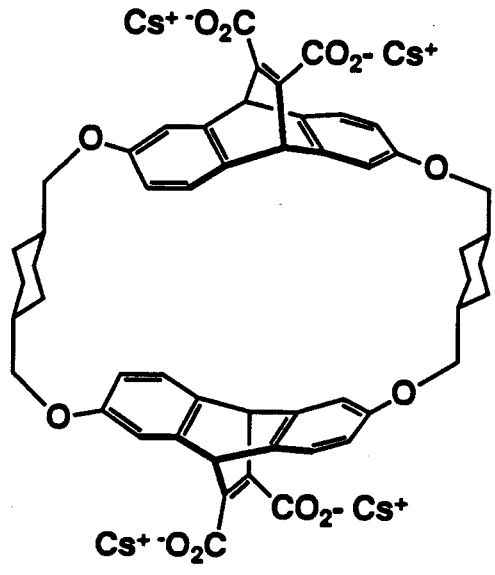

2

could not be the result of electrostatic interactions: the only differences between these hosts are found in the linkers. If hydrophobic interactions dominate, **2** should be the more effective host, because cyclohexane is more hydrophobic than benzene.[4,12,13] However, if specific aromatic ring effects are important, **1** should be the better host. Note that in this comparison, by varying *host* structure, guest-solubility effects are factored out.[9]

The communication[9] on donor/acceptor and ion-dipole interactions dealt specifically with water-soluble guests. Modelling studies suggested that, in addition to the previously described[14] toroid conformation, hosts **1** and **2** could adopt a C_2, rhomboid conformation for encapsulating naphthalene-sized guests (Figure **1.1**). In the rhomboid conformer, one of the two rings of each ethenoanthracene unit and both of the rings of the linker can stack with the guest. Distinctive and characteristic ^{1}H NMR shift patterns in both host and guest have provided compelling evidence for this arrangement.[9,15,16] Current research in the group (intermolecular nuclear Overhauser enhancement spectroscopy) is aimed at determining more precisely the orientation(s) involved in host-guest complexes.

All binding studies, both "past" and "present," were performed with enantiomerically pure hosts in a 10mM cesium borate buffer (borate-*d*, see Experimental) at pD~9, using the ^{1}H NMR titration method. NMR is the method of choice: one obtains information about binding *affinities* as well as *structures* of host-guest complexes. Because only time-averaged signals were observed in the nmr titration, and we generally have been unable to achieve saturating conditions, binding constants for 1:1 complexes were calculated with a computer program written by Barrans called MULTIFIT.[11] MULTIFIT employs an iterative, non-linear least-squares procedure in which the binding constant (K_a) is simultaneously fit to the

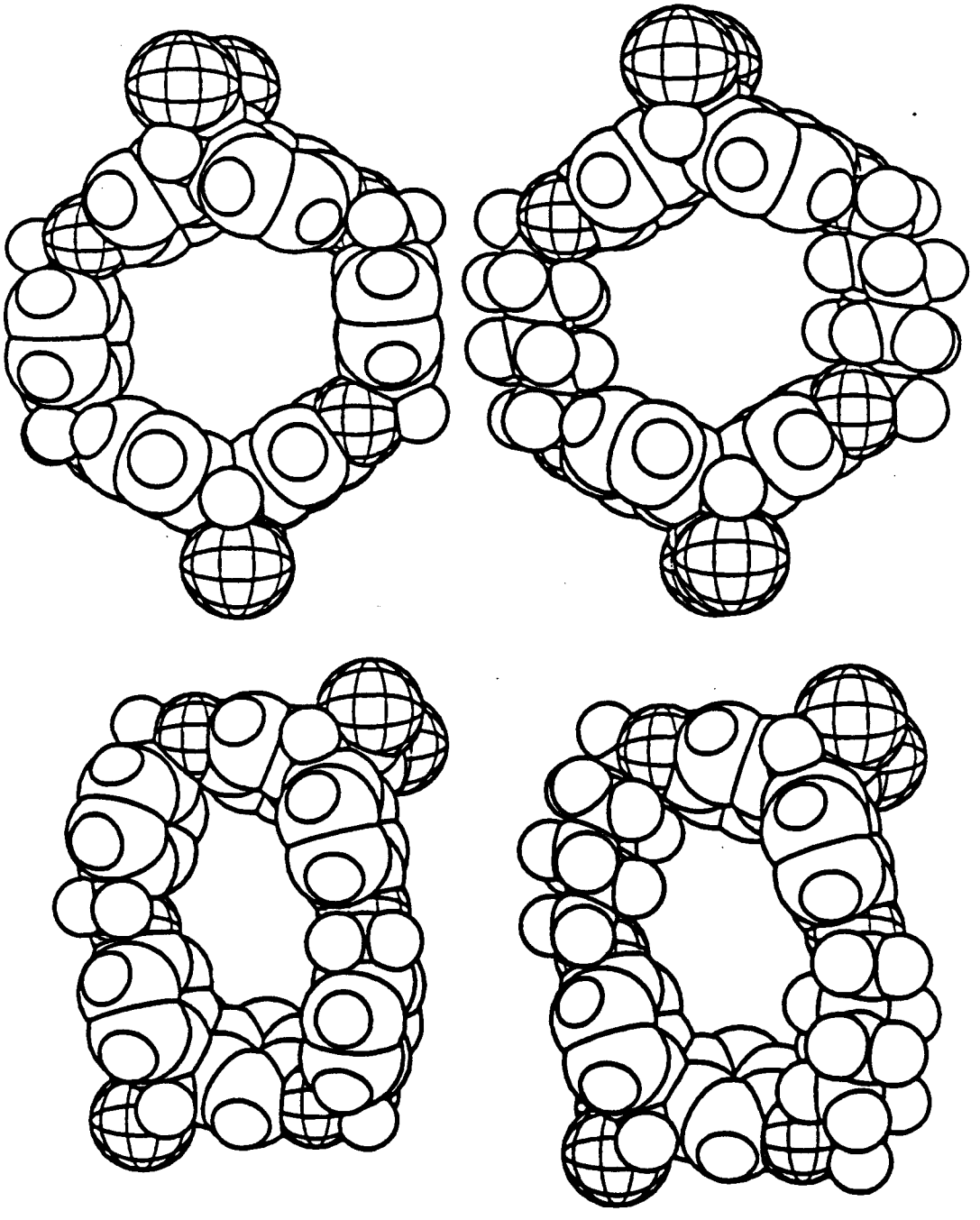

Figure 1.1. Top left: host **1**, toroid conformation; **top right**: host **2**, toroid comformation; **bottom left**: host **1**, rhomboid conformation; **bottom right**: host **2**, rhomboid conformation.

chemical-shift changes for all the observable protons of the guest (and, in some cases, the host; see Chapters 2 and 4).

Table **1.1**,[9] which has been reproduced here to provide a frame of reference for the present work, summarizes binding studies on a series of water-soluble guests with hosts **1** and **2**. These hosts, which are constructed from electron-rich π systems, have been found to preferentially bind electron-deficient guests (**3-7**) more tightly than electron-rich guests (**8** and **9**). The discrimination attributed to these donor/acceptor π-stacking interactions is ca. 1.5 kcal/mol in $\Delta G°_{295}$. The electron-rich oxygen-

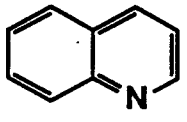

3

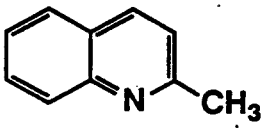

4

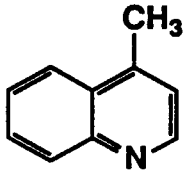

5

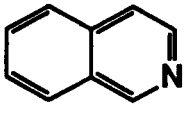

6

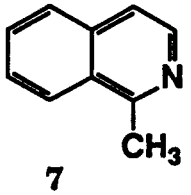

7

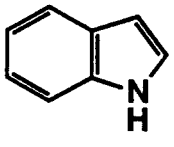

8

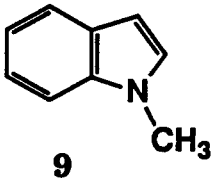

9

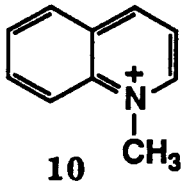

10

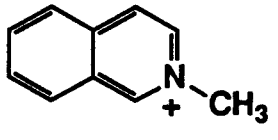

11

Table 1.1: Binding parameters for **1** and **2** with guests (**3-11**) in borate-*d*.

guest	solubility[a] (M)	free energies of complexation ($-\Delta G°$)[b] host **1**	host **2**
3	0.078	5.4	5.9
4	0.023	5.5	5.8
5	0.014	6.2	6.0
6	0.037	6.3	6.3
7	0.030	6.4	6.7
8	0.016	4.2	4.3
9	0.0032	4.5	4.8
10	0.52	7.6	6.3
11	0.45	7.2	6.0

[a]Solubility of the guest determined in the operating buffer pD~9; [b]From reference 9; in kcal/mol at 295K; values listed are accurate to ±0.2kcal/mol.

substituted rings of the ethenoanthracenes apparently dominate this interaction, such that differences between **1** and **2** are small, although the greater donor/acceptor capabilities of **1** could be offset by the greater hydrophobicity of **2**.

It was anticipated that alkylation of **3** and **6** at N to produce **10** and **11**, respectively, should further enhance donor/acceptor interactions. Comparison of the positively-charged guests with their "isostructural" neutral counterparts reveals two important features: first, the positively-charged guests are much more water-soluble than the neutrals, and so the relative constancy of binding affinities for host **2** actually reflects a substantial increase in the favorable host-guest interactions for the cationic guests; second, host **1** complexes the charged guests much more strongly than does host **2**, exhibiting large binding affinities for such freely water-soluble guests. Although it was recognized that this enhanced complexation could be due to the donor/acceptor effects in the linker becoming magnified with the more electron-deficient guests, the greater affinity of **10** and **11** has been interpreted[9] as indicative of the polarization of host **1** in response to the positive charge of the guest. In fact we have found that host **1** has a general, strong affinity for quaternary ammonium and immonium compounds (over 40 to date), an affinity which is attributed to an ion-dipole effect.

In the present context, the ion-dipole effect is defined as the interaction between a cation and the polarizable π-cloud in the face of an aromatic ring (Figure **1.2**). Gas-phase studies have revealed that the association of tetramethylammonium and benzene is driven by a large, favorable enthalpic component.[17] *Ab initio* calculations suggest that this ion-dipole effect is electrostatic in origin.[18]

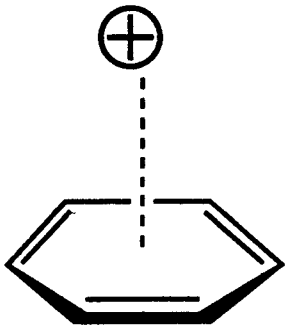

Figure 1.2. Definition of the ion-dipole interaction: localized positive charge over the face of an aromatic ring.

In addition, such an effect apparently is important in stabilizing the secondary structures of proteins. Burley and Petsko have discussed the strong tendency for cationic amino-acid side chains (lys, arg, his) to position the positive charge directly over the face of an aromatic residue (phe, tyr, trp).[19] In the majority of cases, these interactions occur in the hydrophobic interior of globular proteins.

The ion-dipole effect proposed for host **1** is depicted schematically in Figure **1.3**. In effect, the electron-rich faces of the aromatic rings of the host solvate the positive charge of the guest. The fact that **1** is a much better host than **2** suggests that a fully aromatic array is crucial for binding positively-charged guests.

Additional binding data that lend further support to the ion-dipole effect in aqueous media are documented in Table **1.2**. The data have been recast to emphasize the stronger affinity of **1** for positively-charged versus

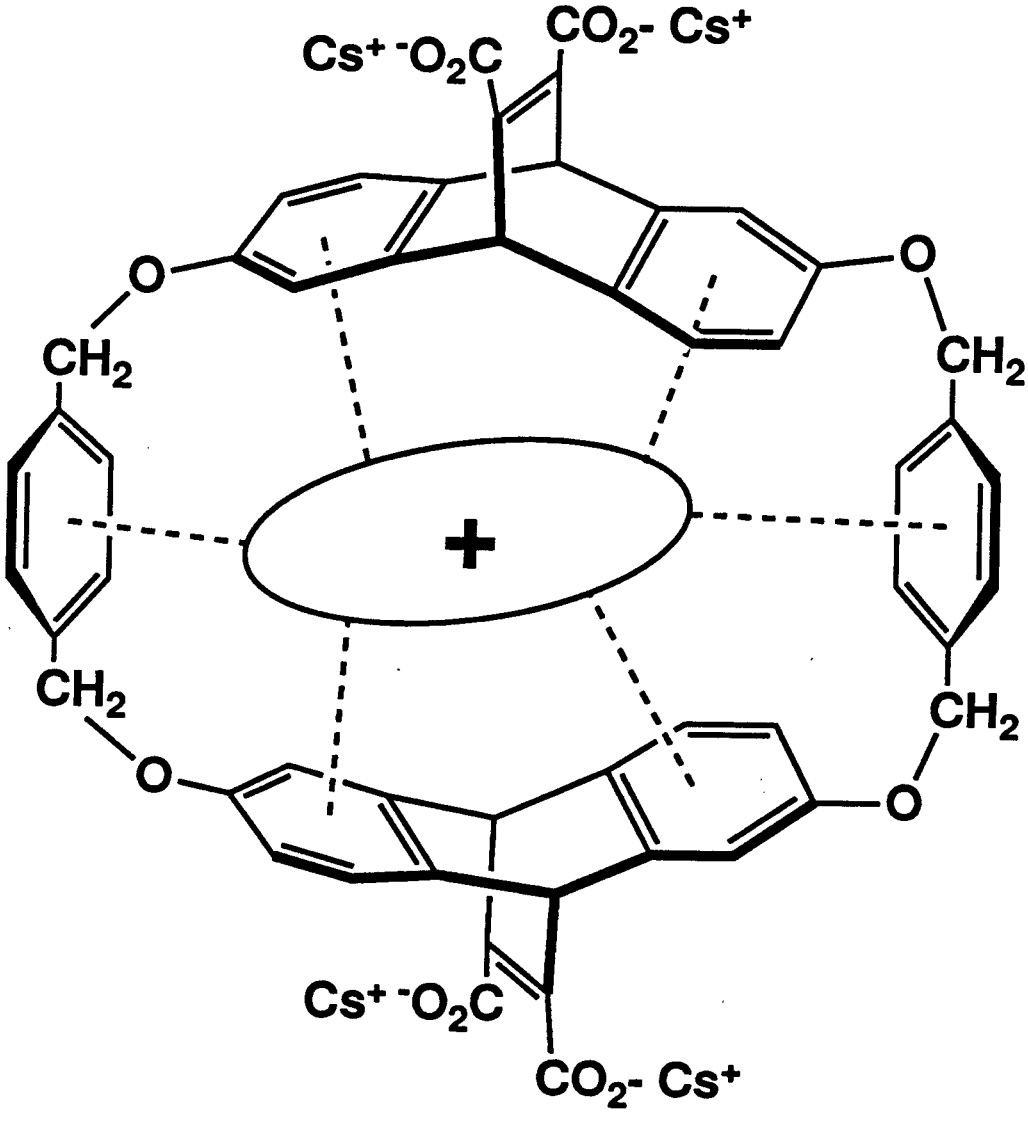

Figure 1.3. The fully aromatic array of host **1** stabilizes positively charged guests via ion-dipole interactions.

Table 1.2: Free energies of complexation for neutral and onium guests with host **1** in borate-*d*.

neutral guest	-ΔG°	onium guest	-ΔG°	ΔΔG°
6	6.3[a]	**11**	7.2[a]	0.9
12	5.4[b]	**13**	7.0[b]	1.6
3	5.4[a]	**10**	7.6[a]	2.2
3	5.4[a]	**14**	7.8[c]	2.4
3	5.4[a]	**15**	7.8[c]	2.4
3	5.4[a]	**16**	7.3[c]	1.9
17	5.8[b]	**18**	6.5[b]	0.7
19	4.7[c]	**20**	6.7[c]	2.0
		21	5.7[c]	

[a]Reference 11, 295K; [b]Present work, 300K; [c]Present work, 295±2K.

neutral guests. Host **1** prefers the naphthalene-sized, cationic immonium guests by 0.9 to 2.2 kcal/mol.

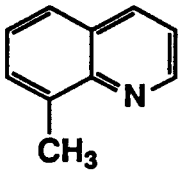

12

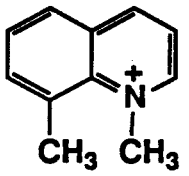

13

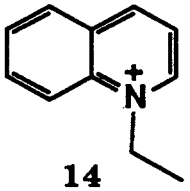

14

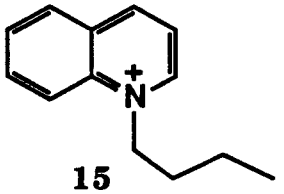

15

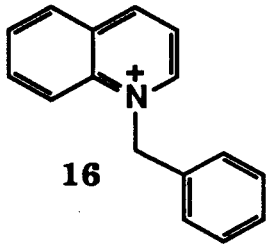

16

Quinolinium guests **14**, **15**, and **16** point out subtle differences related to hydrophobic and steric interactions. Based upon hydrophobicity one would anticipate all three of the guests (with ethyl, butyl, and benzyl groups, respectively) to have slightly higher affinities for **1** than *N*-methylquinolinium (**10**). This expectation is met for ethyl and butyl, but not for benzyl. To understand this result, we turn to nmr shift patterns for the host-guest complexes. For all three guests under consideration, the characteristic "rhomboid conformation" is evident in the host shifts. CPK models, in combination with nmr-induced shifts of the substituents of the

quinolinium guests, suggest that steric interactions in the case of the benzyl group *could* be less than optimal for binding: protons of the aromatic ring of the benzyl group of **16** shift *downfield* in the presence of host **1**, indicating close contact with $H_{3,7}$ and $H_{4,8}$ (which shift *upfield*), leading to a slightly lower affinity as a result of steric repulsion. It should be pointed out, however, that the data are not so compelling as to mandate such a convoluted rationalization.

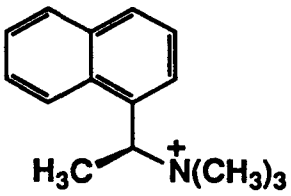

22

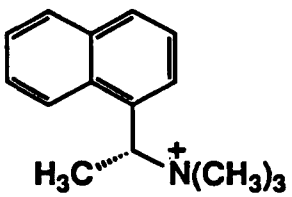

23

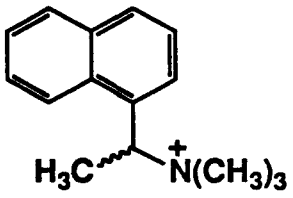

24

One of the design objectives achieved by Shepodd[15] was the synthesis of high-symmetry, chiral hosts in *enantiomerically pure* form in order to examine enantioselective binding. The affinities for the four pairwise combinations of enantiomerically pure (naphthethyl)trimethylammonium guests (**22** and **23**) and hosts **1** (both *S,S,S,S*- and *R,R,R,R*-isomers) suggested rather modest (3:1) selectivities in this case.[11] Since these experiments, racemic (±)-(naphthylethyl)amine has become available commercially from Aldrich. Consequently, a binding study was performed using racemic trimethylammonium (TMA) guest **24** and enantiomerically pure host **1** (*R,R,R,R*-isomer) in borate-*d*. Diastereomeric host-guest

complexes were evident by resonance doubling of guest peaks (for **22** and **23**). Using the known *D* values for the $N(CH_3)_3$ protons of the guest enantiomers **22** and **23**,[15] an average selectivity of 1.56(±0.07):1 (*R* preference, 5 data points) was calculated.[21] While this result may be viewed as a disappointment, one must keep in mind that in this case host **1** recognizes the TMA group rather than the naphthyl moiety.[11]

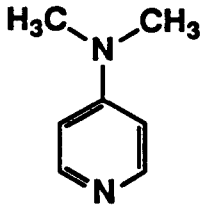

17

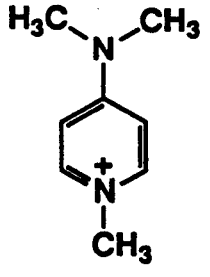

18

Until the present work, pyridine-type (benzene-sized) guests had not been probed with respect to donor/acceptor π-stacking and ion-dipole interactions. Host **1** binds 4-dimethylaminopyridine (DMAP, **17**) with an affinity comparable to quinoline, isoquinoline, and their derivatives (Table **1.2**). CPK models and host-induced nmr shifts together suggest that **17** is buried within the cavity of **1**, oriented with its C_2 axis aligned with the long side of the rectangular (rhomboid) host conformation (Figure **1.4**). Methylation at the pyridine nitrogen (no amine methylation is observed) to afford the positively-charged guest **18** results in only a slight increase (0.7 kcal/mol) in binding free energy with host **1**. To account for this apparently weaker manifestation of the ion-dipole effect, models and shift patterns indicate that, in this case, the rhomboid host geometry is *too small* to accommodate the long axis of **18** (Figure **1.4**).

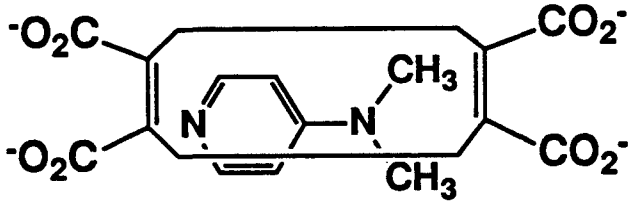

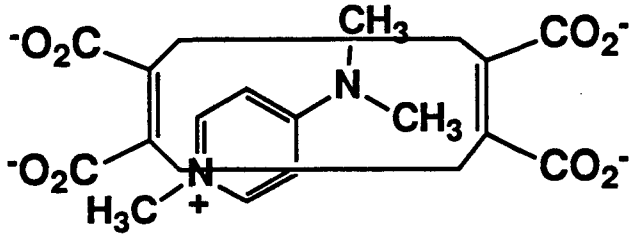

Figure 1.4. Top: Cartoon depicting guest **17** encapsulated in rhomboid conformation of host **1**; **bottom**: cartoon depicting guest **18** unable to fit longitudinally into rhomboid conformation of host **1**.

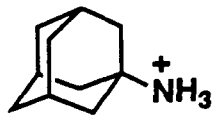

19

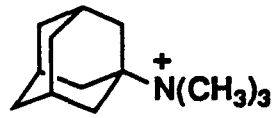

20

An interesting question regarding the ion-dipole effect that heretofore had not been addressed experimentally is this: if host **1** recognizes *tetraalkyl*ammonium guests, can it also recognize ammonium guests in which one (or more) of the alkyl groups is replaced by hydrogen? To answer this question, consider guests **20** (ATMA) and **19** (pK_a~11;[20] at pD~9, ca. 99% of adamantylamine should be ammonium): ATMA and host **1** form a tight, *oriented* complex;[14] in contrast, guest **19** ("demethylated ATMA") and host **1** form a weaker, randomly-oriented complex as evidenced by the 2.0 kcal/mol lower affinity (Table **1.2**) and lower, invariant *D* values (there is a slight preference *away from* the ammonium group, see Table **1.3**). This dramatic difference is rationalized as follows: guest **19** apparently is solvated favorably via hydrogen-bonding in the aqueous medium (vide infra); also, binding of the adamantyl moiety may preclude an *optimal* cation/aromatic ring distance for *effective* ion-dipole interactions.[19]

Current research in our group is aimed at characterizing the complexation properties of the highly-electron-rich host **25**.[22] This host is expected to have a much higher critical aggregation concentration (CAC, see Chapter 4) in borate-*d* than host **1** by virtue of the favorable solvation of the methoxy groups.[2] Also, this "octamethoxy" host may exhibit dramatic ion-dipole interactions with positively-charged guests in aqueous and organic media.

Table 1.3: *D* values for **19** and **20** with host **1** in borate-*d*.[a]

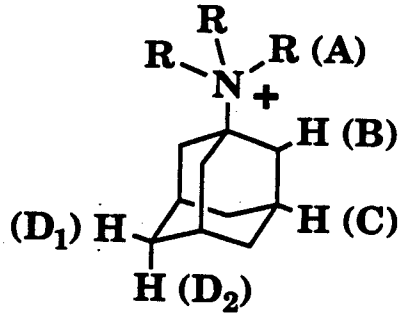

proton	**20**[a] (R=CH_3)	**19**[b] (R=H)
A	1.87	----
B	2.99	0.45
C	1.18	0.63
D_1	1.29	0.62
D_2	0.73	0.64

[a]Reference 14; [b]Present work.

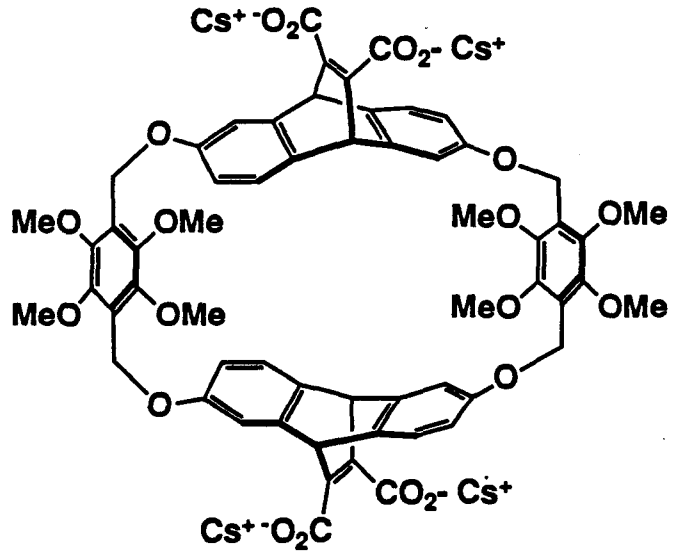

25

Future studies in the Dougherty group include expanding the repertoire of positively-charged guests encapsulated by electron-rich hosts. Toward that end, we have found that trimethylsulfonium (**26**) displaces quinoline (**3**) from the binding site of host **1** in borate-*d* (see Chapter 3) to give an apparent K_a~170M^{-1}. It will be of interest to compare the affinities of sulfonium versus ammonium guests for our hosts.

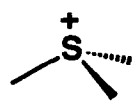

26

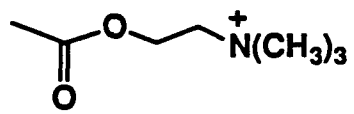

21

As a prelude to future work in other environs, acetylcholine (**21**, a neurotransmitter responsible for activating transient depolarization of post-synaptic membranes in vertebrate neuromuscular junctions[23]) has a moderately strong affinity for host **1** ($\Delta G°_{295}$ ~ -5.7 kcal/mol). CPK models and nmr shift patterns indicate that **1** recognizes the tetraalkylammonium group of this small, aliphatic guest. It is, therefore, a prediction based upon this work that biological receptors will be revealed to recognize

biogenic amines and ammonium compounds through ion-dipole interactions with aromatic amino-acid residues.

Ion-Dipole Effect in Organic Media[24]

If, in the present case, the ion-dipole effect represents a true attraction between the guest and the receptor site, rather than merely a solvent repulsion or an ionic attraction, it should then also be effective with a *neutral host in organic media*. The results presented in Table **1.4** show that this is indeed the case. The negative free energies of complexation for the tetraester of the *p*-xylyl-linked host (**27**) in $CDCl_3$ are compared with the tetracesium tetracarboxylate **1** results in borate-*d*. The binding constants in deuterochloroform were determined by the same nmr method as described for the aqueous results. Again, enantiomerically pure host (tetraester **27**) was used.[25]

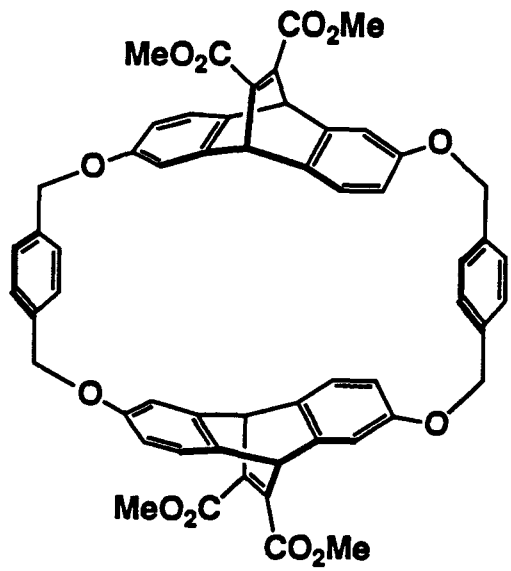

27

Within our error limits,[11] the neutral guests quinoline (**3**) and isoquinoline (**6**) are not bound at all by host **27** in chloroform (observed shifts <1Hz for $[H]_0 >> [G]_0$). However, the cationic guests show substantial

Table 1.4: Comparison of binding in organic and aqueous media: $-\Delta G°_{295}$ values (kcal/mol).[a]

guest[b]		% guest[c] bound	host **27** in $CDCl_3$	host **1** in borate-*d*[d]
6	(>2.9)	<0.6	0.2	6.3
3	(>2.1)	<0.4	0.0	5.4
20	(0.12)	2-23	2.1	6.7
11	(0.035)	2-29	2.5	7.2
10	(0.0028)	7-60	3.5	7.6
15	(0.45)	7-18	2.5	7.8[e]

[a]From reference 24; determined by ^1H NMR (400 MHz); accurate to ±0.2kcal/mol; for all binding studies in $CDCl_3$, $[H]_o$ ranged from 0.5 to 8.0mM, $[G]_o$ ranged from 0.2 to 0.4mM; the *R,R,R,R*-host was used in these studies; [b]Values in parentheses are guest solubilities (M) in $CDCl_3$; [c]Range of the percent guest bound calculated according to MULTIFIT analysis; [d]Values for all but **15** from reference 9; [e]Present work; solubility in borate-*d* = 0.09M.

binding affinities, and their relative magnitudes nicely parallel the aqueous results. Of course, the absolute magnitudes are reduced significantly because of the absence of the hydrophobic effect. Although the 1:1 binding constants in organic solution are lower, a large range of percent guest bound could still be covered in the nmr titration, because the tetraester host does not aggregate at higher concentrations. (For example, for guest **10**, MULTIFIT analysis calculates 60% guest bound for *observed* chemical shifts of greater than 1.5 ppm.)

In all binding studies in $CDCl_3$, the concentration of guest was well below saturation.[26] Nevertheless, we were concerned that the binding free energies for guests **10** and **11** seemed inversely correlated with the guest solubilities in chloroform (Table **1.4**): the less soluble guest (**10**) has the larger binding affinity. The inclusion of the aliphatic guest **20** in our data set fits the developing trend. As one proceeds from **20** to **11** to **10**, the solubilities progressively decrease, while the binding affinities progressively increase. These results suggested that some sort of "solvophobic" effect could be operative in chloroform. We therefore prepared *N*-butylquinolinium (**15**), which is much more soluble (because of the lipophilic butyl group) in chloroform than guests **10**, **11**, and **20**. Gratifyingly, guest **15** still shows a substantial affinity for host **27**, indicating that solvophobic binding is not dominant in this system.

In the preceding section on molecular recognition in aqueous media, it was suggested that hydrogen-bonding (in borate-*d*) could account for the lower affinity of adamantylammonium (**19**) versus adamanty*ltrimethyl*-ammonium (**20**) for host **1**. In chloroform, solvent-guest hydrogen-bonding is alleviated; however, guest **19** experiences no host **27**-induced shifts, and therefore is not bound. The alternate explanation offered may still stand:

optimal distances for ion-dipole interactions cannot be achieved for the positive charge of **19** and the aromatic rings of **27** with concommitant encapsulation of guest.

It was demonstrated in aqueous media that a complete, "intact" macrocyclic host is required for binding guests.[16] This should also be true for complexation in organic media. Thus, the "3/4"-molecule **28** was synthesized from the racemic diol building block **29**[16] and excess 4-bromomethyltoluene. As expected, guests **10** and **20** experienced no chemical-shift changes in the presence of "control" molecule **28**.

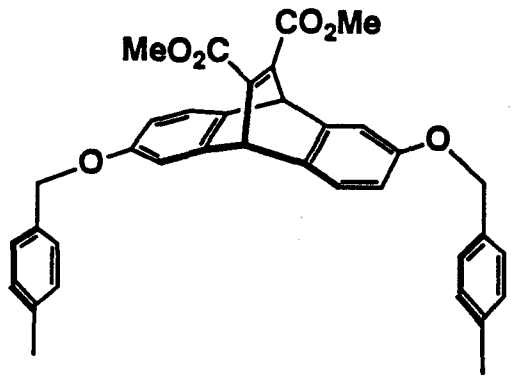

28

In the binding studies in water, it was shown that host **1** encapsulates ATMA (**20**) in a precise orientation.[14] Experimentally, this precise orientation is indicated by distinctive and characteristic nmr shift patterns observed upon complexation (Table **1.5**). In the proposed orientation, the C_3 axis of ATMA passes directly through the binding cavity of **1**, running roughly parallel to the etheno bridges. The A and B protons each form a ring that lies perpendicular to this axis, and both experience substantial shielding because they point toward the aromatic rings of the host. The C and D_1 protons together form a third ring and they are comparably shielded. Most importantly, the D_2 protons lie in a very

Table 1.5: Comparison of binding in organic and aqueous media: *D* values for ATMA (**20**) with hosts **27** and **1**.

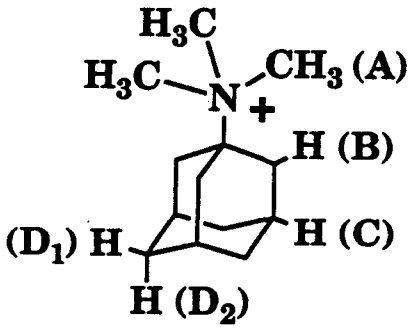

proton	$CDCl_3$[a]	borate-*d*[b]
A	2.99	1.87
B	2.92	2.99
C	1.11	1.18
D_1	1.07	1.29
D_2	0.67	0.73

[a]Host **27** (*R,R,R,R*-isomer); [b]Host **1** (*R,R,R,R*-isomer), reference 14.

different environment and point nearly parallel to the C_3 axis; hence, the D_2 protons point away from the aromatic rings of host **1** and are the least shielded.

A similar shift pattern is observed in chloroform, suggesting a comparable structure for the host-guest complex. The larger shifts of the *N*-methyl protons (labelled A) in $CDCl_3$ could indicate that the trimethylammonium group is buried more deeply in the cavity.

The chemical-shift patterns in both the guest and the host (when $[G]_o >> [H]_o$) upon binding positively-charged, flat aromatic guests (**10**, **11**, **15**) are similar in both $CDCl_3$ and borate-*d*. It is therefore concluded that both toroid and rhomboid host conformations are accessible to host **27** in chloroform as for host **1** in water. It is also expected that similar host-guest structures (with nearly identical *bound* chemical shifts) are formed independent of solvent (and temperature, see Chapter 2).

In an effort to correlate donor/acceptor and ion-dipole interactions with solvent polarity,[2,27] binding studies with host **27** and guests in other deuterated solvents were performed. Using *D* values for guests in borate-*d*,[15] binding constants were estimated for host **27** as follows (guest, solvent, K_a): **20**, CD_3CN, $2.5M^{-1}$; **10**, d_6-DMSO, $6.0M^{-1}$; **6**, CD_3CN, $1.1M^{-1}$. Thus, from this limited data set, it is concluded that host **27** has a significantly reduced affinity in polar, aprotic solvents compared to chloroform.

The present investigation of ion-dipole effects in organic media has focused solely upon *p*-xylyl-linked host **27** with its full array of aromatic rings. However, the results for complexation in aqueous media do not preclude the possible recognition of positively-charged guests by cyclohexyl-linked host **30** in organic media. Preliminary evidence for binding guest **20**

in $CDCl_3$ with host **30** is suggestive of weaker, but potentially measurable, affinities (observed shifts of 5Hz give an estimated K_a~20M^{-1}). More compelling evidence awaited the synthesis of more host **30**; however, in our hands, the attempted synthesis of **30** according to the published procedure (5.5% yield)[11,16] provided none of the desired product. We have since found it easier to isolate the "3/4"-molecule **31**, albeit in low yield (20%, see Experimental), as a more "preorganized" precursor to **30**.

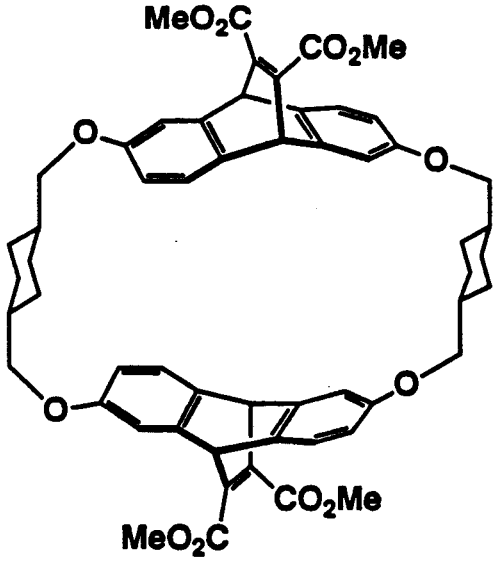

30

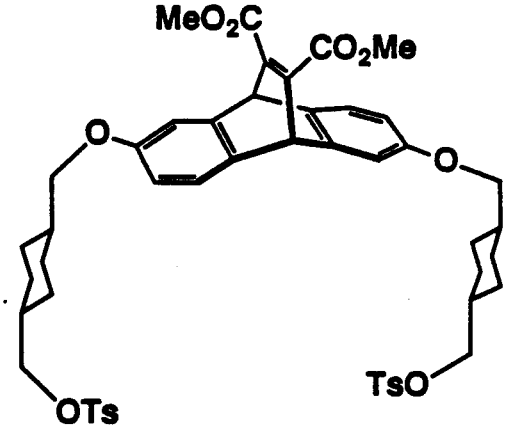

31

Conclusions

Our studies in different solvents have quantified hydrophobic, donor/acceptor, and ion-dipole interactions as forces for molecular recognition. We have found clear evidence for substantial host-guest donor/acceptor π-stacking interactions (ca. 1.5 kcal/mol) in aqueous media. The absence of any detectable complexation of neutral, electron-deficient guests by tetraester host **27** suggests that such interactions are insignificant in organic media.

Most importantly, the ion-dipole effect can serve as an appreciable driving force (worth up to 3.5 kcal/mol) for molecular recognition in *both* aqueous and organic media.

Experimental for Chapter 1

Melting points (corrected) were recorded on a Thomas-Hoover melting point apparatus. NMR spectra were recorded on Varian EM-390, JEOL JNM GX-400, or Bruker WM 500 spectrometers. Routine spectra were referenced to the residual proton and carbon signals of the solvents and are reported (ppm) downfield of 0.0 as δ values. Aqueous binding spectra were referenced to external TSP (0.00ppm) in a coaxial tube or to internal 3,3-dimethylglutarate (DMG, 1.09ppm, CH_3, referenced to TSP) in the borate-*d* buffer described below. Organic binding spectra were referenced to residual proton signals of the solvents: $CDCl_3$ (7.24ppm); d_6-DMSO (2.49ppm); CD_3CN (1.93ppm). Infrared and ultraviolet spectra were recorded on Beckman or Shimadzu infrared spectrometers and a Hewlett-Packard 8451 diode array ultraviolet spectrometer, respectively. Optical rotations were recorded on a Jasco DIP-181 digital polarimeter at 293±2K. Flash chromatography was performed according to the method of Still *et al.*[28] HPLC and reverse-phase HPLC (RPHPLC) were performed on a Perkin-Elmer Series 2 liquid chromatograph. Preparative HPLC employed a 1" X 25cm Vydac 101HS1022 silica column; analytical RPHPLC employed a 5mm X 25cm Whatman Partisil ODS-3 C_{18} column. Electron-impact (EI), fast-atom bombardment (FAB), and high-resolution mass spectrometry (HRMS) were performed by the staff of the University of California, Riverside.

Solvents were distilled from drying agents as noted: dichloromethane, CaH_2; toluene, sodium metal; tetrahydrofuran, sodium benzophenone ketyl; carbon tetrachloride, P_2O_5. Dimethylformamide (DMF) was distilled *in vacuo* at ambient temperature from calcined CaO

onto freshly activated 4Å sieves and stored over at least two successive batches of freshly activated 4Å sieves. Reagent-grade solvents were obtained from commercial sources, and were used without further purification. For sources of guests not synthesized below, see Chapter 4 Experimental.

Guest stock solutions for the organic nmr binding experiments were prepared in volumetric flasks (2mL) with deuterated solvent. The concentrations of both host and guest were quantified separately via nmr integrations against a standardized solution of a carefully tared amount of adamantyltrimethylammonium iodide (ATMA) in $CDCl_3$ (2mL, 19.1mM). All volumetric measurements of organic solutions were made using Hamilton microliter syringes.

Host and guest stock solutions for the aqueous nmr binding experiments were prepared with a standard 10mM deuterated cesium borate buffer at pD~9 (borate-*d*).[11] The buffer was prepared by dissolving 31-32mg of high purity boric oxide (B_2O_3) in 100g of D_2O (Aldrich, 99.8atom% D), adding CsOD in D_2O (*eg* 467μL, 1M), and mixing thoroughly.[15] The concentrations of the solutions were quantified via nmr integrations against a stock solution of 3,3-dimethylglutarate (DMG, 4.20-4.23mM versus potassium hydrogen phthalate, 10.6mM) in borate-*d*. All volumetric measurements of aqueous solutions were made using adjustable volumetric pipets.

Guest solubilities were determined in the following way: solid guest was suspended in a given solvent and dissolved thoroughly via sonication (60Hz, 2min). Solid and liquid phases were separated via centrifugation. An aliquot of the supernate was analyzed by ^1H NMR integration versus the appropriate standard (ATMA in $CDCl_3$; DMG in borate-*d*).

All pulse delays for the aqueous and organic stock-solution-integration experiments (15-20s) were at least 5 times the measured T_1 for the species involved. All binding studies were performed at 400MHz.

8,*N*-Dimethylquinolinium iodide (13)

A solution of 8-methylquinoline (Aldrich, 97%, 100μL, 0.71mmol) and iodomethane (Aldrich, 99%, 200μL, 3.2mmol) was placed in an nmr tube sealed with a screw cap and Teflon-lined, silicone septum. The reaction mixture was heated at 60°C for 22h. The resulting orange precipitate was recrystallized from chloroform/isopropanol to afford **13** as fine yellow needles (36mg, 18%); mp 189-191°C. An aqueous stock solution of **13** (7mg) in borate-*d* (4mL) was prepared (4.65mM): ^{1}H NMR (400 MHz, borate-*d*) δ 3.11 (s, 3H, C8-CH_3), 4.88 (s, 3H, N1-CH_3), 7.84 (t, 1H, J=8Hz, H_6), 7.92 (dd, 1H, J=6, 8Hz, H_3), 8.05 (d, 1H, J=8Hz, H_7), 8.17 (d, 1H, J=9Hz, H_5), 9.04 (d, 1H, J=8Hz, H_4) 9.07 (d, 1H, J=6Hz, H_2); HRMS 158.0963, calcd for $C_{11}H_{12}N$ 158.0970.

***N*-Ethylquinolinium iodide (14)**

A solution of quinoline (Aldrich, 96%, 600μL, 4.89mmol) and ethyl iodide (Baker, 600μL, 7.50mmol) in acetonitrile (3mL) was heated at reflux under argon overnight. The mixture was concentrated via rotary evaporation; the product was crystallized from acetone/H_2O, collected via filtration, and washed well with ether to afford **14** as thick orange plates (unrecorded yield); ^{1}H NMR (400 MHz, $CDCl_3$) δ 1.78 (t, 3H, J=7Hz, β-CH_3), 5.39 (q, 2H, J=7Hz, α-CH_2), 7.95 (t, 1H, J=7Hz, H_6), 8.16 (dd, 1H, J=6, 8Hz, H_3), 8.22 (dt, 1H, J=1, 9Hz, H_7), 8.36 (d, 1H, J=7Hz, H_5), 8.49 (d, 1H, J=9Hz,

H_8), 9.16 (d, 1H, J=8Hz, H_4) 10.26 (d, 1H, J=6Hz, H_2); HRMS 158.0973, calcd for $C_{11}H_{12}N$ 158.0970.

N-Butylquinolinium iodide (15)

A solution of quinoline (Aldrich, 95%, 1.2mL, 9.7mmol) and iodobutane (Aldrich, 99%, 1.4mL, 12mmol) in acetonitrile (5mL) under argon was heated at reflux for 22h. Upon cooling, a yellow solid that deposited was triturated with ether, then collected via filtration and washed well with ether; **15** was isolated as a yellow powder (2.50g, 83%); ^{1}H NMR (400 MHz, $CDCl_3$) δ 0.99 (t, 3H, J=7Hz, δ-CH_3), 1.56 (m, 2H, γ-CH_2), 2.10 (quintet, 2H, J=8Hz, β-CH_2), 5.34 (t, 2H, J=8Hz, α-CH_2), 7.96 (dt, 1H, J=1, 7Hz), 8.20 (m, 2H), 8.30 (dd, 1H, J=1, 8Hz), 8.36 (d, 1H, J=9Hz), 9.04 (d, 1H, J=8Hz, H_4), 10.43 (dd, 1H, J=1, 6Hz, H_2); HRMS 186.1279, calcd for $C_{13}H_{16}N$ 186.1283.

N-Benzylquinolinium bromide (16)

A mixture of quinoline (Aldrich, 96%, 600μL, 4.89mmol) and benzyl bromide (EM, 600μL, 5.05mmol) stirred at ambient temperature under argon for 4h had deposited a purple precipitate within 30min. The product was recrystallized from methanol/$CHCl_3$ as maroon/white plates (unrecorded yield); ^{1}H NMR (400 MHz, $CDCl_3$) δ 7.55 (s, 2H, CH_2), 8.10 (m, 3H, meta- and para-H), 8.26 (dd, 1H, J=2, 8Hz, ortho-H), 8.71 (dt, 1H, J=1, 8Hz, H_6), 8.93 (dt, 1H, J=2, 7Hz, H_7), 9.04 (dd, 1H, J=6, 8Hz, H_3), 9.18 (dd, 1H, J=2, 8Hz, H_5), 9.38 (d, 1H, J=9Hz, H_8), 10.05 (d, 1H, J=8Hz, H_4) 11.38 (dd, 1H, J=1, 6Hz, H_2); HRMS 220.1116, calcd for $C_{16}H_{14}N$ 220.1126. Slow evaporation of an nmr sample ($CDCl_3$) afforded **16** as colorless plates,

which were carefully washed with pentane, then used to prepare an aqueous stock solution in borate-*d*.

4-Dimethylamino-*N*-methylpyridinium iodide (18)

To a solution of 4-dimethylaminopyridine (DMAP, Aldrich, 99%, 213mg, 1.73mmol) in chloroform (1mL) was added iodomethane (Aldrich, 99%, 500μL, 7.95mmol). The reaction mixture, which had deposited a white precipitate within 1min, was stirred at ambient temperature for 6h. The product was crystallized from chloroform/isopropanol, affording **18** as white needles (383mg, 84%); mp 245-246°C; ^{1}H NMR (400 MHz, $CDCl_3$) δ 3.26 (s, 6H, C4-N(CH_3)$_2$), 4.14 (s, 3H, N1-CH_3), 6.92 (d, 2H, J=8Hz, $H_{3,5}$), 8.33 (d, 2H, J=6Hz, $H_{2,6}$); ^{1}H NMR (400 MHz, borate-*d*) δ 3.19 (s, 6H, C4-N(CH_3)$_2$), 3.89 (s, 3H, N1-CH_3), 6.85 (d, 2H, J=8Hz, $H_{3,5}$), 7.93 (d, 2H, J=6Hz, $H_{2,6}$).

((±)-Naphthylethyl)trimethylammonium iodide (24)

To a mixture of racemic (±)-naphthylethylamine (Aldrich, 98%, 1.11g, 6.36mmol) and anhydrous potassium carbonate (Baker, 2.71g, 19.6mmol) in dry DMF (10mL) under argon cooled in an ice-water bath was added iodomethane (Aldrich, 2.0mL, 32mmol). After stirring at ambient temperature for 2d, excess potassium carbonate was removed via filtration. The filtrate was concentrated via rotary evaporation *in vacuo*. The remaining brown residue was taken up in $CHCl_3$, and the insoluble material was removed via filtration. The filtrate was again concentrated *in vacuo* to afford crude **24** as a dark brown oil, which was purified via flash chromatography on silica eluted with a gradient of 20% to 80% methanol/$CHCl_3$; **24** was isolated as a yellow-brown wax (R_f=0.3, 5:1 (v/v) $CHCl_3$/methanol, 1.58g, 73%); ^{1}H NMR (400 MHz, $CDCl_3$) δ 1.98 (d, 3H,

J=7Hz, CH_3), 3.42 (s, 9H, N(CH_3)$_3$), 6.11 (q, 1H, J=7Hz, CH), 7.55 (m, 2H, H_3 and H_7), 7.72 (m, 2H, H_2 and H_6), 7.88 (d, 1H, J=8Hz, H_5), 7.97 (m, 1H, H_4), 8.83 (d, 1H, J=9Hz, H_8).

2,6-Bis[(4-methyl)benzyloxy]-9,10-dihydro-9,10-(1,2-dicarbomethoxy)etheno-anthracene (28)

To a mixture of 4-bromomethyltoluene (Aldrich, 98%, 0.20g, 1.1mmol) and cesium carbonate (Aldrich, 99%, 0.5g, 1.5mmol) was added a solution of racemic 2,6-dihydroxy-9,10-dihydro-9,10-(1,2-dicarbomethoxy)-ethenoanthracene[16] (**29**, 89mg, 0.253mmol) in dry acetonitrile (5mL). The reaction mixture was stirred at ambient temperature for 6h, and monitored by tlc (1:1 (v/v) ether/petroleum ether). Excess cesium salts were removed via filtration; the filtrate was concentrated, and the brown residue was purified via flash chromatography on silica eluted with a gradient of 1:1 to 1:10 (v/v) petroleum ether/ether, affording **28** as a white foam (132mg, 94%); ^{1}H NMR (400 MHz, $CDCl_3$) δ 2.37 (s, 6H, C4'-CH_3), 3.81 (s, 6H, CO_2CH_3), 4.97 (s, 4H, CH_2), 5.38 (s, 2H, $H_{9,10}$), 6.59 (dd, 2H, J=2, 8Hz, $H_{3,7}$), 7.09 (d, 2H, J=2Hz, $H_{1,5}$), 7.20 (d, 2H, J=8Hz, $H_{4,8}$), 7.27 (d, 4H, J=8Hz) 7.30 (d, 4H, J=8Hz).

2,6-Bis[(4-Tosyloxymethyl)cyclohexylmethyloxy]-9*S*,10*S*-dihydro-9,10-(1,2-dicarbomethyoxy)ethenoanthracene (31)

To a mixture of cesium carbonate (Aldrich, 99%, 185mg, 0.562mmol) and *trans*-1,4-bis[4-tosyloxymethyl]cyclohexane[16] (98mg, 0.217mmol) in dry acetonitrile (5mL) heated at reflux under argon was added dropwise via syringe over 3h a solution of racemic 2,6-dihydroxy-9,10-dihydro-9,10-(1,2-

dicarbomethoxy)ethenoanthracene[16] (**29**, 29mg, 0.082mmol) in dry CH_3CN (2.6mL). After heating at reflux for 24h, the mixture was concentrated *in vacuo*. The residue was taken up in CH_2Cl_2 and the insoluble cesium salts were removed via filtration. The filtrate was concentrated and dry-loaded onto silica, then purified via flash chromatography on silica eluted with a gradient of 25% to 50% ethyl acetate/petroleum ether to afford **31** (R_f=0.3, 50% ethyl acetate/petroleum ether) as a colorless oil (15mg, 20%); ^{1}H NMR (400 MHz, $CDCl_3$) δ 0.95 (m, 16H, cyclohexyl-CH_2), 1.62 (m, 4H, cyclohexyl-CH), 1.80 (m, 4H, tosyl-CH_2), 2.42 (s, 6H, tosyl-CH_3), 3.72 (d AB, 4H, J=7Hz, Δν~72Hz, 2,6-O-CH_2), 3.74 (s, 6H, CO_2CH_3), 5.27 (s, 2H, $H_{9,10}$), 6.41 (dd, 2H, J=2, 8Hz, $H_{3,7}$), 6.91 (d, 2H, J=2Hz, $H_{1,5}$), 7.18 (d, 2H, J=8Hz, $H_{4,8}$), 7.32 (d, 4H, J=7Hz, tosyl-$H_{3',5'}$), 7.76 (d, 4H, J=7Hz, tosyl-$H_{2',6'}$), from ^{1}H-^{1}H decoupling.

****

The following experimental procedures represent improved conditions for the synthesis of optically pure macrocycles based upon the published asymmetric Diels-Alder chemistry.[11,15]

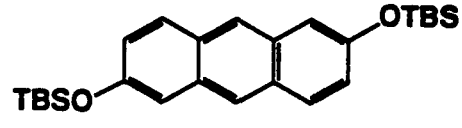

32

Purification of 2,6-bis[*tert*-butyldimethylsilyloxy]anthracene (32)

It is suggested that the workup for the synthesis of **32** could be simplified analogous to that for **33** (see Experimental for Chapter 4): After

removing DMF via rotary evaporation *in vacuo*, addition of methanol (with ice cooling) should afford **32**, which can be collected via filtration and washing with methanol. Golden brown needles isolated in this way from an impure flash chromatography fraction were pure **32** (3.20g): mp 123-125°C; ^{1}H NMR (400 MHz, $CDCl_3$) δ 0.25 (s, 12H, $Si(CH_3)_2$), 1.01 (s, 18H, $SiC(CH_3)_3$), 7.06 (dd, 2H, J=2, 9Hz, $H_{3,7}$), 7.24 (d, 2H, J=2Hz, $H_{1,5}$), 7.81 (d, 2H, J=9Hz, $H_{4,8}$), 8.15 (s, 2H, $H_{9,10}$).

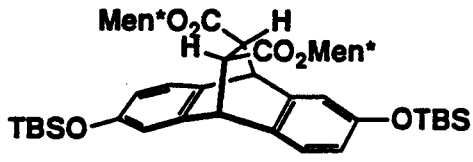

34

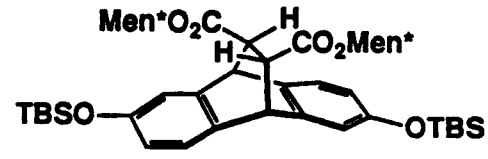

35

2,6-Bis[*tert*-butyldimethylsilyloxy]-9*R*,10*R*-dihydro-9,10-(1*R*,2*R*-dicarbo-(+)-menthoxy)ethanoanthracene (34), and 2,6-bis[*tert*-butyldimethylsilyloxy]-9*S*,10*S*-dihydro-9,10-(1*R*,2*R*-dicarbo-(+)-menthoxy)ethanoanthracene (35).[11]

This is modified from the literature procedure.[11] A solution of di-(+)-menthyl fumarate in toluene (5.2mL, 1M, 5.2mmol, 1.0 eq) was introduced to an oven-dried 100mL, three-necked reaction flask fitted with a thermometer, septum, and reflux condenser under argon. The reaction flask was cooled to ca. -45°C in a dry ice/acetonitrile bath. A solution of diethylaluminum chloride in toluene (17mL, 1.8M, 31mmol, 6.0eq) was added over 3min such that the reaction mixture, which became dark orange, remained below -20°C. After the temperature re-equilibrated, a

solution of **32** (1.594g, 3.64mmol, 0.7eq) in dry toluene (10mL) was added dropwise over 10min, keeping the reaction mixture below -40°C throughout the addition; it appeared that some anthracene **32** had precipitated on the sides of the flask. After stirring at -40°C for 15h, the mixture was allowed to warm slowly to ca. 10°C over 12h, then cooled in an ice/water bath. The mixture was then poured carefully into toluene (30mL) and saturated aqueous sodium potassium tartrate (100mL) cooled in an ice/water bath (*caution: gas evolution!*). The emulsion that formed was broken up via filtration; the phases were separated and the aqueous layer was further extracted with toluene (3x50mL), then with CH_2Cl_2 (50mL). The combined organic layers were dried ($MgSO_4$) and concentrated *in vacuo*. The golden brown foam was subjected to flash chromatography on silica eluted with a gradient of 2% to 12% ether/hexane to afford recovered **32** (0.08g), pure **34** (704mg), a mixture of **34** and **35** (ca. 1:5, 1.76g), and pure **35** (0.24g). The total yield of Diels-Alder adducts was 2.70g (89%, or 94% based upon recovered **32**); Anti diastereomer **34** (R_f=0.18, 3% ether/hexane): ^{1}H NMR (400 MHz, $CDCl_3$) menthyl peaks (δ 0.68 (d, 6H, *J*=7Hz, CH_3), 0.82 (d, 6H, *J*=7Hz, CH_3), 0.92 (d, 6H, *J*=7Hz, CH_3)), δ 0.14 (s, 12H, $Si(CH_3)_2$), 0.94 (s, 18H, $SiC(CH_3)_3$), 3.28 (s, 2H, ethano-C*H*), 4.50 (s, 2H, $H_{9,10}$), 4.54 (dt, 2H, *J*=4, 9Hz, menthyl O-C*H*), 6.49 (dd, 2H, *J*=2, 8Hz, $H_{3,7}$), 6.81 (d, 2H, *J*=2Hz, $H_{1,5}$), 6.99 (d, 2H, *J*=8Hz, $H_{4,8}$); Syn diastereomer **35** (R_f=0.09, 3% ether/hexane): ^{1}H NMR (400 MHz, $CDCl_3$) menthyl peaks (δ 0.72 (d, 6H, *J*=7Hz, CH_3), 0.82 (d, 6H, *J*=7Hz, CH_3), 0.93 (d, 6H, *J*=7Hz, CH_3)), δ 0.111 (s, 6H, Si-CH_3), 0.114 (s, 6H, Si-CH_3), 0.93 (s, 18H, $SiC(CH_3)_3$), 3.27 (s, 2H, ethano-C*H*), 4.49 (s, 2H, $H_{9,10}$), 4.51 (dt, 2H, *J*=4, 11Hz, menthyl O-C*H*), 6.52 (dd, 2H, *J*=2, 8Hz, $H_{3,7}$), 6.67 (d, 2H, *J*=2Hz, $H_{1,5}$), 7.13 (d, 2H, *J*=8Hz, $H_{4,8}$). The mixture of diastereomers (1.76g) was dissolved in pentane (12mL) and

cooled slowly to -100°C. Pure syn diastereomer **35** crystallized from solution and was isolated as a white foam (893mg).

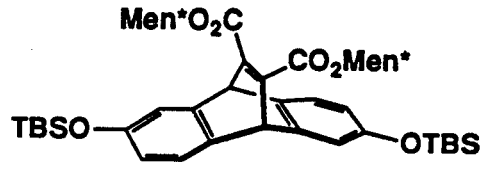

36

2,6-Dihydroxy-9S,10S-dihydro-9,10-(dicarbo-(+)-menthoxy)ethenoanthracene (36)[11]

To a stirred solution of the syn Diels-Alder adduct (**35**, 650mg, 0.783mmol) and diphenyl diselenide (387mg, 1.20mmol) in dry toluene (20mL) under argon was added a freshly prepared solution of potassium *tert*-butoxide in THF (1.7mL, ca. 1.3M). After the mixture was stirred vigorously at ambient temperature *in the dark* for 1h as a light brown precipitate formed, a solution of concentrated hydrochloric acid (8mL) in isopropanol (42mL) was added. After stirring at ambient temperature for 13h, the mixture was neutralized via careful addition of solid sodium bicarbonate. Excess solids were removed via filtration. The filtrate was partitioned between ethyl acetate (50mL) and aqueous pH 7 phosphate buffer (50mL, 1M). After a second extraction of the aqueous layer with ethyl acetate (50mL), the combined organic layers were dried ($MgSO_4$), filtered, and concentrated *in vacuo*. The light brown residue was purified via flash chromatography on silica eluted with a gradient of 1:2 to 1:1 (v/v) ethyl acetate/isooctane to afford **36** (R_f=0.3, 1:1 (v/v) ethyl acetate/isooctane) as a white solid (463mg, 99%): ^{1}H NMR (400 MHz, $CDCl_3$) δ 0.7-2.1 (menthyl

peaks), 4.78 (dt, 2H, J=4, 11Hz, menthyl O-CH), 5.18 (s, 2H, $H_{9,10}$), 5.33 (s, 2H, O-H), 6.29 (dd, 2H, J=2, 8Hz, $H_{3,7}$), 6.81 (d, 2H, J=2Hz, $H_{1,5}$), 7.02 (d, 2H, J=8Hz, $H_{4,8}$).

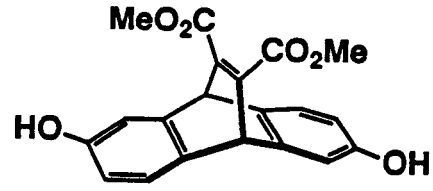

29

2,6-Dihydroxy-9*S*,10*S*-dihydro-9,10-(dicarbomethoxy)ethenoanthracene (29, *S,S*-isomer)[11]

A solution of **36** (640mg, 1.07mmol) and methanesulfonic acid (freshly distilled, 1.5mL) in methanol (30mL) was heated at reflux under argon for 4d and monitored by tlc (ether). The clear yellow solution was partitioned between ethyl acetate (50mL) and aqueous pH 7 phosphate buffer (50mL, 1M). The resultant emulsion was broken up via the addition of ethyl acetate (25mL) and saturated aqueous sodium bicarbonate (25mL; *caution*: vigorous evolution of CO_2). The aqueous phase was further extracted with ethyl acetate (2x50mL). The combined organic layers were dried ($MgSO_4$), filtered, dry-loaded onto silica, then purified via flash chromatography on silica eluted with 1% methanol in 1:1 (v/v) ethyl acetate/petroleum ether to afford **29** (R_f=0.3, 1:1 (v/v) ethyl acetate/petroleum ether) as a white solid (375mg, 100%): ^{1}H NMR (400 MHz, CD_3CN) δ 3.74 (s, 6H, CO_2CH_3), 5.38 (s, 2H, $H_{9,10}$), 6.45 (dd, 2H, J=2, 8Hz, $H_{3,7}$), 6.93 (d, 2H, J=2Hz, $H_{1,5}$), 7.06 (s, 2H, O-H), 7.19 (d, 2H, J=8Hz, $H_{4,8}$). Two samples prepared in this manner were combined and the optical rotation was measured: $[\alpha]_D$ (c=2.6, CH_3CN) -51° (lit.[11] -60°); synthesis of the macrocycle **27** (vide infra) revealed that the

syn/anti separation (**34/35**) via crystallization was imperfect in this case (ca. 4% meso isomer was detected in the **27**-*S,S,S,S*-dimer sample).

In a separate incident, a sample of **29** (350mg) in acetonitrile that was allowed to slowly evaporate *in the dark* over a period of *3 months* afforded golden brown crystals nested in an faint brown oil. NMR analysis of the oil indicated the presence of significant amounts of photo-rearranged (di-π-methane) material. Fortunately, similar analysis of the crystals revealed extremely clean, pure **29**; thus, it appears that recrystallization from acetonitrile *in the dark* is a potentially useful method for purifying **29**.

Macrocycles: host 27 dimer (*S,S,S,S*-isomer)[11]

An oven-dried 500mL, three-necked reaction flask was charged quickly with cesium carbonate (Aldrich, 99%, 1.5g, 4.6mmol) and stirrer, then fitted with septum, 125mL addition funnel with septum, and reflux condenser under argon. The system was evacuated and refilled with argon (5 cycles, using a Firestone valve). The addition funnel was charged with dry DMF (100mL), then drained into the reaction flask; this procedure was repeated with a second aliquot of dry DMF (100mL). The addition funnel was then charged with a solution of **29** (178mg, 0.506mmol) and *p*-xylylene dibromide (purified via flash chromatography, 134mg, 0.508mmol) in dry DMF (100mL). The reaction flask was wrapped in aluminum foil. The contents of the addition funnel were added dropwise over 19h (variable rate), with the first 50mL added in ca. 5h. The addition funnel was subsequently rinsed into the reaction flask with dry DMF (25mL). The mixture was stirred *in the dark* at ambient temperature for 5d under an inert atmosphere of argon. The insoluble cesium salts were removed via filtration and were washed well with CH_3CCl_3 (methyl chloroform). The

filtrate was concentrated via rotary evaporation *in vacuo*. The yellow residue was dry-loaded onto silica and subjected to flash chromatography on silica eluted with 3% ether/chloroform. Fractions containing the highest R_f spot (presumed dimer) were combined and the isolated white solid (105mg) was purified via preparative scale tlc on silica (20cm X 20cm X 2mm) eluted with 5% ether/chloroform (3 elutions) to afford **27** as a white film (59mg, 26%): ^{1}H NMR (400 MHz, $CDCl_3$) shows contamination by the meso isomer;[15] for dimer **27** δ 3.75 (s, 12H, CO_2CH_3), 5.07 (AB q, 8H, J=14Hz, Δν=35Hz, O-CH_2), 5.21 (s, 4H, $H_{9,10}$), 6.38 (dd, 4H, J=2, 8Hz, $H_{3,7}$), 6.89 (d, 4H, J=2Hz, $H_{1,5}$), 7.07 (d, 4H, J=8Hz, $H_{4,8}$), 7.20 (s, 8H, xylyl-H).

Adamantyltrimethylammonium iodide (20)[15]

To a stirred mixture of amantadine (Sigma, 1.52g, 10.1mmol), cesium carbonate (Fluka, 4.40g, 13.5mmol), and some 4Å sieves in dry dimethylformamide (DMF, 15mL) under nitrogen was added iodomethane (Aldrich, 98%, 3.7mL, 58mmol). After stirring at ambient temperature for 24h, the mixture was poured into 2:1 (v/v) acetonitrile/ether. The cesium salts were removed via filtration and were washed well with 2:1 (v/v) acetonitrile/ether. The filtrate was concentrated via rotary evaporation. The product was crystallized as white plates from acetonitrile, collected via filtration, and washed well with cold 2:1 (v/v) acetonitrile/ether (1.19g). The mother liquor afforded a second crop of **20** from acetonitrile (0.59g; total 1.78g, 55%); ^{1}H NMR (400 MHz, $CDCl_3$) δ 1.68 (AB, 6H, J=14Hz, Δν=8Hz, D_1 and D_2 protons), 2.05 (d, 6H, J=3Hz, B protons), 2.36 (br, 3H, C protons), 3.28 (s, 9H, A protons); ^{1}H NMR (400 MHz, D_2O) δ 1.54 (AB, 6H, J=13Hz, Δν=26Hz, D_1 and D_2 protons), 1.92 (d, 6H, J=2Hz, B protons), 2.16 (br, 3H, C protons), 2.84 (s, 9H, A protons); ^{13}C NMR (100 MHz, $CDCl_3$) δ 30.19, 35.14,

35.27, 48.79 (t, 1:1:1), 73.13. El. anal. C (47.22) H (7.28), N (4.39); calcd for $C_{13}H_{24}IN$: C (48.61), H (7.53), N (4.36); calcd for $2(C_{13}H_{24}IN)\cdot H_2O$: C (47.28), H (7.63), N (4.24).

((*S*)-Naphthylethyl)trimethylammonium iodide (22)[11]

To a mixture of (*S*)-naphthylethylamine (Aldrich, 99+%, 1g, 6mmol) and anhydrous potassium carbonate (Baker, 2.42g, 17.5mmol) in dry DMF (10mL) under argon cooled in an ice-water bath was added iodomethane (Aldrich, 1.8mL, 29mmol). After stirring at ambient temperature for 24h, excess potassium carbonate was removed via filtration. The filtrate was concentrated via rotary evaporation *in vacuo*. The remaining brown residue was taken up in $CHCl_3$, and the insoluble material was removed via filtration. The filtrate was again concentrated *in vacuo* to afford crude **22** as an orange-brown oil, which was purified via flash chromatography on silica eluted with a gradient of 10% to 50% methanol/$CHCl_3$; **22** was isolated as an off-white foam (R_f=0.3, 5:1 (v/v) $CHCl_3$/methanol, 1.83g, 92%); ^1H NMR (400 MHz, $CDCl_3$) δ 1.99 (d, 3H, J=7Hz, CH_3), 3.42 (s, 9H, $N(CH_3)_3$), 6.15 (q, 1H, J=7Hz, CH), 7.58 (m, 2H, H_3 and H_7), 7.67 (dd, 1H, J=1, 7Hz, H_2), 7.76 (m, 1H, H_6), 7.90 (d, 1H, J=8Hz, H_5), 7.99 (d, 1H, J=8Hz, H_4), 8.83 (d, 1H, J=9Hz, H_8).

((*R*)-Naphthylethyl)trimethylammonium iodide (23)[11]

To a mixture of (*R*)-naphthylethylamine (Aldrich, 99+%, 1g, 6mmol) and anhydrous potassium carbonate (Baker, 2.46g, 17.8mmol) in dry DMF (10mL) under argon cooled in an ice-water bath was added iodomethane (Aldrich, 1.8mL, 29mmol). After stirring at ambient temperature for 2d,

excess potassium carbonate was removed via filtration. The filtrate was concentrated via rotary evaporation *in vacuo*. The remaining brown residue was taken up in $CHCl_3$, and the insoluble material was removed via filtration. The filtrate was again concentrated *in vacuo* to afford crude **23** as a brown oil, which was purified via flash chromatography on silica eluted with a gradient of 20% to 60% methanol/$CHCl_3$; **23** was isolated as an off-white foam (R_f=0.3, 5:1 (v/v) $CHCl_3$/methanol, 2.38g, 119%); ^1H NMR (400 MHz, $CDCl_3$) δ 1.99 (d, 3H, J=7Hz, CH_3), 3.42 (s, 9H, $N(CH_3)_3$), 6.14 (m, 1H, CH), 7.57 (m, 2H, H_3 and H_7), 7.67 (m, 1H, H_2), 7.76 (m, 1H, H_6), 7.90 (d, 1H, J=8Hz, H_5), 7.99 (d, 1H, J=8Hz, H_4), 8.83 (d, 1H, J=9Hz, H_8).

References to Chapter 1

(1) Tanford, C. *The Hydrophobic Effect*, 2nd ed.; Wiley: New York, 1980.

(2) Diederich, F. *Angew. Chem. Int. Ed. Engl.* **1988**, *27*, 362-386.

(3) Petti, M. A.; Shepodd, T. J.; Dougherty, D. A. *Tetrahedron Lett.* **1986**, *27*, 807-810.

(4) Franke, J.; Vögtle, F. *Top. Curr. Chem.* **1986**, *132*, 135-170.

(5) (a) Rebek, J., Jr. *Science (Washington, D. C.)* **1987**, *235*, 1478-1484; (b) Rebek, J., Jr.; Askew, B.; Ballester, P.; Buhr, C.; Jones, S.; Nemeth, D.; Williams, K. *J. Am. Chem. Soc.* **1987**, *109*, 5033-5035; (c) Hamilton, A. D.; van Engen, D. *J. Am. Chem. Soc.* **1987**, *109*, 5035-5036.

(6) Lehn, J.-M. *Science* **1985**, *227*, 849-856.

(7) Saenger, W. *Principles of Nucleic Acid Structure*; Springer-Verlag: New York, 1984; Chapter 6.

(8) Diederich has studied the binding of a wide range of substituted naphthalenes with a single host. Evidence for favorable donor/acceptor interactions was obtained in methanol but not in water. Differential guest solubilities were not considered: Ferguson, S. B.; Diederich, F. *Angew. Chem. Int. Ed. Engl.* **1986**, *25*, 1127-1129.

(9) Shepodd, T. J.; Petti, M. A.; Dougherty, D. A. *J. Am. Chem. Soc.* **1988**, *110*, 1983-1985.

(10) Cram, D. J. *Angew. Chem. Int. Ed. Engl.* **1986**, *25*, 1039-1134.

(11) Petti, M. A.; Shepodd, T. J.; Barrans, R. E., Jr.; Dougherty, D. A. *J. Am. Chem. Soc.* **1988**, *110*, 6825-6840.

(12) Wolfenden, R. *Science (Washington, DC)* **1983**, *222*, 1087-1093.

(13) Odashima, K.; Soga, T.; Koga, K. *Tetrahedron Lett.* **1981**, *22*, 5311-5314.

(14) Shepodd, T. J.; Petti, M. A.; Dougherty, D. A. *J. Am. Chem. Soc.* **1986**, *108*, 6085-6087.

(15) Shepodd, T. J. Ph. D. Thesis, California Institute of Technology, 1988.

(16) Petti, M. A. Ph. D. Thesis, California Institute of Technology, 1988.

(17) Meot-Ner (Mautner), M.; Deakyne, C. A. *J. Am. Chem. Soc.* **1985**, *107*, 469-474.

(18) Meot-Ner (Mautner), M.; Deakyne, C. A. *J. Am. Chem. Soc.* **1985**, *107*, 474-479.

(19) (a) Burley, S. K.; Petsko, G. A. *FEBS Letters* **1986**, *203*, 139-143; (b) Burley, S. K.; Petsko, G. A. *Adv. Protein Chem.* **1988**, *39*, 125-189.

(20) Lowry, T. H.; Richardson, K. S. *Mechanism and Theory in Organic Chemistry*; 3rd ed.; Harper and Row: New York, 1987; pp 259-326.

(21) Within the error limits for binding free energies (±0.2 kcal/mol), the affinities of **23** and **24** for host **1** (*S,S,S,S*-isomer) were reproduced in the present work. No selectivity was discernible for binding of **23** and **24** by host **27** ($P_{S,S,S,S}$) in $CDCl_3$ (each estimated K_a~30M^{-1}).

(22) Kearney, P. C., unpublished results.

(23) Kandel, E. R.; Schwartz, J. H. *Principles of Neural Science*; 2nd ed; Elsevier: New York, 1985.

(24) Stauffer, D. A.; Dougherty, D. A. *Tetrahedron Lett.* **1988**, *29*, 6039-6042.

(25) Host **27** could be recovered from the binding-study solutions by chromatography. Improved syntheses of host **27** precursors are presented in the Experimental.

(26) The positively charged guests exhibited concentration-dependent chemical shifts in $CDCl_3$, suggesting aggregation. Therefore,

binding studies in $CDCl_3$ were performed at a low, narrow range of $[G]_0$.

(27) Reichardt, C. *Solvent Effects in Organic Chemistry*; Verlag Chemie: New York, 1979; pp 270-272.

(28) Still, W. C.; Kahn, M.; Mitra, A. *J. Org. Chem.* **1978**, *43*, 2923-2925.

Chapter 2

Heat Capacity and Thermodynamics of Complexation

Introduction

Host-guest chemistry has focused upon defining specific interactions that stabilize intermolecular complexes. The understanding of weak, non-bonded interactions involved in association equilibria is crucial, whether in small systems such as the benzene dimer in the gas phase or in large systems such as protein secondary and tertiary structures in solution.

Theoretical methods for predicting association processes in large biological molecules (*eg* proteins, DNA, polysaccharides) must use as their benchmarks structures and energies derived from studies in molecular recognition. Although the available computing power continues to advance rapidly,[1] it is evident that *ab initio* calculations on even modestly-sized structures will require some empirical parametrization. Free-energy perturbation techniques[2] have begun to gain favor for calculating *relative* affinities for simpler, closely related intermolecular complexes. If molecular recognition studies are to be useful, clear and compelling evidence regarding thermodynamics and kinetics of association processes is mandatory. The extrapolation to more complex systems will depend, therefore, upon a more detailed understanding of the many driving forces for binding.

It is in this context that we seek in the present work to define more specifically hydrophobic, donor/acceptor, and ion-dipole interactions as forces for molecular recognition in aqueous and organic media. As described earlier[3-5] (Chapter 1), we have quantified these interactions in terms of free energies ($\Delta G°$) for 1:1 host-guest complexation:

$$\Delta G° = -RT \ln K_a \qquad (2.1)$$

$$K_a = \frac{[HG]}{[H][G]} \tag{2.2}$$

where R is the gas constant; T is absolute temperature; and [H], [G], and [HG] are the concentrations of host, guest, and host-guest complex, respectively. In order to obtain a more detailed, "physically meaningful" understanding of these driving forces, one typically considers the binding event in terms of enthalpic and entropic contributions.

$$\Delta G° = \Delta H° - T\,\Delta S° \tag{2.3}$$

Eqn. 2.3 relates free energy ($\Delta G°$) to enthalpy ($\Delta H°$) and entropy ($\Delta S°$). Combining Eqns. 2.1 and 2.3 gives

$$-RT \ln K_a = \Delta H° - T\,\Delta S° \tag{2.4}$$

or

$$R \ln K_a = (-\Delta H°)(\frac{1}{T}) + \Delta S° \tag{2.5}$$

Eqn. 2.5 suggests that enthalpic and entropic terms can be evaluated by determining the binding constant (K_a) as a function of temperature (T). This straightforward van't Hoff analysis[6] makes one critical assumption: $\Delta H°$ and $\Delta S°$ must be temperature-invariant. This assumption often holds up under the scrutiny of experiments for gas-phase and "small-molecule," solution-phase equilibria.[7] However, this assumption breaks down for systems involving polar solutes and/or solvents. Examples include acid-base (ionic) equilibria in protic solvents[8,9] and protein folding and denaturation in water.[10] We are therefore forced to consider thermodynamic parameters as functions of temperature:

$$\Delta G°(T) = \Delta H°(T) - T\,\Delta S°(T) \tag{2.6}$$

The temperature dependence of enthalpy is defined:[7,8]

$$\Delta C_p = \left(\frac{\partial \Delta H}{\partial T}\right)_p \tag{2.7}$$

where ΔC_p is the change in heat capacity between multiple states at constant pressure. If ΔC_p is assumed to be independent of temperature, integration of Eqn. 2.7 gives

$$\Delta H = (\Delta C_p \cdot T) + A \tag{2.8}$$

Substitution of Eqn. 2.9[6]

$$\frac{\partial (\ln K_a)}{\partial T} = \frac{\Delta H}{RT^2} \tag{2.9}$$

into Eqn. 2.8 gives

$$\frac{\partial (\ln K_a)}{\partial T} = \frac{\Delta C_p}{RT} + \frac{A}{RT^2} \tag{2.10}$$

Integration of Eqn. 2.10 gives

$$\ln K_a = \frac{\Delta C_p}{R} \ln T - \frac{A}{RT} + B \tag{2.11}$$

Evaluation of the constants of integration (A and B) gives a temperature-dependent van't Hoff equation ($A=\Delta H_o$; $B=\Delta S_o - \Delta C_p$):[11]

$$R \ln K_a = -\left(\frac{\Delta H_o}{T}\right) + \Delta C_p \ln T + (\Delta S_o - \Delta C_p) \quad (2.12)$$

where ΔH_o and ΔS_o are constants of integration representing enthalpy and entropy of complexation, respectively, at 0 K. Eqn. 2.12 assumes that the heat capacity of complexation (ΔC_p) is independent of temperature. Experimentally, examples of temperature-dependent ΔC_p-values have been reported.[12] In the present case (as well as in many other cases[10]), the assumption of a temperature-independent ΔC_p is valid according to statistical analysis (vide infra).

In aqueous media, the hydrophobic effect is often invoked as the driving force for enzyme-substrate association.[13] The "classical" hydrophobic effect is attributed to a specific, highly positive entropic contribution. Nominally insoluble solutes associate to minimize the amount of "structured" water required for solvation in bulk, "disordered" water. In contrast, a large, favorable enthalpic term (with a small, sometimes unfavorable entropic term) has been found with more water-soluble guests as evidence for a "non-classical" hydrophobic effect.[14-16] A large, negative heat capacity is often correlated with hydrophobic binding.[13] Consistent with this view of hydrophobicity are studies of heat capacities of organic compounds in solution: in comparison to other polar protic (and aprotic) solvents, water shows a large, *positive* ΔC_p for the *dissolution* of many classes of organic solutes.[17]

Sturtevant has discussed heat capacity and entropy changes in processes involving proteins.[10] Table **2.1** illustrates a trend persistent in macromolecular association/dissociation thermodynamics in aqueous media: heat capacity changes for association are large and negative, whereas those for dissociation are large and positive. Conformational, hydrophobic, and vibrational effects were deemed primarily responsible for the magnitudes of these changes.[10] More significantly, such large values for ΔC_p underscore the fact that the apparent driving force for an equilibrium process changes dramatically from enthalpy-driven to entropy-driven over a very narrow range of temperature (ΔC_p = 100 cal/mol-K means ΔH (or $T\Delta S$) changes 1 kcal/mol each 10°). It has been noted that care must be taken in comparing thermodynamic parameters from measurements that cover different ranges of temperature.[18] These considerations emphasize the importance of determining carefully ΔC_p in addition to the "traditional" parameters $\Delta G°$, $\Delta H°$, and $\Delta S°$.[18]

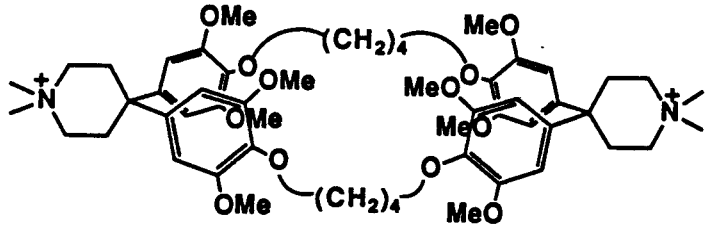

37

With respect to the present work, Diederich and co-workers reported recently that hydrophobic binding of benzene guests with macrocycle **37** in water was driven by a large, favorable *enthalpic* component.[19] Also, the complexation of aromatic compounds with cyclodextrins in water is reported to be enthalpically driven.[20] Of particular relevance to our work,

Table 2.1: Heat capacity and entropy changes in biochemical reactions at 25°C.[a]

	ΔS_u[b] (cal/mol-K)	ΔC_p[c] (cal/mol-K)	References
<u>association processes</u>			
aldolase + hexitol-1,6-diphosphate	34	-410	34
heart LDH[d] + NADH	-2.8	-170	35
tRNA ligase + isoleucine	19.7	-430	36
hemoglobin + haptoglobin	-73	-940	37
<u>dissociation (unfolding) processes</u>			
α-chymotrypsin (pH 7)	330	+3080	38,39
lysozyme (pH 7)	140	+1560	40
ribonuclease (pH 2, 31°C)	215	+1220	41,42
$tRNA_1^{Val}$	210	+1500	43

[a]Excerpted from reference 10; [b]Unitary entropy, reference 44; [c]ΔC_p appears to be temperature-independent in the vicinity of 25°; all values are average values per site in multisite cases; [d]LDH, lactate dehydrogenase.

the binding of adamantyl derivatives by β-cyclodextrin has been found to be favorable enthalpically.[14]

Aside from the routine determination of $\Delta H°$ and $\Delta S°$, there are scant studies regarding the "effect" of heat capacity upon thermodynamics of complexation for synthetic macrocycles in aqueous media. Most of the recent investigations in the field of molecular recognition have shown a glaring absence of reported ΔC_p values: the temperature-dependence of $\Delta H°$ and $\Delta S°$ appears virtually to have been ignored up to this point. It is suggested that difficulties in determining ΔC_p values have limited their report in the literature of synthetic host-guest chemistry. The present work deals with rectifying this dearth of important information by attempting to address ΔC_p in terms of the forces for molecular recognition we have uncovered.

Petti described the initial evaluation of thermodynamics of complexation with our hosts.[15] Values for $\Delta H°$ and $\Delta S°$ were calculated using van't Hoff analysis (temperature-dependent, Eqn. 2.5) for the binding of guest **20** (ATMA) by hosts **38** and **39** in aqueous media (Figure **2.1**). The Petti binding studies employed the ^1H NMR titration method (see Chapters 1 and 4). The aqueous medium was a pD~9.5 phosphate buffer. MULTIFIT analysis[4] afforded values for K_a at each temperature (Table **2.2**), and the van't Hoff plots ($R\ln K_a$ vs T^{-1}) provided $\Delta H°$ and $\Delta S°$. These thermodynamic parameters had been interpreted in the context of the non-classical hydrophobic effect:[15] the binding of ATMA was enthalpically driven, with a small, favorable entropic contribution. These variable-temperature binding studies in aqueous media helped provide a frame of reference for the present work.

Table 2.2: Temperature dependence of the association constant (K_a) for guest **20** with hosts **38** and **39** in aqueous media.[a]

temperature (K)	host **38** K_a (M^{-1})	host **39** K_a (M^{-1})
290.5	2351	2027
299.6	1890	1804
309.7	1549	1599
319.4	1222	1357
329.0	934	1104

[a]Reproduced from reference 15, p 60; [b]Determined by ^1H NMR (400 MHz) in pD~9.5 phosphate buffer.

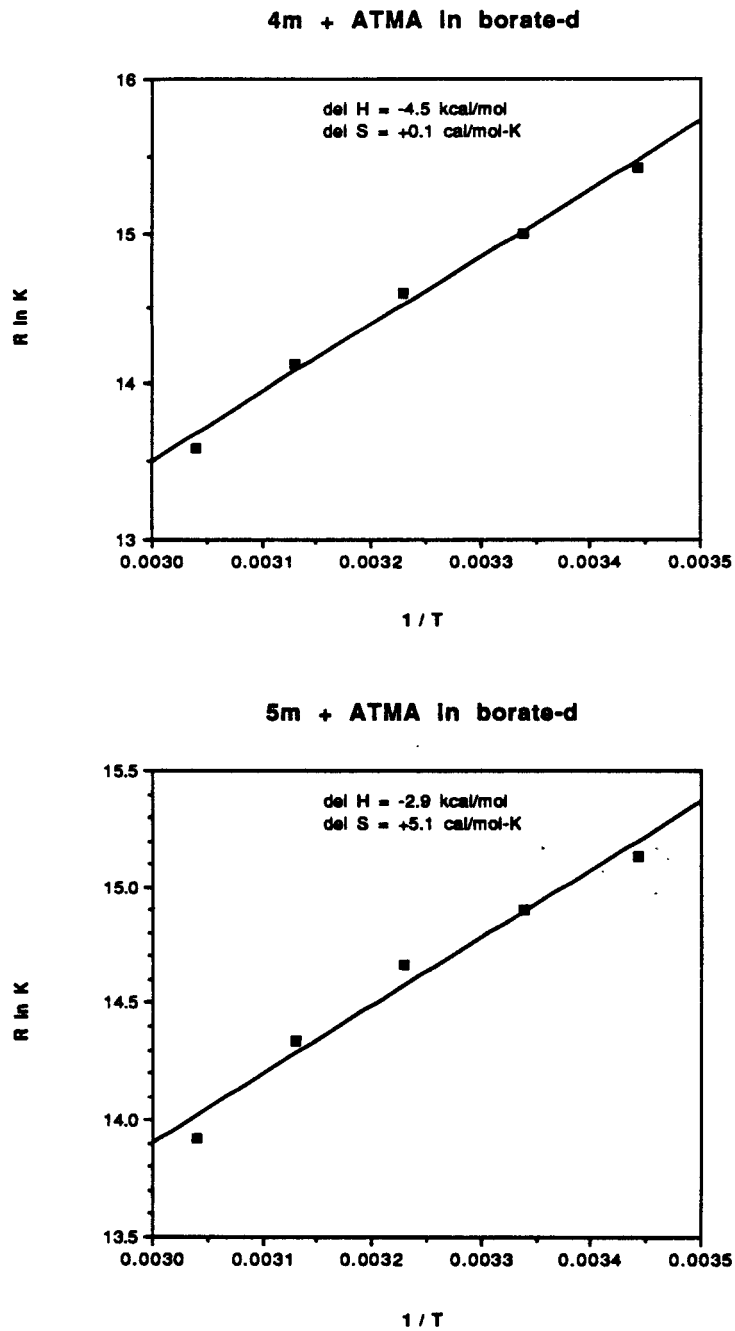

Figure 2.1. "Complete" VT binding studies by Petti.[15] **Top**: van't Hoff plot for host **38** and guest **20** in borate-*d*; **bottom**: van't Hoff plot for host **39** and guest **20** in borate-*d*.

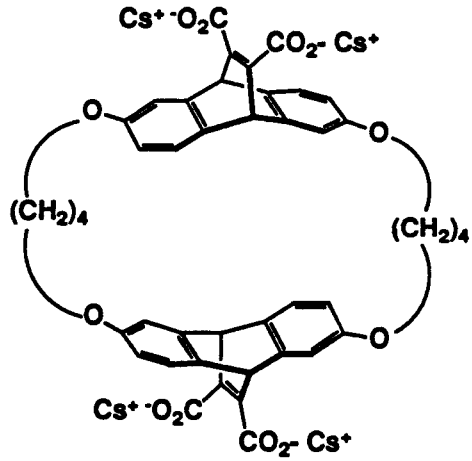

38

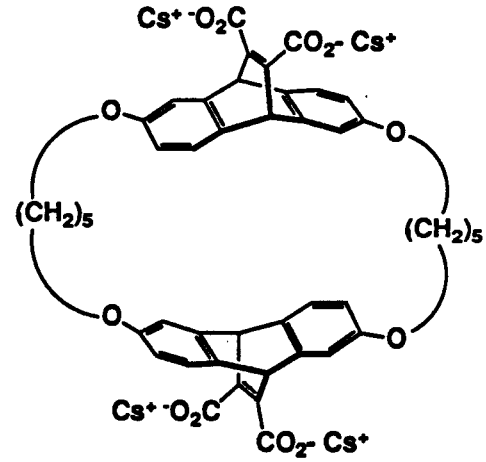

39

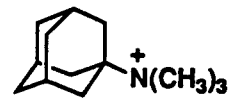

20

As mentioned earlier, our objective is to understand the binding force in terms of those interactions that we have identified. The binding of positively-charged guests in organic media[21] stimulated us to reconsider the nature of the ion-dipole effect: is complexation driven enthalpically, entropically, or both? Furthermore, if we could partition the ion-dipole effect into $\Delta H°$ and $\Delta S°$ contributions, could we then also assign hydrophobic and donor/acceptor interactions enthalpy and entropy terms? We find that for binding guests with our hosts, ΔC_p is not insignificant, and $\Delta H°$ and $\Delta S°$ are correspondingly temperature-dependent. Because the accuracy attained depends upon several unknowns, we cannot comment with confidence about the absolute ΔC_p values calculated; fortunately, certain trends are apparent so that solvation and binding forces can be evaluated.

Methods of determining ΔH, ΔS, and ΔC_p of complexation

According to Eqns. 2.7, 2.13, and 2.14, if one determines the heat capacity of complexation, all other thermodynamic parameters ($\Delta G°$, $\Delta H°$, $\Delta S°$) can be calculated for a given temperature.[22] In solution, microcalorimetry has been applied to the determination of heat capacities for dissolving solutes in an array of solvents as a measure of solvophobicity (i.e., to reflect the ordered structure of the solvent around the solute).[23,24] Differential scanning calorimetry (DSC) has been used for measuring ΔC_p in intramolecular equilibrium processes.[10,18] In host-guest complexation, as noted above, calorimetry has been employed to obtain thermodynamic parameters for complexes of cyclodextrins and adamantyl derivatives. Negative ΔC_p values were interpreted as evidence for hydrophobic binding.[14]

An alternative approach for obtaining thermodynamic parameters for molecular recognition involves the temperature-dependent van't Hoff analysis: determination of K_a as a function of T and evaluation of Eqn. 2.12 should give parameters that describe $\Delta H°$ and $\Delta S°$ as temperature-dependent variables according to:

$$\Delta H°(T) = \Delta H_o + \Delta C_p \cdot T \qquad (2.13)$$

$$\Delta S°(T) = \Delta S_o + \Delta C_p \ln T \qquad (2.14)$$

This method is employed herein for determining thermodynamic parameters to define hydrophobic, donor/acceptor, and ion-dipole interactions. Barrans has written a computer program (VANT HOFF) for

calculating ΔH°(T), ΔS°(T), and ΔCp given data relating K_a versus T (vide infra).

Variable-temperature binding studies in organic media

In order to unravel thermodynamic parameters for the ion-dipole effect, we focused first upon the complexation of positively-charged guests with host **27** in organic media. As in the earlier studies by Petti,[15] ^{1}H NMR was employed to determine binding affinities as a function of temperature.

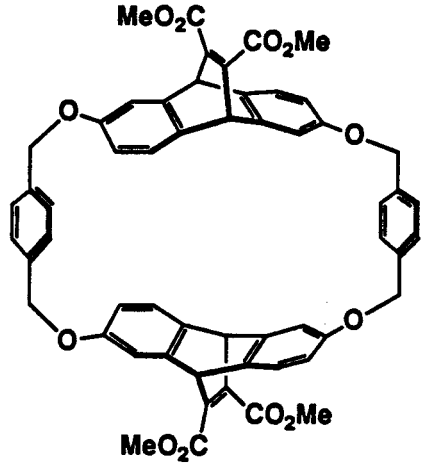

27

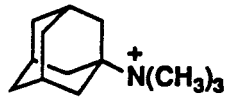

20

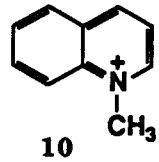

10

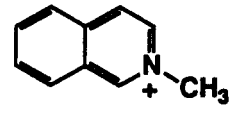

11

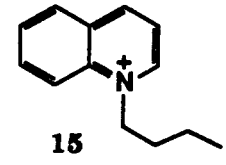

15

The first host-guest pair studied in deuterated organic solvents was host **27**/guest **10** in chloroform.[25] Binding constants were calculated at each temperature according to:

$$K_a = \left(\frac{1}{[H]_o - (P \cdot [G]_o)}\right)\left(\frac{P}{1 - P}\right) \qquad (2.15)$$

$$P = \frac{\text{observed upfield shift}}{D \text{ value}} \qquad (2.16)$$

where $[H]_o$ and $[G]_o$ are total concentrations of host and guest, respectively; P is percent guest bound (Eqn 2.16). Concentrations of host and guest were corrected for volume changes with temperature (see Experimental). As an initial assumption, the *D* values for guest protons were held constant for "single-point" determinations of K_a (one set of $[H]_o$ and $[G]_o$). Table **2.3** shows the K_a at each T determined in this way. Note that for a 100°-temperature range, K_a changes by a factor of 6.5.

To address the validity of the constant-*D*-value assumption in organic media, "complete" binding studies (several sets of $[H]_o$ and $[G]_o$) were performed at -40°C and +60°C (Table **2.4**). Comparison of *D* values (N-CH_3 of **10**) with temperature finds no trend, although approximately 10% changes in *D* are calculated by MULTIFIT. More importantly, the affinities at -40°C, room temperature, and +60°C for the "complete" binding studies are very close to the "single-point" affinities. Further discussion of *D* values will be withheld until the section on variable-temperature binding studies in aqueous media.

The van't Hoff plot for the data in Table **2.3** is shown in Figure **2.2**. Surprisingly, thermodynamic parameters obtained from the slope (-ΔH°) and intercept (ΔS°) suggest a binding force similar to the non-classical hydrophobic effect discussed above: ΔG° is composed of a relatively large, favorable ΔH° and a smaller, favorable ΔS°. However, the van't Hoff plot does show some curvature, which suggests that ΔC_p is non-zero.

Table 2.3: Temperature dependence of K_a for guest **10** with host **27**[a] in $CDCl_3$.

temperature (K)	K_a (M^{-1} x 10^2)[b]
234.2	12.3
244.3	9.9
254.3	8.0
264.3	6.6
274.3	5.4
284.2	4.5
294.4	3.7
296.4	3.6
293.8	3.8
304.3	3.1
324.5	2.2
334.6	1.9

[a]*R,R,R,R*-isomer; [b]Determined by "single-point" variable-temperature ^1H NMR (400 MHz) binding study assuming a constant *D* value for N-C*H*$_3$ (1060Hz, 2.65ppm).

Table 2.4: Comparison of K_a for "complete" and "single-point" variable-temperature binding studies of guest **10** and host **27**[a] in $CDCl_3$.

probe T (°C)	corrected T (K)	"complete" K_a (M^{-1} x 10^2)	"single-point" K_a (M^{-1} x 10^2)	*D* value[b] (ppm)
-40	234.2	12.2	12.3	2.87
ambient[c]	296.4	4.1	3.8	2.65
+60	334.6	1.9	1.9	2.80

[a]*R,R,R,R*-isomer; [b]For N-C*H*$_3$; [c]Ambient temperature not recorded for "complete" binding study.

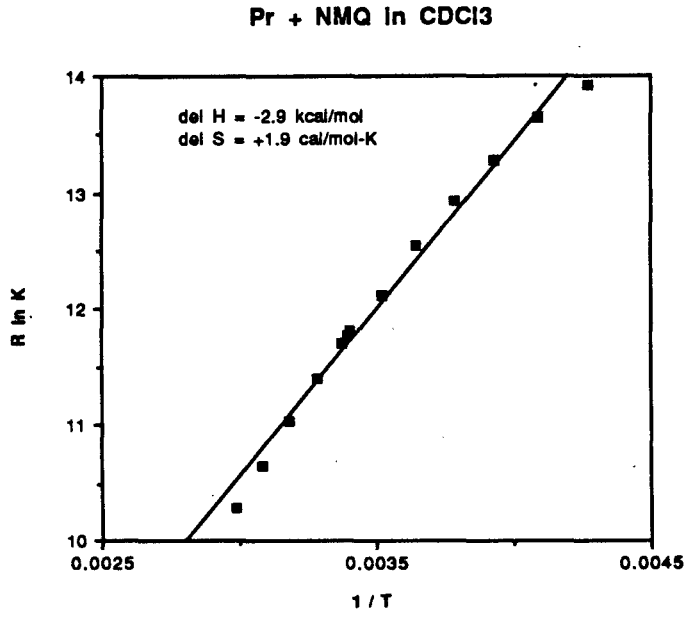

Figure 2.2. "Single-point" VT binding studies: van't Hoff plot for host **27** and guest **10** in $CDCl_3$.

The curvature in the van't Hoff plot is even more dramatic for host **27** with guest **20** (ATMA) in $CDCl_3$ (Figure **2.3**): At sufficiently low temperatures, K_a begins to *decrease*. This phenomenon was also to be observed in aqueous media. This unprecedented result led us to calculate thermodynamic parameters according to the temperature-dependent van't Hoff Equation 2.12 (referred to hereafter as the "log" equation). The validity of adding a second term (ln T) to the mathematical expression for thermodynamic parameters was verified by statistical analysis included in VANT HOFF.[26] We find that the log equation fits our data quite well.[27] Figure **2.4** shows the data for host **27** with guests **10** and **20**. The fitted curves are interpolated for $R\ln K_a$ calculated at each temperature according to the log equation.

Overall, single-point, variable-temperature binding studies were performed for host **27** and the positively-charged guests **10**, **11**, **15**, and **20**. The van't Hoff data and interpolated log fits for guests **11** and **15** are shown in Figure **2.5**: again, the curvature is obvious.

The heat capacities and thermodynamics of complexation for binding onium guests in chloroform are summarized in Table **2.5**. It is imperative that we report the temperature for discussing the nature of the binding force. As noted earlier, care must be taken when characterizing equilibria as either entropy- or enthalpy-driven if ΔC_p is significant. In such cases, one may partition $\Delta H°$ and $\Delta S°$ into "motive" and "compensation" terms,[28] wherein motive ΔH and ΔS are intrinsic to the free energy for the interaction, while compensation ΔH and ΔS reflect ΔC_p and thereby cancel their contributions to $\Delta G°$. It has been noted also that, in addition to thermodynamic parameters for equilibria, activation parameters for

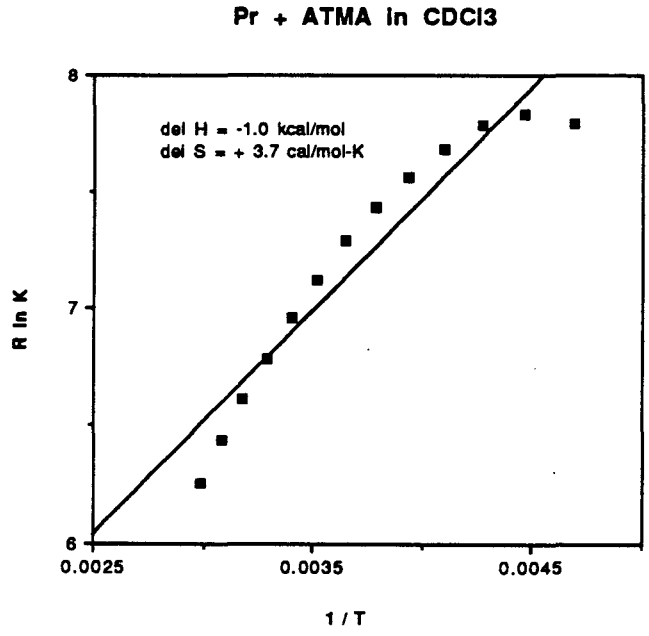

Figure 2.3. "Single-point" VT binding studies: van't Hoff plot for host **27** and guest **20** in $CDCl_3$.

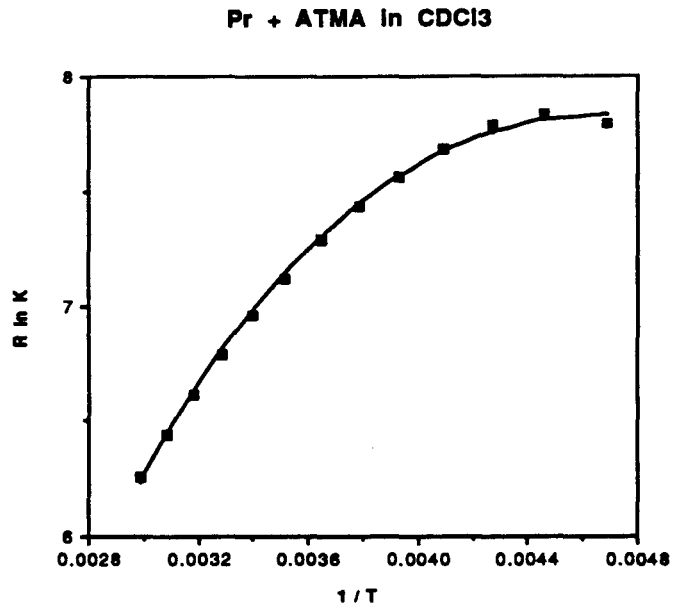

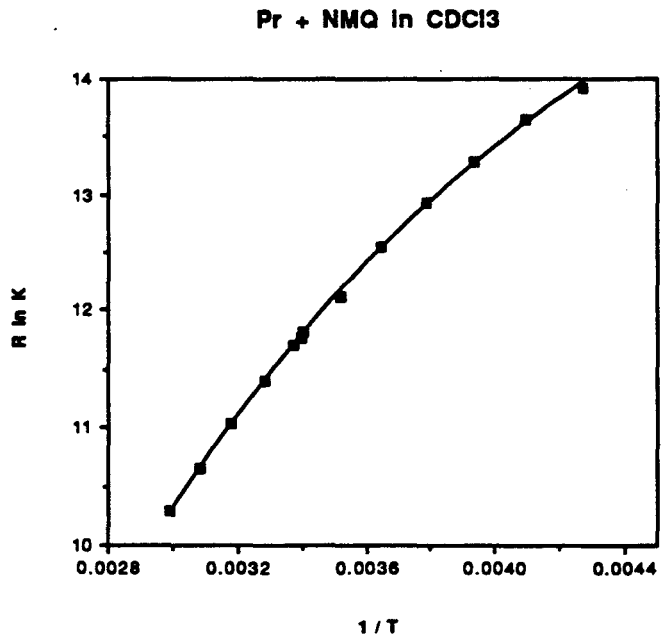

Figure 2.4. Log fits (Eqn. 2.12) for single-point VT binding studies. **Top**: host **27** and guest **20** in $CDCl_3$; **bottom**: host **27** and guest **10** in $CDCl_3$.

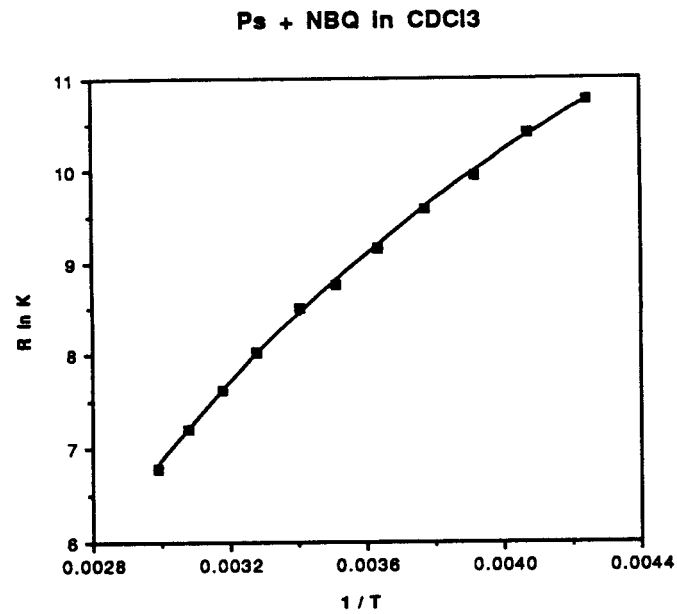

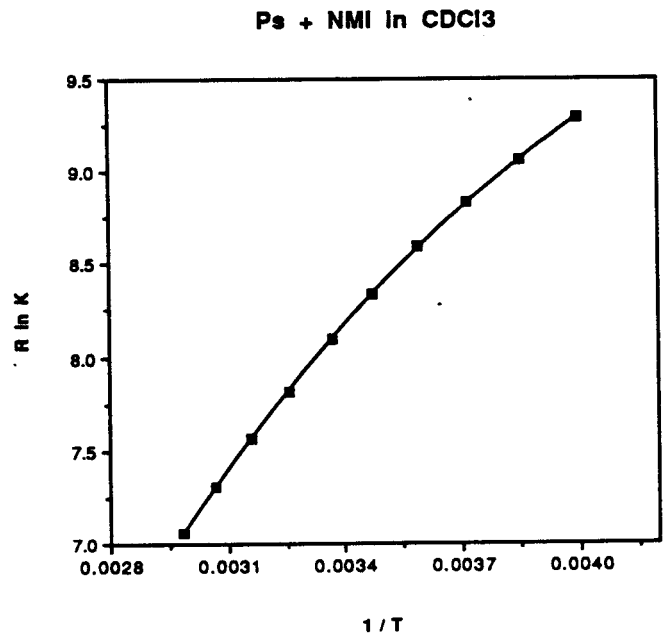

Figure 2.5. Log fits (Eqn. 2.12) for single-point VT binding studies. **Top**: host **27** and guest **15** in $CDCl_3$; **bottom**: host **27** and guest **11** in $CDCl_3$.

Table 2.5: Thermodynamic parameters for complexation in organic media: host **27** and guests in $CDCl_3$.[a]

guest	ΔC_p (cal/mol-K)	$\Delta H°_{298}$ (kcal/mol)	$\Delta S°_{298}$ (cal/mol-K)	$\Delta G°_{298}$ (kcal/mol)
20[b]	-18.0	-1.54	+1.76	-2.06
10[b]	-23.6	-3.34	+0.43	-3.47
15[c]	-24.0	-3.59	-3.76	-2.47
11[c]	-18.9	-2.39	+0.05	-2.40

[a]Calculated from Eqns. 2.6, 2.13, and 2.14 using ΔC_p determined from "single-point" VT binding studies; [b]*R,R,R,R*-isomer of host **27**; [c]*S,S,S,S*-isomer of host **27**.

kinetics in several reaction classes exhibit compensation of enthalpy and entropy[29] (see Chapter 3).

While we hesitate to ascribe specific motive and compensation values in the present work, we do find that $\Delta H°$ and $\Delta S°$ exhibit the anticipated compensation behavior in organic media. Figure **2.6** illustrates the dramatic compensation of $\Delta H°$ and $T\Delta S°$ as a function of temperature: $\Delta G°$ remains relatively unchanged. Thus, to reiterate, enthalpic/entropic origins of the binding force in molecular recognition require a specific temperature for comparison. Hence, the thermodynamic parameters in Table **2.5** are specified for 298K, so that comparisions to other studies can be made. We suggest that caution be used when making any such comparisons to ΔC_p-deficient parameters. Our discussion will rest upon the ideas regarding host-guest, host-solvent, guest-solvent, and solvent-solvent interactions.

The heat capacities for binding in organic media are consistent with biochemical association processes[10] in that all ΔC_p values are negative, although their magnitudes are smaller, as would be expected for a non-hydrophobic environment.[17] Several tentative conclusions can be drawn from this data: (1) based upon the values for $\Delta H°$ and $\Delta S°$ at 298K, the ion-dipole effect for binding onium guests in organic media is primarily enthalpic, with a small, favorable entropic contribution (Table **2.5**); (2) the lower affinity of guest **15** versus **10** (butyl vs methyl) suggests that the host pays an entropic price to orient the butyl group upon encapsulation; (3) based upon the higher affinity for the flat, aromatic guests, the host is better-suited in the rhomboid conformation than in the toroid conformation for strong, enthalpic ion-dipole interactions. (Alternatively, the additional affinity could be due to donor/acceptor interactions with the aromatic guests

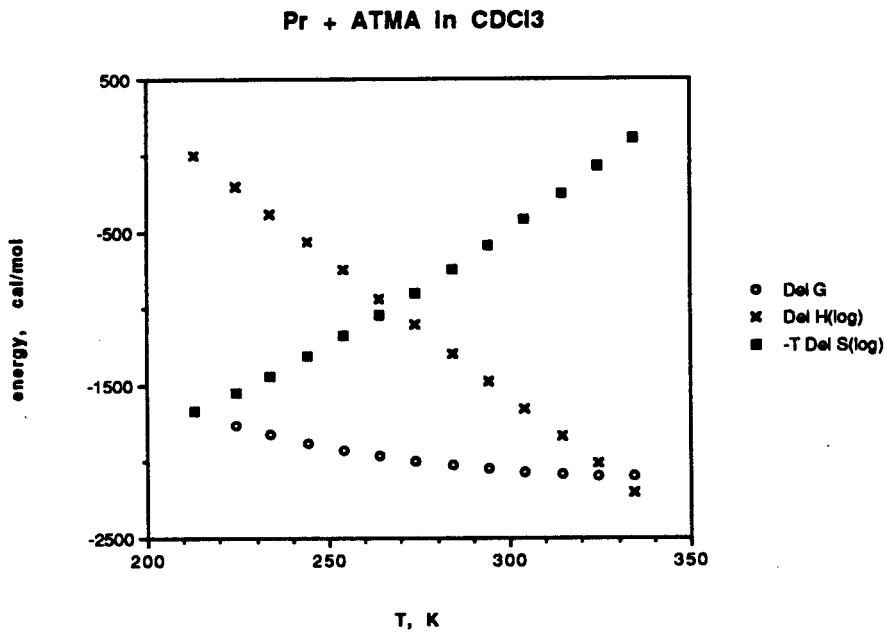

Figure 2.6. Temperature-dependence of thermodynamic parameters. Compensation of $\Delta H°$ and $T\Delta S°$ with a relatively constant $\Delta G°$ for host **27** and guest **20** in $CDCl_3$.

in the rhomboid geometry; however, we discount this argument because no such interactions are observed in organic media for the neutral analogs, as detailed in Chapter 1.)

The primary conclusion that the ion-dipole effect in chloroform is an enthalpic binding force contrasts the results obtained in other host-guest systems in organic solvents.[30] Binding of related guests with crown ether hosts typically exacts a large entropic cost, which has been attributed to the order necessary to bring two species together as one. We therefore wondered whether the slightly favorable entropy term in our system was due to the presence of the counterion: are two species in equilibrium with two species, as in Equation 2.17?

$$\text{host} + \text{guest}^{+}\cdot X^{-} \rightleftharpoons \text{host}\cdot\text{guest}^{+} + X^{-} \qquad (2.17)$$

We therefore postulated that guest$^{+}\cdot X^{-}$ could form a tight-ion pair in chloroform.[31] Host **27** would then break guest^{+} and X^{-} into a separated-ion pair. We hoped to probe this issue by forcing the putative guest$^{+}\cdot X^{-}$ species to be separated in the absence of host. Unfortunately, the attempted exchange of iodide anion for the bulky tetraphenylborate anion with guest **10** was unsuccessful in our hands.

Variable-temperature binding studies in aqueous media

Adamantyltrimethylammonium (**20**, ATMA)

We begin our evaluation of heat capacity and thermodynamics of complexation in aqueous media by considering guest **20** (ATMA) with several hosts. As alluded to earlier, the van't Hoff plots reported by Petti[15] for ATMA with hosts **38** and **39** showed distinct curvature, much like that

for the variable-temperature binding in chloroform. The Petti data have been subjected to fitting with the log equation (Eqn. 2.12), and the results for these hosts and hosts **1**, **2**, **40**, and **41** with ATMA are summarized in Table **2.6**. Interpolated log fits are shown in Figures **2.7**, **2.8**, and **2.9**. Binding constants for the recent variable-temperature studies were determined in a pD~9 borate buffer according to the single-point analysis described above: *D* values were held constant (within a host-guest pair) with the values as tabulated for the *N*-methyl protons. (Only the *D* value for ATMA with host **1** has been modified from the reported room-temperature binding studies[15,32] to reflect more recent MULTIFIT analysis (vide infra) for nearly 100% bound guest.) The magnitude of the calculated ΔC_p values is greater in aqueous media than in chloroform, as is expected for hydrophobic binding.

The thermodynamic parameters for hosts with ATMA invite several interesting comparisons, which are outlined below. Because we are comparing data for a single guest, guest-solvent interactions are factored out.

The ion-dipole effect has been invoked primarily to explain the enhanced affinity of host **1** versus **2**[3] (Chapter 1) for positively-charged guests. These hosts, which possess similar binding site dimensions and comparable degrees of preorganization, show significantly different $\Delta H°_{298}$ and $\Delta S°_{298}$ values: the more favorable entropy term for host **2** is consistent with "classical" hydrophobicity (cyclohexyl is more hydrophobic than phenyl;[33] the hydrophobic effect is defined classically in terms of a large, positive $\Delta S°$ for binding[13]). As found for host **27** in organic media, host **1** in aqueous media displays a favorable enthalpic contribution as evidence for strong ion-dipole interactions.

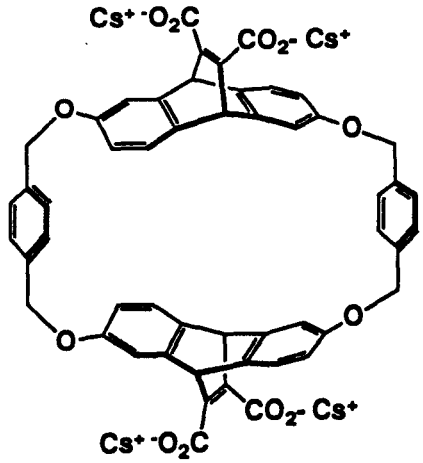
Cs+ -O2C
CO2- Cs+
O
O
O
O
CO2- Cs+
Cs+ -O2C

1

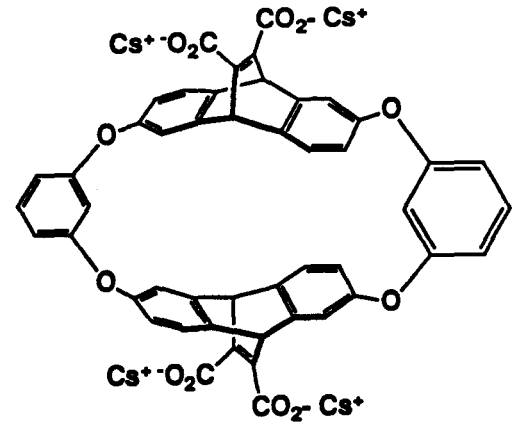
CO2- Cs+
Cs+ -O2C
O
O
O
O
Cs+ -O2C
CO2- Cs+

40

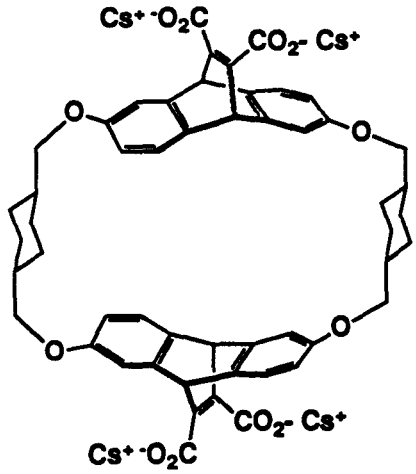
Cs+ -O2C
CO2- Cs+
O
O
O
O
CO2- Cs+
Cs+ -O2C

2

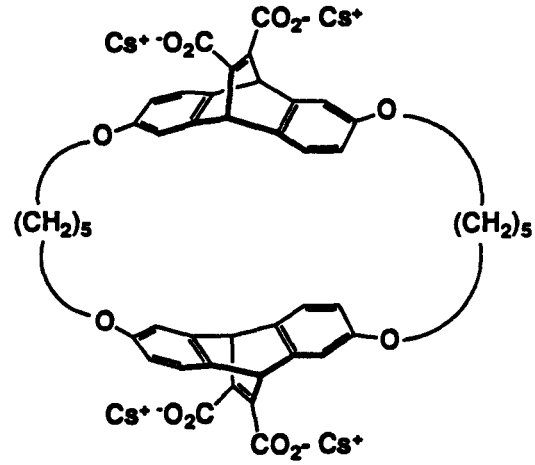
CO2- Cs+
Cs+ -O2C
O
O
(CH2)5
(CH2)5
O
O
Cs+ -O2C
CO2- Cs+

41

Table 2.6: Thermodynamic parameters for complexation in aqueous media: guest **20** (ATMA) and a series of hosts in borate-*d*.[a]

host	ΔC_p (cal/mol-K)	$\Delta H°_{298}$ (kcal/mol)	$\Delta S°_{298}$ (cal/mol-K)	$\Delta G°_{298}$ (kcal/mol)	*D* value[b] (Hz)
1	-102	-4.69	8.62	-7.26	670
40	-131	-3.39	9.95	-6.35	410
2	-109	-1.35	14.2	-5.57	502
41	-34.0	-4.86	2.16	-5.50	565
39[c]	-81.9	-2.04	8.12	-4.46	N/A
38[c]	-65.5	-3.76	2.50	-4.50	N/A

[a]Single-point VT binding analysis; [b]For $N(CH_3)_3$ (A protons) of ATMA; [c]Reference 15.

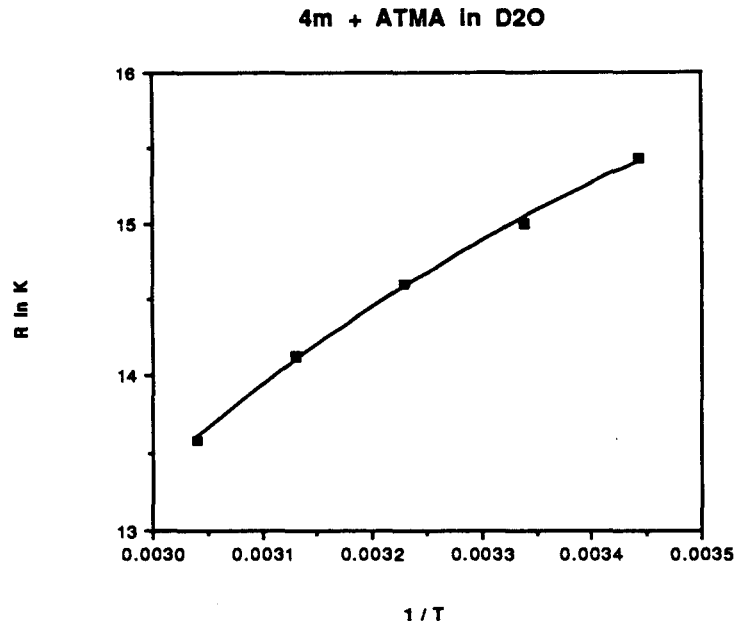

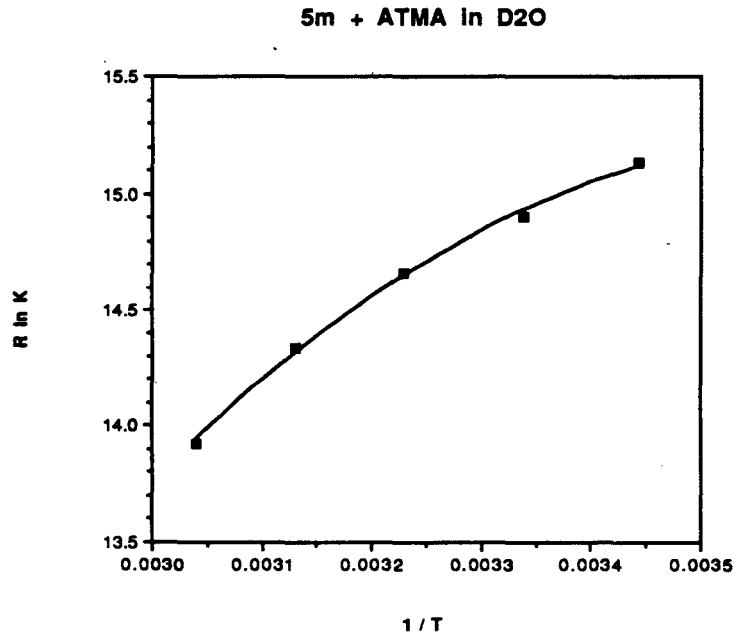

Figure 2.7. Log fits (Eqn. 2.12) for complete VT binding studies by Petti.[15] **Top**: host **38** and guest **20** in borate-*d*; **bottom**: host **39** and guest **20** in borate-*d*.

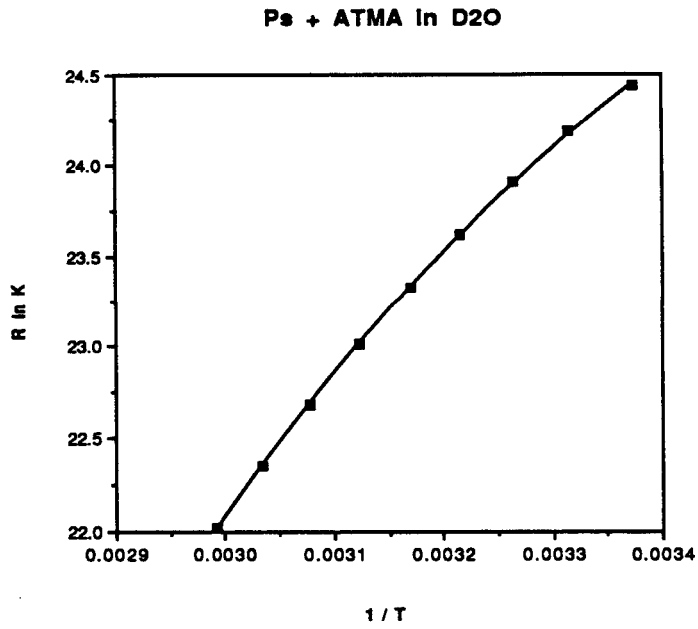

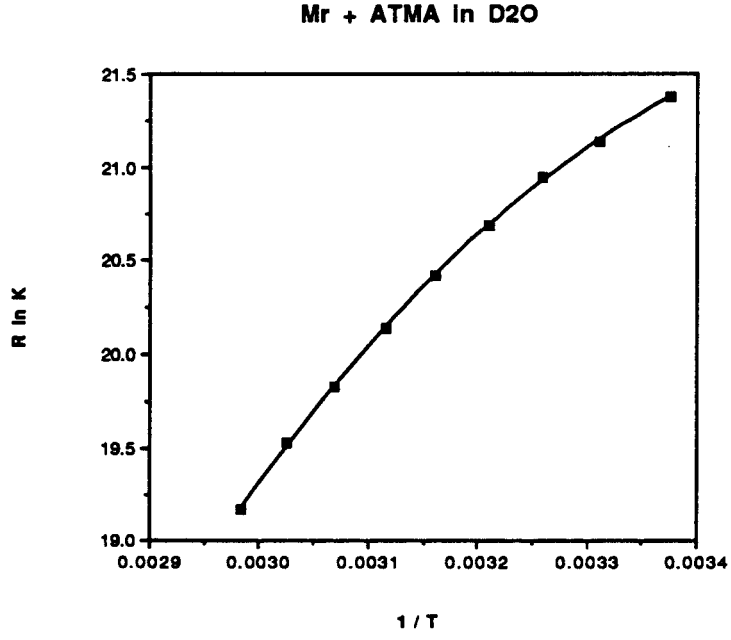

Figure 2.8. Log fits (Eqn. 2.12) for single-point VT binding studies. **Top**: host **1** and guest **20** in borate-*d*; **bottom**: host **40** and guest **20** in borate-*d*.

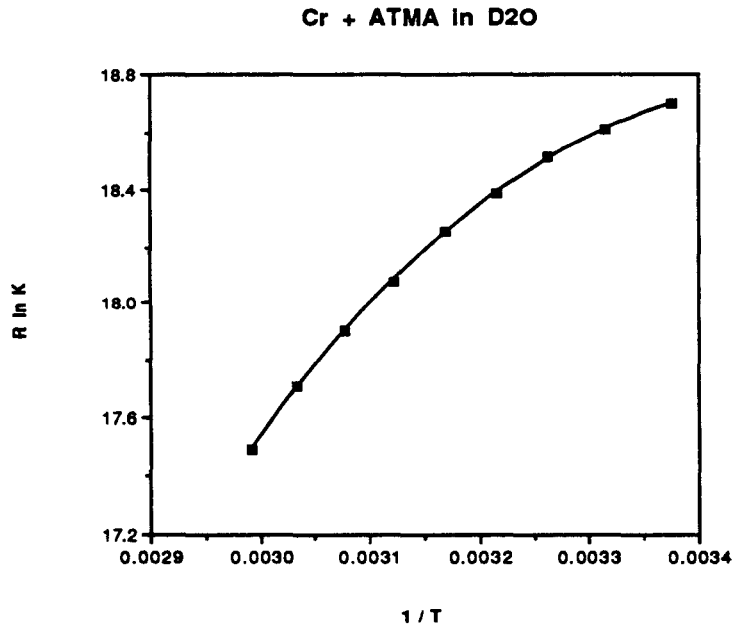

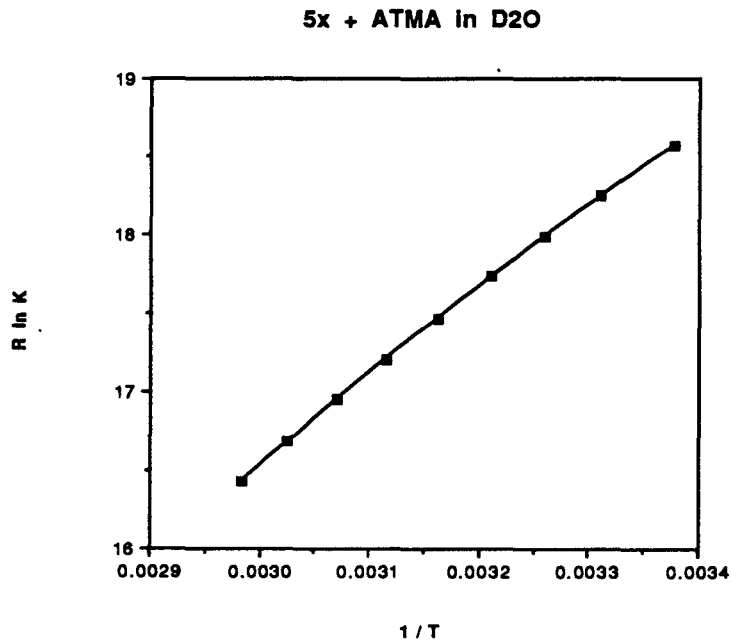

Figure 2.9. Log fits (Eqn. 2.12) for single-point VT binding studies. **Top:** host **2** and guest **20** in borate-*d*; **bottom:** host **41** and guest **20** in borate-*d*.

Comparison of hosts **1** and **40** suggests that the *p*-xylyl linkers achieve better ion-dipole interactions ($\Delta H°$) than the *m*-xylyl linkers. Modelling studies had suggested that the lower affinity for host **40** was the result of a greater number of low energy conformations accessible to **40**.[4] We anticipated, therefore, a less favorable entropy term; however, according to the ΔC_p-log fit, these views are not compatible.

With ATMA as a probe for host-guest structure, differences between hosts **1** and **41** have been delineated. The thermodynamic parameters at 298K are consistent with the model for binding of ATMA by hosts **1** and **41**. The lower affinity for host **41** has been attributed to the flexibility of the polymethylene linkers, which allow the host to collapse into a bowl-shaped conformation:[45] the lower $\Delta S°$ for complexation attests to the randomly-oriented binding of ATMA with host **41**. A more favorable entropy term is found with the more preorganized host **1**, which exhibits tight, oriented binding with ATMA. Perhaps the larger negative $\Delta H°$ for host **41** reflects the ability of the bowl-shaped host to exert even stronger ion-dipole interactions than host **1** with its fully aromatic array!

Because the Petti data (Table **2.6**) were determined in a pD~9.5 phosphate buffer, we hesitate to make any direct comparisons with our more recent data. As with the data in pD~9 borate buffer, ΔH and ΔS are *both* favorable for hosts **38** and **39** with ATMA. Overall, we have partitioned the 298K-thermodynamic parameters for binding ATMA in aqueous media into three catergories: (1) the host-guest ion-dipole effect is evident by a favorably large, negative $\Delta H°$, as was found also in organic media; (2) the classical hydrophobic effect, through host-solvent and solvent-solvent interactions, is evident by a large, positive $\Delta S°$; and (3) disordered host conformations (host-solvent interactions) reduce the favorable entropic

contribution. It is in the context of these points that we consider the binding of other guests in aqueous media.

Alkylation substrates and products

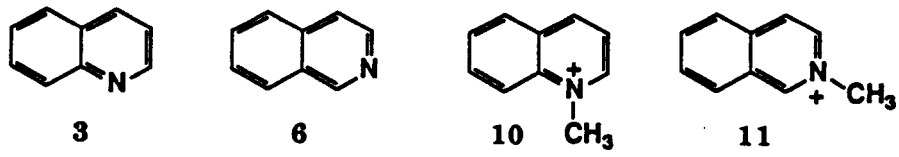

3 6 10 11

Detailed variable-temperature (VT) binding studies (^{1}H NMR, 400MHz) for methylation substrate/product pairs **3/10** and **6/11** with host **1** were performed (for the single guests) in anticipation of the nmr kinetics for the host-catalyzed alkylation reactions described in Chapter 3. The temperature-dependent thermodynamic parameters for these four guests were determined from both "single-point" and "complete" VT binding studies. Single-point K_a determinations were performed initially, assuming constant D values.[32] When the reported $-\Delta G°_{295}$ values were not reproduced within the assigned error limits (±0.2 kcal/mol), complete VT binding studies were carried out wherein nmr titration data *at each temperature* were evaluated by MULTIFIT to give temperature-dependent sets of K_a and D values. However, because the room-temperature affinities measured in the complete VT binding studies did not reproduce adequately the Shepodd results,[32] we examined more carefully host-guest complexation near guest saturation ($[H]_o >> [G]_o$). In this way, we came full circle to establish new D values for the single-point VT analyses. Temperature-dependent affinities for very tightly bound guests (**10, 11**) were

scaled to the reported values.[3] Below is the detailed discussion of this *tour de force.*

Single-point VT binding studies were performed for onium guests **10** and **11** and neutral guest **6** with host **1** in borate-*d*. Shifts for selected guest protons were monitored as a function of temperature for single $[H]_0$ and $[G]_0$ pairs. As in the chloroform studies, the nmr probe temperature was calibrated with a methanol standard, and total concentrations of host and guest were corrected for volume changes with termperature[46] (see Experimental). Data reduction was carried out according to Eqns. 2.15 and 2.16. Almost immediately, a flaw in the single-point method was detected: for guest **10**, the observed shifts and the *D* values reported by Shepodd[32] gave values for P that specified negative values for the concentrations of free host (i.e., $P \cdot [G]_0 > [H]_0$), which specified *negative* K_as. It was found in this case that introducing slight changes in the *D* values (or, alternatively, substantial changes in $[H]_0$ and/or $[G]_0$) led to positive K_a values. Unfortunately, for very tightly bound guests (K_as greater than ~$10^5 M^{-1}$), such as **10** with host **1**, this problem withstood all of our efforts to determine heat capacity and thermodynamics of complexation in aqueous media.

These initial difficulties in applying the single-point VT binding method to guests other than **20** (ATMA) forced us to re-evaluate the constant-*D*-value assumption in aqueous media. Consequently, tedious complete binding studies were performed at four different temperatures (25-55°C) for guests **3**, **6**, **10**, and **11** in borate-*d*. Data were subjected to MULTIFIT analysis to obtain unique K_a and *D* values at each temperature. The range in *D* values, which are tabulated with the corresponding log-fit thermodynamic parameters in Table **2.7**, varied dramatically with temperature. Even more distressing, all *D* values at 25°C determined in the

Table 2.7: Thermodynamic parameters for complexation in aqueous media from complete VT binding studies: methylation substrate/product guests **3/10** and **6/11** and host **1** in borate-*d*.

guest	ΔC_p (cal/mol-K)	$\Delta H°_{298}$ (kcal/mol)	$\Delta S°_{298}$ (cal/mol-K)	$\Delta G°_{298}$ (kcal/mol)	*D* range[a] (proton, Hz)
3	-223	-1.30	12.6	-5.06	1048-880 (H_2)
6	-120	-1.93	11.6	-5.40	1256-1133 (H_1)
10	+21.6	-4.03	9.50	-6.86	877-910 (N-CH_3)
11	-34.5	-1.19	16.0	-5.94	635-620 (N-CH_3)

[a]*D* values were calculated by MULTIFIT at each temperature (25-55°C).

present work were appreciably higher than those calculated by Shepodd.[32] In addition, all binding affinities were lower than, and outside the error limits for, the values reported (Table **2.8**).[3]

Tables **2.9** and **2.10** present MULTIFIT-analyzed room-temperature[47] binding studies from Shepodd[32] and the present work, respectively. We find that when essentially identical binding studies are performed, significantly different results are obtained. Most notably, as has been found repeatedly in our research, MULTIFIT compensates K_a and D values: relatively high K_as go "hand-in-hand" with relatively low D values (and, vice versa, low K_as compensate high D values).

As discussed in detail below in the section on the constant-D-value assumption for the specific example of host **1** and guest **20** (ATMA), several factors exposed by MULTIFIT may be responsible for this discrepancy in D values. Host- and guest-stock-solution concentrations are determined by nmr integration (see Experimental) and can introduce errors propagated throughout the MULTIFIT analysis. As noted in the previous VT binding studies, observed host-induced guest shifts can be highly temperature-dependent, although this factor alone cannot account for the magnitude of the differences between the Shepodd work and the present work. The MULTIFIT analysis could be the culprit, in part, in that it seeks the *best* fit for *all* the data, even if only a single proton is analyzed. In many cases, the present work includes *guest*-induced *host* shifts in the MULTIFIT data reduction (see also Chapter 4). The much smaller host shifts do not significantly alter K_a or D values (for guest protons), but they artificially improve the overall rms deviation in the fit. Further comments about MULTIFIT and other complete-binding data-reduction procedures shall be deferred to Barrans.[48]

Table 2.8: Comparison of reported and complete "room-temperature" binding studies: affinities and *D* values for methylation substrate/product guests **3/10** and **6/11** and host **1** in borate-*d*.

guest	reported[a]		complete[b]	
	$\Delta G°_{295}$ (kcal/mol)	*D* value (Hz, proton)	$\Delta G°_{300}$ (kcal/mol)	*D* value (Hz, proton)
3	-5.4	661 (H_2)	-5.06	1048 (H_2)
6	-6.3	736 (H_1)	-5.40	1256 (H_1)
10	-7.6	658 (N-CH_3)	-6.86	877 (N-CH_3)
11	-7.2	420 (N-CH_3)	-5.94	635 (N-CH_3)

[a]Reference 32; room temperature not recorded; [b]From log-fit thermodynamic parameters from complete binding studies; *D* values at probe temperature setting of 25°C (actual T=300.3K).

Table 2.9: MULTIFIT analysis of room-temperature binding study for guest **6** and host **1** in borate-*d*, performed by Shepodd.[32]

Best Binding constant = 39126.69
Overall RMS deviation = 0.5407

Chemical Shift of free guest = 3702.3600
Maximum Upfield Shift = 746.1661
RMS deviation = 0.5407

[H]o (μM)	[G]o (μM)	Chem Shift Observed	Up. Shift Obs'd	Up. Shift Calc'd	Calc'd -Obs'd	(C-O)/O (%)	% G Bound	% H Bound
29.0	426	3653.56	48.80	47.74	1.06	2.18	6.397	93.976
69.8	410	3583.74	118.62	118.27	0.35	0.30	15.850	93.103
132.	386	3469.97	232.39	232.77	-0.38	-0.16	31.195	91.222
207.	357	3324.72	377.64	377.85	-0.21	-0.06	50.639	87.334
288.	326	3179.70	522.66	522.52	0.14	0.03	70.027	79.267

Table 2.10: MULTIFIT analysis of room-temperature binding study for guest **6** and host **1** in borate-*d*, present work.

Best Binding constant = 8844.78
Overall RMS deviation = 5.9356

Chemical Shift of free guest = 3702.3600
Maximum Upfield Shift = 1260.2151
RMS deviation = 5.9356

[H]o (μM)	[G]o (μM)	Chem Shift Observed	Up. Shift Obs'd	Up. Shift Calc'd	Calc'd -Obs'd	(C-O)/O (%)	% G Bound	% H Bound
20.6	363	3647.13	55.23	53.96	1.27	2.30	4.282	75.449
59.4	349	3539.71	162.65	156.57	6.08	3.74	12.424	72.997
112.	330	3397.19	305.17	295.47	9.70	3.18	23.446	69.083
175.	308	3240.63	461.73	454.81	6.92	1.50	36.090	63.518
242.	285	3103.00	599.36	606.40	-7.04	-1.17	48.119	56.669
239.	374	3175.26	527.10	529.38	-2.28	-0.43	42.007	65.734
235.	460	3242.16	460.20	463.57	-3.37	-0.73	36.785	72.004

The significance of the complete VT binding studies was to point out the need for more accurate, "correct" *D* values. As is evident from the aforementioned binding studies, and from other complete binding studies evaluated by MULTIFIT, all single-point VT binding studies demand that we have confidence in the *D* values. Therefore, we have pushed the limits of nmr detection for small amounts of guest in the presence of host (maintained below its CAC, see Chapter 4) in the nmr titration experiments. *D* values determined by MULTIFIT analyses of the high-percent-guest-bound[49] data are listed in Table **2.11**. Also tabulated are the log-fit thermodynamic parameters for these four guests from single-point VT binding studies using these "correct" *D* values. Difficulties are still encountered for very tightly bound guests: the problem of negative K_a values persists for guest **10**; also, note that $-\Delta G°_{298}$ for guest **11** is extremely large. Table **2.12** compares the single-point affinities to the reported values.[3] As an indication that the VT binding analysis is again manageable, the room-temperature affinities for neutral guests **3** and **6** are quite close to those found by Shepodd,[32] even though the *D* values differ significantly for **6**.

The binding of neutral, electron-deficient guests by host **1** in aqueous media has been attributed to a combination of donor/acceptor π-stacking and hydrophobic interactions.[3] The small, negative heat capacities for guests **3** and **6** resemble ΔC_p values for the chloroform VT binding studies. The signs and magnitudes for $\Delta H°$ and $\Delta S°$ hint that hydrophobic interactions may be overridden by donor/acceptor interactions as evidenced by highly favorable enthalpic contributions against large unfavorable entropic terms. Alternatively, a non-classical hydrophobic effect could be operative with assistance from the donor/acceptor interaction, although one

Table 2.11: Thermodynamic parameters for complexation in aqueous media from single-point VT binding studies: methylation substrate/product guests **3/10** and **6/11** and host **1** in borate-*d*.

guest	ΔC_p (cal/mol-K)	$\Delta H°_{298}$ (kcal/mol)	$\Delta S°_{298}$ (cal/mol-K)	$\Delta G°_{298}$ (kcal/mol)	*D* value[a] (proton, Hz)
3	-11.6	-11.0	-16.7	-5.99	665 (H_2)
6	-24.6	-9.80	-11.3	-6.43	875 (H_1)
10	+32.0	-4.30	8.57	-6.85	710 (N-CH_3)
11	-2.9	-11.6	-10.6	-8.42	420 (N-CH_3)

[a]*D* values were estimated from MULTIFIT analysis of high-percent-bound-guest data at a probe temperature setting of 25°C (actual T=300.3K).

Table 2.12: Comparison of reported and single-point "room-temperature" binding studies: affinities and *D* values for methylation substrate/product guests **3/10** and **6/11** and host **1** in borate-*d*.

guest	reported[a]		single-point[b]	
	$\Delta G°_{295}$ (kcal/mol)	*D* value (Hz, proton)	$\Delta G°_{298}$ (kcal/mol)	*D* value (Hz, proton)
3	-5.4	661 (H_2)	-5.99	665 (H_2)
6	-6.3	736 (H_1)	-6.43	875 (H_1)
10	-7.6	658 (N-CH_3)	-6.85	710 (N-CH_3)
11	-7.2	420 (N-CH_3)	-8.42	420 (N-CH_3)

[a]Reference 32; room temperature not recorded; [b]From log-fit thermodynamic parameters from single-point binding studies; *D* values from MULTIFIT analysis of high-percent-bound-guest binding data at probe temperature setting of 25°C (actual T=300.3K).

would expect a larger $-\Delta C_p$ for hydrophobic binding (see comparison of hosts **1** and **2** below).

In order to obtain K_as as a function of temperature for the VT nmr kinetics analysis to follow in Chapter 3, the free energies calculated from the complete binding studies (Table **2.7**) for guests **10** and **11** with host **1** were scaled to match the reported values[3] at room temperature. Scaled K_as were calculated for the range of temperatures covered in the single-point studies, then re-evaluated to give the log-fit thermodynamic parameters in Table **2.13**. In contrast to the neutral guests **3** and **6**, the onium guests **10** and **11** show large positive $\Delta S°$ values and more modestly favorable $\Delta H°$ values at 298K. This result is surprising in that it suggests classic hydrophobic interactions ($\Delta S°$) assist a milder ion-dipole effect ($\Delta H°$) for these very tightly bound guests with host **1**.

The constant-*D*-value assumption

An examination of host-guest pair **1/20** in borate-*d* further illustrates the dilemma confronted in the constant-*D*-value assumption. Most importantly, again, "correct" *D* values are mandatory for proper evaluation of the single-point VT binding studies. Table **2.14** lists log-fit thermodynamic parameters for host **1** with ATMA determined by single-point and complete analyses of VT data.

For the complete VT binding study (Figure **2.10**) at four temperatures (25-55°C), the MULTIFIT *D* values for the *N*-methyl protons (as well as other observable protons) of ATMA progressively decrease with increasing temperature (Table **2.15**). Interestingly, K_a remains basically unchanged with temperature, which is evident by the small $-\Delta C_p$ and near-zero $\Delta H°_{298}$.

Table 2.13: Thermodynamic parameters for complexation from scaled,[a] complete VT binding studies in aqueous media for onium guests **10** and **11** with host **1** in borate-*d*.

guest	ΔC_p (cal/mol-K)	$\Delta H°_{298}$ (kcal/mol)	$\Delta S°_{298}$ (cal/mol-K)	$\Delta G°_{298}$ (kcal/mol)
10	+32.0	-4.30	11.3	-7.67
11	-27.9	-1.20	20.2	-7.24

[a]Scaled to free energies reported in reference 3.

Table 2.14: Thermodynamic parameters for complexation in aqueous media: comparison of single-point and complete VT binding studies for guest **20** (ATMA) and host **1** in borate-*d*.

method	ΔC_p (cal/mol-K)	$\Delta H°_{298}$ (kcal/mol)	$\Delta S°_{298}$ (cal/mol-K)	$\Delta G°_{298}$ (kcal/mol)	*D* values[a] (Hz)
complete	-13.3	-0.14	21.3	-6.49	938-784[b]
single-point	-98.2	-3.05	12.6	-6.80	747[c]
single-point	-102	-4.69	8.62	-7.26	670[d]

[a]For $N(CH_3)_3$ (A protons) of ATMA; [b]*D* values were calculated by MULTIFIT at each temperature (25-55°C); [c]Reference 32; ambient temperature ~295K; [d]From MULTIFIT analysis of high-percent-bound-guest data at a probe temperature setting of 25°C (actual T=300.3K), performed by McCurdy.

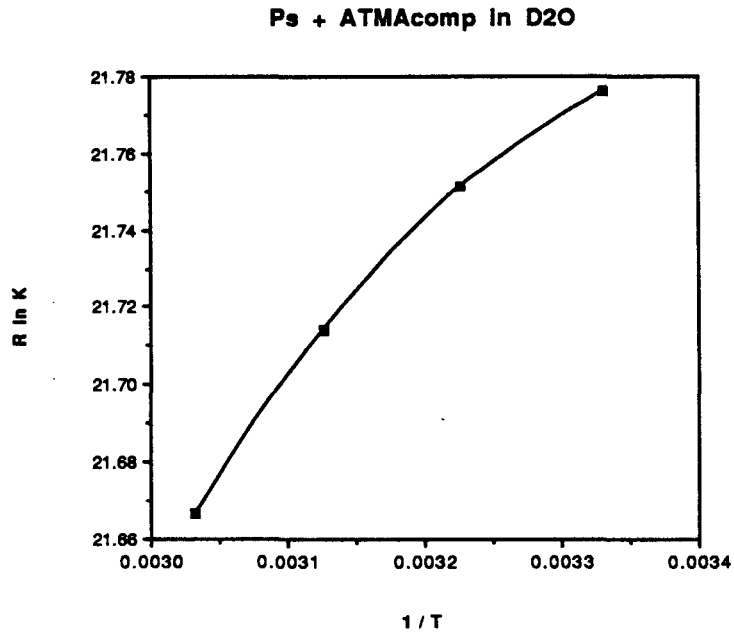

Figure 2.10. Log fit (Eqn. 2.12) for complete VT binding study: host **1** and guest **20** in borate-*d*.

Table 2.15: *D* values as a function of temperature from complete VT binding studies for guest **20** (ATMA) and host **1** in borate-*d*.[a]

temperature[b] (°C)	*D* value[c] (Hz)
25	939
35	897
45	843
55	784

[a]$[H]_0$~0-120μM; $[G]_0$~60-50μM; [b]Probe temperature setting; [c]For $N(CH_3)_3$ (A protons) of ATMA; *D* values were calculated by MULTIFIT at each temperature.

The correspondingly large, positive $\Delta S°$ suggests classic hydrophobic binding.

The complete study contrasts the single-point VT binding studies: using the reported *D* value (747Hz[32]) and a more recently determined *D* value (670Hz, from MULTIFIT analysis of high-percent-bound-guest data), greater curvature in the $R\ln K_a$ vs T^{-1} plot is noted, and the interpolated log fits are shown in Figure **2.11**. The log-fit thermodynamic parameters suggest a greater $-\Delta C_p$ and a larger, favorable enthalpic contribution, particularly as the *D* value decreases;[50] as another example of $\Delta H°/\Delta S°$ compensation, $\Delta S°$ is less favorable. In the first section on ATMA-binding in aqueous media, this result was attributed to the dominant ion-dipole interaction ($-\Delta H°$) with a mild, classic hydrophobic interaction ($+\Delta S°$).

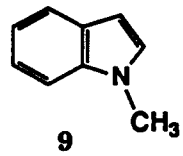

9

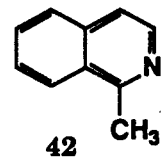

42

Single-point VT binding studies for host-guest pair **2/42** were also considered to assess the constant-*D*-value assumption. The reported room-temperature *D* value for the methyl group of **42** is 370Hz.[32] We wondered whether *D* might vary as a function of absolute temperature. Consequently, *D* was artificially weighted in a "positive" sense (Eqn. 2.18, D_+) and in a "negative" sense (Eqn. 2.19, D_-) versus temperature (T):

$$D_+(T) = \left(\frac{T}{295}\right) \cdot 370\ \text{Hz} \qquad (2.18)$$

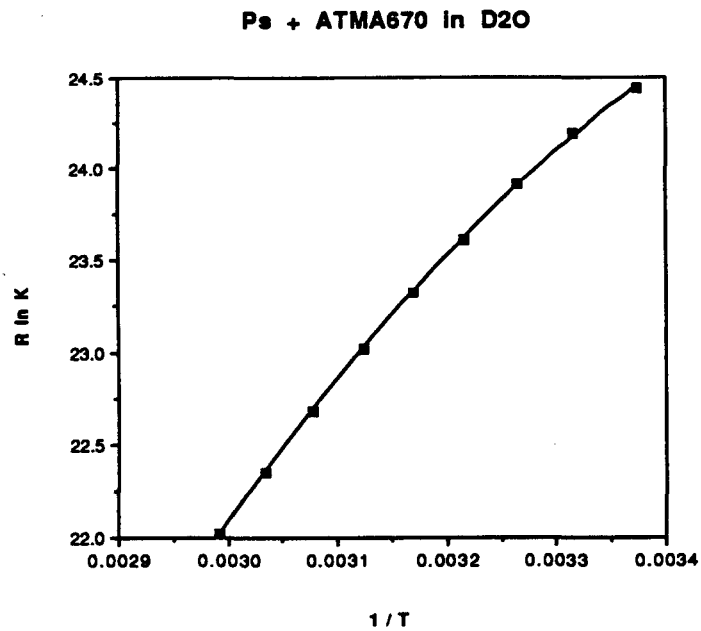

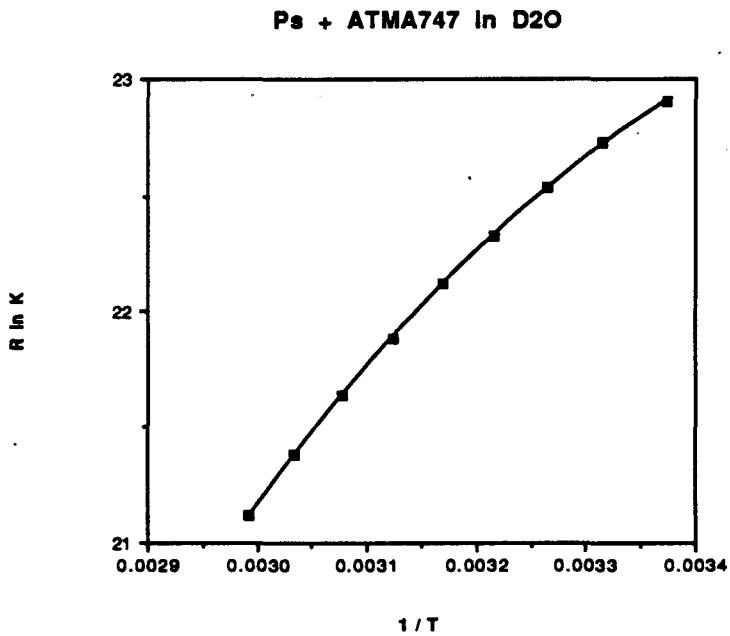

Figure 2.11. Log fits (Eqn. 2.12) for single-point VT binding studies with different D values for host **1** and guest **20** in borate-*d*. **Top**: D=670Hz from present work; **bottom**: D=747Hz from Shepodd.[32]

$$D_{-}(T) = \left(\frac{295}{T}\right) \cdot 370\ \text{Hz} \qquad (2.19)$$

The van't Hoff plot for the two weighted *D* values (D_+ and D_-) and the constant *D* values (D_0) is shown in Figure **2.12**. The log-fit thermodynamic parameters are listed in Table **2.16**. In all cases, ΔC_p is large and negative, while $\Delta S°_{298}$ is large and positive; however, $\Delta H°_{298}$ ranges from favorable (D_+, -2.28 kcal/mol) to unfavorable (D_-, +4.13 kcal/mol), whereas $\Delta G°_{298}$ is basically unchanged. If *D* is some function of temperature, this result casts serious doubt upon conclusions we might draw with respect to $\Delta H°$ or $\Delta S°$ contributions to the binding force.

Nevertheless, we are convinced that the only meaningful comparisons for VT binding data demand an assumption of constant *D* values. For every guest subjected to ^1H NMR VT binding studies in aqueous media, a survey of the free chemical shifts as a function of temperature was undertaken. The free shifts were nearly temperature-invariant: the largest shift changes observed per 10° were *less than 1.5 Hz*. Recall that *D* is the difference between the bound- and free-guest shifts. Because (1) the bound shift corresponds to the guest in the host-guest complex, (2) we can develop no argument for a change in host-guest structure with temperature, and (3) free guest shifts are temperature invariant, we conclude that *D* values do not change *significantly* as a function of temperature, and we will therefore continue to employ the constant-*D*-value assumption.

Keep in mind that there are errors inherent to both the single-point and complete VT binding studies. The single-point analysis depends upon

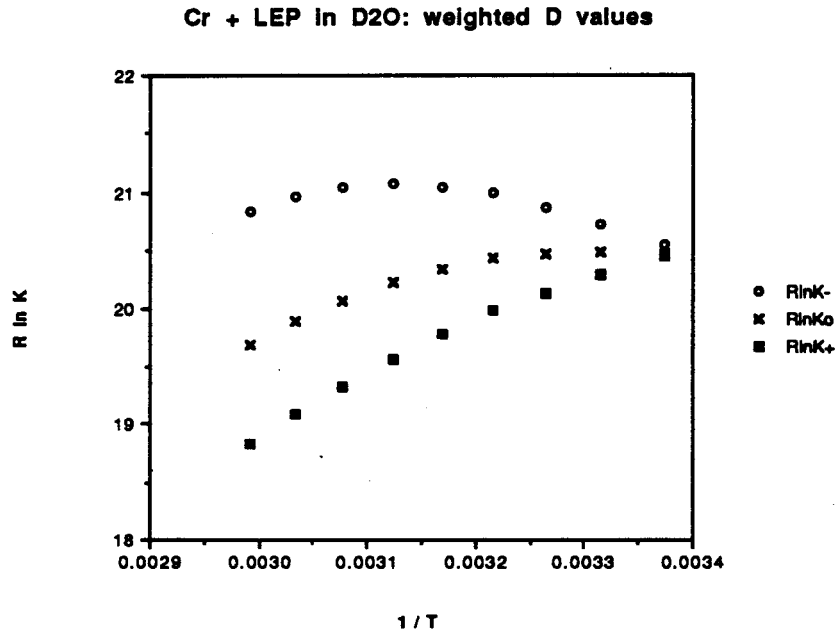

Figure 2.12. Log fits (Eqn. 2.12) for single-point VT binding study with weighted *D* values for host **2** and guest **42** in borate-*d*.

Table 2.16: Comparison of thermodynamic parameters for *D* values[a] weighted as a function of temperature from single-point VT binding study for guest **42** and host **2** in borate-*d*.

weight	ΔC_p (cal/mol-K)	$\Delta H°_{298}$ (kcal/mol)	$\Delta S°_{298}$ (cal/mol-K)	$\Delta G°_{298}$ (kcal/mol)
D.	-191	+4.13	34.5	-6.13
$\mathbf{D_o}$	-159	+0.72	22.9	-6.10
$\mathbf{D_+}$	-112	-2.28	12.8	-6.08

[a]*D* values for CH_3 of guest **42**; [b]See text for description of weighting procedures.

"correct" D values, and even for very tightly bound guests, correct D values do not always suffice for VT log-fit analysis (negative K_as are sometimes obtained). As noted above, MULTIFIT, which calculates significantly different D values as a function of temperature, may not adequately handle complete VT binding data.

Comparison of hosts 1 and 2

Log-fit thermodynamic parameters for guests **9**, **10**, **11**, and **42** with structurally-related hosts **1** and **2** (see Chapter 1) have been determined (Table **2.17**). Unfortunately, the parameters for onium guests **10** and **11** do not yield to straightforward evaluation.

However, the values for $\Delta H°$ and $\Delta S°$ at room temperature for guest **42** with host **1** parallel those values for other electron-deficient guests (**3** and **6**, vide supra). These parameters have been defined above in terms of an enthalpically favorable/entropically unfavorable donor/acceptor interaction with a non-classical hydrophobic effect. In contrast, the large, favorable $\Delta S°$ and near-zero $\Delta H°$ for guest **42** with host **2** indicate almost exclusively *classic* hydrophobic binding, with little hint of donor/acceptor interactions.

We are further confounded when guest **9** is included. Gratifyingly, host **1** displays a much less favorable enthalpic contribution, as one would expect if donor/acceptor interactions are poor between the electron-rich host and electron-rich guest. Also, entropy is now favored, such that classic hydrophobic binding may be invoked (**9** is much less water-soluble than **42**[3]). Surprisingly, with host **2**, the only significant difference between guests **42** and **9** is a slightly reduced $\Delta S°$, which indicates reduced hydrophobic binding: no distinction for donor/acceptor interactions with host **2** is evident!

Table 2.17: Thermodynamic parameters for complexation from single-point VT binding studies in aqueous media: comparison of guests with hosts **1** and **2** in borate-*d*.

guest	ΔC_p (cal/mol-K)	$\Delta H°_{298}$ (kcal/mol)	$\Delta S°_{298}$ (cal/mol-K)	$\Delta G°_{298}$ (kcal/mol)	*D* values[a] (Hz, proton)
host **1**					
10[b]	+32.0	-4.30	11.3	-7.67	N/A
11[b]	-27.9	-1.20	20.2	-7.24	N/A
9	-123	-1.58	8.11	-4.00	750 (N-C*H*$_3$)
42	-131	-9.79	-9.11	-7.08	450 (C*H*$_3$)
host **2**					
10	-86.7	-0.06	20.1	-6.05	530 (N-C*H*$_3$)
11	-7.5	-5.94	1.80	-6.47	180 (N-C*H*$_3$)
9	-123	+0.34	17.8	-4.97	650 (N-C*H*$_3$)
42	-188	+0.96	24.3	-6.27	350 (C*H*$_3$)

[a]For host **1**, reference 32; for host **2**, reference 15; [b]From complete VT binding studies with free energies scaled to values in reference 3.

In general, the thermodynamic parameters in Table **2.16** are consistent with **2** as the more hydrophobic host and **1** as the better donor/acceptor host. Unfortunately, some unresolved holes appear: this comparison is not consistent with an enthalpically-driven ion-dipole effect for the enhanced binding of guests **10** and **11** by host **1** versus **2**.

Conclusion

The variable temperature binding studies have revealed significant values for the heat capacities of complexation in organic and aqueous media. These ΔC_p values reflect the temperature-dependence of enthalpic and entropic contributions to binding.

Hydrophobic, donor/acceptor, and ion-dipole interactions are tentatively partitioned into $\Delta H°$ and $\Delta S°$ contributions *at 298K*. "Classic" hydrophobic binding is characterized by a large, positive $\Delta S°$ and a near-zero $\Delta H°$ term. Strong donor/acceptor π-stacking interactions are typically balanced between large, favorable enthalpic and unfavorable entropic contributions. The ion-dipole effect is primarily an enthalpically-driven binding force.

Experimental for Chapter 2

All variable-temperature (VT) ^1H NMR spectra were recorded on a JEOL JNM GX-400 spectrometer. Organic binding spectra were referenced to the residual proton signal of $CDCl_3$ (7.24ppm) at all temperatures. Aqueous binding spectra were referenced to internal 3,3-dimethylglutarate (DMG, 1.09ppm vs TSP) in borate-*d* at all temperatures.

Syntheses for hosts and guests are described (or referenced) elsewhere in this thesis. Following each binding study in organic media, tetraester host **27** was recovered with slight material loss after purifying via flash chromatography[51] on silica eluted with 3% ether/chloroform.

Guest stock solutions for the organic VT nmr binding experiments were prepared in volumetric flasks (2mL) with deuterochloroform. The concentrations of both host and guest were quantified separately via nmr integrations against a standardized solution of a carefully tared amount of adamantyltrimethylammonium iodide (**20**, ATMA) in $CDCl_3$ (2mL, 19.1mM). All volumetric measurements of organic solutions were made using Hamilton microliter syringes.

Host and guest stock solutions for the aqueous VT nmr binding experiments were prepared with a standard 10mM deuterated cesium borate buffer at pD~9 (borate-*d*).[4] The buffer was prepared as described in Chapter 1. The concentrations of the host and guest stock solutions were quantified via nmr integrations against a stock solution of DMG (4.20-4.23mM, vs potassium hydrogen phthalate, KHP) in borate-*d*. All volumetric measurements of aqueous solutions were made using adjustable volumetric pipets.

All pulse delays for the organic and aqueous stock solution integration experiments (15-20s) were at least 5 times the measured T_1 for the species involved.

The probe temperature was calibrated versus a methanol standard, using an equation[52] relating the difference in observed methanol peaks ($\Delta\nu$) versus temperature:

$$y = c + bx + ax^2 \qquad (2.20)$$

where
y = actual temperature, K
x = $\Delta\nu$ in Hz
a = -1.491×10^{-4}
b = -7.369×10^{-2}
c = 403.0

(x, a, b, and c for 400MHz spectrometer only). An example of this calibration is given in Table **2.18** and Figure **2.13**.

Volumes for $CDCl_3$ variable-temperature binding studies were corrected for thermal expansion of solvent according to:

$$v_t = v_0 (1 + \alpha t_0) \qquad (2.21)$$

where
v_t = volume at corrected probe temperature
v_0 = volume of solution at temperature t_0
t_0 = corrected probe temperature (°C)
α = coefficient of thermal expansion
= 0.00126 $cm^3/°$ for $CHCl_3$.[53]

Volumes for borate-*d* variable-temperature binding studies were corrected for density changes from a plot of densities of H_2O (10-65°C)[53] versus temperature, which fit a quadratic equation:

$$y = a + bx + cx^2 \qquad (2.22)$$

where

y = density at corrected temperature (°C)

x = corrected temperature (°C)

a = 1.0011

b = -6.7589×10^{-5}

c = -3.8471×10^{-6}.

Table 2.18: Temperature calibration of nmr probe using the methanol standard.

Probe reading (°C)	Δν for methanol (Hz)	Actual temperature[a] (K)
-40.6	845.483	234.1
-30.3	814.718	244.0
-20.4	782.030	254.2
-10.2	747.969	264.5
-0.3	713.908	274.4
9.6	679.023	284.2
19.6	643.589	293.8

[a]Calculated according to Eqn. 2.20.

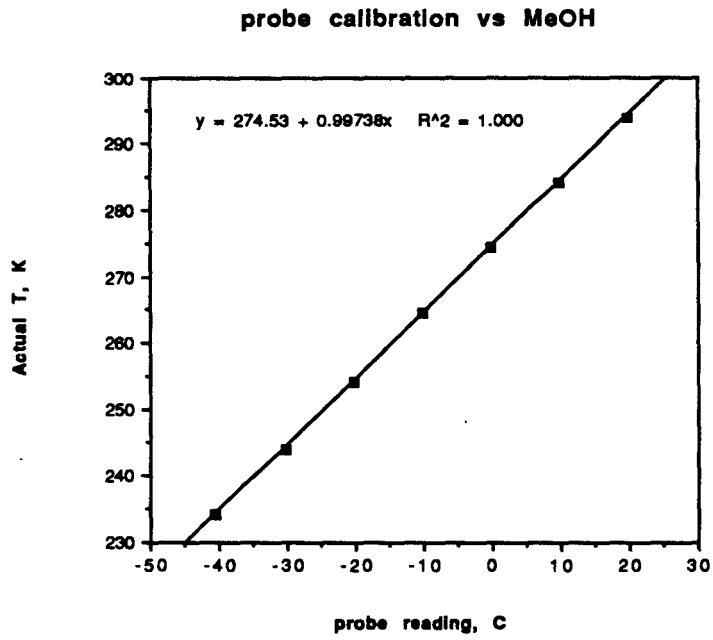

Figure 2.13. "Dedicated ^{1}H-only" nmr probe temperature calibration versus methanol.

References to Chapter 2

(1) Frühbeis, H.; Klein, R.; Wallmeier, H. *Angew. Chem. Int. Ed. Engl.* **1987**, *26*, 403-418.

(2) Wong, C. F.; McCammon, J. A. *J. Am. Chem. Soc.* **1986**, *108*, 3830-3832; Singh, U. C.; Brown, F. K.; Bash, P. A.; Kollman, P. A. *J. Am. Chem. Soc.* **1987**, *109*, 1607-1614.

(3) Shepodd, T. J.; Petti, M. A.; Dougherty, D. A. *J. Am. Chem. Soc.* **1988**, *110*, 1983-1985.

(4) Petti, M. A.; Shepodd, T. J.; Barrans, R. E., Jr.; Dougherty, D. A. *J. Am. Chem. Soc.* **1988**, *110*, 6825-6840.

(5) Stauffer, D. A.; Dougherty, D. A. *Tetrahedron Lett.* **1988**, *29*, 6039-6042.

(6) Sturtevant, J. M., in *Bioenergetics and Thermodynamics: Model Systems*; Braibanti, A., Ed.; Reidel: Boston, 1980; pp 391-404.

(7) Atkins, P. W. *Physical Chemistry*; Freeman: San Francisco, 1978; pp 75-101.

(8) (a) Everett, D. H.; Wynne-Jones, W. F. K. *Trans. Faraday Soc.* **1939**, *35*, 1380-1401; (b) Clarke, E. C. W.; Glew, D. N. *Trans. Faraday Soc.* **1966**, *62*, 539-547.

(9) (a) Ives, D. J. G.; Marsden, P. D. *J. Chem. Soc.* **1965**, 649-676; (b) Feates, F. S.; Ives, D. J. G. *J. Chem. Soc.* **1956**, 2798-2812.

(10) Sturtevant, J. M. *Proc. Natl. Acad. Sci. USA* **1977**, *74*, 2236-2240.

(11) Alternatively, Eqn. 2.12 can be derived from the separate definitions of ΔH (Eqn. 2.7) and ΔS (Eqn. 2.20) with ΔC_p:

$$\frac{1}{T}\,\Delta C_p = \left(\frac{\partial\,\Delta S}{\partial T}\right)_p \qquad (2.23)$$

Eqn. 2.7 gives $\Delta H(T) = \Delta H_o + \Delta C_p T$ (2.24)

Eqn. 2.23 gives $\Delta S(T) = \Delta S_o + \Delta C_p \ln T$ (2.25)

Combining Eqns. 2.24 and 2.25 leads to Eqn. 2.12.

(12) Hearn, R. P.; Richards, F. M.; Sturtevant, J. M.; Watt, G. D. *Biochemistry* **1971**, *10*, 806-817.

(13) Tanford, C. *The Hydrophobic Effect*, 2nd ed.; Wiley: New York, 1980.

(14) (a) Harrison, J. C.; Eftink, M. R. *Biopolymers* **1982**, *21*, 1153-1166; (b) Cromwell, W. C.; Byström, K.; Eftink, M. R. *J. Phys. Chem.* **1985**, *89*, 326-332; (c) Gelb, R. I.; Schwartz, L. M.; Laufer, D. A. *J. Chem. Soc. Perkin Trans 2* **1984**, 15-21.

(15) Petti, M. A. Ph. D. Thesis, California Institute of Technology, 1988.

(16) Jencks, W. P. *Catalysis in Chemistry and Enzymology*; McGraw-Hill: New York, 1969.

(17) Mirejovsky, D.; Arnett, E. M. *J. Am. Chem. Soc.* **1983**, *105*, 1111-1117.

(18) (a) Sturtevant, J. M., in *Bioenergetics and Thermodynamics: Model Systems*; Braibanti, A., Ed.; Reidel: Boston, 1980; pp 391-404; (b) Takahashi, K.; Casey, J. L.; Sturtevant, J. M. *Biochemistry* **1981**, *20*, 4693-4697.

(19) These authors reported linear van't Hoff plots over a narrow (35-40°) temperature-range: Ferguson, S. B.; Seward, E. M.; Diederich, F.; Sanford, E. M.; Chou, A.; Inocencio-Szweda, P.; Knobler, C. B. *J. Org. Chem.* **1988**, *53*, 5593-5595.

(20) Saenger, W. *Angew. Chem. Int. Ed. Engl.* **1980**, *19*, 344-362.

(21) Cram, D. J. *Angew. Chem. Int. Ed. Engl.* **1986**, *25*, 1039-1134; Cram, D. J.; Lam, P. Y.-S.; Ho, S. P. *J. Am. Chem. Soc.* **1986**, *106*, 839-841.

(22) Benzinger has discussed the importance of determining ΔCp to absolute zero: Benzinger, T. H. *Nature* **1971**, *229*, 100-102.

(23) (a) Arnett, E. M.; Campion, J. J. *J. Am. Chem. Soc.* **1970**, *92*, 7097-7101; (b) Arnett, E. M.; Kover, W. B.; Carter, J. V. *J. Am. Chem. Soc.* **1969**, *91*, 4028-4034; (c) Abraham, M. H. *J. Am. Chem. Soc.* **1982**, *104*, 2085-2094.

(24) (a) Niekamp, C. W.; Sturtevant, J. M.; Velick, S. F. *Biochemistry* **1977**, *16*, 436-445; (b) Breslauer, K. J.; Terrin, B.; Sturtevant, J. M. *J. Phys. Chem.* **1974**, *78*, 2363-2366; (c) Sturtevant, J. M.; Velicelebi, G. *Biochemistry* **1981**, *20*, 3091-3096.

(25) A single-point VT binding study for host **27** and guest **10** in d_6-DMSO suggested a small, negative ΔCp; however, because $-\Delta G°_{298}$ ~1kcal/mol, we cannot attribute binding to ΔH° or ΔS°.

(26) Both log and parabolic[27] fits were evaluated according to the significance-of-regression *F*-distribution: Snedecor, G. W. *Statistical Methods*; 5th ed.; Iowa State Univ. Press: Ames, Iowa, 1956.

(27) We initially used a parabolic fit: $y = c + bx + ax^2$, where $y = R\ln K_a$; $x = T^{-1}$; $\Delta C_p = 2aT^{-2}$.

(28) Lumry, R., in *Bioenergetics and Thermodynamics: Model Systems*; Braibanti, A., Ed.; Reidel: Boston, 1980; pp 435-454.

(29) Leffler, J. O. *J. Org. Chem.* **1955**, *20*, 1202-1231.

(30) (a) Cram, D. J.; Stewart, K. D.; Goldberg, I.; Trueblood, K. N. *J. Am. Chem. Soc.* **1985**, *107*, 2574-2575; (b) Diederich, F.; Dick, K.; Griebel, D. *J. Am. Chem. Soc.* **1986**, *108*, 2273-2286.

(31) Lowry, T. H.; Richardson, K. S. *Mechanism and Theory in Organic Chemistry*; 3rd ed.; Harper and Row: New York, 1987; pp 127-247.

(32) Shepodd, T. J. Ph. D. Thesis, California Institute of Technology, 1988.

(33) Wolfenden, R. *Science (Washington, D. C.)* **1983**, *222*, 1087-1093.

(34) Hinz, H.-J.; Shiao, D. D. F.; Sturtevant, J. M. *Biochemistry* **1973**, *14*, 2780.

(35) Schmid, F.; Hinz, H.-J.; Jaenicke, R. *Biochemistry* **1976**, *15*, 3052-3059.

(36) Hinz, H.-J.; Wever, K.; Flossdorf, J.; Kula, M. R. *Eur. J. Biochem.* **1976**, *71*, 427-433.

(37) Lavaille, F.; Rogard, M.; Alfsen, A. *Biochemistry* **1974**, *13*, 2231-2234.

(38) Privalov, P. L. *FEBS Lett.* **1974**, *40*, 5140-5153.

(39) Privalov, P. L.; Khechinashivili, N. N. *J. Mol. Biol.* **1974**, *86*, 665-684.

(40) Pfeil, W.; Privalov, P. L. *Biophys. Chem.* **1976**, *4*, 41-50.

(41) Privalov, P. L.; Khechinashivili, N. N.; Atanasov, B. P. *Biopolymers* **1971**, *10*, 1865-1890.

(42) Tsung, T. Y.; Hearn, R. P.; Wrathall, D. P. Sturtevant, J. M. *Biochemistry* **1970**, *9*, 2666-2677.

(43) Privalov, P. L.; Filimonov, V. V.; Venkstern, T. V.; Bayer, A. A. *J. Mol. Biol.* **1975**, *97*, 279-288.

(44) Gurney, R. W. *Ionic Processes in Solution*; McGraw-Hill: New York, 1953.

(45) Shepodd, T. J.; Petti, M. A.; Dougherty, D. A. *J. Am. Chem. Soc.* **1986**, *108*, 6085-6087.

(46) For aqueous VT binding data, volume corrections for temperature changes did not change significantly the log-fit parameters.

(47) The magnitude of the chemical shift changes with temperature in some cases suggests that comparison to earlier work by Petti[15] and Shepodd[32] (where ambient temperature was unrecorded) may not be meaningful; all recent (and future) "room-temperature" binding studies have been (and should be) performed with the nmr VTON (probe setting 25°C).

(48) In unpublished work, Barrans is attempting to statistically evaluate and simulate errors in our binding studies.

(49) Deranleau, D. A. *J. Am. Chem. Soc.* **1969**, *91*, 4044-4049; Deranleau, D. A. *J. Am. Chem. Soc.* **1969**, *91*, 4050-4054.

(50) Log-fit parameters for single-point VT binding data for host **1** and guest **20** with D=1250Hz ($N(CH_3)_3$) are: ΔC_p -61.8cal/mol-K; $\Delta H°_{298}$ -1.18 kcal/mol; $\Delta S°_{298}$ +15.2cal/mol-K; $\Delta G°_{298}$ -5.71kcal/mol.

(51) Still, W. C.; Kahn, M.; Mitra, A. *J. Org. Chem.* **1978**, *43*, 2923-2925.

(52) Gordon, A. J.; Ford, R. A. *The Chemist's Companion*; Wiley: New York, 1972; p 303.

(53) Riddick, J. A.; Bunger, W. B. *Organic Solvents*; 3rd ed.; Wiley: New York, 1970.

Chapter 3

Ion-Dipole Effect as a Force for Biomimetic Catalysis in Aqueous Media

Introduction

Mechanisms of enzymatic catalysis continue to receive considerable attention from enzymologists and bioorganic and biophysical chemists. Several proposals have been advanced to account for the extraordinary rate acceleration imparted by enzymes upon their substrates.[1] Among these proposals, two are especially pertinent to the present work: proximity (or propinquity) effects[2] and transition-state stabilization.[3] The idea of proximity has been derived from a comparison of intra- versus intermolecular reactivity of small molecules in solution.[4,5] The extension to biological macromolecules has been suggested wherein an enzyme can lock its substrate in a reactive conformation in the vicinity of its catalytic groups. Transition-state stabilization was introduced to explain the same results: enzymes preferentially bind transition states[3] versus ground states *or intermediates*. The design of transition-state analogs[6] as inhibitors[7] of enzyme-catalyzed reactions attests to this description of the problem. However, while the various concepts make sense intuitively, it remains extremely difficult experimentally to confirm that any one explanation encompasses the nature of enzymatic reactivity.

The continued success of catalytic antibodies[8] and other semisynthetic enzymes[9] demonstrates the ability of scientists to re-engineer catalysts borrowed from nature. Because of the structural complexity involved, this relatively new enzymology has focused more upon discovering novel transformations and less upon mechanisms for the reactions.

Biomimetic chemistry[10] complements enzymology in that it attempts to extract the "essence" of enzyme structure and function, then reconstruct

it in simpler, structurally well-defined systems. The design and synthesis of "supramolecular"[11] catalysts for chemical transformations is represented by numerous examples. Many of these catalysts have been constructed with some degree of proximity in mind: well-characterized binding sites have been functionalized with appropriately directed catalytic groups to create active sites for biomimetic reactions. Cyclodextrins, primarily through the studies of Breslow and co-workers, have been modified according to this concept to serve as mimics for acyl-transferases,[12] esterases,[13] thiamine-dependent enzymes,[14] ribonucleases,[15] metal-assisted peptidases,[16] and other enzymes. Similarly, synthetic receptors have been functionalized with catalytic moieties for acyl-transfer reactions,[17] ester hydrolyses,[11] and acyloin condensations.[18] In all of the above examples, substrates were designed to bind in orientations that placed their reacting groups in proximity to catalytic groups on the receptors.

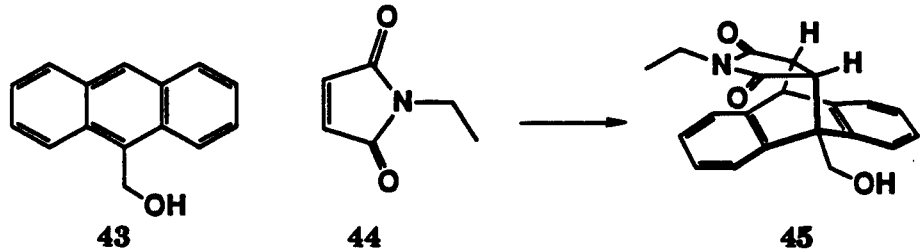

43 44 45

There are fewer examples in molecular recognition of rate accelerations due to a binding event alone. Diels-Alder reactions (*eg* between **43** and **44**) have been found to proceed faster in water than in organic solvents because of hydrophobic effects.[19] By providing a more favorable solvation environment than water, cyclodextrins accelerated (only

modestly) such reactions.[20] The rate of the intramolecular Diels-Alder reaction of **46** to give **47** also was enhanced by cyclodextrins.[21] Apparently, the dithiane unit of **46** was bound in the cyclodextrin cavity, forcing the two reactive groups (diene and dienophile) together. In this case, it was not established whether the transition state was stabilized relative to substrate and product. (Our own efforts to use binding in a synthetic receptor to direct reactive moieties in proximity to one another in intramolecular Diels-Alder reactions analogous to the Sternbach work are described in Appendix 1.)

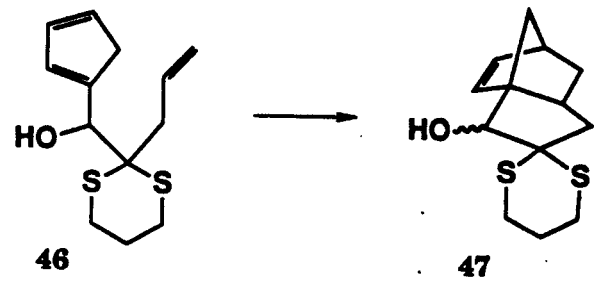

With respect to transition-state stabilization, Rebek has reported the transition-metal-catalyzed racemization of **48**.[22] Normally unfavorable steric interactions were overcome when the bipyridyl moiety became planar to optimize coordination to the metal: the achiral metal complex is the transition state for racemization.

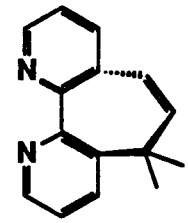

48

Chapters 1 and 2 of this thesis established the ion-dipole effect as a force for molecular recognition in organic and aqueous media.[23-25] Electron-rich synthetic macrocyclic hosts complex positively charged guests such as **10**, **11**, and **20** more strongly than neutral guests **3** and **6**. Host **1** has a general affinity for tetraalkylammonium and alkylpyridinium compounds. The detailed binding studies of these guests were a necessary prelude to catalysis studies.

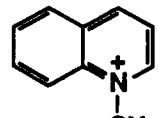

10

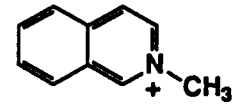

11

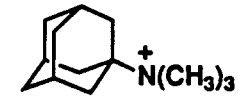

20

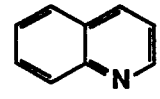

3

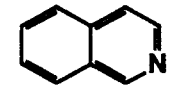

6

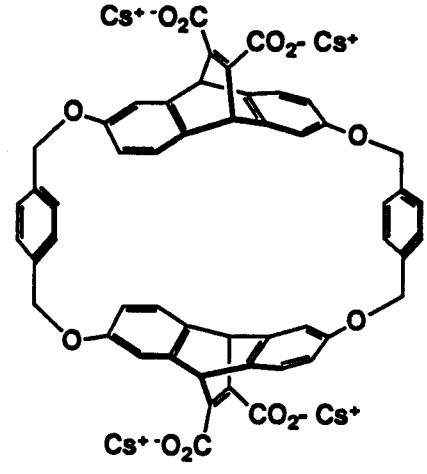

1

Since host **1** shows a strong affinity for the positive charge of an onium compound, it was anticipated that **1** could produce a special stabilization for a developing charge in a reaction transition state. Thus,

for example, one would expect that the rate of the alkylation of quinoline (**3**) with R-X to afford an alkylquinolinium salt (**49**) should be accelerated in the presence of host **1**. We describe herein a class of methylation reactions with host **1** that demonstrate the ion-dipole effect to be a force for biomimetic catalysis in aqueous media. Most significantly, we find that host **1** stabilizes transition states in preference to substrates or products.

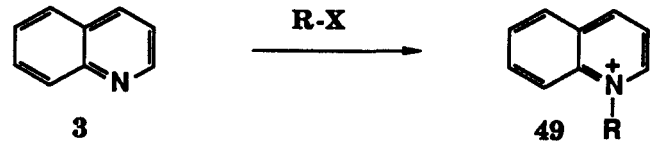

To understand precisely what is meant by transition-state stabilization, consider the reaction-coordinate diagram depicted in Figure **3.1**, which shows the free energy relationships between substrate, transition state, and product of uncatalyzed and catalyzed reactions. This diagram represents a single mechanistic step in a reaction scheme, although, of course, it can be extended to multistep processes. In an enzymatic reaction, it is often impossible to determine the affinities for *both* substrate and product (much less for the transition state) with accuracy: one usually reports the observed rate constant ($k_{obs}=k_{cat}/K_m$) in terms of the rate constant for the catalyzed reaction (k_{cat}) and the dissociation constant for enzyme-substrate complex (Michaelis constant, K_m).[26] Figure **3.1** suggests that the binding affinity of an "enzyme" for the transition state ($\Delta G°_T$) can be obtained:

$$\Delta G°_T = \Delta G°_S + \Delta G^{\ddagger}_{un} - \Delta G^{\ddagger}_{cat} \qquad (3.1)$$

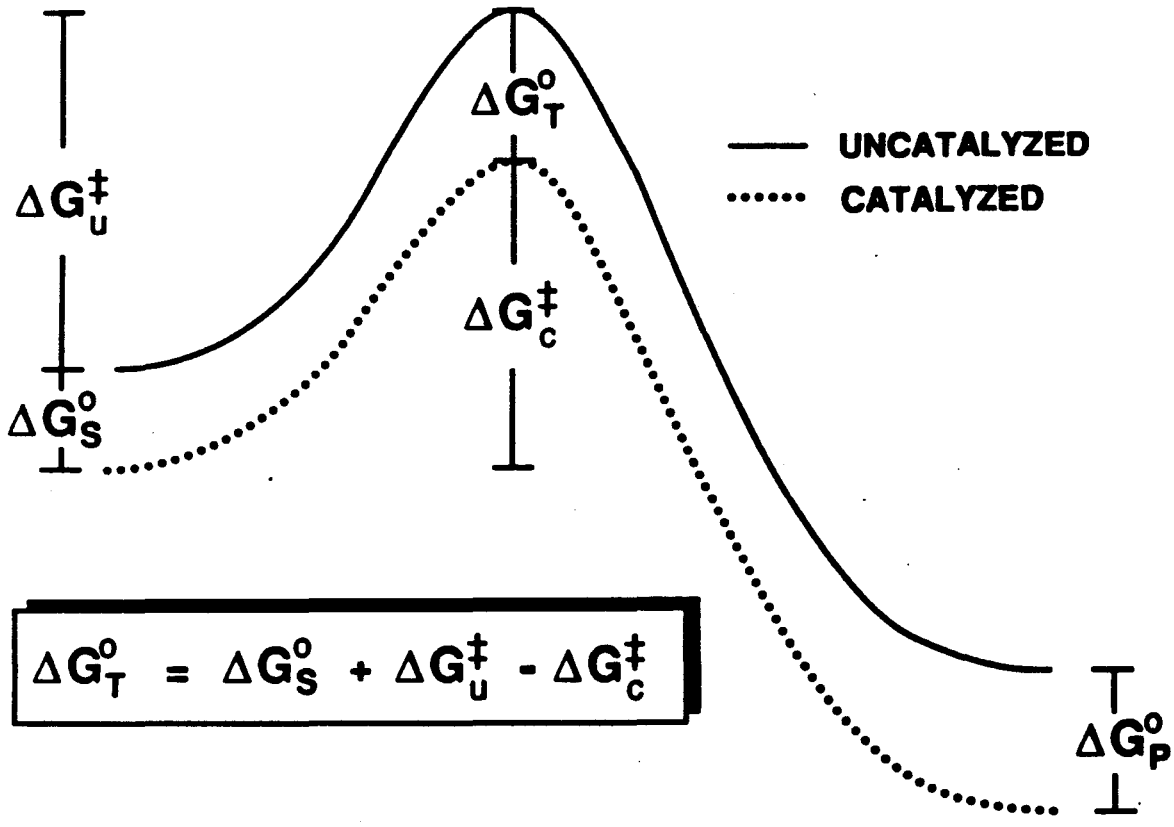

Figure 3.1. Reaction-coordinate diagram for uncatalyzed and catalyzed reactions: relationship between free energies of complexation and activation.

$$\Delta\Delta G^{\ddagger}_{for} = \Delta G^{\ddagger}_{un} - \Delta G^{\ddagger}_{cat} \qquad (3.2)$$

where ΔG°_{S} = free energy of complexation for substrate

$\Delta G^{\ddagger}_{un}$ = activation energy for uncatalyzed reaction

$\Delta G^{\ddagger}_{cat}$ = activation energy for catalyzed reaction

$\Delta\Delta G^{\ddagger}_{for}$ = difference in $\Delta G^{\ddagger}$ for forward reaction

With respect to transition-state stabilization, if the product is bound more tightly than the substrate, all that is required to discern whether the transition state (T) is stabilized preferentially to the ground states (S/P) is the ratio of rate constants versus binding constants:

$$\frac{k_{cat}}{k_{un}} > \frac{K_P}{K_S} \qquad (3.3)$$

where k_{cat} and k_{un} are the rate constants for catalyzed and uncatalyzed reactions, respectively; K_P and K_S are association constants for product and substrate ($K_P > K_S$) with enzyme/host, respectively.

The specific reaction of a methyl halide with a pyridine-type nucleophile is called a Menschutkin reaction.[27] It has been clearly established that the Menschutkin reaction proceeds by an S_N2 mechanism.[28] Consequently, the transformation of substrate to product occurs in a single step, and therefore it comes under the jurisdiction of the reaction-coordinate diagram in Figure **3.1**. In the present work, we have focused upon the Menschutkin reactions of substrates **3** and **6** with iodomethane to give products **10** and **11**, respectively. In this context, we

shall discuss sequentially the design of the kinetics experiments; rates for the uncatalyzed reactions; rates for the host-catalyzed reactions; other selected examples of biomimetic catalysis; and attempts to dealkylate products.

Design of kinetics experiments

Several factors guided the choice of alkylating reagents in the present work. To meaningfully apply the data from our aqueous binding studies to the kinetics analysis for the host-catalyzed reactions, the reagent should be soluble in the pD~9 cesium borate buffer (borate-*d*) in which the earlier studies were done. The reagent should be sufficiently reactive with pyridine-type nucleophiles at a convenient rate at (or slightly above) ambient temperatures. Additionally, the reagent should be sufficiently *unreactive* with nucleophiles in the buffer ([DO^-] ~10μM in borate-*d*), such that pseudo-first-order kinetics (with excess alkylating reagent) for the disappearance of substrates can be followed.

Among the alkylating reagents considered, only iodomethane (MeI) most nearly fulfilled the criteria listed above. MeI is ca. 90mM-soluble in borate-*d*;[29] it reacts slowly with deuteroxide in the buffer (k_2~2×10^{-5} s^{-1} M^{-1} at 300K); it reacts at an adequate rate with isoquinoline (**3**) at 25°C (half-life on the order of several hours). Perhaps the most satisfying aspect is the fact that products **10** and **11** were synthesized (for binding studies) as their iodide salts from MeI and substrates **3** and **6**, respectively.

Other reagents examined for host-catalyzed alkylation reactions were not as satisfactory as MeI. Alkyl halides and water-soluble, putative methyl-group donors were considered. Iodoethane (for **14** from **3**) was roughly an order of magnitude less soluble than MeI in borate-*d*, and not

sufficiently reactive in the uncatalyzed reaction; butyl iodide (for **15** from **3**) was minimally soluble in borate-*d*; benzyl bromide (for **16** from **3**) was too reactive with deuteroxide in the buffer to permit quantitative pseudo-first-order kinetics, although evidence of host-catalyzed benzylation was indicated (vide infra). Of the water-soluble reagents, trimethylsulfonium iodide (**26**) and methyl sulfate (**50**) did not react with **3**, **6**, or deuteroxide.

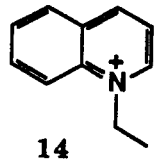

14

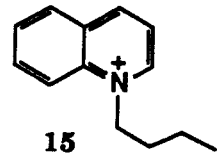

15

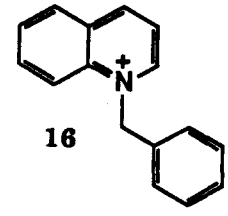

16

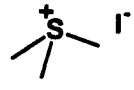

26

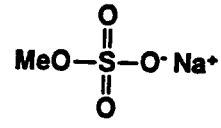

50

Subsequent to the choice of alkylating agent, we set out to determine a method for following the alkylation kinetics. It was crucial that we report concentrations for substrate (S), product (P), alkylating reagent (A), and host (H, where appropriate) as a function of time. Ultraviolet spectroscopy was quickly eliminated from consideration, as the distinction between substrates, products, and host was insufficient (Figure **3.2**). High-performance liquid chromatography separated all components of the reaction mixture, but could not report their concentrations reproducibly. Therefore, we turned again to ^{1}H NMR (400MHz) spectroscopy, which had been employed to characterize S, P, H, HS, and HP species.

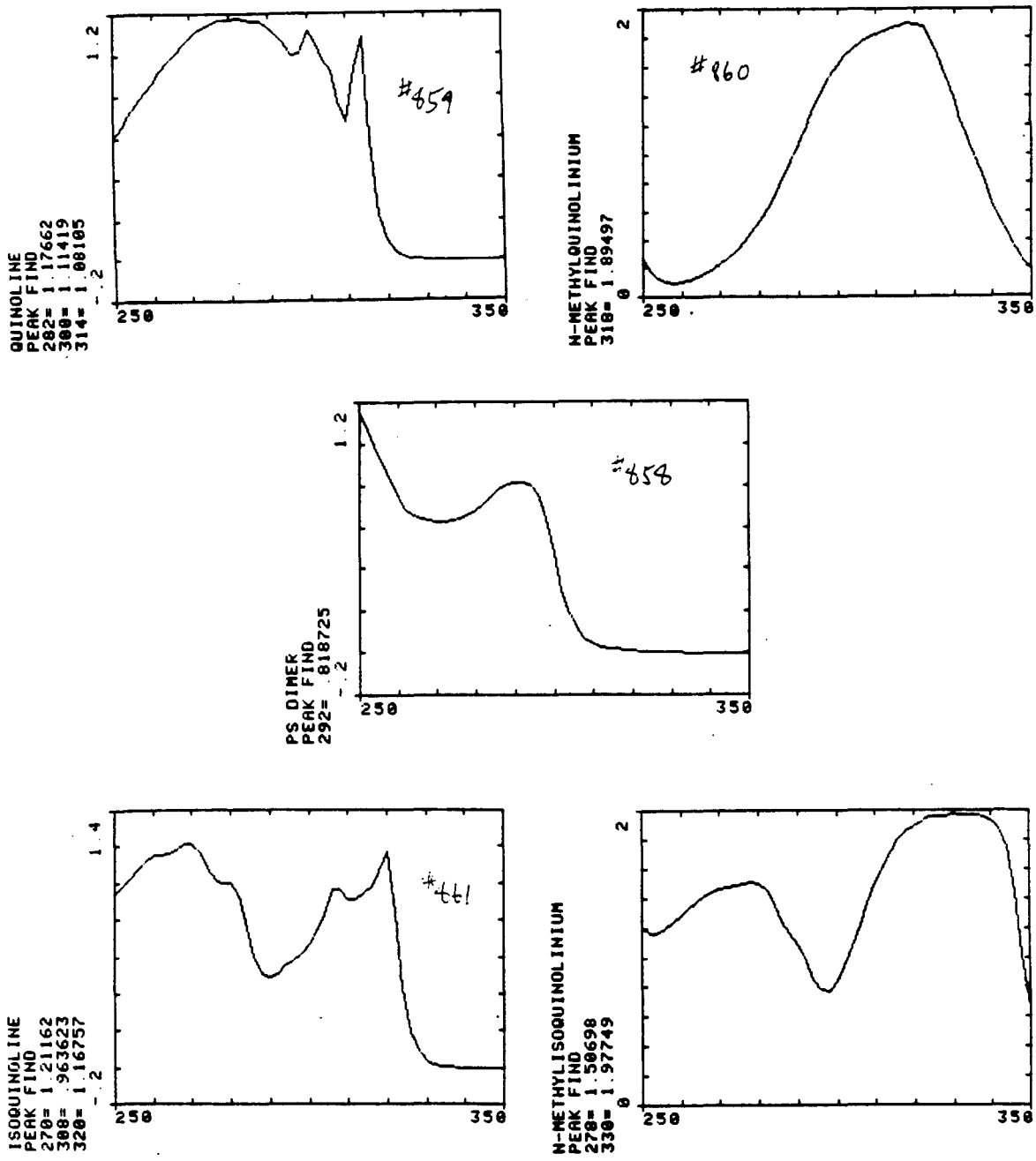

Figure 3.2. UV-VIS spectra. Top left: guest **3** in borate-*d*, [**3**] = 361μM; top right: guest **10** in borate-*d*, [**10**] = 332μM; middle: host **1** in borate-*d*, [**1**] = 72.7μM; bottom left: guest **6** in borate-*d*, [**6**] = 455μM; bottom right: guest **11** in borate-*d*, [**11**] = 960μM.

The limiting factor for obtaining pseudo-first-order kinetics was maintaining a constant concentration of excess MeI. Because of the volatility of MeI (bp 40°C), an airtight, sealed reaction vessel was mandatory. Thus, specially designed reaction "vessels" were constructed from regular nmr tubes and sealable screw-cap vials. These vessels were used for all rate determinations in the present work: time-dependent total concentrations of S, P, H, and A were adequately measured (25-55°C) by nmr spectroscopic integration versus an internal standard of 3,3-dimethylglutarate (DMG). For further details of the kinetics experiments, see Experimental.

Uncatalyzed alkylation reactions

For the uncatalyzed alkylation reactions, pseudo-first-order kinetics (over two half-lives) were determined for isoquinoline (**6**) plus MeI at 40°, 45°, 50°, and 55°C:

$$S \xrightarrow{k_{un}[A]} P \qquad (3.4)$$

$$\frac{d[P]}{dt} = -\frac{d[S]}{dt} = k_{un}[S][A] \qquad (3.5)$$

$$= k_{obs}[S] \qquad (3.6)$$

$$\ln \frac{[S]_t}{[S]_o} = -k_{obs} \cdot t \qquad (3.7)$$

or

$$\ln (\%S) = -k_{obs} \cdot t \qquad (3.8)$$

where we monitor the disappearance of substrate (S) as a function of time (t); %S is the fraction of S at time=t versus S at time=0. Plotting ln (%S) vs t

gives the pseudo-first-order rate constant (slope=$-k_{obs}$). The second-order rate constant is readily obtained ($k_{un}=k_{obs}/[A]$). In this case, [A] is the *average* concentration of MeI *in solution at the probe temperature* during the time we monitor the reaction.

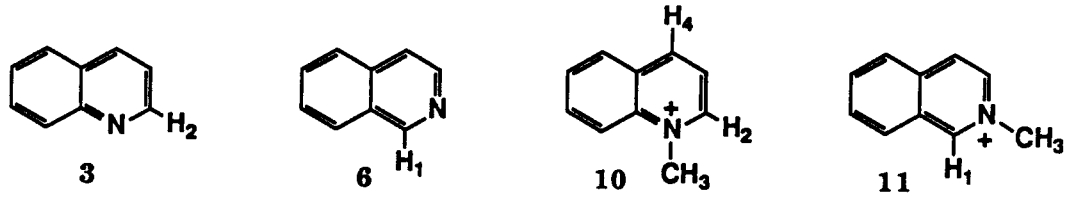

Because 10μM-deuteroxide reacts with MeI faster than does quinoline (**3**), and peaks for **3**, **6**, **10**, and **11** can be resolved by nmr spectroscopy, uncatalyzed rates for substrates (**3**/**6**) were measured simultaneously. The relative amounts of substrate and product in each spectra (time increments of 26-27min) were measured by nmr integration. The following protons were used for the respective compounds: **3**, H_2; **6**, H_1; **10**, H_2 and H_4; **11**, H_1. The amount of each product, $[P]_t$, was determined according to:

$$[P]_t = ([S]_o + [P]_o)\left(\frac{\chi P}{\chi P + \chi S}\right) \qquad (3.9)$$

where χS and χP are the integral areas, and $[S]_o$ and $[P]_o$ are the starting concentrations, for S and P, respectively. Figure **3.3** plots the pseudo-first-order dependence for the disappearance of **3** and **6** with MeI at 45°C.

The second-order rate constants determined at different

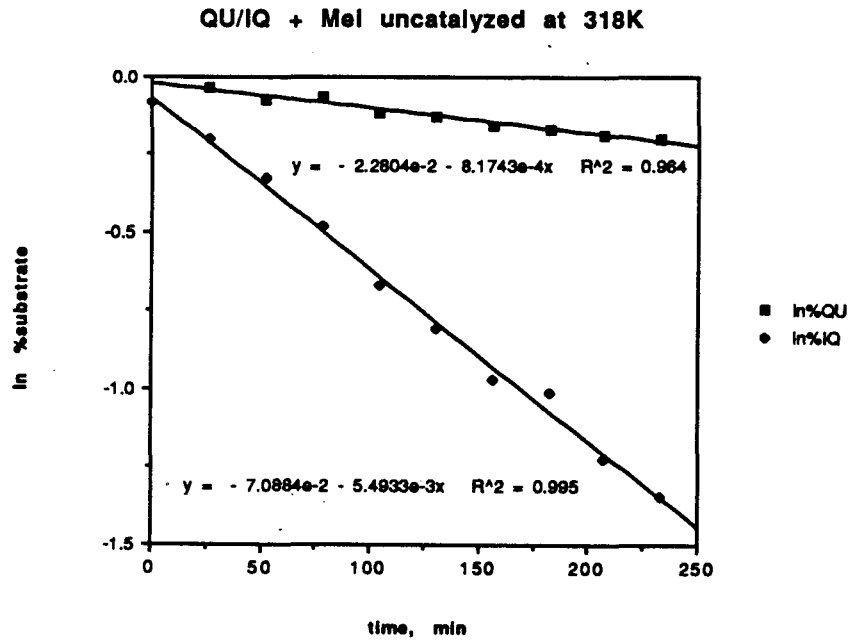

Figure 3.3. Pseudo-first-order kinetics for the disappearance of substrates quinoline (**3**) and isoquinoline (**6**) in uncatalyzed alkylation reactions; calculated second-order rate constants: k_2 (**3**) = 2.55 x $10^{-4}s^{-1}M^{-1}$; k_2 (**6**) = 1.72 x $10^{-3}s^{-1}M^{-1}$.

temperatures (Table **3.1**) were evaluated according to Eqn. 3.11 from Eyring transition-state theory to obtain activation parameters:[30]

$$k = \frac{\kappa \cdot k_B}{h} \cdot T \cdot \exp\left(\frac{-\Delta H^{\ddagger}}{RT}\right) \exp\left(\frac{\Delta S^{\ddagger}}{R}\right) \quad (3.10)$$

$$R \ln Y = (-\Delta H^{\ddagger})\left(\frac{1}{T}\right) + \Delta S^{\ddagger} \quad (3.11)$$

where

$$Y = \frac{k \cdot h}{\kappa \cdot k_B \cdot T} \quad (3.12)$$

k = pseudo-first-order rate constant, s^{-1}

κ = transmission coefficient (assumed κ=1)

k_B = Boltzmann's constant (1.381×10^{-23} J/K)

h = Planck's constant (6.626×10^{-34} J-sec)

T = absolute temperature, K

R = universal gas constant (8.314 J/mol-K)

and where $\Delta H^{\ddagger}$ and $\Delta S^{\ddagger}$ are the enthalpy and entropy of activation, respectively. The Eyring plots (RlnY vs T^{-1}) for **3** (Figure **3.4**) and **6** (Figure **3.5**) provide the activation parameters reported in Table **3.2**, along with values for these Menschutkin reactions in benzene and chloroform.[31] The reaction with **3** is about a factor of 7 slower than **6** independent of solvent. The lower reactivity of **3** has been attributed to the unfavorable steric interaction between the peri-hydrogen (H_8) and incoming electrophiles.[32]

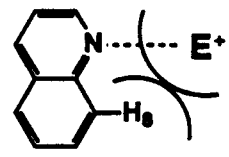

Table 3.1: Uncatalyzed alkylation reactions of **3** and **6**: second-order rate constants for pseudo-first-order reactions with excess MeI versus temperature.

	probe setting (°C)	actual temperature (K)	k_2 (s^{-1} M^{-1})
quinoline (**3**)	35	310.1	7.87×10^{-5}
	40	315.0	1.47×10^{-4}
	45	320.0	2.55×10^{-4}
	50	324.9	4.50×10^{-4}
	55	329.8	7.30×10^{-4}
isoquinoline (**6**)	30	305.3	3.38×10^{-4}
	35	310.1	5.48×10^{-4}
	40	315.0	9.87×10^{-4}
	45	320.0	1.72×10^{-3}
	50	324.9	2.71×10^{-3}
	55	329.8	4.33×10^{-3}

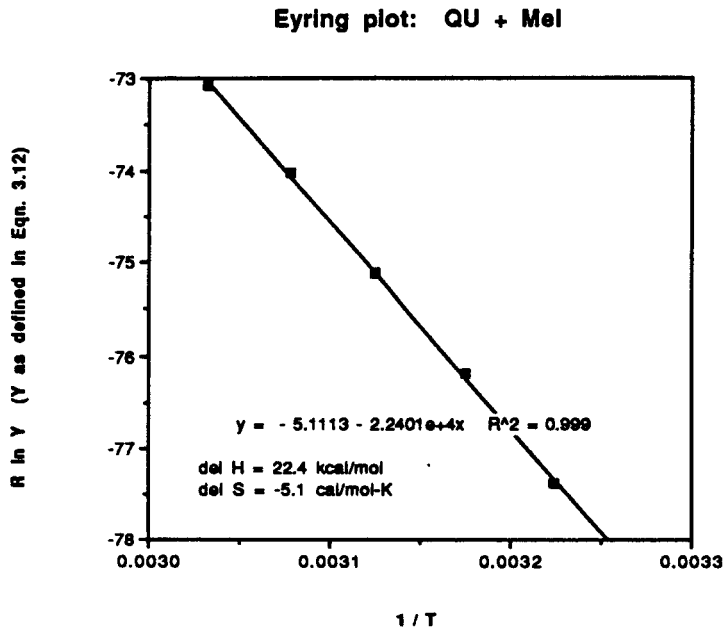

Figure 3.4. Eyring plot for second-order rate constants from Table 3.1 for uncatalyzed alkylation reaction of 3 with excess MeI in borate-*d*.

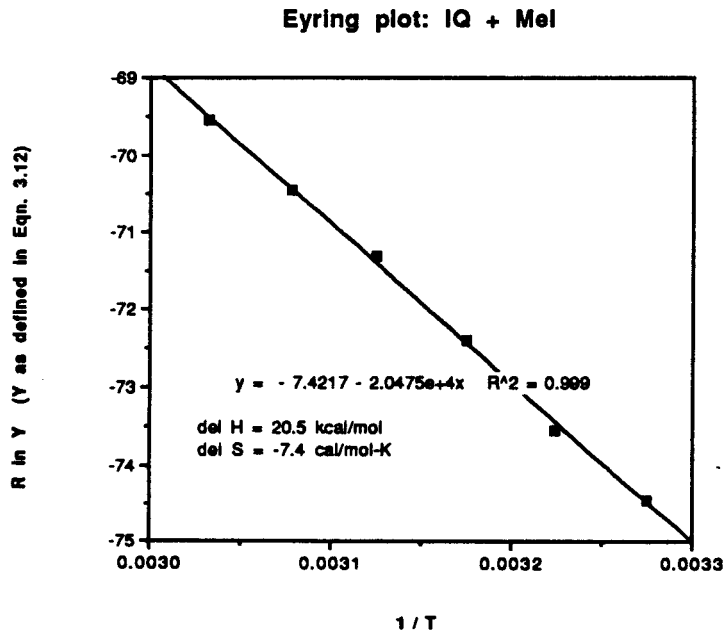

Figure 3.5. Eyring plot for second-order rate constants from Table 3.1 for uncatalyzed alkylation reaction of **6** with excess MeI in borate-*d*.

Table 3.2: Activation parameters for Menschutkin reactions in different solvents: **3** and **6** with MeI.

quinoline (**3**)

solvent	$\Delta G^{\ddagger}_{298}$ (kcal/mol)	$\Delta H^{\ddagger}$ (kcal/mol)	$\Delta S^{\ddagger}$ (cal/mol-K)
C_6H_6[a]	24.8	11.9	-43.2
$CHCl_3$[a]	24.4	13.8	-35.4
D_2O (pD~9)	23.9	22.4	-5.1

isoquinoline (**6**)

solvent	$\Delta G^{\ddagger}_{298}$ (kcal/mol)	$\Delta H^{\ddagger}$ (kcal/mol)	$\Delta S^{\ddagger}$ (cal/mol-K)
C_6H_6[a]	23.8	13.4	-34.9
$CHCl_3$[a]	23.3	13.9	-31.5
D_2O (pD~9)	22.7	20.5	-7.4

[a]Reference 31.

These parameters illustrate two important points regarding the host-accelerated alkylations. First, the room-temperature rates ($\Delta G^{\ddagger}_{298}$) are comparable as a function of solvent. However, the relatively large $\Delta H^{\ddagger}$ term in water (versus organic solvents) is offset by a much smaller, less unfavorable $\Delta S^{\ddagger}$ term. (S_N2 reactions typically display large, negative entropies of activation, which reflect the order required to bring two reacting species together in the transition state.[33]) As alluded to in Chapter 2, the Menschutkin reaction is just one of many reaction classes that exhibit this kind of compensation of enthalpy and entropy contributions to the activation free energy.[34] (The temperature dependence of activation parameters $\Delta H^{\ddagger}$ and $\Delta S^{\ddagger}$ has not been addressed.) Second, the reaction in aqueous media is faster ($\Delta G^{\ddagger}$) than in organic solvents, which is crucial from the standpoint of the host-catalyzed reactions described below: the rate acceleration in the presence of host cannot be attributed to what is often considered a more favorable "organic" (hydrophobic) environment provided by the host.[35]

The activation parameters for **3** and **6** with MeI in borate-*d* were necessary to calculate uncatalyzed rate constants (Eqn. 3.10) for the determination of catalyzed rate constants in the host-accelerated reactions at lower temperatures.

Host-catalyzed alkylation reactions

For the host-catalyzed alkylation reactions, we must consider Figure **3.1** and Eqn. 3.1. The rates for the uncatalyzed reaction provided $\Delta G^{\ddagger}_{un}$. The binding studies (Chapter 2) provided ΔG°_{S}. All that remain are values for $\Delta G^{\ddagger}_{cat}$, which can be obtained from a determination of the catalyzed rates. The kinetics scheme used in the analysis of the host-catalyzed

alkylation reactions is shown in Figure **3.6**. (We have found no evidence for the reversibility of alkylation under the reaction conditions; see below the section on attempted dealkylations.) The catalyzed step involves the bimolecular reaction between host-substrate complex (HS) and alkylating reagent (A):

$$\mathrm{HS} \xrightarrow{k_{cat}\,[A]} \mathrm{HP} \tag{3.13}$$

$$\frac{d[HP]}{dt} = -\frac{d[HS]}{dt} = k_{cat}\,[HS]\,[A] \tag{3.14}$$

$$[HS] = K_S\,[H][S] \tag{3.15}$$

$$-\frac{d[HS]}{dt} = k_{cat} \cdot K_S\,[H][S][A] \tag{3.16}$$

Combining Eqns. 3.5 and 3.16:

$$-\left(\frac{d[S]}{dt} + \frac{d[HS]}{dt}\right) = (k_{un} + k_{cat} \cdot K_S\,[H])\,[S][A] \tag{3.17}$$

$$[S]_{total} = [S] + [HS] \tag{3.18}$$

Because the total concentration of substrate ($[S]_{total}$) and the concentrations of the individual substrate species ([S], [HS]) change during the course of the reaction, the solution to Eqn. 3.17 is complex and must be solved analytically. Additionally, because the product of the alkylation reaction also is bound by the host, product inhibition (as the reaction proceeds) must be evaluated. Barrans has written a QuickBasic program (Kinetics

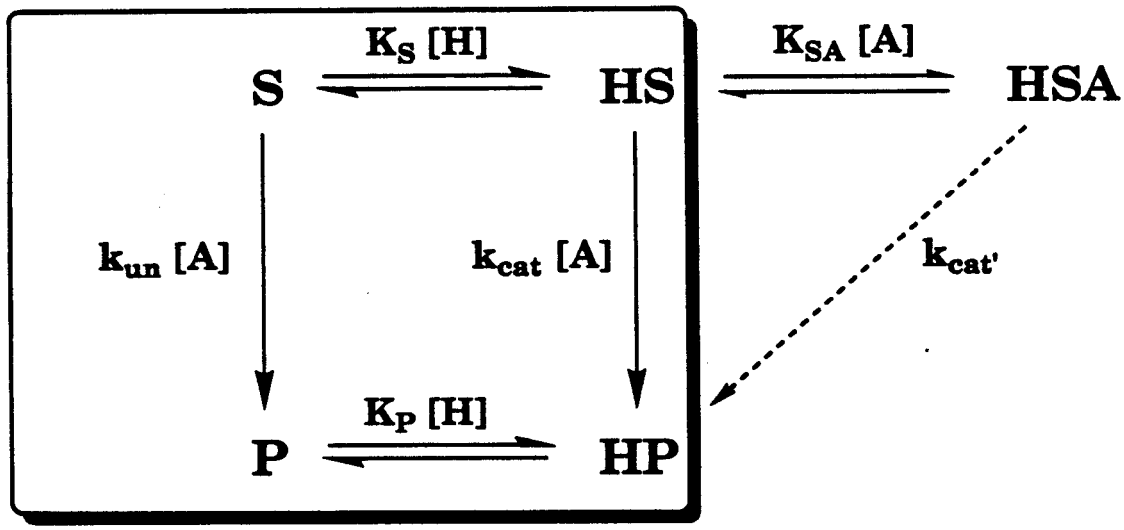

Figure 3.6. Kinetics scheme for determining k_{cat} in host-catalyzed alkylation reactions.

Simulator) to help determine k_{cat} given the following input parameters *specific for the reaction temperature*:

(1) K_S, association constant for host/substrate (M^{-1})

(2) K_P, association constant for host/product (M^{-1})

(3) k_{un}, uncatalyzed rate constant (s^{-1} M^{-1})

(4) $[A]_t$, concentration of alkylating agent (M)

(5) $[H]_t$, concentration of host (M)

(6) $[S]_o$, starting concentration of substrate (M)

(7) $[P]_o$, starting concentration of product (M)

The reaction temperature was maintained in the nmr probe throughout the course of the reaction. Values for K_S and K_P were calculated from the thermodynamics parameters in Chapter 2 according to Eqn 2.12. As noted earlier, k_{un} was calculated from the activation parameters and Eqn 3.9. The Experimental section details how $[A]_t$, $[H]_t$, $[S]_o$, and $[P]_o$ were determined. The relative amounts of substrate (S + HS) and product (P + HP) species were determined as described for the uncatalyzed reactions (Eqn. 3.9), using the following protons: **3**, H_2 and **10**, N-CH_3; or **6**, H_1, **11**, N-CH_3. The integration data for **3/10** and **6/11** at 25°C are reported in Tables **3.3** and **3.4**, respectively. Because the hosts have different affinities (and *D* values, see Chapter 2) for substrates and products, the chemical shifts of these species can change dramatically during the course of the reaction to reflect the percents of S and P bound by H (Figure **3.7**). As a result, in several experiments, the N-CH_3 peak for each product moved through regions of other peaks.

The simulation program, which is coupled to a plotting program, uses these seven values and a user-chosen k_{cat} to calculate the concentration of product as a function of time. The simulated curve is then

Table 3.3: Data reduction for the host **1**-catalyzed alkylation reaction of **3** with MeI at 25°C.[a]

elapsed time (min)	**3** (H_2) integration[b]	**10** (N-CH_3) integration[b]	calculated fraction **10**	[**10**] (M)[c]
0	3.189	0.446	0.045	0.0000097
27	3.666	1.365	0.110	0.0000240
54	2.815	1.726	0.170	0.0000368
80	3.818	1.791	0.135	0.0000293
107	3.781	2.167	0.160	0.0000348
134	2.932	2.967	0.252	0.0000547
161	2.572	3.247	0.296	0.0000643
188	2.977	3.611	0.288	0.0000625
214	2.599	3.794	0.327	0.0000710
241	3.287	4.988	0.336	0.0000729
268	2.493	4.290	0.365	0.0000791
295	2.603	4.828	0.382	0.0000829
322	1.958	4.819	0.451	0.0000978
375	1.901	5.246	0.479	0.0001040
455	1.590	5.728	0.546	0.0001184
587	1.554	7.375	0.613	0.0001330
720	1.668	8.325	0.625	0.0001355
852	0.896	9.004	0.770	0.0001671

[a]Experimental data for kinetics simulation in Figure **3.8**; [b]Referenced to DMG (10.000) at 1.09ppm; [c]Based upon $[\mathbf{3}]_0 + [\mathbf{10}]_0 = 217\mu M$.

Table 3.4: Data reduction for the host **1**-catalyzed alkylation reaction of **6** with MeI at 25°C.[a]

elapsed time (min)	**6** (H_2) integration[b]	**11** (N-CH_3) integration[b]	calculated fraction **11**	[**11**] (M)[c]
0	25.467	3.733	0.047	0.0000635
26	25.144	9.252	0.109	0.0001490
53	22.172	10.354	0.135	0.0001837
79	21.452	12.490	0.163	0.0002217
105	21.308	15.464	0.195	0.0002657
131	19.517	15.425	0.209	0.0002844
157	21.265	19.734	0.236	0.0003222
182	19.665	20.494	0.258	0.0003517
208	18.622	20.633	0.270	0.0003679
234	18.151	21.745	0.285	0.0003893
260	17.850	23.871	0.308	0.0004206
286	16.500	25.025	0.336	0.0004580
312	17.282	27.851	0.349	0.0004767
364	15.318	29.266	0.389	0.0005307
442	14.713	32.506	0.424	0.0005785
546	13.285	39.384	0.497	0.0006779
651	13.025	41.862	0.517	0.0007055

[a]Experimental data for kinetics simulation in Figure **3.9**; [b]Referenced to DMG (10.000) at 1.09ppm; [c]Based upon $[\mathbf{6}]_o + [\mathbf{11}]_o = 1364\mu M$.

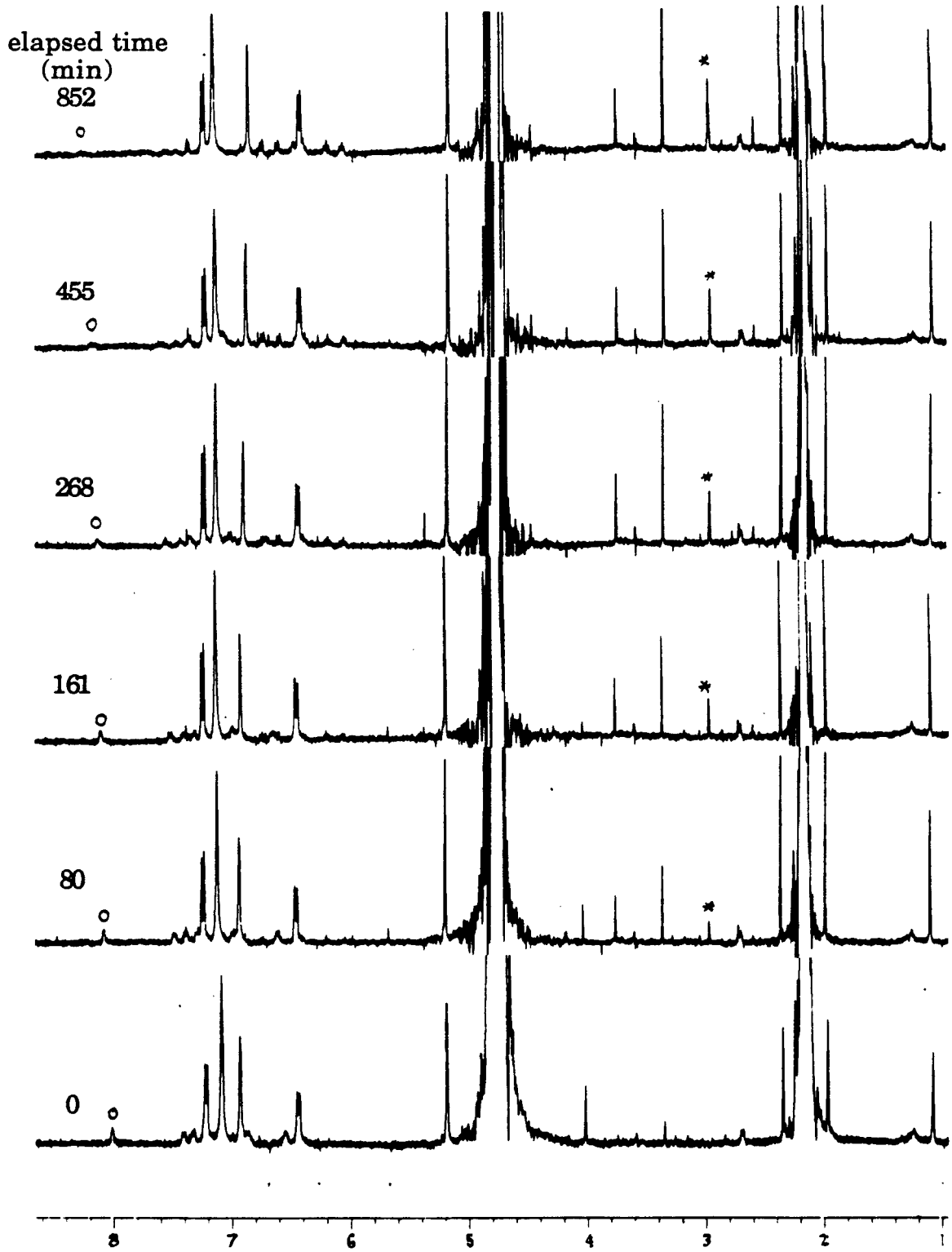

Figure 3.7. ^{1}H NMR spectra for the host **1**-catalyzed alkylation reaction of **3** with MeI at 25°C: time-evolution of catalysis with shifting of peaks for substrate, product, and host; H_2 of **3** (o); N-CH_3 of **10** (*).

compared to the experimental data, and the user can choose a new value for k_{cat} to iteratively minimize the rms deviation between the simulation and the experiment. The kinetics simulation for the host **1**-catalyzed alkylation of **3** with MeI at 25°C is plotted in Figure **3.8**; the simulation for **6** at 25°C is plotted in Figure **3.9**. In each case, most of the "effective" host catalysis occurs in the early part of the reaction. As product is formed, competitive inhibition decreases the amount of free host, such that $k_{un} \sim k_{cat}K_S[H]$. We have observed up to five turnovers for the host **1**-catalyzed reaction of **6** with MeI.[41] From Eqn. 3.1, the binding affinities of host **1** for transition states were calculated: $\Delta G°_T$ (**3/10**) = -8.1kcal/mol; $\Delta G°_T$ (**6/11**) = -7.8kcal/mol. In both cases, *transition states are bound more tightly than substrates or products* (Table **3.5**).

We wondered whether appreciable errors in any of the parameters used in the kinetics simulations could lead to $-\Delta G°_T$ less than $-\Delta G°_S$ or $-\Delta G°_P$. When changes were seperately introduced into each of the seven variables of Figure **3.9** for **6/11** at 25°C, $-\Delta G°_T$ remained larger than $-\Delta G°_P$ in all cases. Also, kinetics simulations for host-catalyzed alkylation reactions at other temperatures gave k_{cat}/k_{un} greater than K_P/K_S (Eqn. 3.3), further confirming that transition states are stabilized preferentially.

Figure **3.6** suggests the possibility of a ternary host-substrate-alkylating reagent (HSA) complex that could react to give HP:

$$\text{HSA} \xrightarrow{k_{cat'}} \text{HP} \qquad (3.19)$$

The addition of MeI to a solution of host and substrate led to decreased HS-binding as indicated by downfield shifting (reduced net upfield shifting) of substrate protons in the nmr. This result suggested that (1) a ternary HSA

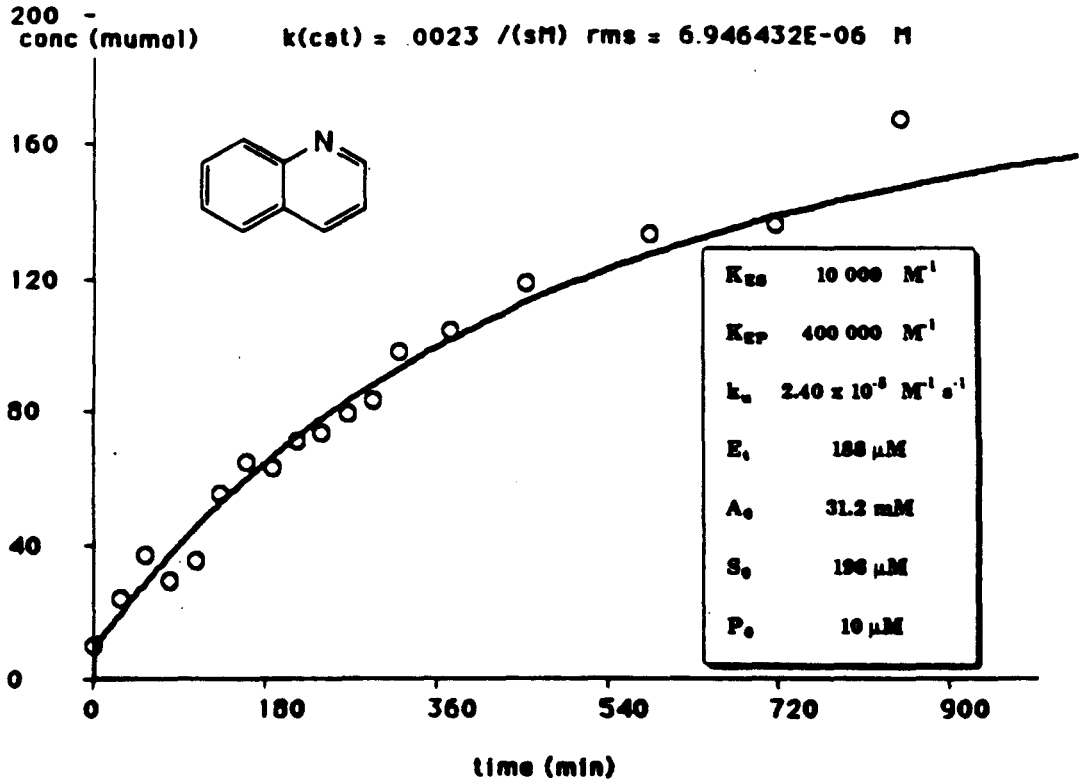

Figure 3.8. Kinetics simulation for the host **1**-catalyzed alkylation reaction of **3** with MeI at 25°C.

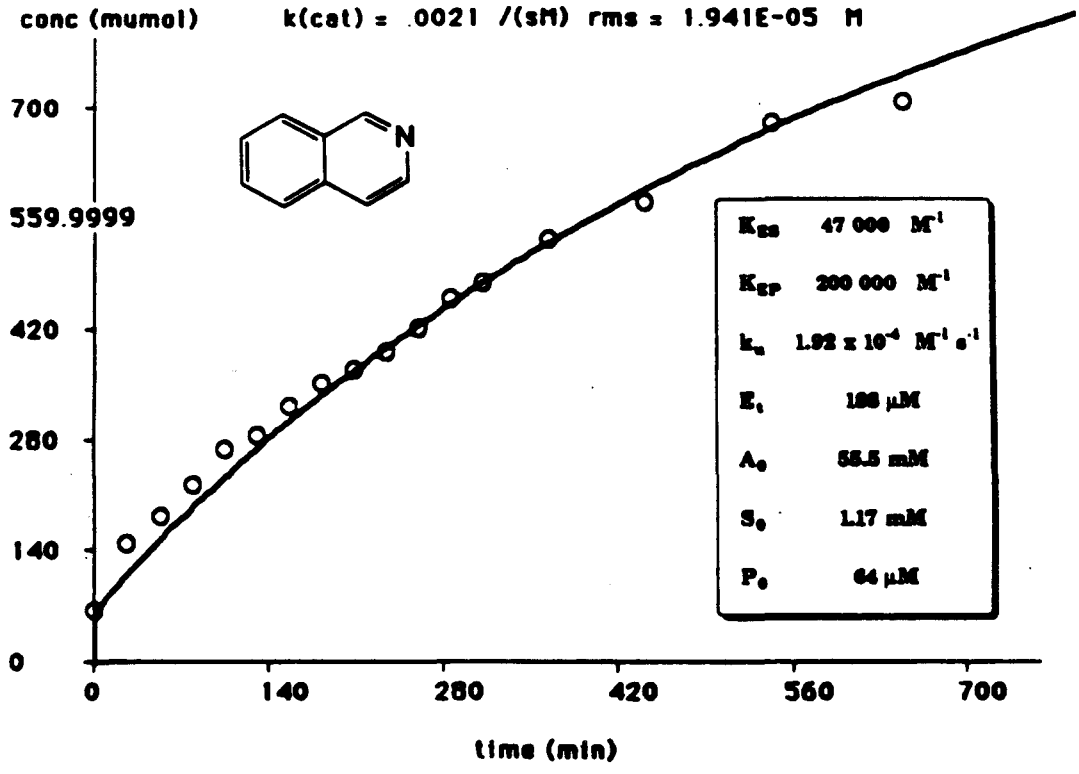

Figure 3.9. Kinetics simulation for the host **1**-catalyzed alkylation reaction of **6** with MeI at 25°C.

Table 3.5: Host-catalyzed reactions: binding affinities (kcal/mol) for host **1** with substrates, transition states, and products at all temperatures.

T (K)	$-\Delta G°_S$[a]	$-\Delta G°_T$	$-\Delta G°_P$[a]	$\Delta\Delta G^{\ddagger}_{for}$[b]	$\Delta\Delta G^{\ddagger}_{rev}$[c]
		quinoline (**3**)/quinolinium (**10**)			
300.3	5.50	8.22	7.70	2.72	0.52
300.3	5.50	7.92	7.70	2.42	0.22
305.3	5.55	8.42	7.76	2.87	0.66
310.1	5.58	8.22	7.82	2.64	0.40
315.0	5.60	8.52	7.88	2.92	0.64
320.0	5.60	8.46	7.95	2.86	0.51
324.9	5.58	8.40	8.01	2.82	0.39
329.8	5.54	8.89	8.09	3.35	0.80
		isoquinoline (**6**)/isoquinolinium (**11**)			
300.3	6.42	7.85	7.28	1.43	0.57
305.3	6.49	8.01	7.38	1.42	0.63
310.1	6.54	8.32	7.48	1.78	0.84
315.0	6.59	8.17	7.57	1.58	0.60
320.0	6.63	8.67	7.66	2.04	1.01

[a]See Chapter 2; [b]$\Delta\Delta G^{\ddagger}_{for} = |\Delta G°_S - \Delta G°_T|$; [c]$\Delta\Delta G^{\ddagger}_{rev} = |\Delta G°_P - \Delta G°_T|$.

complex formed in competition with HS; (2) MeI acted as a competitive inhibitor of HS to form HA; (3) added MeI (ca. 5% of the volume of aqueous buffer) changed the solvent medium sufficiently to reduce the hydrophobicity, leading to a net decrease in HS-complexation; or (4) some combination of points 1-3. Consistent with points 2 and 3, the addition of MeI to a solution of host and product led to decreased HP-binding, as indicated by downfield shifting of product peaks, similar to HS above. As negative evidence for a binary host-alkylating reagent complex (point 2), the proton chemical shift of MeI (ca. 50μM) was unaffected by host **1** (200μM). Attempts to detect a ternary HSA complex were unsuccessful: addition of minute quantities of MeI in borate-*d* (ca. 10μM) to a host-substrate solution led to rapid formation of product, presumably via host catalysis. However, if we consider the rate equation for the formation of HP from the as-yet-uncharacterized HSA:

$$\frac{d[HP]}{dt} = -\frac{d[HSA]}{dt} = k_{cat}'\,[HSA] \qquad (3.20)$$

$$[HSA] = K_3\,[HS]\,[A] \qquad (3.21)$$

$$= K_3 \cdot K_S\,[H][S][A] \qquad (3.22)$$

$$-\frac{d[HSA]}{dt} = k_{cat}' \cdot K_3 \cdot K_S\,[H][S][A] \qquad (3.23)$$

Combining Eqns. 3.17 and 3.23:

$$-\left(\frac{d[S]}{dt} + \frac{d[HS]}{dt} + \frac{d[HSA]}{dt}\right) = \{k_{un} + (k_{cat} + k_{cat}' \cdot K_3)(K_S[H])\}[S][A] \qquad (3.24)$$

Without evidence (and a binding constant, K_3) for the ternary HSA complex, we find that it is impossible to distinguish the bimolecular reaction (HS +

A) from the unimolecular reaction (HSA) to give HP. Thus, HSA has not been included in our kinetics analysis. Most importantly, regardless of the order of the host-catalyzed reaction, our primary conclusion still holds: transition states are bound more tightly than ground states.

These host-catalyzed alkylation reactions have been performed over a range of temperatures in an effort to obtain activation parameters for the catalyzed reaction (Table **3.5**). The parameters for the kinetics simulations are reported in Tables **3.6** and **3.7**. The ion-dipole effect, which was anticipated to be the driving force for catalysis in these reactions, is enthalpically driven (Chapter 2). One would, therefore, expect the catalytic source to be enthalpic as well. Eyring plots for the two alkylation reactions (Figures **3.10** and **3.11**) described above suggest preliminarily (and most surprisingly) that catalysis is *entropically* driven.[42]

We wondered whether the apparently reduced affinities of host **1** for substrates and products under the influence of excess MeI could account for the poorly fit Eyring plots. The magnitudes of the reduced upfield shifts described above suggested that MeI acted as a competitive inhibitor with an apparent association constant, K_A~30-50M^{-1}. Therefore, the Kinetics Simulator was modified by Barrans to include a user-chosen value for K_A. The modified values for k_{cat} are summarized in Table **3.8**: there were only slight increases for the **6/11** reactions; in contrast, significant increases were calculated for the **3/10** reaction, which can be attributed to the lower K_S for **3** with host **1** relative to **6**. Comparative Eyring plots for the data in Table **3.8** are shown in Figures **3.12** and **3.13**. In each case, fits are not substantially improved, and are clearly worsened for the **3/10** reaction.

Figure **3.14** is our working model for the host-catalyzed methylation reaction of **3** with MeI. This model is a simple S_N2 mechanism in which

Table 3.6: Parameters for kinetics simulations of host **1**-catalyzed reaction of **3** with excess MeI.

temp (K)	K_S[a] (M^{-1})	K_P[a,b] (M^{-1})	k_{un}[c] (s^{-1} M^{-1})	$[H]_t$ (μM)	$[A]_t$ (mM)	$[S]_o$ (μM)	$[P]_o$ (μM)	k_{cat}[d] (s^{-1} M^{-1})	rms fit (x 10^{-6})
300.3	9995	399941	2.402 x 10^{-5}	188	31.2	186.3	9.7	0.0023	6.95
300.3	9995	399941	2.402 x 10^{-5}	215	63.78	754.	30.4	0.0014	15.4
305.3	9366	356706	4.46 x 10^{-5}	188	62.68	367.7	24.3	0.0051	15.3
310.1	8566	321973	7.922 x 10^{-5}	188	50.02	909.1	71.	0.0058	32.8
315.0	7643	292660	1.355 x 10^{-4}	188	48.2	241.2	52.6	0.0143	13.3
320.0	6664	267322	2.52 x 10^{-4}	188	45.18	959.	21.1	0.0226	42.9
324.9	5646	245772	4.50 x 10^{-4}	188	40.79	277.5	115.3	0.036	7.77
329.8	4716	227692	7.355 x 10^{-4}	188	44.8	764.7	238.2	0.123	27.5

[a]Affinities at different temperatures obtained as described in Chapter 2; [b]Scaled to reported values (Chapter 2); [c]From $\Delta H^{\ddagger}$ and $\Delta S^{\ddagger}$ and Eqn. 3.10; [d]From best fit of simulated curve to experimental data.

Table 3.7: Parameters for kinetics simulations of host **1**-catalyzed reaction of **6** with excess MeI.

temp (K)	K_S[a] (M^{-1})	K_P[a,b] (M^{-1})	k_{un}[c] (s^{-1} M^{-1})	$[H]_t$ (μM)	$[A]_t$ (mM)	$[S]_o$ (μM)	$[P]_o$ (μM)	k_{cat}[d] (s^{-1} M^{-1})	rms fit ($\times 10^{-6}$)
300.3	46942	199903	1.916×10^{-4}	188	55.48	1300	63.5	0.0021	19.4
305.3	43976	192675	3.334×10^{-4}	188	48.48	549.4	63.6	0.0041	19.7
310.1	40704	185520	5.486×10^{-4}	188	58.06	1134	93.1	0.0097	21.6
315.0	37175	178235	9.87×10^{-4}	143	44.71	1177	49.7	0.0122	29.7
320.0	33456	170733	1.518×10^{-3}	188	50.14	1033	193.5	0.038	18.4

[a]Affinities at different temperatures obtained as described in Chapter 2; [b]Scaled to reported values (Chapter 2); [c]From $\Delta H^{\ddagger}$ and $\Delta S^{\ddagger}$ and Eqn. 3.10; [d]From best fit of simulated curve to experimental data.

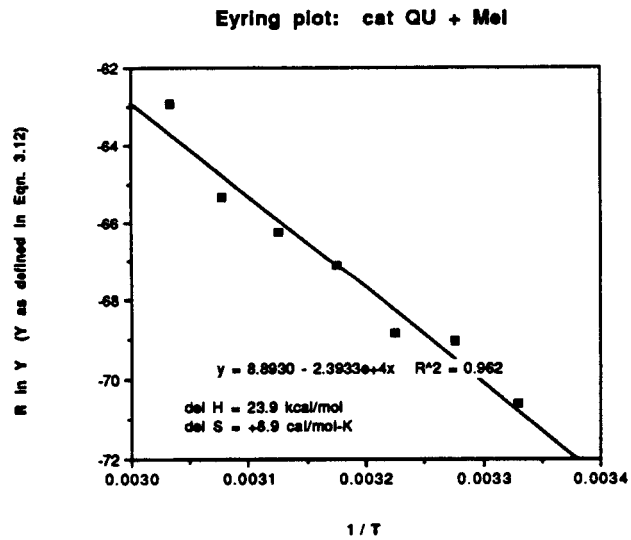

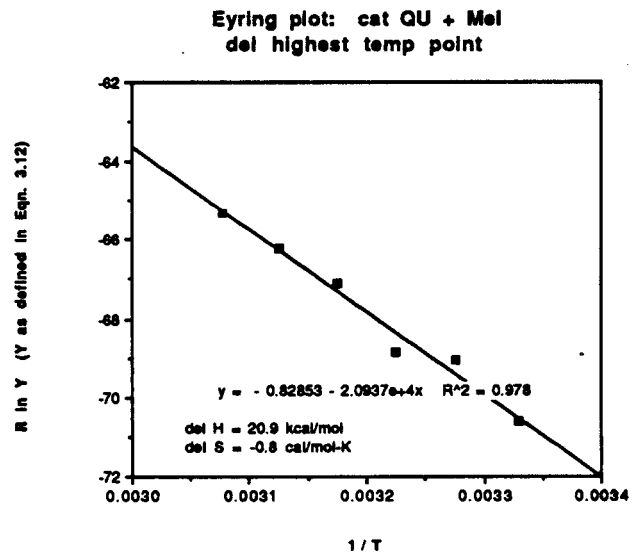

Figure 3.10. Eyring plot for second-order catalytic rate constants (k_{cat}) from kinetics simulations (Table **3.6**) for the host **1**-catalyzed alkylation reaction of **3** with MeI. **Top**: all data; **bottom**: deleted highest temperature point.

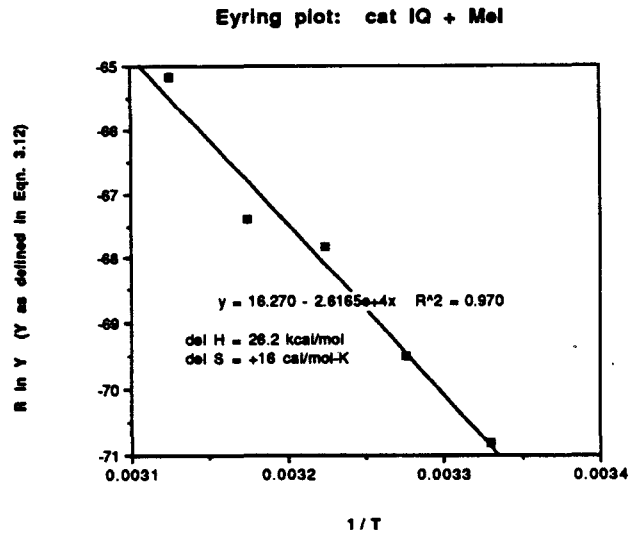

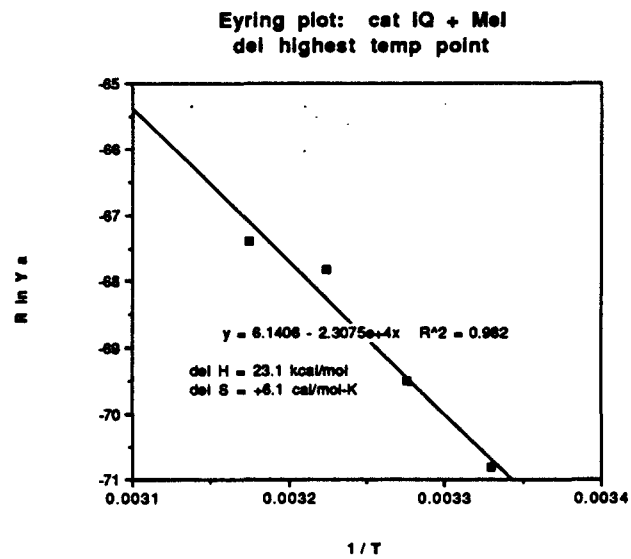

Figure 3.11. Eyring plot for second-order catalytic rate constants (k_{cat}) from kinetics simulations (Table 3.7) for the host **1**-catalyzed alkylation reaction of **6** with MeI. **Top**: all data; **bottom**: deleted highest temperature point.

Table 3.8: MeI as a competitive inhibitor of host-catalyzed alkylation reactions: k_{cat} at different temperatures as a function of K_A.

probe setting (°C)	K_A=1 (M^{-1})	K_A=30 (M^{-1})	K_A=50 (M^{-1})	$[MeI]_t$[a] (mM)
quinoline (**3**)				
25	0.0023	0.0031	0.0036	31.2
25	0.0014	0.0017	0.0019	63.78
30	0.0051	0.0069	0.0081	62.68
35	0.0058	0.0063	0.0067	50.02
40	0.0143	0.020	0.023	48.2
45	0.0226	0.024	0.025	45.18
50	0.036	0.043	0.047	40.79
55	0.123	0.128	0.131	44.8
isoquinoline (**6**)				
25	0.0021	0.0021	0.0022	55.48
30	0.0041	0.0043	0.0044	48.48
35	0.0097	0.0099	0.0100	58.06
40	0.0122	0.0124	0.0125	44.71
45	0.038	0.039	0.039	50.14

[a]From average integration versus DMG at 1.09ppm.

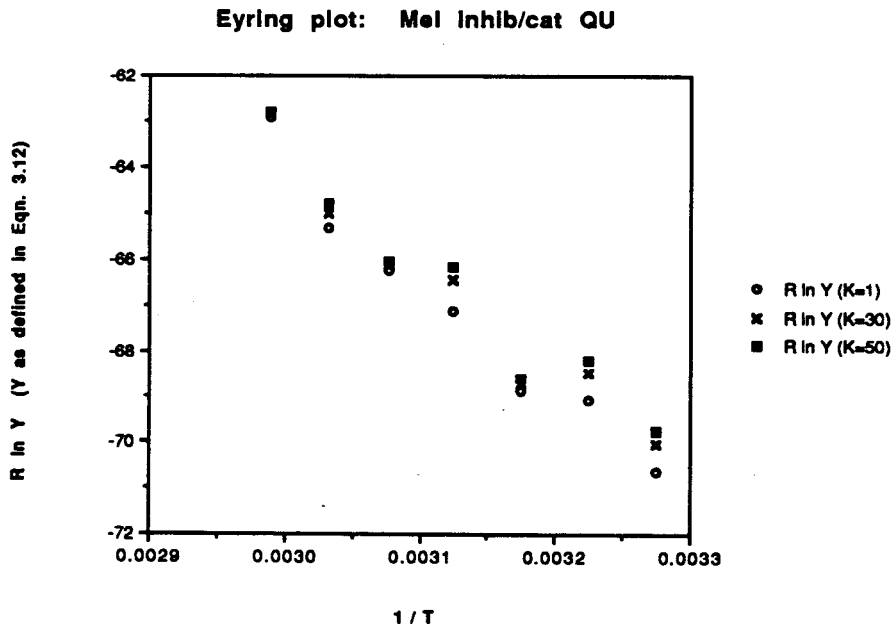

Figure 3.12. Comparative Eyring plots for apparent inhibition by MeI (Table 3.8) from modified kinetics simulations for the host **1**-catalyzed alkylation reaction of **3** with MeI.

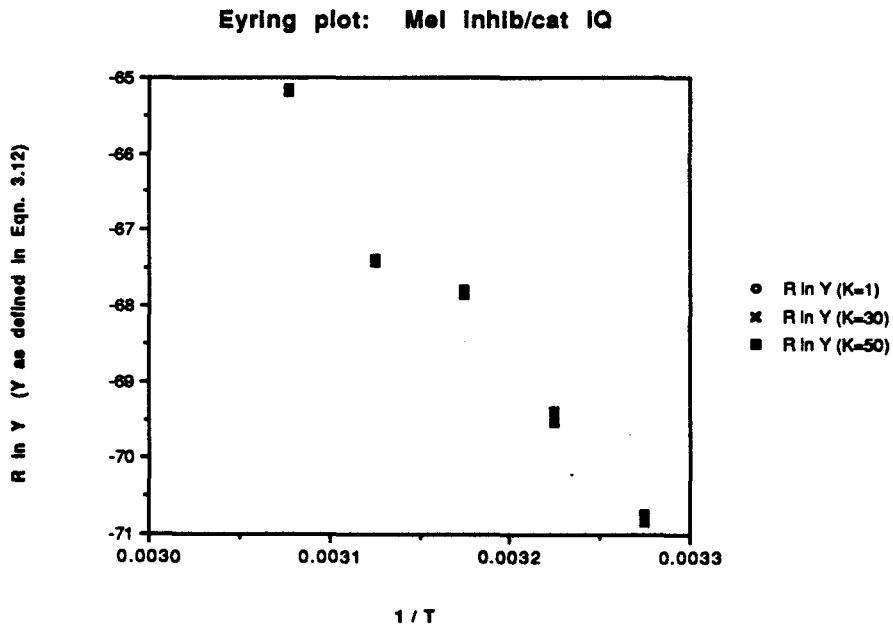

Figure 3.13. Comparative Eyring plots for apparent inhibition by MeI (Table 3.8) from modified kinetics simulations for the host **1**-catalyzed alkylation reaction of **6** with MeI.

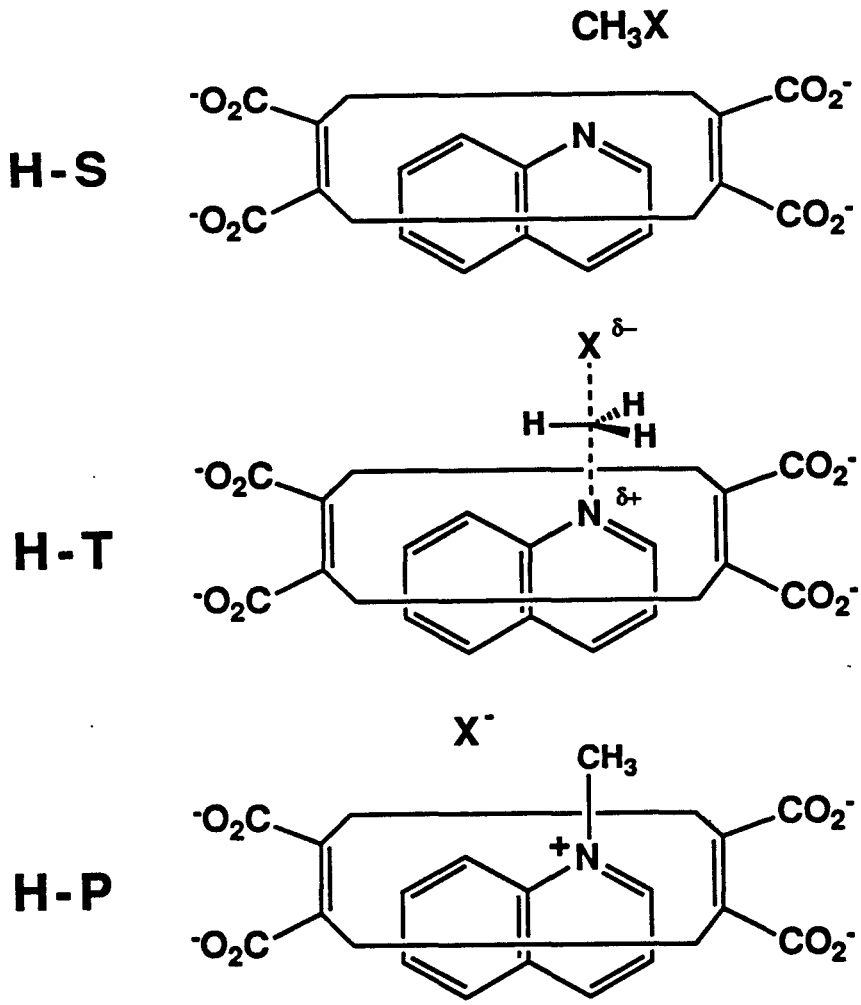

Figure 3.14. Scheme for transition-state stabilization for the host **1**-catalyzed alkylation reaction of **3** with MeI.

the host serves to encapsulate the reacting species. The reactant ground state is represented by the host-substrate complex and MeI. These two species come together in a highly polarized, S_N2 transition state (H-T) wherein the N-C bond is forming with a positive charge developing on the quinoline moiety, and the C-I bond is breaking with a negative charge developing on iodine. In the product ground state, the host-product complex is a "zwitterionic" species with the positive charge delocalized on the quinolinium paired with iodide.[36]

Theoretical calculations have suggested that the more polarized transition state (relative to ground states) in an S_N2 reaction should be stabilized in a dipolar environment.[37] Thus, it is more correct to attribute the rate acceleration of the above reactions to favorable dipole-dipole interactions between host **1** and the S_N2 transition state, rather than ion-dipole interactions that account for host-product stabilization.[37e]

With respect to other features of biomimetic catalysis, the host-catalyzed alkylation reaction could be inhibited competitively. When guest **20** (ATMA, $\Delta G°_{295}$ (**1**/**20**) = -6.7kcal/mol) was included in the kinetics experiment at 25°C with host **1**, substrate **3** and MeI, such that approximately 40% of the "catalytic sites" of **1** would be occupied, k_{cat} was diminished by 40% according to the kinetics simulation.

As testimony to the requirement for a preorganized binding site, the "3/4" molecule **51** was unable to induce chemical shift changes in either substrates (**3**/**6**) or products (**10**/**11**). Not surprisingly, then, **51** was ineffective as a catalyst for the alkylation reactions: whereas host **1** accelerated the methylation of **3** at 40°C by two orders of magnitude, under similar conditions with **3** and **6**, **51** accelerated methylation by less than a factor of 2.

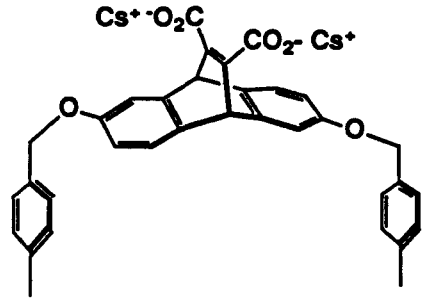

51

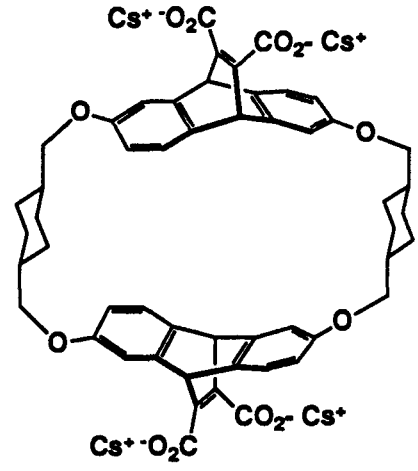

2

Other examples of host-catalyzed alkylation reactions

To further define the scope of the host-catalyzed alkylation reactions, other host-substrate-alkylating reagent combinations have been surveyed.

Host **1** catalyzed the alkylation of **3** with benzyl bromide at 25°C to afford **16**. Because the alkylating reagent also reacted rapidly with deuteroxide to form benzyl alcohol, k_{cat} could not be quantified, although we estimated an approximately 20-fold rate enhancement versus the uncatalyzed reaction.

Host **1** also catalyzed the alkylation of **17** with MeI at 35°C to give pyridinium compound **18**. The uncatalyzed rate constant at 35°C for **17** with MeI (k_2 3.37 x 10^{-4} s^{-1} M^{-1})[38] was determined simultaneously with **6** under pseudo-first-order conditions. Kinetics simulation of the host-catalyzed reaction provided k_{cat}/k_{un}~5. Based upon the relative affinities of **17** and **18** with host **1** (K_P/K_S ~3, see Chapter 1), the transition state was once again bound more tightly than the ground states.

Cyclohexyl-host **2** catalyzed the reaction of **3** with MeI at 25°C to give **10**. Kinetics simulation of the host **2**-catalyzed reaction provided k_{cat}/k_{un} ~20 (K_P/K_S[24] ~2.4). This rate enhancement is a factor of 5 less than with host **1**; nevertheless, host **2** binds the transition state preferentially ($\Delta G°_T$ = -7.7kcal/mol). The importance of this result relates to efforts to catalyze the reverse reaction (vide infra): with host **2**, the product is not bound much more strongly than the substrate, such that the expected rate enhancement for dealkylation of **10** should be greater for host **2** ($\Delta\Delta G^{\ddagger}_{rev}$ = 1.4kcal/mol) than for host **1** ($\Delta\Delta G^{\ddagger}_{rev}$ = 0.5kcal/mol).

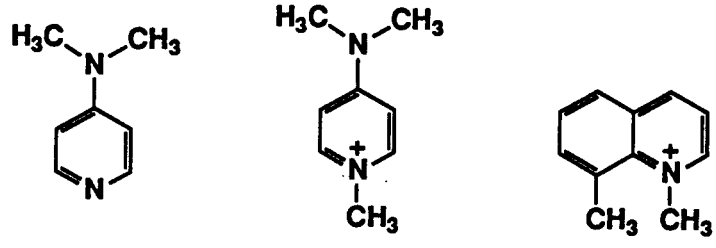

17 **18** **13**

Attempted dealkylation reactions

According to the reaction-coordinate diagram (Figure **3.1**) and the results for the host-catalyzed alkylation reactions, if the transition state is bound more tightly than the product, our hosts should accelerate the reverse reaction (assuming the activation barrier is accessible). In this context, products (**10** and **11**) are reportedly demethylated to substrates (**3** and **6**) and MeI with triphenylphosphine in anhydrous dimethylformamide *at 130-150°C*,[39] which suggests that the thermodynamics for substrate and product are roughly 8-10kcal/mol in favor of product.

The exact microscopic reverse of the forward reaction was attempted with excess cesium iodide (100mM) and alkylation products **10**, **11**, **13**, **15**, **16**, and **18** (each ~1mM) and monitored by nmr spectroscopy. Heating at 60°C for several days provided no distinct changes in the spectra of any of

the onium compounds. In the case of **13**, which is expected to have an activation barrier for demethylation ca. 3kcal/mol lower than **10**,[40] the signal for H_2 disappeared, apparently via deuterium exchange (the remainder of the spectrum, except for ^1H-^1H coupling for H_3 to H_2, was identical to starting **13**). Interestingly, this competing reaction was more clearly established when solutions of **10** and **11** were heated in borate-*d* (pD~9) at 80°C: peaks for H_2 of **10** disappeared after 1d; peaks for H_1, then H_3, of **11** disappeared more slowly (3-5d), and the coupling patterns for each became more complicated.

Thus, our future efforts to dealkylate products must focus upon stronger, weakly-basic nucleophiles. To that end, we have begun to explore water-soluble thiolates (RS^-). To date, we have inconclusive evidence regarding the potential for using such nucleophiles to carry out the desired transformations. In order to avoid side reactions of the sulfur nucleophiles (oxidative dimerization), experiments must be performed in deoxygenated aqueous solutions.

Conclusion

Electron-rich synthetic macrocyclic host **1** accelerates Menschutkin reactions in aqueous media. The rate constants of catalyzed versus uncatalyzed reactions and the binding affinities for substrates and products demand that host **1** binds transition states more tightly than ground states. This extension of molecular recognition through ion-dipole interactions to biomimetic catalysis provides compelling evidence for transition-state stabilization via favorable dipole-dipole interactions in aqueous media.

To date, however, the puzzle remains incomplete without evidence regarding the host-catalyzed dealkylation reactions.

Experimental for Chapter 3

Host and guest stock solutions for the aqueous nmr kinetics experiments were prepared with a standard 10mM deuterated cesium borate buffer at pD~9 (borate-*d*). The buffer was prepared as described in Chapter 1. All volumetric measurements of aqueous solutions were made using adjustable volumetric pipets. All pulse delays for the aqueous stock-solution-integration experiments (21s) were at least 5 times the measured T_1 for the species involved.

NMR tubes, which served as reaction vessels in the kinetics experiments, were made by John Pirolo in the Caltech Chemistry Glass Shop: half-dram screw-cap vials were fused (and balanced) to the tops of Norell 508-UP nmr tubes (7"). The vial portion could then be capped and sealed using the plastic screw-caps in tandem with Teflon-lined, silicone septa, such that the volatile alkylating agent (iodomethane) could be maintained.

For the kinetics experiments, buffered solutions containing substrate(s), 3,3-dimethylglutarate (DMG, internal chemical shift reference at 1.09ppm, concentration standard 4.20-4.23mM (vs KHP standard)), and hosts **1** or **2** (for catalyzed samples) were introduced into the reaction vessels, and buffer was added to give a total volume of 500μL; the vessels were capped and sealed, and then cooled in an ice-water bath. Iodomethane (2.0-3.5μL, ca. 30-55mM) was then injected through the septum with a 10-μL syringe. The cold solution was mixed by shaking vigorously. The reaction mixture was then recooled as the punctured septum was replaced with a pristine one. The cold reaction mixture was

then briefly sonicated to remove air bubbles and to complete mixing prior to loading the sample into the nmr probe.

Relative concentrations of substrate and product in the Menschutkin reactions were monitored by 400-MHz ^{1}H NMR (JEOL JNM GX-400) in an aqueous cesium borate buffer (borate-*d*). Concentrations were determined by careful integration of appropriate peaks such that the "tops" and "bottoms" of the integrals were flat, and the "window" for each peak was reproduced as closely as possible for sequential spectra. Initial concentrations of substrate and host were assumed from their respective stock-solution concentrations as determined by ^{1}H NMR integration versus DMG with the following typical parameters: ACQTM 4.096s; PD 21.0s; PW1 7.0μs; TI 32scans; FR 4000Hz. DMG also was employed as an integration standard to determine the *average* concentration of iodomethane during the course of the experiment. The reaction temperature was maintained in the "dedicated ^{1}H-only" probe and calibrated versus a methanol standard (see Chapter 2 Experimental).

The standard nmr kinetics experiment was prepared by locking and *manually shimming* the sample, adjusting the probe temperature, then setting the following parameters (all others default): ACQTM 4.096s (for FR 4000Hz) or 3.277s (for FR 5000Hz); PD 21.0s; PW1 7.0μs; TI 64scans; total accumulation time 26-27min *per spectrum* (or data point).

Command files (macros, "filename.GLG") were constructed in order to automatically measure the time evolution of the Menschutkin reactions overnight. (An example of such a command file is given below. Note that delays could be created artificially by accumulating but not writing to disk.) Time increments were determined from the time the files were written to disk (default feature of instrument).

Listing of file "SPUD40.GLG"

```
ACC CO H1D2O.3/24/89.H40QIP20 DF DR2:H40QIP20 WTD
ACC CO H1D2O.3/24/89.H40QIP21 DF DR2:H40QIP21 WTD
ACC CO H1D2O.3/24/89.H40QIP22 DF DR2:H40QIP22 WTD
ACC CO H1D2O.3/24/89.H40QIP23 DF DR2:H40QIP23 WTD
ACC CO H1D2O.3/24/89.H40QIP24 DF DR2:H40QIP24 WTD
ACC CO H1D2O.3/24/89.H40QIP25 DF DR2:H40QIP25 WTD ACC
ACC CO H1D2O.3/24/89.H40QIP26 DF DR2:H40QIP26 WTD ACC
ACC CO H1D2O.3/24/89.H40QIP27 DF DR2:H40QIP27 WTD PD 26 ACC PD 21
ACC CO H1D2O.3/24/89.H40QIP28 DF DR2:H40QIP28 WTD PD 26 ACC PD 21
ACC CO H1D2O.3/24/89.H40QIP29 DF DR2:H40QIP29 WTD PD 31 ACC PD 21
ACC CO H1D2O.3/24/89.H40QIP30 DF DR2:H40QIP30 WTD PD 36 ACC PD 21
ACC CO H1D2O.3/24/89.H40QIP31 DF DR2:H40QIP31 WTD
TEM 35 VTON TEM 25 VTON VTOFF
```

2,6-Bis[(4-methyl)benzyloxy]-9,10-dihydro-9,10-(1,2-dicarboxylato)ethenoanthracene, dicesium salt (51)

To a solution of **28** in dimethylsulfoxide (3mL) was added a solution of cesium hydroxide in H_2O (0.5mL, 1.0M); the mixture was sonicated and shaken vigorously. (**Note**: the *ratio* of DMSO to H_2O ($\geq$5:1) appears to be crucial for *complete hydrolysis* for this compound *and for macrocycles* such as tetraester host **27** to tetracarboxylate host **1**.) The resulting emulsion was dissolved in dd H_2O, then frozen and lyophilized (3 cycles). The residue was purified via ion-exchange chromatography (DOWEX, NH_4^+ form). UV-active fractions were combined and lyophilized, affording the dicarboxylic acid as fluffy white flakes. The water-soluble "3/4"-macrocycle was prepared as a stock solution in borate-*d*; **51** (913μM).

References to Chapter 3

(1) (a) Page, M. I.; Williams, A., Eds. *Enzyme Mechanisms*; Royal Soc. Chem.: London, 1987; (b) Lipscomb, W. N. *Acc. Chem. Res.* **1982**, *15*, 232-238.

(2) Jencks, W. P. *Catalysis in Chemistry and Enzymology*; McGraw-Hill: New York, 1969.

(3) (a) Pauling, L. *Nature* **1948**, *161*, 707-709; (b) Pauling, L. *Chem. Eng. News* **1946**, *24*, 1375.

(4) Menger, F. M. *Acc. Chem. Res.* **1985**, *18*, 128-134.

(5) Page, M. I.; Jencks, W. P. *Proc. Natl. Acad. Sci. USA* **1971**, *68*, 1678-1683.

(6) Most "transition-state" analogs resemble high-energy intermediates rather than transition states; likely exceptions are analogs to the prephenate/chrorismate Claisen rearrangement.

(7) (a) Bartlett, P. A.; Kezer, W. B. *J. Am. Chem. Soc.* **1984**, *106*, 4282-4283; (b) Jacobsen, N. E.; Bartlett, P. A. *J. Am. Chem. Soc.* **1981**, *103*, 654-657.

(8) (a) Tramontono, A.; Janda, K. D.; Lerner, R. A. *Science* **1986**, *234*, 1566-1573; (b) Iverson, B. L.; Lerner, R. A. *Science* **1989**, *243*, 1184-1188; (c) Pollack, S. J.; Schultz, P. G. *J. Am. Chem. Soc.* **1989**, *111*, 1929-1931; (d) Benkovic, S. J.; Napper, A.; Lerner, R. A. *Proc. Natl. Acad. Sci. USA* **1988**, , 5355-5358.

(9) Kaiser, E. T. *Angew. Chem. Int. Ed. Engl.* **1988**, *27*, 913-922.

(10) (a) Breslow, R. *Isr. J. Chem.* **1979**, *18*, 187-191; (b) Breslow, R. *Science* **1982**, *218*, 532-537.

(11) (b) Lehn, J.-M. *Science* **1985**, *227*, 849-856; (b) Tabushi, I. *Tetrahedron* **1984**, *40*, 269-292; (c) Tabushi, I. *Acc. Chem. Res.* **1982**, *15*, 66-72.

(12) Breslow, R.; Czarniecki, M. F.; Emert, J.; Hamaguchi, H. *J. Am. Chem. Soc.* **1980**, *102*, 762-770.

(13) (a) Tabushi, I.; Kimura, Y.; Yamamura, K. *J. Am. Chem. Soc.* **1978**, *100*, 1304-1306; (b) Zemel, H. *J. Am. Chem. Soc.* **1987**, *109*, 1875-1876.

(14) Hilvert, D.; Breslow, R. *Bioorg. Chem.* **1984**, *12*, 206-220.

(15) (a) Breslow, R.; Bovy, P.; Hersh, C. L. *J. Am. Chem. Soc.* **1980**, *102*, 2115-2117; (b) Breslow, R.; Doherty, J. B.; Guillot, G.; Lipsey, C. *J. Am. Chem. Soc.* **1978**, *100*, 3227-3229.

(16) Schepartz, A.; Breslow, R. *J. Am. Chem. Soc.* **1987**, *109*, 1814-1826.

(17) Cram, D. J.; Lam, P. Y.-S.; Ho, S. P. *J. Am. Chem. Soc.* **1986**, *106*, 839-841.

(18) Lutter, H.-D.; Diederich, F. *Angew. Chem. Int. Ed. Engl.* **1986**, *25*, 1125.

(19) Grieco, P. A.; Garner, P.; He, Z. *Tetrahedron Lett.* **1983**, *24*, 1897-1901.

(20) Breslow, R.; Rideout, D. *J. Am. Chem. Soc.* **1980**, *102*, 7816-7818.

(21) Sternbach, D. D.; Rossana, D. M. *J. Am. Chem. Soc.* **1982**, *104*, 5853-5854.

(22) (a) Rebek, J., Jr.; Trend, J. E. *J. Am. Chem. Soc.* **1978**, *100*, 4315-4316; (b) Rebek, J., Jr.; Costello, T.; Wattley, R. V. *Tetrahedron Lett.* **1980**, *21*, 2379-2380.

(23) Shepodd, T. J.; Petti, M. A.; Dougherty, D. A. *J. Am. Chem. Soc.* **1988**, *110*, 1983-1985.

(24) Petti, M. A.; Shepodd, T. J.; Barrans, R. E., Jr.; Dougherty, D. A. *J. Am. Chem. Soc.* **1988**, *110*, 6825-6840.

(25) Stauffer, D. A.; Dougherty, D. A. *Tetrahedron Lett.* **1988**, *29*, 6039-6042.

(26) Walsh, C. *Enzymatic Reaction Mechanisms*; Freeman: New York, 1979.

(27) Menschutkin, N. *Z. Physik. Chem.* **1890**, *6*, 41.

(28) (a) Essex, H. Gelormini, O. *J. Am. Chem. Soc.* **1926**, *48*, 882; (b) Norris, J. F.; Prentiss, S. W. *J. Am. Chem. Soc.* **1928**, *50*, 3042.

(29) The solubility was estimated from hplc injection of an aqueous phase of MeI in borate-*d* over an organic phase of MeI.

(30) Lowry, T. H.; Richardson, K. S. *Mechanism and Theory in Organic Chemistry*; 3rd ed.; Harper and Row: New York, 1987; pp 248-253.

(31) Cachaza, J. M.; Herraez, M. A. *An. Quim.* **1971**, *67*, 11-16.

(32) Packer, J.; Vaughan, J.; Wong, E. *J. Am. Chem. Soc.* **1958**, *80*, 905.

(33) Lowry, T. H.; Richardson, K. S. *Mechanism and Theory in Organic Chemistry*; 3rd ed.; Harper and Row: New York, 1987; pp 327-424.

(34) Leffler has tabulated several examples of reactions wherein $\Delta H^{\ddagger}/T\Delta S^{\ddagger}$ compensation occurs: Leffler, J. O. *J. Org. Chem.* **1955**, *20*, 1202-1231.

(35) Breslow, R.; Guo, T. *J. Am. Chem. Soc.* **1988**, *110*, 5613-5617.

(36) In the 10mM borate buffer, iodide is likely to be "washed out" in favor of a borate counter anion.

(37) (a) Carrion, F.; Dewar, M. J. S. *J. Am. Chem. Soc.* **1984**, *106*, 3531-3539; (b) Chandrasekhar, J.; Smith, S. F.; Jorgensen, W. L. *J. Am. Chem. Soc.* **1985**, *107*, 154-163; (c) Chandrasekhar, J.; Smith, S. F.; Jorgensen, W. L. *J. Am. Chem. Soc.* **1984**, *106*, 3049-3050; (d) Bunton, C. A. *Nucleophilic Substitution at a Saturated Carbon Atom*; Elsevier: New York, 1963; (e) Host 1 also probably alleviates solvent reorganization in the alkylation reaction: see Arnett, E. M.; Reich, R. *J. Am. Chem. Soc.* **1980**, *102*, 5892-5902.

(38) Somewhat surprisingly, **6** is a better nucleophile for MeI in borate-*d* than is **17**, according to the relative rates (**17** is ca. 65% of **6**).

(39) (a) Deady, L. W.; Korytsky, O. L. *Tetrahedron Lett.* **1979**, 451-452; (b) Berg, U.; Gallo, R.; Metzger, J. *J. Org. Chem.* **1976**, *41*, 2621-2624.

(40) Deady, L. W.; Finlayson, W. L.; Korytsky, O. L. *Aust. J. Chem.* **1979**, *32*, 1735-1742.

(41) According to nmr analysis, there are several by-products in the alkylation reactions with MeI that require characterization. Host **1** has been observed to precipitate from solution after prolonged heating (60°C) with MeI in borate-*d*; four unidentified singlets appear (δ2.6-3.2) attributable to the host **1** stock solution, although the absence of desymmetrization of the nmr spectra for **1** suggests that host is not undergoing methylation. The carboxylates of the internal reference, 3,3-dimethylglutarate (DMG), become methylated slowly (δ3.8). The 10mM-deuteroxide is converted to methanol, which eventually lowers the pD of the solution (pD~2-4); host **1** precipitates from the reaction mixture, then apparently decomposes under more strongly acidic conditions.

(42) The slope ($-\Delta H^{\ddagger}_{cat}$) and intercept ($\Delta S^{\ddagger}_{cat}$) in Figures **3.10** (top) and **3.11** (top) suggest a large, *positive* $\Delta S^{\ddagger}_{cat}$ and a high, relatively unfavorable $\Delta H^{\ddagger}_{cat}$ compared to the uncatalyzed reaction (Table **3.2**); however, if the highest temperature point is discarded in each case (bottoms of Figures **3.10** and **3.11**), $\Delta S^{\ddagger}_{cat}$ becomes smaller, while $\Delta H^{\ddagger}_{cat}$ is more favorable.

Chapter 4

Design, Synthesis, and Complexation Behavior of a New Class of Water-Soluble, Hydrophobic Binding Sites

Introduction

Synthetic host-guest (molecular recognition) chemistry continues to evolve against a multidisciplinary background of synthetic, bioorganic, and physical-organic chemistry. Principles of stereoelectronic complementarity and preorganization, as developed in the pioneering work in the field of crown ethers and related structures,[1] have guided the design of synthetic macrocycles as hosts for the selective complexation of a variety of guests. The binding of organic guests by cyclodextrins further sparked the development of fully synthetic macrocycles for binding apolar molecules in water.[2] The X-ray structure (Figure 4.1) reported by Koga[3] provided another major advance in the field: true encapsulation of an apolar guest *within* the cavity of a cyclophane host was evident. The rapid evolution of water-soluble cyclophanes with hydrophobic binding sites attests to the importance of the Koga macrocycle.[4]

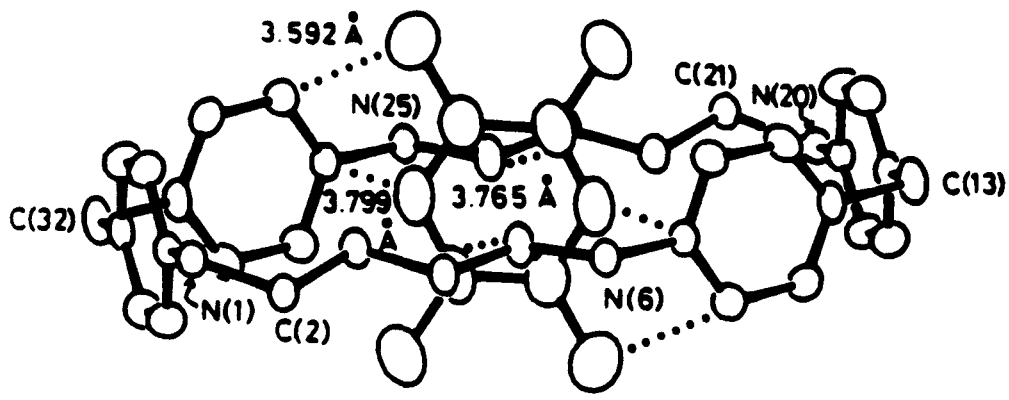

Figure 4.1. Ball-and-stick model of the X-ray crystal structure for durene included in the Koga macrocycle (reproduced from reference 3).

Molecular recognition studies in aqueous media probe the weak, non-covalent forces relevant to biologically important macromolecules. Recently, an excellent review has appeared that describes the complexation of neutral molecules by cyclophane hosts[5] with the goal of understanding the nature of hydrophobic binding. In addition to the hydrophobic effect, our group has sought to understand other, more subtle, forces for molecular recognition in aqueous[6] and organic[7] media (see Chapter 1). For the present work, the studies by Petti[8] and Shepodd[9] provide a blueprint for quantifying the "hydrophobic binding" of water-soluble guests by high-symmetry, chiral hosts.

Design of a New Class of Water-Soluble, Hydrophobic Binding Sites

The work described herein commenced concurrent with the 2,6-host system developed by Petti[8] and Shepodd.[9] A second, related class of hosts, with 1,5-substituents on the rigid ethenoanthracene units, was designed and synthesized.

As with the 2,6-hosts, the design of the 1,5-hosts was guided by several criteria to improve upon the Koga system, which have been described in detail elsewhere,[6] and are summarized as follows: (1) the water-solubilizing groups should be well removed from the putative hydrophobic cavity to take full advantage of the anticipated hydrophobicity of the binding site; (2) these new hosts should be soluble near neutral pH; (3) the binding site should be defined by rigid units, consistent with the principle of preorganization evident from the crown ether systems;[10] (4) the new hosts should be topographically well-defined, "inherently chiral"[11] molecules; and (5) the synthesis of new hosts should proceed in an efficient, straightforward fashion.

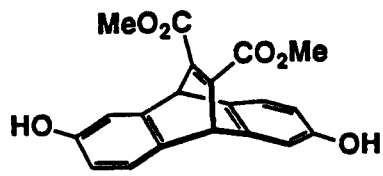

29

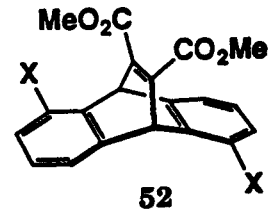

52

The seminal paper to this work[6] presented a structure **29** that most nearly meets the criteria set forth above. Another structure consistent with these same criteria is found in **52**. Both structures feature the bridged ethenoanthracene (9,10-dihydroethenoanthracene, DEA) unit that defines an absolutely rigid, concave, hydrophobic surface[12] in which the aryl rings are locked in a "face-to-face" orientation known to be favorable for binding;[13] also, the masked water-solubilizing groups are necessarily external to the binding site.

The corresponding host structures derived from **29** and **52** are given by **53** and **54**, respectively. These are constructed by connecting two DEA units through linker groups X. For the 2,6-hosts **53**, phenols, which are well-suited to macrocyclization using Cs_2CO_3 in DMF,[14] were chosen as the means to introduce the linkers. In contrast, for the 1,5-hosts **54**, benzoic acids were chosen because they are well-suited to macrocyclization via the corresponding bis(acid chloride) plus diamine[15] under high-dilution conditions to form amide-type linkers. As will be discussed below, circumventing difficulties in the synthesis of 1,5-hosts **54** afforded to us other potentially useful 1,5-DEA building blocks. The present work has been restricted to elaboration of 1,5-DEA units with carboxylic acid substituents.

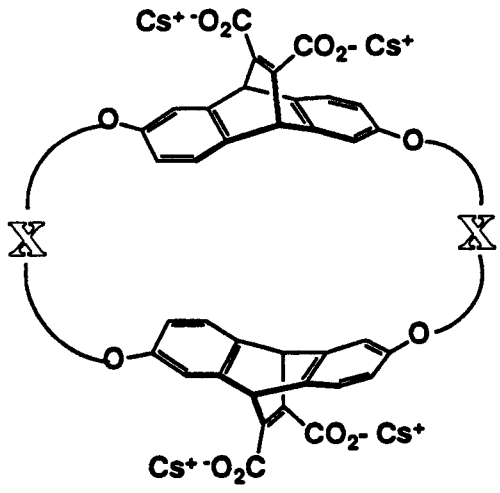

53

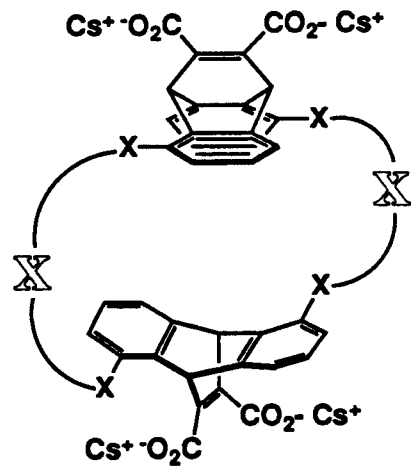

54

Each DEA unit (**29** and **52**) has C_2 symmetry, and hence is chiral, but not dissymmetric. Dimerization of a chiral unit produces two diastereomers (Figure **4.2**). Heterochiral[16] coupling of opposite enantiomers affords a meso compound, which has C_{2h} symmetry in the present case (the original C_2 axis of the DEA unit is perpendicular to a mirror plane that bisects the molecule). Homochiral[16] coupling of like enantiomers affords the chiral, *d,l* diastereomer, which has D_2 symmetry (three mutually perpendicular two-fold axes). In the chiral diastereomer, the linkers run "front-to-back" and "back-to-front," which imparts a sense of twist to the macrocycle (Figure **4.2**). Each host, therefore, contains a helical cavity that is inherently chiral. Examination of CPK models suggests that the 1,5-DEA unit **52** could impart an even greater sense of twist to the chiral macrocycle **54** in comparison to the 2,6-DEA unit **29** and macrocycle **53**, such that perhaps greater enantiodiscriminatory properties could be obtained. Isolation of enantiomerically pure DEA units **29** and **52** will necessarily afford a single enantiomer of the appropriate chiral diastereomer in the macrocyclization reaction.

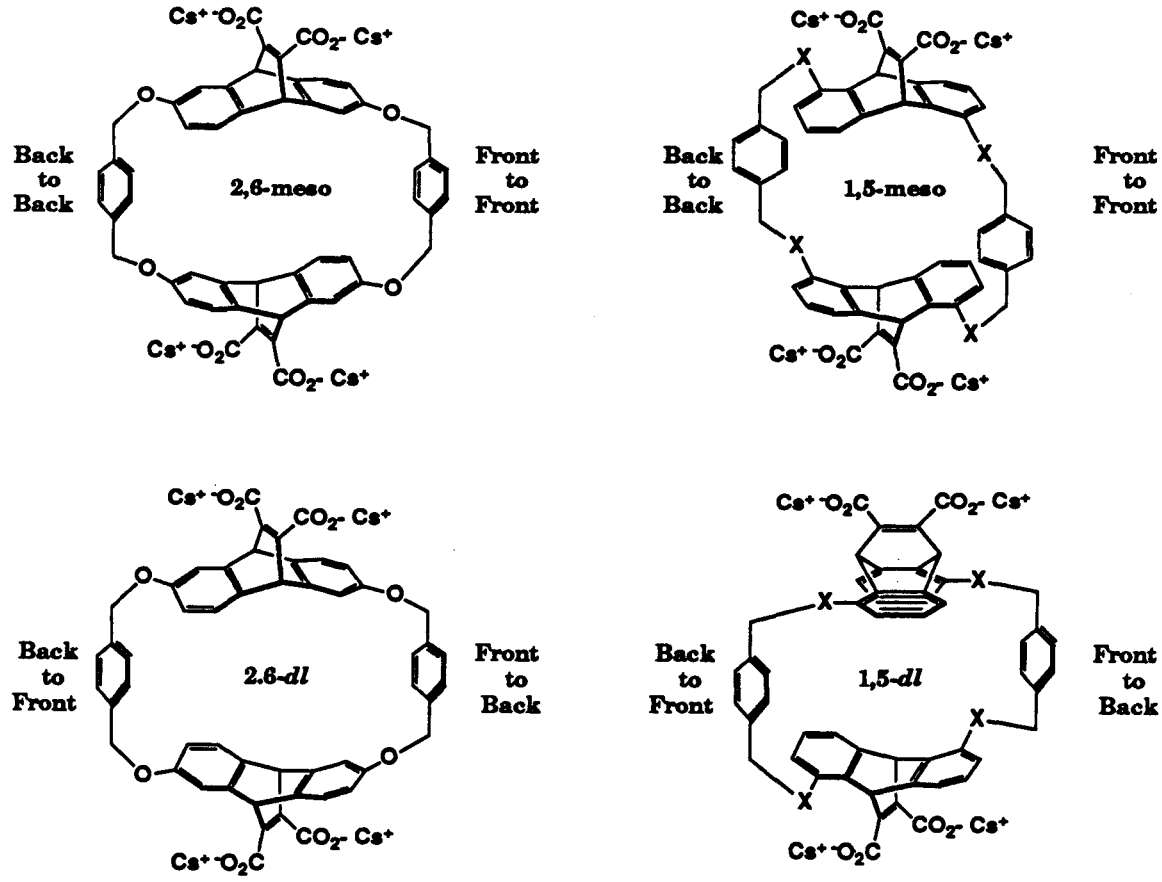

Figure 4.2. Schematic for meso (Front-to-Front, Back-to-Back) and *d,l* (Front-to-Back, Back-to-Front) diastereomers. **Left**: 2,6-hosts; **right**: 1,5-hosts.

In the earlier work,[6] enantiomerically pure 2,6-DEA units were obtained in an elegant, efficient, straighforward synthesis featuring an asymmetric Diels-Alder reaction. Efforts to extend such methodology to the 1,5-DEA units **52** have proven as yet unsuccessful. Also, attempts to separate 1,5-DEA **52** diastereomers (see Appendix 3) synthesized by coupling racemic **63** to chiral auxiliaries have met with limited success.

The aqueous complexation properties of the 1,5-hosts **54** in the present work are compared to those for the 2,6-hosts **53**[6] by surveying a range of water-soluble guests. Because these guests must choose between water and the environment of the host cavity, primarily attractions between host and guest are delineated, rather than repulsions between guest and water (hydrophobic effect[17]). It is observed that the 1,5-hosts **54** (with amide linkers) exhibit consistently lower affinities for guests when compared to 2,6-hosts **53** (with ether linkers). In hindsight, this general result is consistent with concepts of hydrophobicity and solvation set forth in the design criteria: while the amide group was chosen for its facile synthesis and for its anticipated conformational rigidity in the 1,5-hosts **54**, hydrophobicity (and consequently binding affinity) appear to have been sacrificed because of the favorable solvation (hydrogen-bonding) of the amides by the aqueous medium. Efforts to take advantage of hydrogen-bonding amide groups using tetraester 1,5-host **55** in organic media revealed no complexation with either hydrogen-bond donors (to carbonyl) or acceptors (to N-H). Further discussion regarding the amides is presented in the section on Binding. As described in the section on Structures, an unexpected geometry change for 1,5-hosts **54** is indicated from nmr chemical-shift changes upon binding guests.

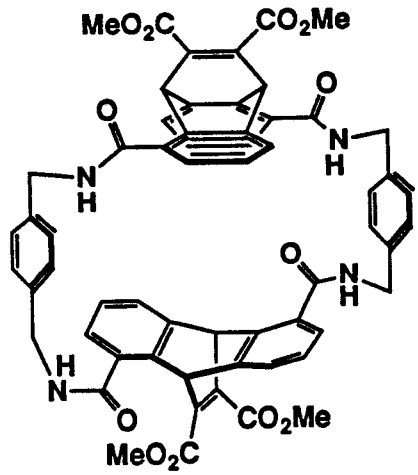

55

Synthesis and Physical Characterization

The synthetic approach to 1,5-hosts **54** is shown in Figure **4.3**. Commercially available 1,5-dichloroanthraquinone (**56**) was converted to 1,5-dicarboxyanthracene (**59**) in three steps.[18] The attempted Diels-Alder reactions of **59** or 1,5-dicarbomethoxyanthracene (**61**) with dimethyl acetylenedicarboxylate (DMAD) in refluxing dioxane were unsuccessful. Probable sources of failure include the low solubility of **59** in the reaction mixture and the electron-withdrawing carboxyl groups of **59** and **61** that render the diene moiety unreactive. In any case, a suitable Diels-Alder diene component was synthesized via reduction of dicarboxylic acid **59** with borane-tetrahydrofuran[19] to afford diol **60** in 52% yield. The low yield for this step can be attributed to the fact that with the synthesis of diol **60** one can purify the product via recrystallization from methanol: in all previous steps, because of their insolubility in organic solvents, isolated materials were carried through the synthesis without purification.

Diol **60** was protected as the bis(silyl) ether **33**. This protection step was necessary to avoid the Michael-addition reaction between DMAD and

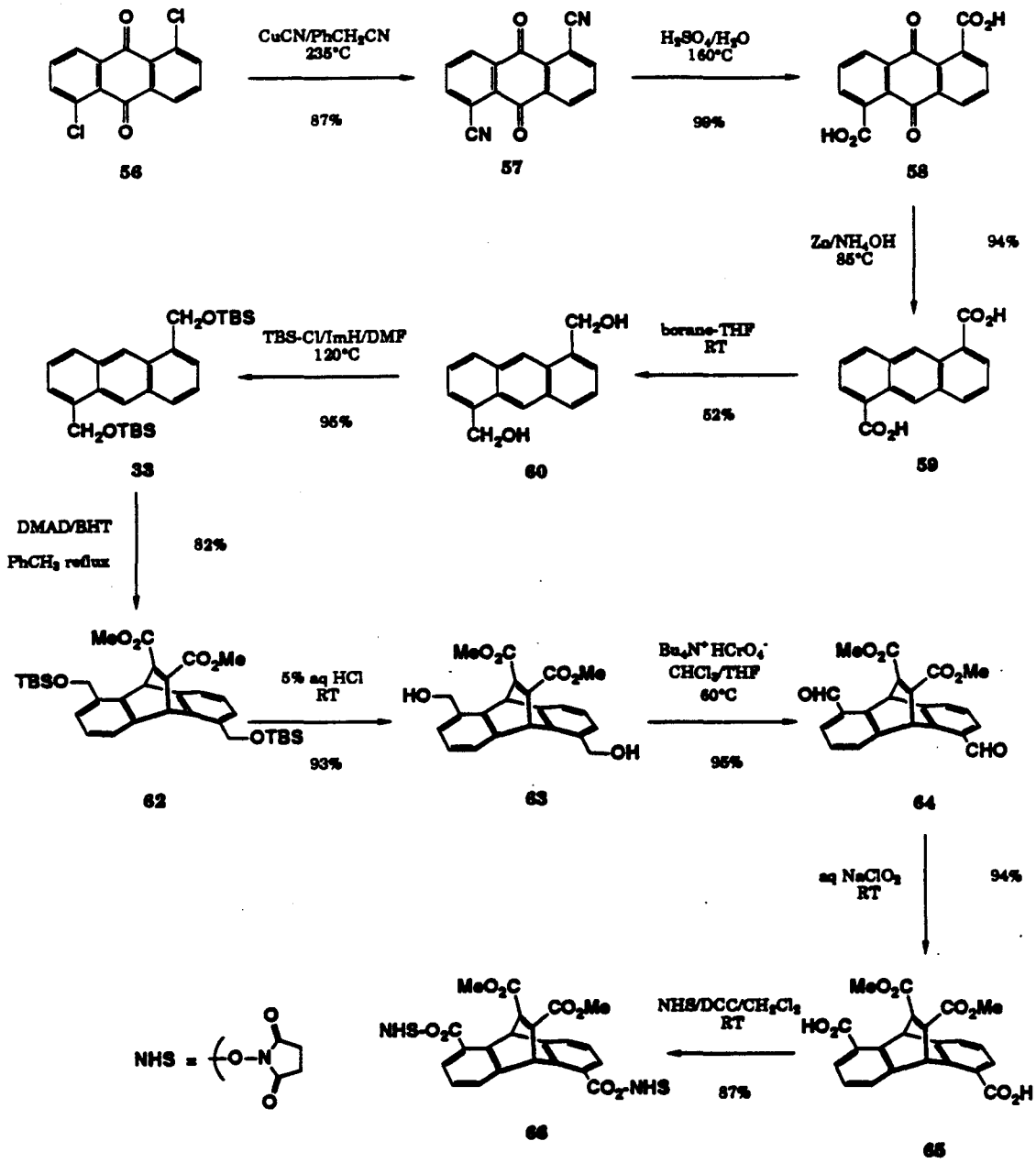

Figure 4.3. Synthetic scheme for 1,5-DEA units/host precursors.

the alcohols, as well as to increase the diene solubility. The Diels-Alder reaction between **33** and DMAD proceeded in refluxing toluene to afford the racemic, C_2-symmetric DEA building block **62**. Bis(silyl) ether **33** is the 1,5-analog to the diene component **32** in the previously reported asymmetric Diels-Alder reaction with dimenthyl fumarate (Figure **4.4**).[6,9] The attempted extension of this methodology using **33** is described in Appendix 3.

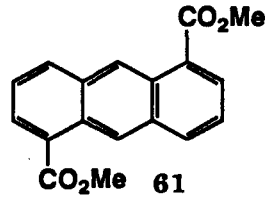

61

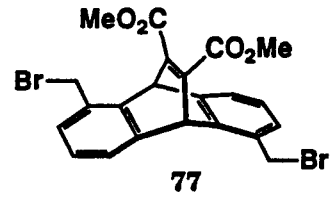

77

DEA **62** was converted to the target DEA **65** in three steps: **62** was deprotected in 5% aqueous hydrochloric acid to give diol **63**; oxidation with tetrabutylammonium chromate[20] afforded dialdehyde **64**; and oxidation with buffered aqueous sodium chlorite[21] yielded diacid **65**. The alcohol and aldehyde oxidation steps both employed milder reagents in order to avoid oxidation of the etheno bridge. The overall, nine-step yield from **56** to **65** was 27%.

The three DEA units **63-65** are potential building blocks for novel host structures. Of particular interest to future work is the prospect of a hydrophobic cavity with an all-carbon periphery, which could be derived from Wittig-type coupling of bis(phosphonium) salts with dialdehyde **64** to give **76**. Alternatively, one could envision Grignard-type coupling of bis(alkyllithium) or bis(Grignard) reagents with dibromide **77** (readily obtained from PPh_3/Br_2 treatment of diol **63**) to give **78**.

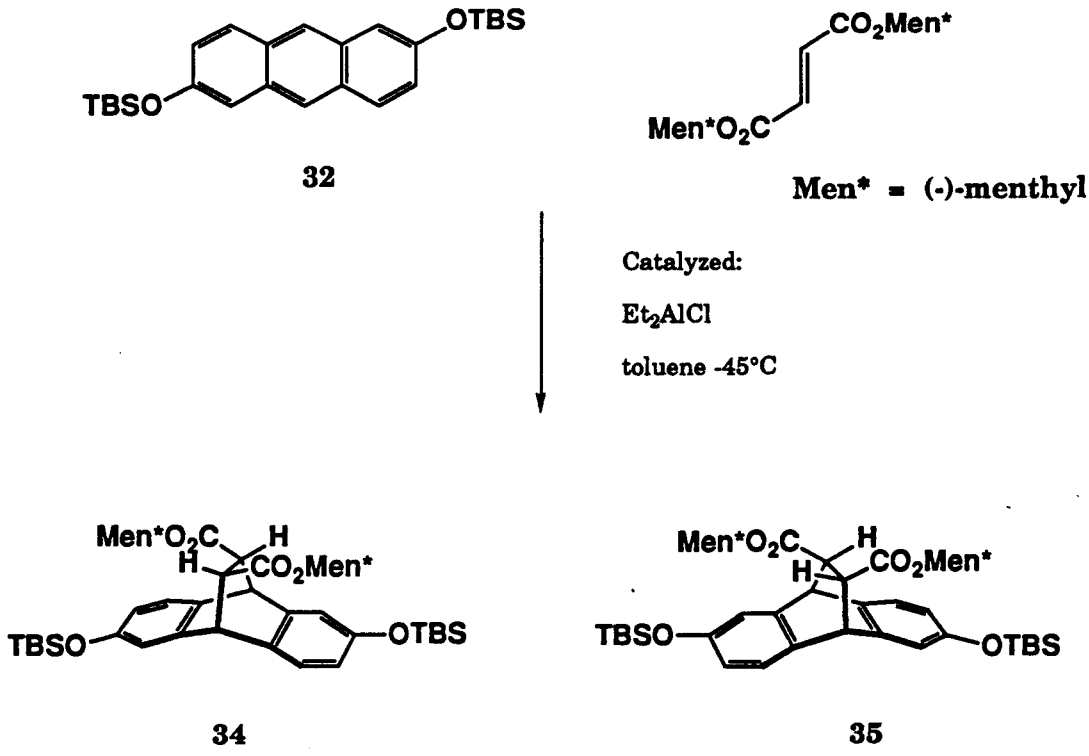

Figure 4.4. Asymmetric Diels-Alder reaction scheme for 2,6-DEAs (from reference 6).

With the target DEA **65** in hand, attention was turned toward macrocyclization through amide-bond formation. Several methods have been developed for this purpose, especially in the field of solid-phase peptide synthesis, wherein rapid and quantitative peptide coupling is crucial.[22] This coupling reaction is also crucial in the present case: we intend to form four bonds in a single macrocyclization step, while minimizing oligomerization. Consequently, before proceeding with the macrocyclization reactions, model reactions were performed to assess which of the various methods would be appropriate for our purposes. To that end, it was found that *N*-hydroxysuccinimidyl (NHS) esters **66** (from carbodiimide-coupling of **65** with two equivalents of *N*-hydroxysuccinimide) were best-suited for amide-bond formation when allowed to react with primary amines in dichloromethane. "Control" molecules (see Binding) **72** and **74** were synthesized cleanly in this way. Unfortunately, the use of NHS esters **66** and diamines in high-dilution macrocyclization reactions was less successful. Incomplete amide-bond formation was noted even after two weeks. More importantly, chromatographic separation of macrocyclic products from starting **6** was non-trivial. Attempts to synthesize and characterize "3/4"-hosts **79** using excess **6** plus diamines was defeated by similar chromatography problems. Because the macrocyclization could be achieved in a simpler way, as described below, the approach with NHS esters was abandoned.

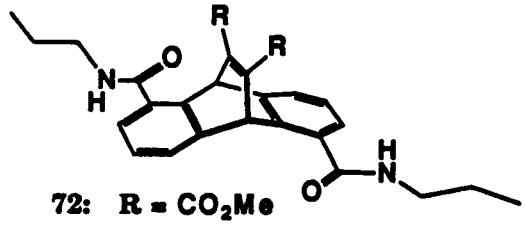

72: R = CO_2Me
73: R = $CO_2^- Cs^+$

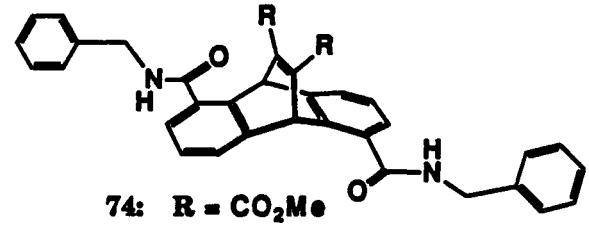

74: R = CO_2Me
75: R = $CO_2^- Cs^+$

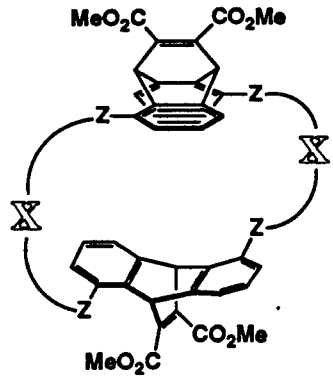

76: Z = CH═CH

78: Z = CH_2—CH_2

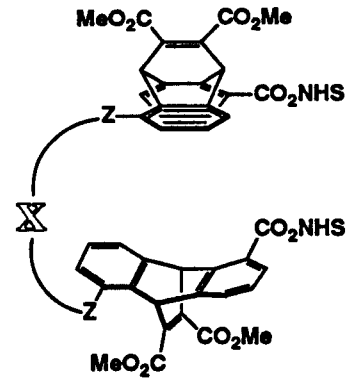

79

Z = CONH

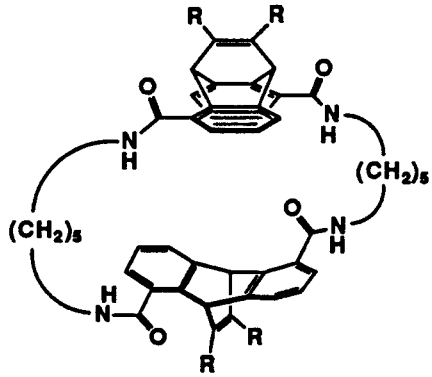

67/68: R = CO_2Me

69/70: R = CO_2^- Cs^+

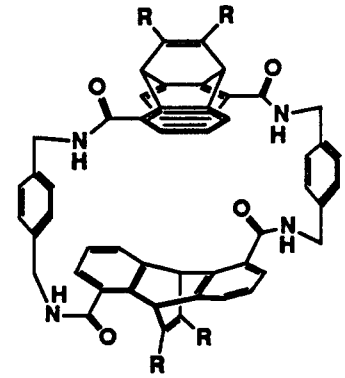

55: R = CO_2Me

71: R = CO_2^- Cs^+

Macrocycles **67/68** and **55** were synthesized successfully in a more conventional fashion.[23] Bis(acid chloride) **80** was prepared *in situ*, then coupled to either 1,5-diaminopentane or *p*-xylylenediamine under high-dilution conditions in dichloromethane to afford **67** and **68** (5C macrocycles, 12%) and **55** (PX macrocycle, 9%), respectively. When the basic building block (e.g., **65**) is racemic, coupling two units together yields roughly equal amounts of the two previously discussed diastereomers (Figure **4.2**), with the chiral diastereomer being racemic.[6] In addition, all macrocyclization reactions afford higher molecular weight oligomers. In contrast to the 2,6-macrocycles,[6] which required preparative high-performance liquid chromatography to separate diastereomeric tetraesters **53**, the 1,5-5C-macrocycles **67** and **68** were separated and isolated cleanly using flash chromatography.[24] In the case of the 1,5-PX-macrocycles **55**, one of the two diastereomeric tetraesters could be isolated cleanly via flash chromatography; however, the alleged second dimer eluted with higher oligomers. Overall, then, dimeric **55**, **67**, and **68** amide macrocycles were characterized: mass spectrometry (EI/FAB), ^{1}H NMR, and ^{13}C NMR data indicated that these structures were the desired dimers.

The meso/*d,l*-stereochemistry of the 5C macrocycles can be distinguished (in principle) by focusing upon the γ-methylene group: these protons are diastereotopic in the C_{2h}, achiral isomer, and homotopic in the D_2, chiral isomer (Figure **4.5**). Homonuclear decoupling of the β-CH_2 *may* reveal the stereochemistry: the γ-CH_2 of the achiral isomer should appear as an AB pattern; the γ-CH_2 of the chiral isomer should appear as a singlet. In all nmr solvents examined ($CDCl_3$, d_6-DMSO, d_5-pyridine, borate-*d*), the chemical shifts of the β-CH_2 and γ-CH_2 groups overlapped in at least one

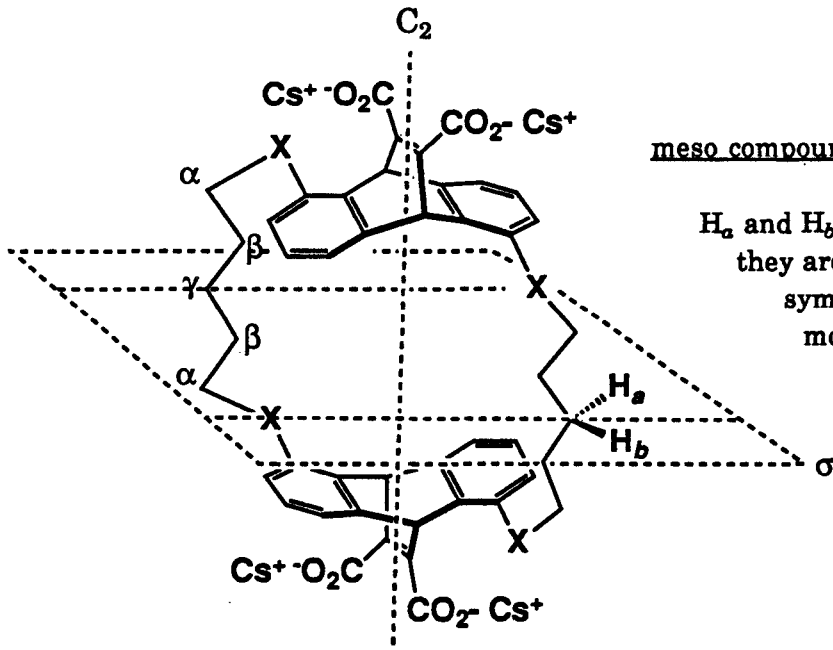

meso compound: γ-CH_2

H_a and H_b are diastereotopic--
they are not interconverted by a
symmetry operation of the
molecule

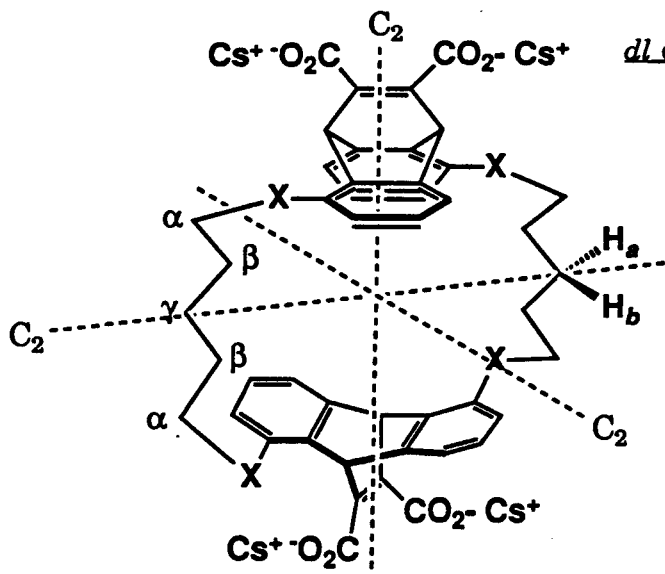

dl compound: γ-CH_2

H_a and H_b are homotopic--
they are interconverted by
a C_2 axis

Figure 4.5. Differentiation of meso/*dl* diastereomers for 5C hosts.

isomer, such that the stereochemistry of the 5C macrocycles could not be assigned unambiguously.

Similarly, the stereochemistry of the PX macrocycles can be distinguished by focusing upon the aromatic xylyl-linker protons *in a chiral environment*: in the absence of a chiral influence, these protons in either diastereomer appear as a singlet in the ^{1}H NMR spectrum. However, a chiral influence necessarily reduces the time-averaged symmetry of the diastereomers (Figure **4.6**): adjacent protons of the achiral isomer are diastereotopically coupled, and could appear as an AB pattern; those of the chiral isomer are homotopically coupled, and could appear as isolated singlets. In the presence of increasing amounts of a chiral guest in water (e.g., **81**, see Binding), the aromatic xylyl-linker protons of the single PX macrocycle **55** in hand were resolved cleanly as two singlets, suggesting that we had isolated the chiral isomer as a racemate. However, without performing the same experiment with the other PX diastereomer to confirm this approach, we cannot have full confidence in this assignment.

Efforts to (1) further purify host dimers, (2) synthesize hosts from other diamines, or (3) resolve DEA units **62-65** (see Appendix 3) were to await characterization of 1,5-hosts in hand according to binding studies, to determine whether such efforts were to be warranted.

Unmasking of the water-solubilizing functionality was achieved through hydrolysis of diesters **72** and **74**, and of tetraesters **67**, **68**, and **55**, using a slight excess of aqueous cesium hydroxide in dimethyl sulfoxide. Each reaction mixture was purified via cation-exchange chromatography (DOWEX, NH_4^+ resin), lyophilized, then neutralized with CsOD and dissolved in aqueous pD~9 borate-*d* buffer to produce stock solutions of

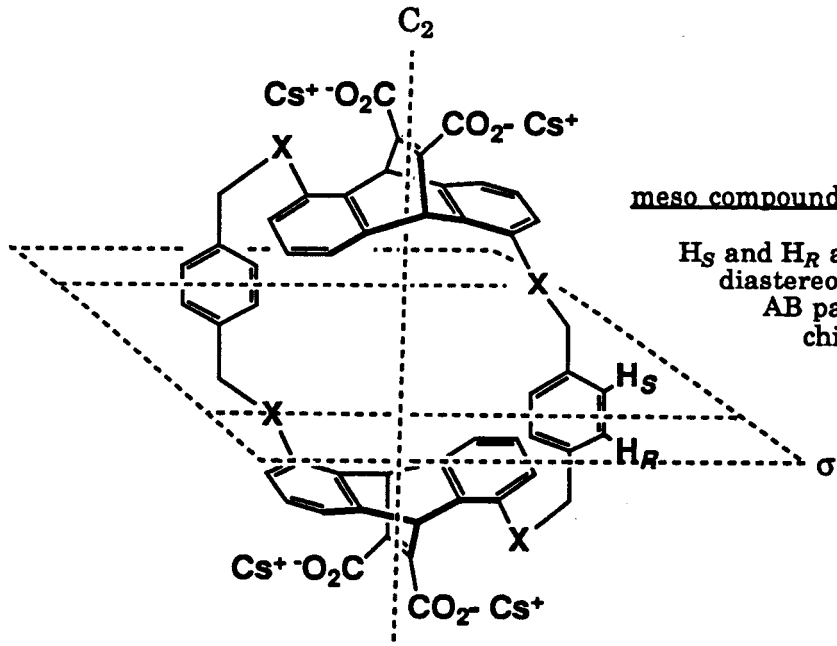

meso compound:

H_S and H_R are time-averaged diastereotopically coupled--AB pattern under a chiral influence

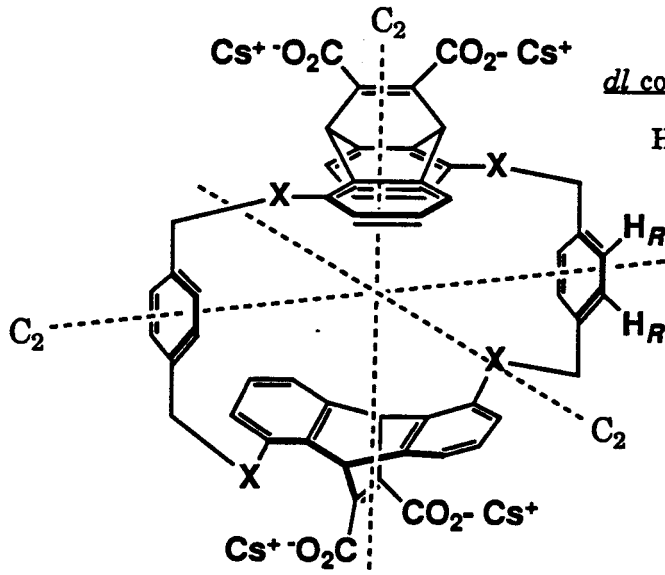

dl compound:

H_R and H_R are time-averaged enantiotopically coupled--two singlets under a chiral influence

Figure 4.6. Differentiation of meso/*dl* diastereomers for PX hosts.

"control" molecules **73** and **75**, and hosts **69**, **70**, and **71**, for binding studies in water.

CAC Studies

As for the 2,6-hosts, the 1,5-hosts possess both hydrophilic and hydrophobic parts, such that aggregation occurs at sufficiently high concentrations. In order to evaluate properly the 1:1 host-guest interaction, it is necessary to operate at concentrations below a critical aggregation concentration (CAC) where only monodispersed host is present. All binding studies described herein were performed with each host well below its CAC. We used ^{1}H NMR to evaluate the aggregation behavior of hosts, where chemical shift changes were monitored as a function of host concentration (monodispersed host exhibits no further change in its spectrum). We find the following CACs: **69** (>7mM); **70** (>5mM); **71** (0.6mM).

The limited data on CACs in the present work suggest a correlation that is consistent with earlier observations[6] wherein the favorable solvation by water raises the CAC, and correspondingly reduces the hydrophobicity of the binding site. The lower affinities of the 1,5-amide hosts versus the 2,6-ether hosts can be ascribed (in part) to the solvation of the amides by water.

Binding Studies: Determination of Binding Affinities from NMR Shift Data

All aqueous binding studies for 1,5-hosts were performed following the protocol for 2,6-hosts.[6] Binding affinities were obtained from ^{1}H NMR titration data in which all spectra exhibit only time-averaged signals for both complexed and uncomplexed host and guest. Assignment of the association constant (K_a) was made from a best fit between the observed

positions of the guest (and host) resonances at varying host and guest concentrations and the resonances predicted from our 1:1 complexation model. The unknowns are K_a and the maximum upfield shifts (D values) of fully complexed guest (host) relative to those for free guest (host). These unknowns were calculated using a non-linear least-squares fitting procedure called MULTIFIT,[6] in which the nmr data from all guest (and host) protons were simultaneously fit with a single K_a. The details of MULTIFIT have been described elsewhere.[6]

In order to compare directly the binding affinities of 1,5- versus 2,6-hosts, a series of common guests was surveyed. By virtue of significantly lower affinities versus 2,6-hosts,[6] the results obtained for the binding of organic guests with 1,5-hosts in aqueous media attest to the effectiveness of the 2,6-host systems, as well as the necessity for rigorous separation of hydrophobic and hydrophilic moieties.

Specific and *sizeable* upfield shifts of guest protons provide strong evidence for binding by encapsulation in the host cavity.[6] We have performed, therefore, "single-point" binding studies (see also Chapter 2) to assess more quickly the 1,5-hosts' ability to complex guests in water.

1,5-5C-Hosts **69** and **70** have no significant influence upon the chemical shifts of guests **11**, **20**, and **82**, as summarized in Table **4.1**. From this limited data set, and from the relatively high (as a lower limit of 5mM) CAC, it is suggested preliminarily that there is no molecular recognition in aqueous media by 1,5-5C-hosts.

Fortunately, the 1,5-PX-host **71** *does* induce significant upfield shifts of guest protons, indicating some degree of complexation in water. In an effort to understand steric and electronic factors important to recognition by **71**, a wide variety of guests was examined (Figure **4.7**). However, of these

Table 4.1: "Single-point" binding analysis for guests in the presence of 1,5-5C-hosts **69** and **70** in borate-*d*.[a]

host	guest	[H]o (μM)	[G]o (μM)	observed shift for N-C*H*$_3$ (Hz)[b]
69	**20**	204	386	6.1
70	**20**	194	382	6.6
69	**11**	202	429	4.4
70	**11**	194	429	4.6
69	**82**	202	465	3.7
70	**82**	192	460	4.4

[a]Determined by ^{1}H NMR (400 MHz); [b]Positive, upfield position from chemical shift of free guest.

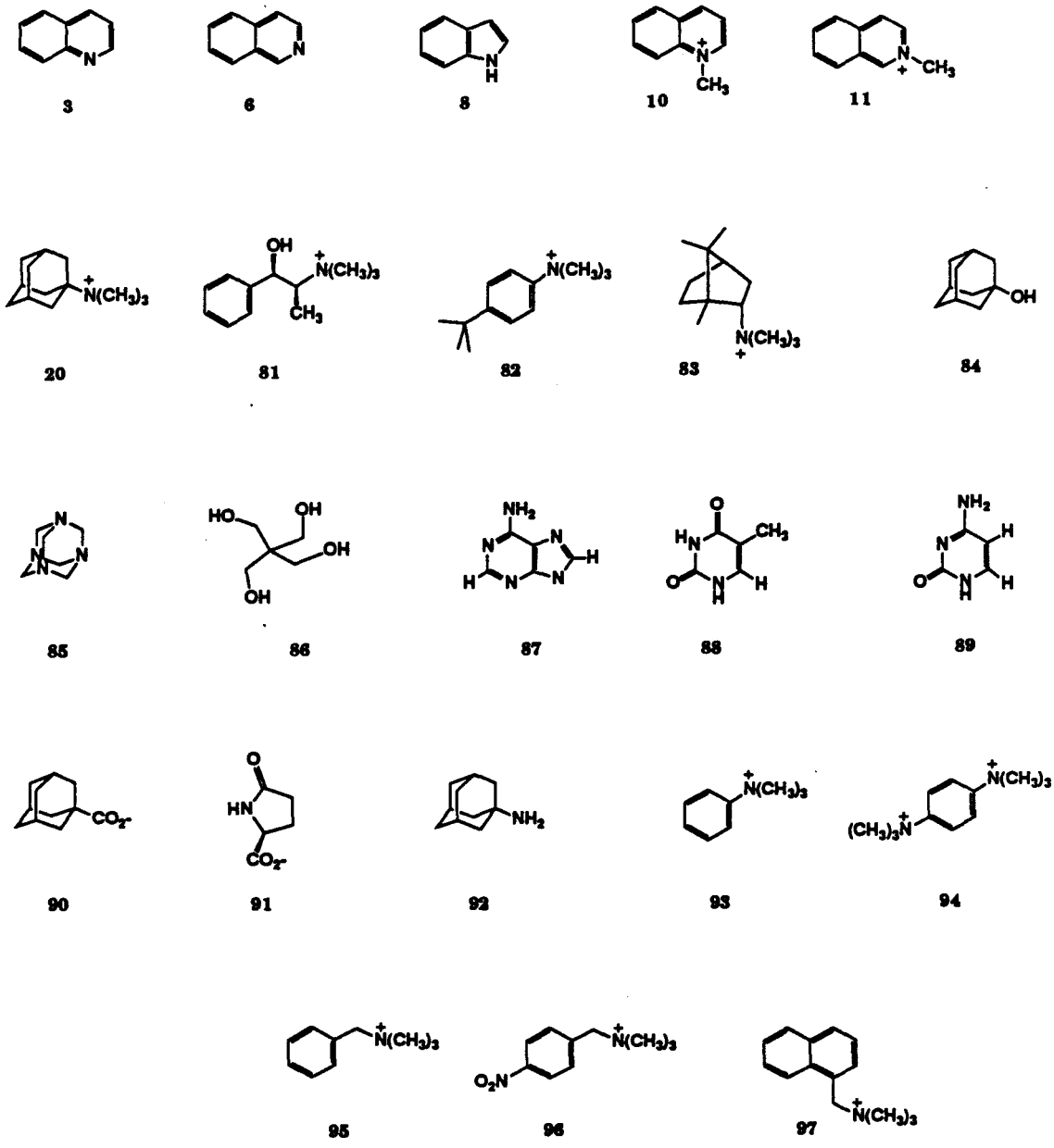

Figure 4.7. Guest list for Chapter 4.

guests, only positively-charged, ammonium guests are bound in the host cavity. Complete binding studies for 1,5-host **71** and guests **11, 20, 81,** and **83** were subjected to MULTIFIT analysis (Table **4.2**). Compared to 2,6-host **1**, the 1,5-host **71** binds the ammonium guests less strongly by ca. 2-3 kcal/mol. Note, however, that with the lower K_as, it is not possible to cover an adequate range of percent guest bound (see Chapter 2) in the nmr titration while maintaining host **71** below its CAC. Interestingly, we can cover an adequate range of percent host bound in this titration (Table **4.2**). Because the *host* experiences significant and sizeable shifts upon complexation, we include host protons in the MULTIFIT analysis. (*D* values for host-guest pairs are given in Appendix 5.)

Guest **84**, adamantanol, has been included in Table **4.2** because of its calculated K_a (1100 M^{-1}), which further illustrates a point discussed in Chapter 2: MULTIFIT tends to compensate high K_as with low *D* values (or, vice versa, low K_as with high *D* values). The largest *observed* upfield shifts for protons of **84** are *only 12Hz* (MULTIFIT calculates 19% **84** bound, 7% **71** bound). We normally attribute small shifts such as these to an *absence* of significant complexation. (Indeed, in a "control" binding experiment employing "3/4"-molecule **75** with guest **20**, ATMA, the largest observed upfield shifts are 6Hz, consistent with a lack of association by inclusion. Amazingly, MULTIFIT calculates K_a~1400M^{-1} (*larger* than guest **20** with host **71**) with very small *D* values (<20Hz).)

Structures of Host-Guest Complexes

With regard to host-guest structures, chemical-shift changes in 1,5-host **71** upon binding positively-charged, ammonium guests indicate an unanticipated change in host conformation to accommodate many

Table 4.2: Binding studies of guests exhibiting significant upfield shift the the presence of 1,5-PX host **71**. Comparison to 2,6-PX host **1**.[a]

guest	K_a[b] (M^{-1})	$-\Delta G°_{295}$[c] with host **71**	range of %G bound	range of %H bound	$-\Delta G°_{295}$[c,d] with host **1**
20	7.7×10^2	3.9	3-14	6-78	6.7
81	1.3×10^2	2.9	1-3	1-17	4.7
83	1.1×10^3	4.1	5-16	4-50	6.5
11	8.9×10^2	4.0	3-12	6-73	7.2
84	1.5×10^3	4.3	12-19	7-33	---

[a]Determined by ^{1}H NMR (400 MHz); [b]From MULTIFIT analysis; [c]Free energies of complexation (± 0.2 kcal/mol); [d]Reference 6.

differently shaped guests in a similar fashion. For comparison, 2,6-host **1** can adopt two different conformations[6] (Figure **4.8**) to bind guests, as discussed earlier (Chapter 1): the toroid conformation binds aliphatic guests (e.g., **20**); the rhomboid conformation binds flat, aromatic, naphthalene-sized guests (e.g., **11**). In contrast, CPK models suggest that 1,5-host **71** cannot adopt an analogous rhomboid conformation. However, it appeared that both aliphatic and flat, aromatic guests could be accommodated by the "sandwich" conformation of 1,5-host **71** (Figure **4.9**). The unexpected geometry change alluded to many times earlier involves the collapse of **71** into a "bowl" conformation.

To dissect the evidence for the "bowl" conformation, we shall consider adamantyltrimethylammonium (**20**, ATMA), which is a high-symmetry, water-soluble guest useful for probing host-guest structure.[25] The chemical-shift changes upon complexation of **20** with **AF** seem most consistent with the structure depicted in Figure **4.10**. ATMA is oriented with the trimethylammonium (TMA) group located *away from* the time-averaged, collapsed, bowl-shaped host. As evidence in support of this structure, for **71**, DEA protons ($H_{2,6}$, $H_{3,7}$, $H_{4,8}$, and $H_{9,10}$) shift downfield, while xylyl-linker protons (both methylene and aromatic) shift upfield;[26] for ATMA, C, D_1, and D_2 protons (Figure **4.11**) are shifted upfield most, then B protons, then A protons. This result contrasts sharply what has been found for ATMA (and other TMA guests) and 2,6-host **1** in aqueous[6] and organic[7] media. It appears that whereas it has been established clearly from *D* values (Table **4.3**) that the electron-rich 2,6-host **1** recognizes the TMA group (A protons of ATMA), it is much more difficult to rationalize the ability of the more electron-deficient 1,5-host **71** to recognize TMA

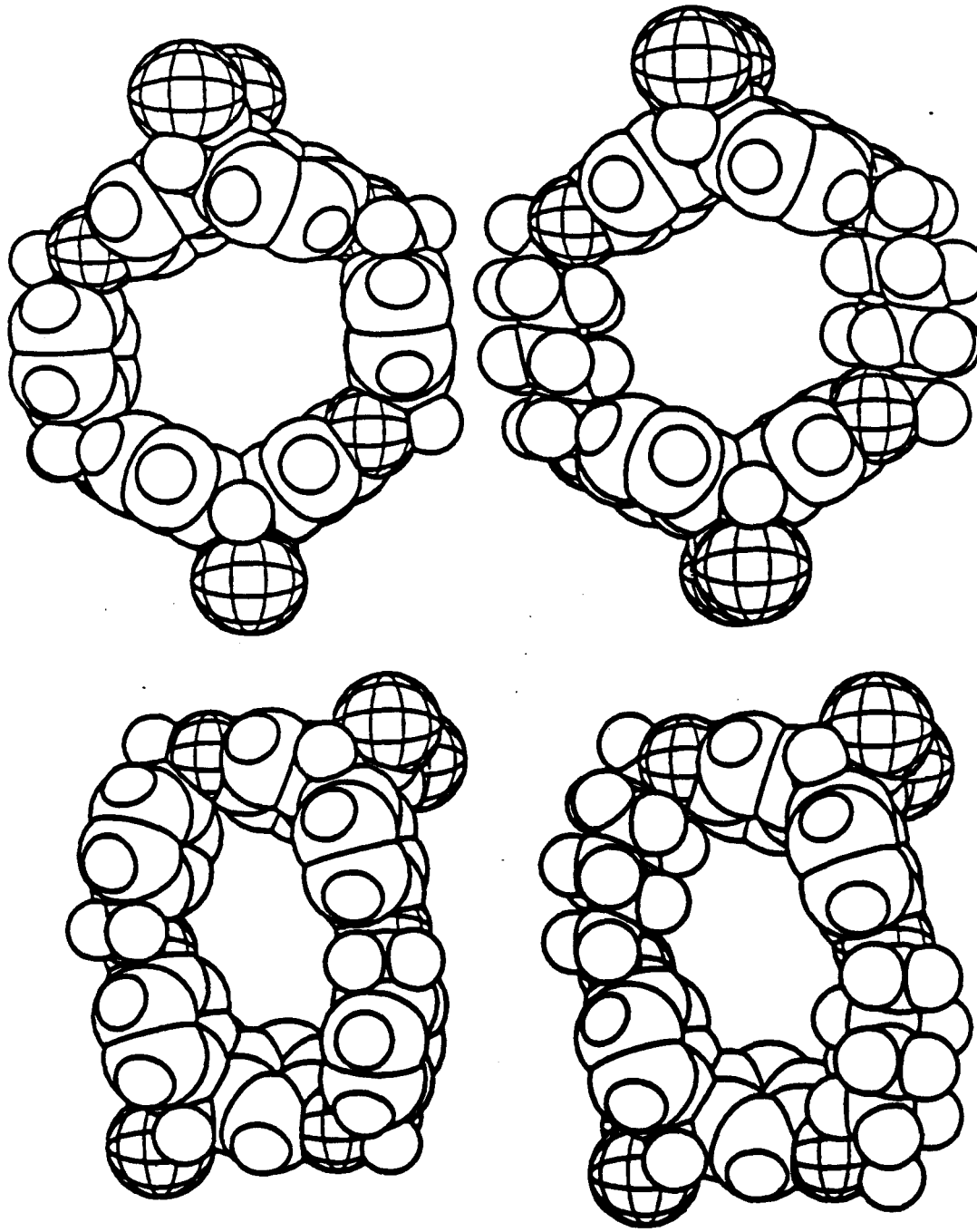

Figure 4.8. 2,6-Host conformations. **Top left**: host **1**, toroid conformation; **top right**: host **2**, toroid comformation; **bottom left**: host **1**, rhomboid conformation; **bottom right**: host **2**, rhomboid conformation.

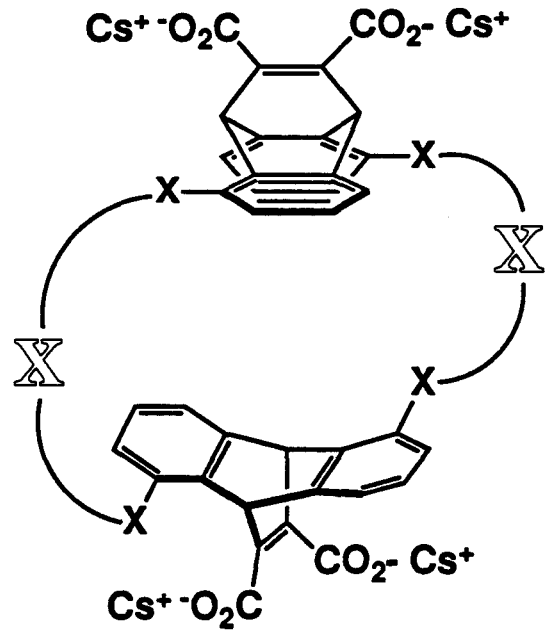

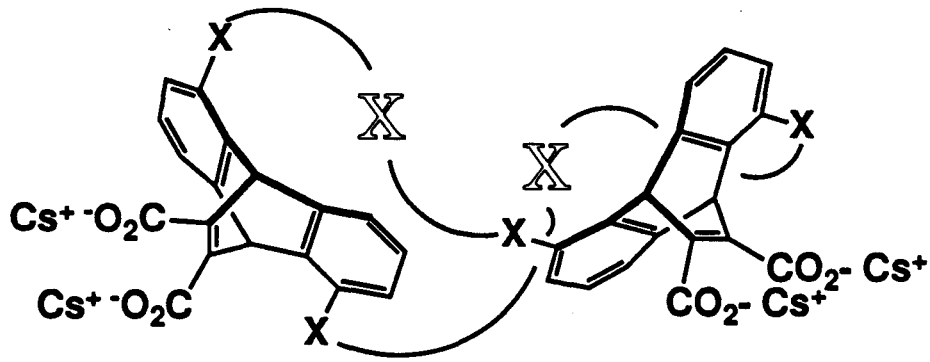

Figure 4.9. 1,5-Host conformations: host **71**. **Top**: "sandwich" conformation; **bottom**: "bowl" conformation.

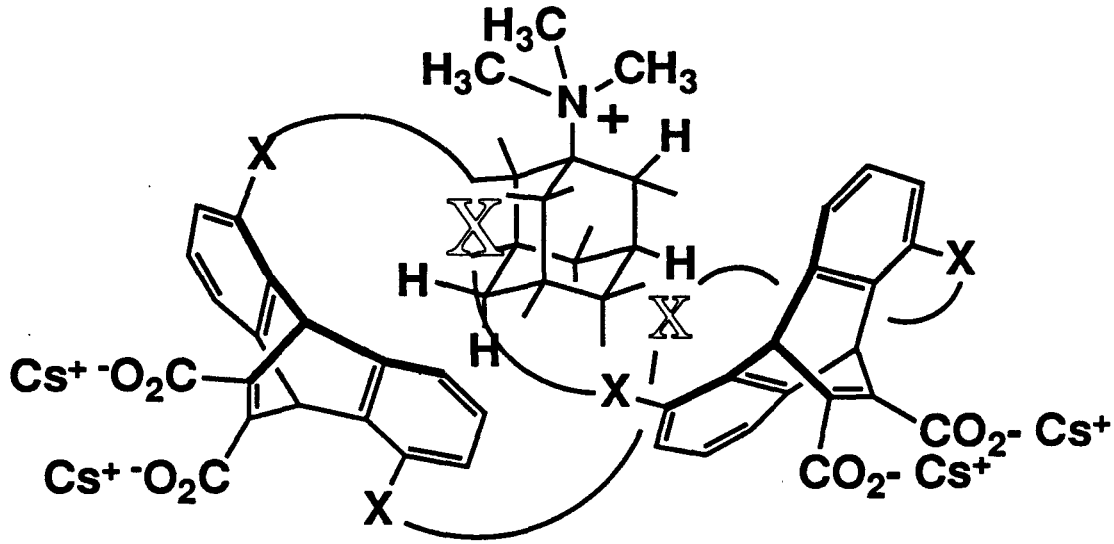

Figure 4.10. Host-guest structure for host **71** ("bowl" conformation) and guest **20** (ATMA).

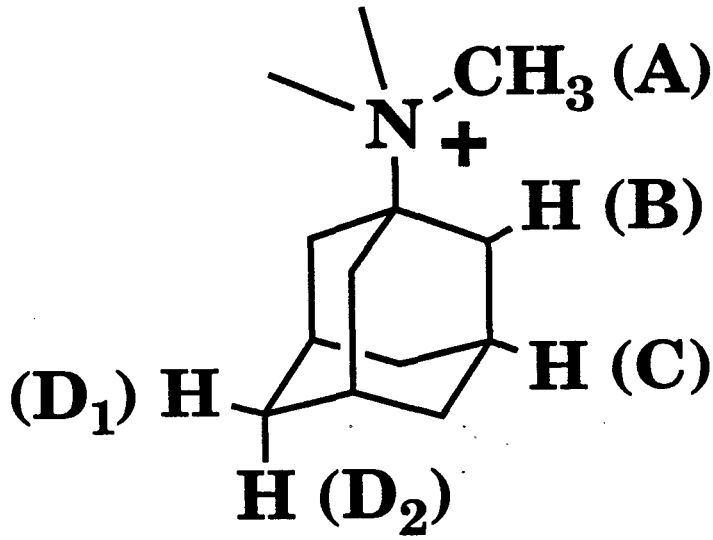

Figure 4.11. Guest **20** (ATMA) with protons labelled.

Table 4.3: *D* values for ATMA with hosts **1**, **27**, and **71**.[a]

proton[b]	**27**[c] in $CDCl_3$	**1**[d] in borate-*d*	**71**[e] in borate-*d*
A	2.99	1.87	1.34
B	2.92	2.99	2.18
C	1.11	1.18	2.58
D_1	1.07	1.29	2.56
D_2	0.67	0.73	2.46

[a]Maximum upfield shifts (ppm) for bound guest protons calculated with MULTIFIT; [b]For designation of protons, see Figure **4.11**; [c]Reference 7; [d]Reference 25; [e]Present work.

compounds (according to K_as) without binding the TMA group directly (according to the pattern of D values, Appendix 5).

The observation of sizeable shift changes in the 1,5-host in the presence of the *aliphatic* guest ATMA is unprecedented and thus marks a surprising deviation from previous binding studies with 2,6-hosts.[27] The only change observed for 2,6-host **1** upon binding ATMA (or other aliphatic guests) in aqueous[9] or organic[7] media is a slight downfield shift of the xylyl-linker protons, which is attributed to restricted rotation of the linker groups such that time-averaged shielding by the DEA units is reduced.

With all guests that exhibit significant, upfield, 1,5-host **71**-induced shifts, a similar host-shift pattern is observed as detailed above. However, it is not clear from guest-shift patterns whether precise host-guest orientations are involved, or if the guest is randomly-oriented in the time-averaged, host "bowl" conformation.

Aside from TMA guests, the present survey did not reveal any compelling evidence for binding by 1,5-host **71**. Several classes of guests exhibited insignificant shifting in the presence of **71** (Table **4.4**). Neutral, naphthalene-sized guests were used to probe favorable donor/acceptor π-stacking interactions: **3** and **6** are electron-deficient; **8** is electron-rich. Aliphatic guests **85** and **86**, and aromatic, nucleotide bases **87-89** revealed no hydrogen-bonding interactions. Carboxylate guests **90** and **91** were not bound in the electron-deficient host interior.

At this point, the ineffectiveness of 1,5-host **71** to bind significantly an array of organic guests in water (analogous to the 2,6-hosts) led us to question the amide-linker design. We surmised that the amides could be solvated favorably by water through hydrogen-bonding, such that it would be unfavorable energetically for a guest to displace water and thereby

Table 4.4: "Single-point" binding analysis for guests in the presence of 1,5-PX-host **71** in borate-*d*.[a]

guest	[H]o (μM)	[G]o (μM)	observed shift[b] (Hz)	observed proton
20	222	189	139	D_1 protons
10	172	358	131	H_4
11	177	168	116	H_1
81	177	74	35	$N(CH_3)_3$
82	176	393	44	N-CH_3
83	177	45	64	C7-CH_3
93	176	383	29	N-CH_3
94	175	384	37	N-CH_3
95	174	393	43	N-CH_3
96	169	380	28	CH_2
97	172	377	68	N-CH_3
3	167	365	8	H_4
6	173	234	16	H_5
8	177	122	12	H_7
84	173	64	12	D_1 protons
85	180	77	3	CH_2
86	177	390	0	CH_2
87	172	<379	0	
88	172	<380	3	H_6
89	174	398	3	H_5
90	169	378	2	C protons
91	177	378	3	CH_2

[a]Determined by ^{1}H NMR (400 MHz); [b]Positive, upfield position from chemical shift of free guest (for largest shifting proton).

desolvate the binding site. We have no physical evidence bearing upon the orientation of the amide groups in the macrocycle; however, CPK models suggest that an amide (in a rigid *E* conformation, Figure **4.12**) should point all four N-H groups into the host cavity. (The N-*H* protons are exchanged for deuteria in the borate-*d* buffer.) Directing one or more carbonyl groups into the host cavity introduces strain into the model. (Variable-temperature ^{1}H NMR analysis (25-60°C) of tetraester **55** gave no indication of a dynamic process such as hindered rotation about the C-N bonds of the amides.)

We therefore sought to take advantage of potential hydrogen-bonding interactions between 1,5-host **55** and donor/acceptor guests in an organic solvent. We hoped to determine if the amide functionality could be used for convergent hydrogen-bond-type recognition akin to the studies of Rebek[28] and Hamilton.[29] Guests **85** and **92** were surveyed for binding with host **55** in $CDCl_3$; additionally, guest **20** was studied as a point of reference. None of these guests exhibited significant shift changes (Table **4.5**) in the presence of **55**. Because of the low solubility of host **55** in $CDCl_3$, only "moderately strong" complexation (*ie* K_a>20M^{-1}) could have been demonstrated. Complete binding studies were therefore out of the question.

Discussion

Compared to the 2,6-hosts, the 1,5-hosts described above do not fulfill sufficiently the design criteria for water-soluble, hydrophobic binding sites. While these new hosts are readily soluble in water, they are too much so because of favorable hydration of the amide linkers. Although the incorporated water-solubilizing carboxylate groups are well-removed from the host cavity, the amides reduce the "net hydrophobicity" of the binding site.

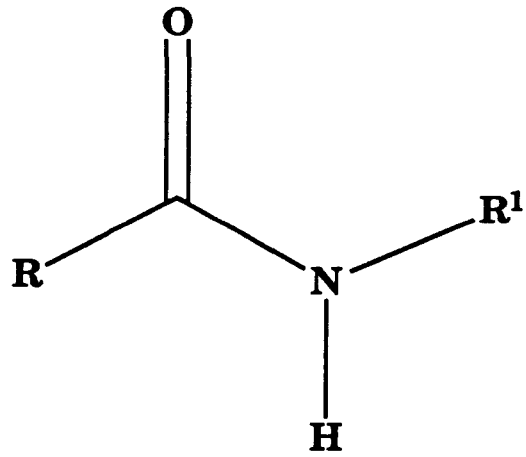

E-isomer

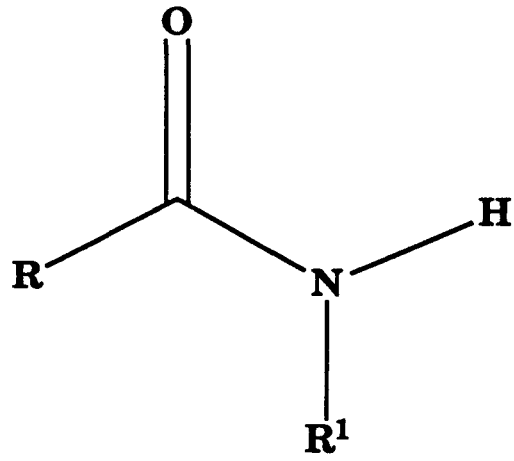

Z-isomer

Figure 4.12. Amide geometric (E/Z) isomers.

Table 4.5: "Single-point" binding analysis for guests in the presence of 1,5-PX-host **55** in $CDCl_3$.[a]

guest	[H]o (μM)	[G]o (μM)	observed shift[b] (Hz)	observed proton
20	206	448	2	A protons
85	206	392	-17	CH_2
92	206	310	53[c]	NH_2

[a]Determined by ^1H NMR (400 MHz); [b]Positive, upfield position from chemical shift of free guest (for largest shifting proton); [c]The amine protons of guest **92** exhibited concentration-dependent shifts in $CDCl_3$ in the *absence* of host **55**.

The synthesis of these new 1,5-hosts was achieved in a relatively high-yield, but more roundabout manner than in the case of the 2,6-hosts. Also, in contrast to the 2,6-hosts, the efficient synthesis of enantiomerically pure 1,5-hosts has thus far proven elusive. It is suggested that efforts toward this end be withheld until it is demonstrated convincingly (using racemic materials) that hydrophobic binding sites would be created. Nevertheless, a benefit of the synthetic approach taken here is the development of a series of DEA building blocks for the construction of hosts with even more pronounced hydrophobic character.

There is one final thorn in the side of the 1,5-host structure. While the binding sites designed herein are composed of topographically well-defined, rigid units to give a chiral host (with a "greater sense of twist"), the disposition of the 1,5-substituents allows the collapse of hosts into a "bowl" conformation. This is reminiscent of a problem encountered by Diederich and co-workers in their efforts to design and synthesize chiral, macrocyclic hosts.[30] These investigators had prepared a host structure that was found experimentally to fold back upon itself. Computer-modelling studies[31] suggested that the distance between (and the directionality of) substituents was crucial for connecting rigid building blocks via linkers (in a related fashion to the 1,5-hosts) to encapsulate efficiently guests in the binding site of the host. This observation leads us to speculate that the more successful high-symmetry, hydrophobic binding sites are to be found with 2,6-DEA-constructed hosts rather than with 1,5-DEA-constructed hosts.

Experimental for Chapter 4

Melting points (corrected) were recorded on a Thomas-Hoover melting point apparatus. NMR spectra were recorded on Varian EM-390, XL-200, JEOL JNM GX-400, or Bruker WM-500 spectrometers. Routine spectra were referenced to the residual proton and carbon signals of the solvents and are reported (ppm) downfield of 0.0 as δ values. Aqueous binding spectra were referenced to external TSP (0.00 ppm) in a coaxial tube. Infrared and ultraviolet spectra were recorded on Beckman or Shimadzu infrared spectrometers and a Hewlett-Packard 8451 diode array ultraviolet spectrometer, respectively. Optical rotations were recorded on a Jasco DIP-181 digital polarimeter at 293±2K. Flash chromatography was performed according to the method of Still *et al.*[24] HPLC and reverse-phase HPLC (RPHPLC) were performed on a Perkin-Elmer Series 2 liquid chromatograph. Preparative HPLC used a 1" X 25cm Vydac 101HS1022 silica column; analytical RPHPLC used a 5mm X 25cm Whatman Partisil ODS-3 C_{18} column. Electron-impact (EI), fast-atom bombardment (FAB), and high-resolution mass spectrometry (HRMS) were performed by the staff of the University of California, Riverside.

Solvents were distilled from drying agents as noted: dichloromethane, CaH_2; carbon tetrachloride, P_2O_5; toluene, sodium metal; tetrahydrofuran, sodium benzophenone ketyl. Dimethylformamide (DMF) was distilled *in vacuo* at ambient temperature from calcined CaO onto freshly activated 4Å sieves and stored over at least two successive batches of freshly activated 4Å sieves. Reagent-grade solvents were obtained from commercial sources, and were used without further purification.

Host and guest stock solutions for the nmr binding experiments were prepared with a standard 10mM deuterated cesium borate buffer at pD~9 (borate-*d*).[9] The buffer was prepared as described in Chapter 1. All volumetric measurements of aqueous solutions were made using adjustable volumetric pipets. The concentrations of host and guest stock solutions were quantified via nmr integrations against a stock solution of 3,3-dimethylglutarate (DMG, 4.20-4.23mM, vs potassium hydrogen phthalate, KHP) in borate-*d*. All pulse delays for the aqueous stock-solution-integration experiments (15-20s) were at least 5 times the measured T_1 for the species involved. All binding studies were performed at 400 MHz.

Guests **11**, **81**, and **83** were synthesized and characterized by Timothy Shepodd.[9] Guests **82** and **93-97** were synthesized and characterized by Michael Petti.[8] Other guests were obtained from commercial sources and were used without further purification.

1,5-Dicyanoanthraquinone (57)[18]

A mechanically stirred mixture of 1,5-dichloroanthraquinone (**56**, Aldrich, 96%, 98.7g, 342mmol), cuprous cyanide (81.1g, 906mmol), and benzyl cyanide (1000g) was heated at reflux under N_2 for 2h. The reaction mixture gradually became black and was allowed to cool overnight. The mixture was then filtered and washed well with benzene, leaving a gray solid. To a stirred suspension of this gray solid in H_2O (300mL) was added dropwise a 40% aqueous nitric acid solution (500mL) over 15min. (*Any evolved HCN gas was passed through a bleach bubbler.*) The mixture was heated at reflux under N_2 for 4h. After cooling overnight, the mixture was filtered and washed well with H_2O, and then with benzene. The dark

brown solid was dried *in vacuo* (74.46g, 87%); mp>355°C (lit.[18] mp>360°C); IR (nujol mull): 2210 (w); 1670 (m), 1460 (vs), 1370 (s) (lit.[18] ν_{CN}=2200 cm^{-1}).

1,5-Dicarboxyanthraquinone (58)[18]

To a mixture of 1,5-dicyanoanthraquinone (**57**, 37.34g, 144.7mmol) and concentrated H_2SO_4 (400mL) cooled in an ice-water bath under N_2 was added dropwise H_2O (80mL) over 15min. The mixture was heated at 180°C for 1.5h; upon cooling, the mixture was poured into H_2O (600mL) and cooled in ice. The resulting gray-black solid was filtered and washed with H_2O, then dried *in vacuo* over P_2O_5 (42.75g, 99%); mp>270°C (lit.[18] mp>360°C); IR (nujol mull): 2650 (br), 1690 (vs), 1580 (m), 1460 (s), (lit.[18] ν_{CO}=1690 cm^{-1}); ^1H NMR (200 MHz, d_6-DMSO) δ 7.84 (dd, 2H, J=1, 8Hz, $H_{4,8}$), 7.96 (t, 2H, J=8Hz, $H_{3,7}$), 8.23 (dd, 2H, J=1, 8Hz, $H_{2,6}$).

1,5-Dicarboxyanthracene (59)[18]

A mixture of 1,5-dicarboxyanthraquinone (**58**, 24.00g, 81.1mmol), excess zinc dust (50g), and 15% aqueous ammonia (1.2L) was heated at 85-90°C with stirring under N_2 for 6h. After cooling and filtering through a pad of Celite, the reaction mixture was acidified (pH<2) with concentrated hydrochloric acid. The resulting dark green solid was filtered and washed with H_2O, then dried *in vacuo* over P_2O_5 (20.36g, 94%); mp>270°C (lit.[18] mp>360°C); ^1H NMR (400 MHz, d_6-DMSO) δ 7.61 (dd, 2H, J=7, 8Hz, $H_{4,8}$), 8.25 (dd, 2H, J=1, 7Hz, $H_{3,7}$), 8.38 (d, 2H, J=8Hz, $H_{2,6}$), 9.61 (s, 2H, $H_{9,10}$).

1,5-Dicarbomethoxyanthracene (61)

To a mixture of 1,5-dicarboxyanthracene (**59**, 251mg, 0.94mmol) and cesium bicarbonate (Thiokol, 428mg, 2.2mmol) in dimethyl sulfoxide

(40mL) was added iodomethane (Aldrich, 99%, 1.0mL, 16mmol). The mixture was stirred at ambient temperature under N_2 for 20h, and monitored by tlc (8:1 (v/v) petroleum ether/ethyl acetate). The viscous orange solution was partitioned between H_2O (40mL) and CH_3CCl_3 (40mL). The aqueous layer was further extracted with CH_3CCl_3 (5x50mL). The combined organic layers were dried ($MgSO_4$) and concentrated. The resulting yellow solid was purified via flash chromatography on silica eluted with a gradient of 5% to 15% ethyl acetate/petroleum ether to afford **61** as fluorescent green, yellow needles (89mg, 32%); mp 170-175°C (lit.[18] mp 200-201°C); ^{1}H NMR (90 MHz, $CDCl_3$) δ 4.1 (s, 6H, CH_3), 7.6 (m, 2H), 8.3 (m, 4H), 9.7 (s, 2H, $H_{9,10}$). The Diels-Alder adduct of **61** with tetracyanoethylene (TCNE) was prepared by adding excess TCNE to the nmr sample: ^{1}H NMR (90 MHz, $CDCl_3$) δ 4.0 (s, 6H, CH_3), 6.9 (s, 2H, $H_{9,10}$), 7.6 (m, 2H), 7.8 (m, 2H), 8.1 (m, 2H).

1,5-Bis[hydroxymethyl]anthracene (60)

To a stirred suspension of 1,5-dicarboxyanthracene (**59**, 16.51g, 62.1mmol) in THF (325mL) cooled in an ice-water bath, under N_2, was added dropwise a solution of borane in THF[19] (Aldrich, 1.0*M*, 325mL, 325mmol) over 30min. The mixture was allowed to warm and was stirred at room temperature for 3d. Excess borane was destroyed via careful dropwise addition of THF/H_2O (1:1 (v/v), 100mL) over 1h. The mixture was saturated carefully with anhydrous potassium carbonate. The phases were separated; the organic layer was dried ($MgSO_4$) and concentrated, leaving a greenish brown solid. The product was recrystallized from methanol to afford **60** as golden green needles (7.73g, 52%); mp 226-227°C; ^{1}H NMR (400 MHz, d_6-DMSO) δ 5.10 (d, 4H, *J*=5Hz, CH_2), 5.39 (t, 2H, *J*=5Hz, O*H*), 7.48 (dd,

2H, J=7, 8Hz, $H_{3,7}$), 7.55 (d, 2H, J=7Hz, $H_{4,8}$), 8.02 (d, 2H, J=8Hz, $H_{2,6}$), 8.69 (s, 2H, $H_{9,10}$); ^{13}C NMR (100 MHz, d_6-DMSO) δ 61.19, 122.34, 122.91, 124.62, 127.46, 128.25, 130.84, 137.19; HRMS 238.0988, calcd for $C_{16}H_{14}O_2$ 238.0994.

1,5-Bis[*tert*-butyldimethylsilyloxymethyl]anthracene (33)

A stirred mixture of 1,5-bis[hydroxymethyl]anthracene (**60**, 3.56g, 15.0mmol), imidazole (Aldrich, 97%, 4.17g, 60.7mmol), and *tert*-butyldimethylsilyl chloride (Aldrich, 97%, 11.24g, 72.4mmol) in dry DMF[32] (125mL) was heated under N_2 at 120°C for 4h. After cooling, the mixture was concentrated via rotary evaporation *in vacuo*. Methanol (ca. 50mL) was added, and the product crystallized from solution when cooled in ice. Golden green needles were collected via filtration and washed well with methanol, then dried *in vacuo* (6.62g, 95%); mp 114-115°C; ^{1}H NMR (400 MHz, $CDCl_3$) δ 0.16 (s, 12H, $Si(CH_3)_2$), 0.97 (s, 18H, $SiC(CH_3)_3$), 5.32 (s, 4H, CH_2), 7.43 (dd, 2H, J=7, 9Hz, $H_{3,7}$), 7.56 (d, 2H, J=7Hz, $H_{4,8}$), 7.92 (d, 2H, J=9Hz, $H_{2,6}$), 8.53 (s, 2H, $H_{9,10}$); ^{13}C NMR (100 MHz, $CDCl_3$) δ -4.75, 26.25, 61.98, 63.68, 122.36, 122.82, 124.80, 127.91, 128.66, 131.43, 136.18.

1,5-Bis[*tert*-butyldimethylsilyloxymethyl]-9,10-dihydro-9,10-(1,2-dicarbomethoxy)ethenoanthracene (62)

A stirred solution of 1,5-bis[*tert*-butyldimethylsilyloxymethyl]-anthracene (**33**, 6.28g, 13.5mmol), dimethyl acetylenedicarboxylate (DMAD, Aldrich, 99%, 15mL, 120mmol), and trace BHT (ca. 50mg) in dry toluene (75mL) was heated at reflux under argon for 2d. The solvent was removed via rotary evaporation. Methanol (ca. 50mL) was added, and the product crystallized from solution upon cooling in ice. Fine white needles were collected via filtration and washed with methanol, then dried *in vacuo*

(6.75g, 82%); mp 126-127°C; ^{1}H NMR (400 MHz, $CDCl_3$) δ 0.03 (s, 6H, Si-CH_3), 0.10 (s, 6H, Si-CH_3), 0.92 (s, 18H, SiC(CH_3)$_3$), 3.76 (s, 6H, CO_2CH_3), 4.88 (AB, 4H, J=13Hz, Δν=47Hz, CH_2), 5.80 (s, 2H, $H_{9,10}$), 6.95 (t, 2H, J=7Hz, $H_{3,7}$), 7.01 (d, 2H, J=7Hz, $H_{4,8}$), 7.28 (d, 2H, J=7Hz, $H_{2,6}$); ^{13}C NMR (100 MHz, $CDCl_3$) δ -4.82, -4.70, 18.72, 26.26, 48.78, 52.44, 63.11, 122.97, 124.24, 124.68, 135.07, 141.73, 143.41, 146.78, 165.48; HRMS 608.2986, calcd for $C_{34}H_{48}O_6Si_2$ 608.2989.

1,5-Bis[hydroxymethyl]-9,10-dihydro-9,10-(1,2-dicarbomethoxy)etheno-anthracene (63)

A mixture of 1,5-bis[*tert*-butyldimethylsilyloxymethyl]-9,10-dihydro-9,10-(1,2-dicarbomethoxy)ethenoanthracene (**62**, 4.97g, 8.17mmol) in THF (50mL) and 5% aqueous HCl (50mL) was stirred under argon at ambient temperature for 48h, and monitored by tlc (10% methanol/chloroform). The brown biphasic solution was neutralized carefully with solid sodium bicarbonate. Excess bicarbonate was removed via filtration, and the filtrate phases were separated. The aqueous layer was washed with THF (4x50mL). The combined organic layers were dried ($MgSO_4$) and the solvent was removed via rotary evaporation. The remaining off-white solid was triturated with petroleum ether (2.89g, 93%); mp 200-202°C; ^{1}H NMR (400 MHz, $CDCl_3$) δ 3.70 (s, 6H, CO_2CH_3), 4.68 (d AB, 4H, J=5, 13Hz, Δν=31Hz, CH_2), 5.23 (t, 2H, J=5Hz, OH), 5.89 (s, 2H, $H_{9,10}$), 6.98 (t, 2H, J=7Hz, $H_{3,7}$), 7.03 (d, 2H, J=7Hz, $H_{4,8}$), 7.37 (d, 2H, J=8Hz, $H_{2,6}$); ^{13}C NMR (100 MHz, $CDCl_3$) δ 47.66, 52.31, 60.47, 122.56, 123.92, 124.22, 136.18, 141.58, 143.27, 146.27, 164.81.

1,5-Bis[bromomethyl]-9,10-dihydro-9,10-(1,2-dicarbomethoxy)etheno-anthracene (77)

To an ice-cooled solution of triphenylphosphine (Aldrich, 99%, 1.00g, 3.82mmol) in acetonitrile (40mL) under N_2 was added bromine (Baker, 200μL, 3.87mmol).[33,34] After the orange solution warmed to room temperature, 1,5-bis[hydroxymethyl]-9,10-dihydro-9,10-(1,2-dicarbomethoxy)ethenoanthracene (**63**, 667mg, 1.76mmol) was added from a solid-addition ampoule. The mixture was stirred at ambient temperature for 1h. The brown suspension was concentrated, then subjected to flash chromatography on silica eluted with CH_2Cl_2 to afford **77** as a white solid (846mg, 95%); mp 257-258°C; ^{1}H NMR (500 MHz, $CDCl_3/d_6$-DMSO) δ 3.7 (s, 6H, CO_2CH_3), 4.65 (AB, 4H, CH_2), 5.85 (s, 2H, $H_{9,10}$), 6.95 (t, 2H, $H_{3,7}$), 7.0 (d, 2H), 7.4 (d, 2H).

1,5-Diformyl-9,10-dihydro-9,10-(1,2-dicarbomethoxy)ethenoanthracene (64)

Preparation of tetrabutylammonium chromate: A solution of tetrabutylammonium chloride (Fluka, 97%, 2.37g, 8.27mmol) in H_2O (40mL) was poured at once into a rapidly stirring solution of chromium (III) trioxide (Mallinckrodt, dried over P_2O_5, 843mg, 8.43mmol) in H_2O (20mL).[20] The mixture was stirred at room temperature for 20min. The precipitated orange reagent was extracted with $CHCl_3$ (3x100mL), concentrated, then placed in an addition funnel and diluted to 30mL with $CHCl_3$.

The reagent solution was added dropwise over 45min to a stirred solution of 1,5-bis[hydroxymethyl]-9,10-dihydro-9,10-(1,2-dicarbomethoxy)-ethenoanthracene (**63**, 748mg, 1.97mmol) in 1:1 (v/v) $CHCl_3$/THF (30mL) heated at 60°C under argon. The mixture then was heated at 60°C for 4d.

After cooling, the reaction mixture was diluted with ether (60mL) and stirred for 15min, then poured onto saturated aqueous $NaHCO_3$ (30mL). The phases were separated and the aqueous layer was extracted with 2:1 (v/v) ether/$CHCl_3$ (2x60mL) and $CHCl_3$ (2x40mL). The combined organic layers were dried ($MgSO_4$) and concentrated. The product was purified via flash chromatography on silica eluted with 5% methanol/$CHCl_3$. The desired component (**64**, R_f=0.8, 10% methanol/$CHCl_3$) was isolated as a yellow solid (700mg, 95%); ^{1}H NMR (400 MHz, $CDCl_3$) δ 3.78 (s, 6H, CO_2CH_3), 6.99 (s, 2H, $H_{9,10}$), 7.21 (t, 2H, J=7Hz, $H_{3,7}$), 7.45 (dd, 2H, J=1, 8Hz, $H_{4,8}$), 7.67 (d, 2H, J=7Hz, $H_{2,6}$), 10.19 (s, 2H, C*H*O); ^{13}C NMR (100 MHz, d_6-DMSO) δ 48.26, 52.53, 125.20, 126.58, 126.62, 127.63, 144.37, 144.51, 146.23, 164.56, 166.90; HRMS 376.0949, calcd for $C_{22}H_{16}O_6$ 376.0947.

1,5-Dicarboxy-9,10-dihydro-9,10-(1,2-dicarbomethoxy)ethenoanthracene (65)

To a stirred mixture of 1,5-diformyl-9,10-dihydro-9,10-(1,2-dicarbomethoxy)ethenoanthracene (**64**, 1.42g, 3.78mmol) in 2-methyl-2-butene (10mL) and *tert*-butyl alcohol (40mL) was added dropwise under argon a solution of sodium chlorite (Aldrich, 80%, 1.83g, 16.2mmol) in pH 3.5 buffer (aq NaH_2PO_4, 6mL) over 5min.[21] The biphasic mixture was stirred vigorously at room temperature for 48h. The yellow solution was neutralized (pH 8) with saturated aqueous $NaHCO_3$ (20mL), then diluted with H_2O (10mL). The organic solvents were removed carefully via rotary evaporation. The remaining aqueous layer was washed with petroleum ether (80mL). To the aqueous layer was added 3:1 (v/v) ether/$CHCl_3$ (80mL); concentrated HCl then was added carefully until pH<2. The phases were separated and the aqueous layer was further extracted with 3:1 (v/v) ether/$CHCl_3$ (4x80mL). The combined ether/$CHCl_3$ layers were dried

($MgSO_4$) and concentrated *in vacuo*, leaving **65** as a white solid (1.45g, 94%); mp>270°C; ^{1}H NMR (400 MHz, d_6-DMSO) δ 3.70 (s, 6H, CO_2CH_3), 6.85 (s, 2H, $H_{9,10}$), 7.16 (t, 2H, J=8Hz, $H_{3,7}$), 7.59 (d, 2H, J=8Hz, $H_{4,8}$), 7.64 (d, 2H, J=7Hz, $H_{2,6}$); ^{13}C NMR (100 MHz, d_6-DMSO) δ 48.19, 52.48, 125.14, 126.51, 126.58, 127.57, 144.31, 144.43, 146.15, 164.49, 166.83; HRMS 408.0838, calcd for $C_{22}H_{16}O_8$ 408.0845.

1,5-Bis[succinimidyloxycarbonyl]-9,10-dihydro-9,10-(1,2-dicarbomethoxy)-ethenoanthracene (66)

To a stirred mixture of 1,5-dicarboxy-9,10-dihydro-9,10-(1,2-dicarbomethoxy)ethenoanthracene (**65**, 1.25g, 3.06mmol), *N*-hydroxysuccinimide (NHS, recrystallized from benzene, 1.07g, 9.30mmol), and 4-dimethylaminopyridine (DMAP, Aldrich, 99%, 109mg, 0.884mmol) in dioxane (30mL) under argon was added a solution of *N,N'*-dicyclohexylcarbodiimide (DCC) in CH_2Cl_2 (1.11*M*, 9.0mL, 10mmol) via syringe. The mixture was stirred at room temperature for 24h. Precipitated *N,N'*-dicyclohexylurea (DCU) was removed via filtration; the filtrate was concentrated via rotary evaporation, leaving a white solid. The product was recrystallized from $CHCl_3$/isopropanol to afford **66** as fine white needles (1.30g, 71%); mp 267-270°C (dec); ^{1}H NMR (400 MHz, $CDCl_3$) δ 2.92 (br s, 8H, CH_2), 3.77 (s, 6H, CO_2CH_3), 6.75 (s, 2H, $H_{9,10}$), 7.17 (t, 2H, J=8Hz, $H_{3,7}$), 7.69 (d, 2H, J=7Hz, $H_{4,8}$), 7.78 (d, 2H, J=8Hz, $H_{2,6}$); ^{13}C NMR (100 MHz, $CDCl_3$) δ 25.95, 49.12, 52.72, 121.13, 125.86, 127.40, 130.03, 144.79, 146.21, 146.27, 161.23, 164.51, 168.59.

1,5-Bis[*N*-propylcarboxamido]-9,10-dihydro-9,10-(1,2-dicarbomethoxy)-ethenoanthracene (72)

To a solution of 1,5-bis[succinimidyloxycarbonyl]-9,10-dihydro-9,10-(1,2-dicarbomethoxy)ethenoanthracene (**66**, 27.2mg, 0.0452mmol) in dry CH_2Cl_2 (30mL) under argon was added via syringe *n*-propylamine (Aldrich, 99+%, 9.0μL, 0.11mmol). The mixture was stirred at ambient temperature for 16h, then filtered through a pad of silica and washed with 10% methanol/chloroform. The filtrate was concentrated *in vacuo*, leaving a white solid (23mg, 104%). The product was recrystallized from $CHCl_3$/isopropanol to afford **72** as fine white plates; mp 265-267°C; ^{1}H NMR (400 MHz, $CDCl_3$) δ 1.01 (t, 6H, *J*=7Hz, γ-C*H*$_3$), 1.69 (sextet, 4H, *J*=7Hz, β-C*H*$_2$), 3.47 (m, 4H, α-C*H*$_2$), 3.78 (s, 6H, CO_2C*H*$_3$), 6.21 (s, 2H, *H*$_{9,10}$), 6.40 (t, 2H, *J*=5Hz, N*H*), 7.00 (t, 2H, *J*=8Hz, *H*$_{3,7}$), 7.19 (dd, 2H, *J*=1, 8Hz, *H*$_{4,8}$), 7.43 (d, 2H, *J*=7Hz, *H*$_{2,6}$); ^{13}C NMR (100 MHz, $CDCl_3$) δ 11.78, 23.17, 42.05, 49.55, 52.73, 124.09, 125.37, 126.13, 132.05, 141.57, 143.83, 146.56, 165.67, 167.52.

1,5-Bis[*N*-propylcarboxamido]-9,10-dihydro-9,10-(1,2-dicarboxylato)-ethenoanthracene, dicesium salt (73)

To a solution of **72** (9mg, 18μmol) in d_6-DMSO (0.7mL) was added a solution of cesium deuteroxide in D_2O (60μL, 0.8M) in an nmr tube. The tube was sonicated and shaken vigorously. NMR analysis showed diester hydrolysis was completed after 1h. The emulsion was dissolved in dd H_2O, then frozen and lyophilized. The residue was purified via ion-exchange chromatography (DOWEX, NH_4^+ form). UV-active fractions were combined and lyophilized, affording the dicarboxylic acid as fluffy white flakes. The water-soluble "half-molecule" **73** was prepared as a stock solution in borate-*d* (10.4mM); ^{1}H NMR (400 MHz, borate-*d*) δ 1.04 (t, 6H,

J=7Hz, γ-CH_3), 1.72 (sextet, 4H, J=7Hz, β-CH_2), 3.45 (dt, 4H, J=1, 7Hz, α-CH_2), 5.75 (s, 2H, $H_{9,10}$), 7.14 (t, 2H, J=8Hz, $H_{3,7}$), 7.16 (d, 2H, J=8Hz), 7.55 (dd, 2H, J=2,6Hz), NH exchanged for deuterium.

1,5-Bis[*N*-benzylcarboxamido]-9,10-dihydro-9,10-(1,2-dicarbomethoxy)-ethenoanthracene (74)

To a solution of 1,5-bis[succinimidyloxycarbonyl]-9,10-dihydro-9,10-(1,2-dicarbomethoxy)ethenoanthracene (**66**, 32mg, 0.053mmol) in dry CH_2Cl_2 (1mL) under argon was added benzylamine (Kodak, 20μL, 0.18mmol) and dry CH_2Cl_2 (1mL). The mixture was stirred at ambient temperature for 24h. The cloudy white mixture was diluted with saturated aqueous sodium bicarbonate (1mL). The aqueous layer was extracted with CH_2Cl_2; the combined organic layers were dried ($MgSO_4$) and concentrated *in vacuo*, leaving a white solid (90mg). The product was purified via flash chromatography on silica eluted with 2% methanol/chloroform to afford **74** as white flakes (26.3mg, 86%). The product also was recrystallized from $CHCl_3$/isopropanol to afford **74** as white flakes; mp 225-227°C; ^{1}H NMR (400 MHz, $CDCl_3$) δ 3.71 (s, 6H, $CO_2C$$H_3$), 4.69 (d AB, 4H, J=6, 15Hz, Δν=30Hz, N-CH_2), 6.24 (s, 2H, $H_{9,10}$), 6.67 (t, 2H, J=6Hz, NH), 7.00 (t, 2H, J=8Hz, $H_{3,7}$), 7.21 (d, 2H, J=8Hz, $H_{4,8}$), 7.30 (d, 2H, J=7Hz, $H_{2,6}$), 7.32-7.43 (m, 10H, phenyl groups); ^{13}C NMR (100 MHz, $CDCl_3$) δ 44.22, 49.35, 52.70, 124.03, 125.42, 126.31, 127.34, 127.67, 128.50, 131.58, 137.96, 141.87, 143.94, 146.54, 165.46, 167.28.

1,5-Bis[*N*-benzylcarboxamido]-9,10-dihydro-9,10-(1,2-dicarboxylato)-ethenoanthracene, dicesium salt (75)

To a solution of **74** (9mg, 15μmol) in d_6-DMSO (0.7mL) was added a solution of cesium deuteroxide in D_2O (50μL, 0.8M) in an nmr tube. The tube was sonicated and shaken vigorously. NMR analysis showed diester hydrolysis was completed after 2h. The emulsion was dissolved in dd H_2O, then frozen and lyophilized. The residue was purified via ion-exchange chromatography (DOWEX, NH_4^+ form). UV-active fractions were combined and lyophilized, affording the dicarboxylic acid as fluffy white flakes. The water-soluble "3/4-molecule" **75** was prepared as a stock solution in borate-*d* (7.65mM) ^{1}H NMR (400 MHz, borate-*d*) δ 4.68 (AB, 4H, J=15Hz, Δν=19Hz, N-CH_2), 5.74 (s, 2H, $H_{9,10}$), 7.12 (t, 2H, J=8Hz, $H_{3,7}$), 7.19 (d, 2H, J=8Hz, $H_{4,8}$), 7.40 (d, 2H, J=7Hz, $H_{2,6}$), 7.52 (s, 10H, phenyl groups), N*H* exchanged for deuterium.

Macrocycles–5C dimers (67 and 68)

<u>Preparation of bis(acid chloride):</u> A suspension of 1,5-dicarboxy-9,10-dihydro-9,10-(1,2-dicarbomethoxy)ethenoanthracene (**65**, 203mg, 0.498mmol) in CCl_4 (8mL) and excess oxalyl chloride (freshly distilled, 2mL) under nitrogen was heated at reflux for 3h. The mixture was concentrated *in vacuo*, leaving a yellow-white solid.

The crude bis(acid chloride) was dissolved in dry CH_2Cl_2 and placed in a 500mL, three-necked flask equipped with stirrer and reflux condenser under nitrogen. To this solution were added CH_2Cl_2 (ca. 250mL), pyridine (1mL), and 1,5-diaminopentane (Aldrich, 60μL, 0.514mmol). The solution, which became cloudy upon the addition of the diamine, was stirred at

ambient temperature for 5d, then concentrated *in vacuo*. The resultant orange solid was partially purified via flash chromatography on silica eluted with 15% methanol in 1:1 (v/v) ether/CH_2Cl_2. Further purification with a second flash chromatography step on silica eluted with a gradient of 3% to 12% methanol/CH_2Cl_2 afforded *separate* dimer diastereomers: higher R_f isomer **67** (17mg, 7%, R_f=0.4, 10% methanol/CH_2Cl_2) ^{1}H NMR (400 MHz, $CDCl_3/d_6$-DMSO) δ 1.52 (m, 4H, γ-CH_2), 1.74 (m, 8H, Δν~31Hz, β-CH_2), 3.59 (m, 8H, Δν~100Hz, α-CH_2), 3.64 (s, 12H, CO_2CH_3), 5.85 (t, 4H, *J*=8Hz, $H_{3,7}$), 6.17 (s, 4H, $H_{9,10}$), 6.73 (d, 4H, *J*=8Hz), 6.99 (d, 4H, *J*=7Hz), 7.89 (t, 4H, *J*=5Hz, N*H*); ^{1}H NMR (400 MHz, d_5-pyridine) δ 1.78 (m, 4H, γ-CH_2), 1.88 (m, 8H, Δν~80Hz, β-CH_2), 3.54 (s, 12H, CO_2CH_3), 3.70 (m, 8H, Δν~165Hz, α-CH_2), 5.98 (t, 4H, *J*=8Hz, $H_{3,7}$), 7.00 (s, 4H, $H_{9,10}$), 7.13 (d, 4H, *J*=8Hz), 7.31 (d, 4H, *J*=7Hz), 8.62 (t, 4H, *J*=5Hz, N*H*); ^{1}H NMR (400 MHz, d_6-DMSO) δ 1.46 (m, 4H, γ-CH_2), 1.67 (m, 8H, β-CH_2), 3.36 (m, 8H, Δν~170Hz, α-CH_2), 3.67 (s, 12H, CO_2CH_3), 6.01 (t, 4H, *J*=8Hz, $H_{3,7}$), 6.15 (s, 4H, $H_{9,10}$), 6.75 (d, 4H, *J*=8Hz), 7.03 (d, 4H, *J*=7Hz), 8.12 (t, 4H, *J*=6Hz, N*H*); ^{13}C NMR (100 MHz, $CDCl_3/d_6$-DMSO) δ 23.64, 28.74, 38.32, 48.05, 51.85, 123.08, 123.36, 124.80, 131.06, 141.55, 143.55, 145.77, 164.45, 166.78; EI/MS 948 (M^+); lower R_f isomer **68** (12mg, 5%, R_f=0.3, 10% methanol/CH_2Cl_2) ^{1}H NMR (400 MHz, $CDCl_3/d_6$-DMSO) δ 1.58 and 1.69 (m, 12H, β– and γ-CH_2), 3.42 (m, 8H, Δν~182Hz, α-CH_2), 3.69 (s, 12H, CO_2CH_3), 5.87 (t, 4H, *J*=8Hz, $H_{3,7}$), 6.13 (s, 4H, $H_{9,10}$), 6.73 (d, 4H, *J*=8Hz), 6.98 (d, 4H, *J*=7Hz), 7.97 (t, 4H, *J*=5Hz, N*H*); ^{1}H NMR (400 MHz, d_5-pyridine) δ 1.78 (m, 4H, γ-CH_2), 1.86 (m, 8H, β-CH_2), 3.54 (s, 12H, CO_2CH_3), 3.70 (m, 8H, Δν~280Hz, α-CH_2), 6.15 (t, 4H, *J*=8Hz, $H_{3,7}$), 6.95 (s, 4H, $H_{9,10}$), 7.16 (d, 4H, *J*=7Hz), 7.40 (d, 4H, *J*=7Hz), 8.66 (dd, 4H, *J*=4, 7Hz, N*H*); ^{1}H NMR (400 MHz, d_6-DMSO) δ 1.54 (m, 4H, γ-CH_2), 1.65 (m, 8H, β–CH_2), 3.38 (m, 8H, Δν~200Hz, α-CH_2), 3.67 (s, 12H, CO_2CH_3), 5.71 (t, 4H,

J=7Hz, $H_{3,7}$), 6.12 (s, 4H, $H_{9,10}$), 6.73 (d, 4H, J=8Hz), 6.98 (d, 4H, J=7Hz), 8.20 (t, 4H, J=6Hz, NH); ^{13}C NMR (100 MHz, $CDCl_3/d_6$-DMSO) δ 22.07, 27.55, 37.33, 48.07, 51.72, 122.97, 123.35, 124.68, 130.77, 141.92, 143.50, 145.77, 164.29, 166.88; EI/MS 948 (M^+).

Water-soluble macrocycles--5C dimers (69 and 70)

To a solution of **67** (13mg, 14μmol) or **68** (11mg, 12μmol) in d_6-DMSO (0.7mL) was added a solution of cesium deuteroxide in D_2O (80μL, 0.85M) in an nmr tube. Each tube was sonicated and shaken vigorously. NMR analysis showed each tetraester hydrolysis was completed after 10min. Each emulsion was dissolved in dd H_2O, then frozen and lyophilized. Each brownish yellow residue was purified via ion-exchange chromatography (DOWEX, NH_4^+ form). UV-active fractions were combined and lyophilized, affording each tetracarboxylic acid as fluffy white flakes. Following a study of their respective critical aggregation concentrations (CACs), the water-soluble macrocycles were prepared as stock solutions in borate-d; **69** (2.89mM) ^{1}H NMR (400 MHz, borate-d) δ 1.63 (m, 4H, γ-CH_2), 1.85 (m, 8H, β–CH_2), 3.60 (m, 8H, Δν~76Hz, α-CH_2), 5.78 (s, 4H, $H_{9,10}$), 5.96 (t, 4H, J=8Hz, $H_{3,7}$), 6.67 (d, 4H, J=8Hz), 7.08 (d, 4H, J=7Hz); **70** (1.94mM) ^{1}H NMR (400 MHz, borate-d) δ 1.63 (m, 4H, γ-CH_2), 1.81 (m, 8H, β–CH_2), 3.56 (m, 8H, Δν~147Hz, α-CH_2), 5.86 (s, 4H, $H_{9,10}$), 5.98 (t, 4H, J=8Hz, $H_{3,7}$), 6.76 (d, 4H, J=8Hz), 7.05 (d, 4H, J=7Hz).

Macrocycles--PX dimers (55)

<u>Preparation of bis(acid chloride):</u> A suspension of 1,5-dicarboxy-9,10-dihydro-9,10-(1,2-dicarbomethoxy)ethenoanthracene (**65**, 408mg, 1.00mmol)

in dry THF (20mL) and excess thionyl chloride (freshly distilled, 2mL) under argon was heated at reflux for 2.5h. The mixture was rotary evaporated, then taken up in benzene and reconcentrated (twice), leaving a yellow-white solid. The crude bis(acid chloride) was dissolved in dry CH_2Cl_2 (25mL) and placed into an addition funnel. A solution of *p*-xylylene diamine (recrystallized from benzene, 142mg, 1.04mmol) in dry CH_2Cl_2 (25mL) was placed into a second addition funnel.

To an oven-dried 500mL, three-necked reaction flask equipped with stirrer and reflux condenser under argon were added 4Å sieves, 10% diisopropylethylamine/CH_2Cl_2 (25mL), and dry CH_2Cl_2 (225mL). The reaction flask was cooled in an ice-water bath. The contents of both addition funnels were added simultaneously and at approximately equal rates over 90min. The mixture was allowed to warm to room temperature and stirred for 2d. The sieves were removed via filtration. The solvent was removed via rotary evaporation and the residue was dried *in vacuo*. The residue was partitioned between CH_2Cl_2 (50mL) and half-saturated aqueous sodium bicarbonate (30mL). The aqueous layer was further extracted with CH_2Cl_2 (3x50mL), and the combined organic layers were dried ($MgSO_4$) and concentrated. The residue was dry-loaded onto silica and purified via flash chromatography on silica eluted with a gradient of 2% to 10% methanol in 1:1 (v/v) ether/CH_2Cl_2. Of the two highest R_f spots on tlc, only the higher spot was isolated as a dimer (white film); the lower spot was contaminated with higher oligomers; higher R_f isomer **55** (18mg, 9%): ^{1}H NMR (400 MHz, d_6-DMSO) δ 3.70 (s, 12H, CO_2CH_3), 3.96 (dd, 4H, J=4, 14Hz, half of CH_2), 4.84 (dd, 4H, J=8, 14Hz, half of CH_2), 6.44 (s, 4H, $H_{9,10}$), 7.02 (t, 4H, J=8Hz, $H_{3,7}$), 7.19 (s, 8H, xylyl-H), 7.20 (d, 4H, J=8Hz), 7.39 (d, 4H, J=7Hz), 8.70 (dd, 4H,

J=4, 8Hz, N*H*); ^{13}C NMR (100 MHz, d_6-DMSO) δ 42.26, 47.88, 52.38, 123.67, 124.73, 125.61, 127.22, 131.33, 138.28, 143.29, 144.73, 146.45, 165.08, 166.41; FAB/MS 1039 (M-Na+).

Water-soluble macrocycles--PX dimer (71)

To a solution of **55** in d_6-DMSO (0.7mL) was added a solution of cesium deuteroxide in D_2O (120μL, 0.85M) in an nmr tube. The tube was sonicated and shaken vigorously. NMR analysis showed tetraester hydrolysis was completed. The emulsion was dissolved in dd H_2O, then frozen and lyophilized. The residue was purified via ion-exchange chromatography (DOWEX, NH_4^+ form). UV-active fractions were combined and lyophilized, affording the tetracarboxylic acid as fluffy white flakes. Following a study of its critical aggregation concentration (CAC), the water-soluble macrocycle was prepared as a stock solution in borate-*d*; **71** (3.36mM) ^1H NMR (400 MHz, borate-*d*) δ 4.37 (CH_2), 5.59 (s, $H_{9,10}$), 6.49 (m, $H_{2,6}$ and $H_{3,7}$), 7.04 (m, $H_{4,8}$), 7.60 (s, xylyl-*H*).

References to Chapter 4

(1) (a) Lehn, J.-M. *Science* **1985**, *227*, 849-856; (b) Cram, D. J. *Angew. Chem. Int. Ed. Engl.* **1986**, *25*, 1039-1134; (c) Cram, D. J.; Lam, P. Y.-S.; Ho, S. P. *J. Am. Chem. Soc.* **1986**, *106*, 839-841.

(2) (a) Bender, M. L.; Komiyama, M. *Cyclodextrin Chemistry*; Springer-Verlag: Berlin, 1978; (b) Saenger, W. *Angew. Chem. Int. Ed. Engl.* **1980**, *19*, 344-362.

(3) Odashima, K.; Itai, A.; Iitaka, Y.; Koga, K. *J. Am. Chem. Soc.* **1980**, *102*, 2504-2505.

(4) (a) Takahashi, I.; Odashima, K.; Koga, K. *Tetrahedron Lett.* **1984**, *25*, 973-976, and references therein; (b) Dhaenens, M.; Lacombe, L.; Lehn, J.-M.; Vigneron, J. P. *J. Chem. Soc., Chem. Commun.* **1984**, 1097-1099; (c) Vogtle, F.; Muller, W. M.; Werner, U.; Losensky, H.-W. *Angew. Chem. Int. Ed. Engl.* **1987**, *26*, 901-903, and references therein; (d) Jarvi, E. T.; Whitlock, H. W. *J. Am. Chem. Soc.* **1982**, *104*, 7196-7204; (e) Breslow, R.; Czarnik, A. W.; Lauer, M.; Leppkes, R.; Winkler, J.; Zimmerman, S. *J. Am. Chem. Soc.* **1986**, *108*, 1969-1979; (f) O'Krongly, D.; Denmeade, S. R.; Chiang, M. Y.; Breslow, R. *J. Am. Chem. Soc.* **1985**, *107*, 5544-5545; (g) Gutsche, C. D. *Acc. Chem. Res.* **1983**, *16*, 161-170; (h) Canceill, J.; Lacombe, L.; Collet, A. *J. Chem. Soc., Chem. Commun.* **1987**, 219-221; (i) Schneider, H.-J.; Philippi, K.; Pohlmann, J. *Angew. Chem. Int. Ed. Engl.* **1984**, *23*, 908-909; (j) Murakami, Y.; Kikuchi, J.-I.; Suzuki, M.; Takaki, R. *Chem. Lett.* **1984**, 2139-2142; (k) Tobe, Y.; Fujita, H.; Wakai, I.; Terashima, K.; Kobiro, K.; Kakiuchi, K.; Odaira, Y. *J. Chem. Soc., Perkin Trans. 1* **1984**, 2681-2684; (l) Saigo, K.; Lin, R.-J.; Kubo, M.; Youda, A.; Hasegawa, M. *J. Am. Chem. Soc.* **1986**, *108*, 1996-2000;

(m) Wilcox, C. S.; Greer, L. M.; Lynch, V. *J. Am. Chem. Soc.* **1987**, *109*, 1865-1867.

(5) Diederich, F. *Angew. Chem. Int. Ed. Engl.* **1988**, *27*, 362-386.

(6) Petti, M. A.; Shepodd, T. J.; Barrans, R. E., Jr.; Dougherty, D. A. *J. Am. Chem. Soc.* **1988**, *110*, 6825-6840.

(7) Stauffer, D. A.; Dougherty, D. A. *Tetrahedron Lett.* **1988**, *29*, 6039-6042.

(8) Petti, M. A. Ph. D. Thesis, California Institute of Technology, 1988.

(9) Shepodd, T. J. Ph. D. Thesis, California Institute of Technology, 1988.

(10) Cram, D. J. *Angew. Chem. Int. Ed. Engl.* **1986**, *25*, 1039-1134.

(11) This terminology has been used also to describe optically active chromophores; see Mislow K. *Introduction to Stereochemistry*; W. A. Benjamin: Menlo Park, CA, 1965; pp 64-67.

(12) Petti, M. A.; Shepodd, T. J.; Dougherty, D. A. *Tetrahedron Lett.* **1986**, *27*, 807-810.

(13) (a) Franke, J.; Vogtle, F. *Top. Curr. Chem.* **1986**, *132*, 135-170; (b) Tabushi, I.; Yamamura, K. *Top. Curr. Chem.* **1983**, *113*, 145-183.

(14) (a) van Keulen, B.; Kellogg, R. M.; Piepers, O. *J. Chem. Soc., Chem. Commun.* **1979**, 285-286; (b) Dijkstra, G.; Kruizinga, W. H.; Kellogg, R. M. *J. Org. Chem.* **1987**, *52*, 4230-4234.

(15) Okuno, Y.; Horita, K.; Yonemitsu, O.; Shibata, K.; Amemiya, T. *J. Chem. Soc., Perkin Trans. 1* **1984**, 1115-1118.

(16) Anet, F. A. L.; Miura, S. S.; Siegel, J.; Mislow, K. *J. Am. Chem. Soc.* **1983**, *105*, 1419-1426.

(17) (a) Tanford, C. *The Hydrophobic Effect*, 2nd ed.; Wiley: New York, 1980; (b) Jencks, W. P. *Catalysis in Chemistry and Enzymology*;

McGraw-Hill: New York, 1969; (c) Saenger, W. *Angew. Chem. Int. Ed. Engl.* **1980**, *19*, 344-362.

(18) Kuritani, M.; Sakata, Y.; Ogura, F.; Nakagawa, M. *Bull. Chem. Soc. Jpn.* **1973**, *46*, 605-610.

(19) Yoon, N. M.; Pak, C. S.; Brown, H. C.; Krishnamurthy, S.; Stocky, T. P. *J. Org. Chem.* **1973**, *38*, 2786-2792.

(20) Bal, B. S.; Childers, W. E., Jr.; Pinnick, H. W. *Tetrahedron* **1981**, *37*, 2091-2096.

(21) Cacchi, S.; LaTorre, F.; Misiti, D. *Synthesis* **1979**, 356-359.

(22) Stewart, J. M.; Young, J. D. *Solid Phase Peptide Synthesis*; 2nd ed.; Pierce Chemical: Rockford, IL, 1984.

(23) Okuno, Y.; Horita, K.; Yonemitsu, O.; Shibata, K.; Amemiya, T. *J. Chem. Soc., Perkin Trans. 1* **1984**, 1115-1118.

(24) Still, W. C.; Kahn, M.; Mitra, A. *J. Org. Chem.* **1978**, *43*, 2923-2925.

(25) Shepodd, T. J.; Petti, M. A.; Dougherty, D. A. *J. Am. Chem. Soc.* **1986**, *108*, 6085-6087.

(26) This shift pattern, with slight changes in the magnitudes of the shifts, is upheld for both aliphatic and aromatic guests (see Appendix 5).

(27) The rhomboid host **1** conformation (Chapter 1) is evidenced by upfield shifts of all aromatic host protons (under the influence of naphthalene-sized guests), except for $H_{4,8}$, which shift *downfield*.

(28) (a) Rebek, J., Jr. *Science (Washington, D. C.)* **1987**, *235*, 1478-1484; (b) Rebek, J., Jr.; Askew, B.; Ballester, P.; Buhr, C.; Jones, S.; Nemeth, D.; Williams, K. *J. Am. Chem. Soc.* **1987**, *109*, 5033-5035.

(29) Hamilton, A. D.; van Engen, D. *J. Am. Chem. Soc.* **1987**, *109*, 5035-5036.

(30) Rubin, Y.; Dick, K.; Diederich, F.; Georgiadis, R. M. *J. Org. Chem.* **1986**, *51*, 3270-3276.

(31) Dharanipragada, R.; Ferguson, S. B.; Diederich, F. *J. Am. Chem. Soc.* **1988**, *110*, 1679-1690.

(32) Corey, E. J.; Venkateswarlu, A. *J. Am. Chem. Soc.* **1972**, *94*, 6190-6191.

(33) *Org. Syn. Coll. Vol. V* **1973**, *5*, 249-251.

(34) Wiley, G. A.; Hershkowitz, R. L.; Rein, B. M.; Chung, B. C. *J. Am. Chem. Soc.* **1964**, *86*, 964-965.

Appendix 1

Attempted Catalysis of Intramolecular Diels-Alder Reactions

Prior to the successful host-catalyzed alkylation reactions described in Chapter 3, we attempted to use host **1** to catalyze intramolecular Diels-Alder (iDA) reactions in a manner analogous to the work with cyclodextrins.[1] We hoped to use the proximity effect[2] whereby binding of the quaternary ammonium functionality would bring the diene and dienophile together within the receptor. Because **1** has a strong affinity for quaternary ammonium compounds via the ion-dipole effect (Chapters 1 and 2), a tetraalkylammonium group was chosen as the delivery agent for the diene and dienophile. Additionally, we sought to take advantage of the chiral environment provided in the cavity of the D_2-symmetric host to induce enantioselectivity for the products of an achiral substrate (Figure **A1.1**). Because the generalized iDA reaction[3] is an intramolecular addition to a π system, it therefore has a helical transition state, which could potentially match the topography of the helical catalytic site of host **1**.

Compound **98** was the prototypical iDA substrate: it reacted at a "convenient" rate (Chapter 3) in water;[4] a series of analogs (Figure **A1.2**) was readily synthesized (Figures **A1.3** and **A1.4**). Binding studies of the iDA substrates and products revealed K_as in the range 10^3-$10^4 M^{-1}$ (Table **A1.1**), indicating that the quaternary ammonium group indeed delivered the substrate to the putative catalytic site.

Rate enhancement for the iDA reactions was expected to result from two effects. First, as discussed above, the proximity effect should force diene and dienophile together. Second, host **1** should stabilize the diffuse, polarized transition state (Chapter 3) typical of an unsymmetrical Diels-Alder reaction.[3]

The conversion of iDA substrates **98**, **99**, and **100** to their respective products (**101**, **102**, and **103**) was each monitored by nmr in side-by-side

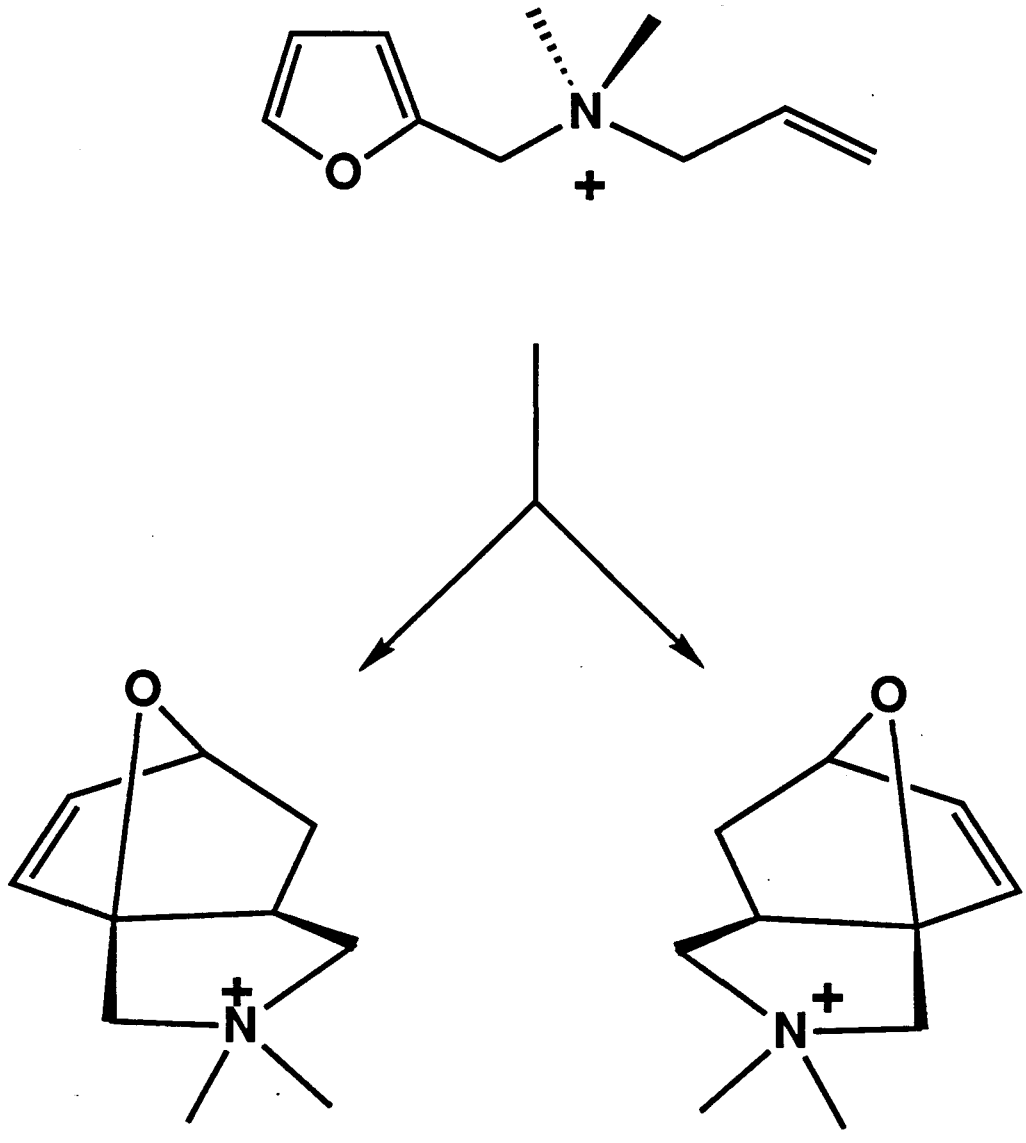

Figure A1.1. Intramolecular addition to a π system: iDA of an achiral substrate gives a racemic, chiral product.

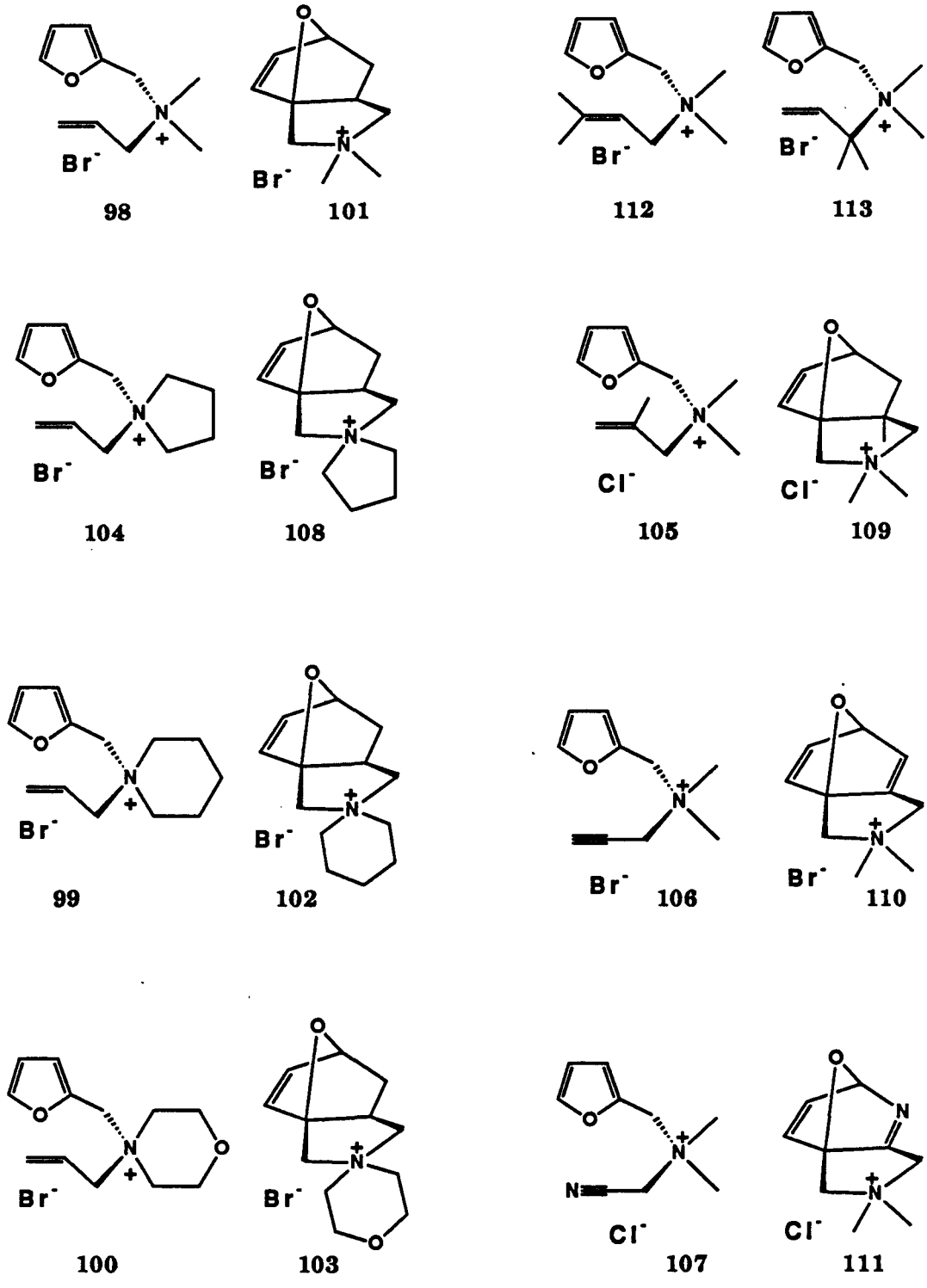

Figure A1.2. Tetraalkylammonium intramolecular Diels-Alder substrates and products.

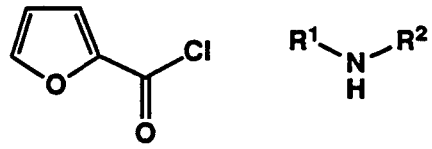

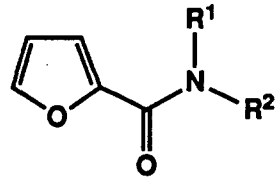

114: R^1=H, R^2=allyl
115: R^1=R^2=CH_3
116: R^1,R^2=$(CH_2)_4$
117: R^1,R^2=$(CH_2)_5$
118: R^1,R^2=$(CH_2)_2$-O-$(CH_2)_2$

$LiAlH_4$

THF

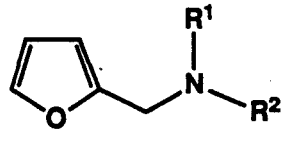

119: R^1=R^2=CH_3
120: R^1,R^2=$(CH_2)_4$
121: R^1,R^2=$(CH_2)_5$
122: R^1,R^2=$(CH_2)_2$-O-$(CH_2)_2$

Figure A1.3. Synthetic scheme for amine precursors to iDA dialkylallylfuranylammonium substrates.

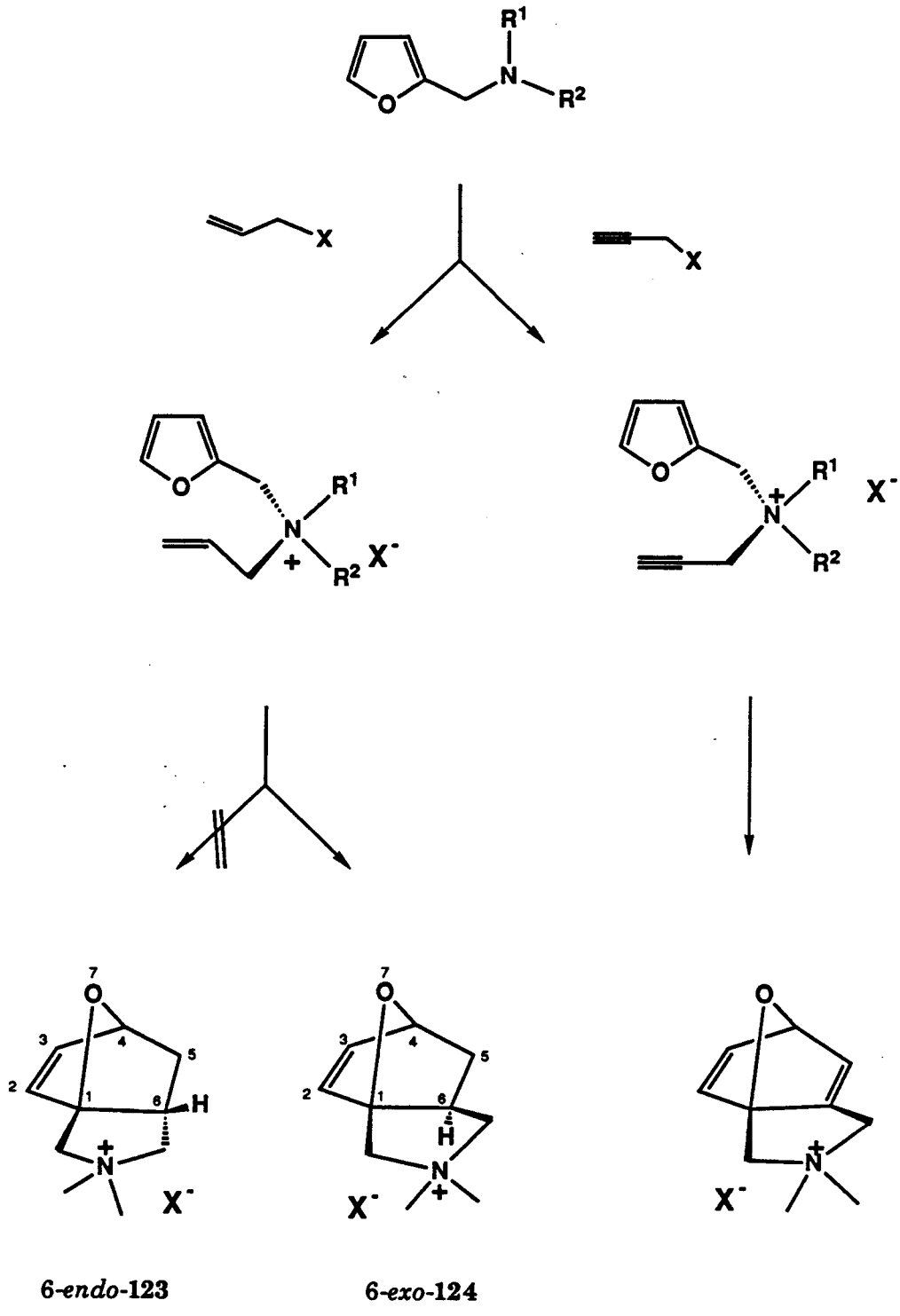

6-*endo*-123 6-*exo*-124

Figure A1.4. Synthetic scheme for series of iDA dialkylallylfuranylammonium substrates; stereochemistry of products obtained in iDA reaction.

Table A1.1: Binding parameters for iDA substrates and products with host **1** in borate-*d*.

substrate	K_a[a] (M^{-1})	$-\Delta G°_{295}$[b] (kcal/mol)	product	K_a[a] (M^{-1})	$-\Delta G°_{295}$[b] (kcal/mol)
98	4260	4.9	**101**	2280	4.6
99	3610	4.8	**102**	6170	5.2
100	2570	4.6	**103**	2510	4.6
104	2300	4.6	**108**	1940	4.5
105	8470	5.3	**109**	N/A[c]	
106	13900	5.6	**110**	8650	5.4
107	4420	5.0	**111**	N/A[d]	

[a]From MULTIFIT analysis of nmr chemical shift data (400MHz); [b]Ambient temperature not recorded, 295±2K; [c]Only obtained ca. 85% **105** conversion to product; [d]Product not stable at room temperature, undergoes retro-iDA reaction to **107**.

reactions with and without host **1**. Of the two possible diastereomers from **98** and its analogs, only the 6-*exo*, bridgehead-substituted adduct (**124**) was observed (Figure **A1.4**).[3] In all three cases, there were no significant increases or decreases in the rates of the iDA reactions. Additionally, careful examination of product peaks revealed both enantiomers were formed in nearly identical amounts. Hence, we observed no rate enhancement and no enantioselectivity.

The absence of an appreciable rate change indicated the possibility of unproductive binding between iDA substrates and host **1**. ^{1}H-^{1}H Decoupling was employed to assign protons in the nmr spectra (Figure **A1.5**; see also Appendix 5). The host **1**-induced chemical shift patterns for substrate **98** and product **101** were consistent with **98** bound in either a linear, extended conformation, or a conformation that would lead to the disfavored 6-*endo*, bridgehead-substituted adduct (**123**).

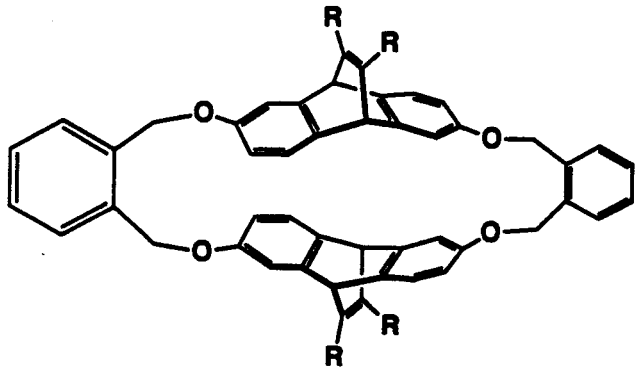

125: R = CO_2^- Cs^+

126: R = CO_2Me

CPK models suggested that perhaps the cavity of host **1** was *too large* to force **98** and its analogs into a *productive* conformation to catalyze the iDA reaction. We therefore turned our attention to a receptor with a smaller cavity: host **125** may force the diene and dienophile together upon binding the quaternary ammonium group only. Macrocyclization of **29** and

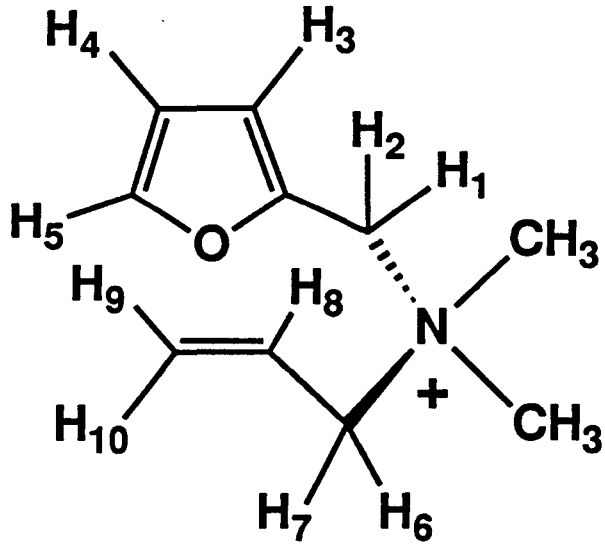

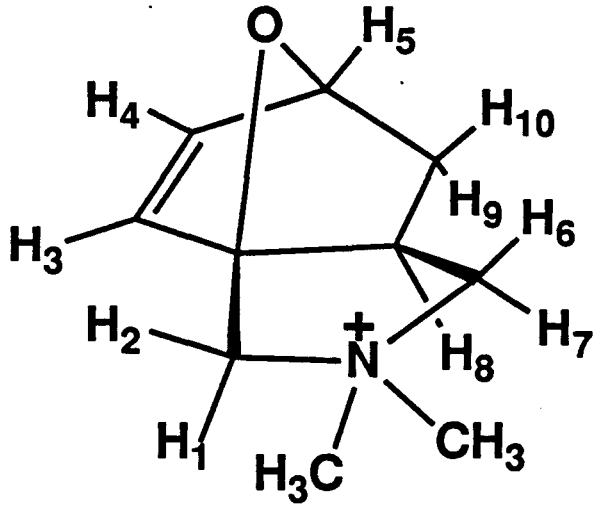

Figure A1.5. Numbering scheme for nmr assignments of iDA substrates and products, with **98** and **101** as specific examples, respectively.

o-xylylene dibromide with Cs_2CO_3/DMF[5] afforded enantiomerically pure dimer[6] (**126**), which was partially purified (contaminated with alleged trimer) by preparative-scale tlc.

The studies with host **125** were abandoned once we uncovered the host-catalyzed alkylation reactions described in Chapter 3.

Experimental for Appendix 1

Melting points (corrected) were recorded on a Thomas-Hoover melting point apparatus. NMR spectra were recorded on a JEOL JNM GX-400 spectrometer. Routine spectra were referenced to the residual proton and carbon signals of the solvents and are reported (ppm) downfield of 0.0 as δ values. Reagent-grade solvents were obtained from commercial sources and were used without further purification.

Host and guest stock solutions for the aqueous kinetics experiments were prepared with a standard 10mM deuterated cesium borate buffer at pD~9 (borate-*d*). The buffer was prepared as described in Chapter 1. The concentrations of the solutions were quantified via nmr integrations against a stock solution of DMG (4.20-4.23mM, vs potassium hydrogen phthalate, KHP) in borate-*d*. All volumetric measurements of aqueous solutions were made using adjustable volumetric pipets. All pulse delays for the aqueous stock-solution-integration experiments (15-20s) were at least 5 times the measured T_1 for the species involved.

For the kinetics experiments, buffered solutions containing substrate, 3,3-dimethylglutarate (DMG, internal chemical shift reference at 1.09ppm, concentration standard 4.20-4.23mM (vs KHP standard)), and host **1** (for catalyzed samples) were employed.

Relative concentrations of substrate and product in the intramolecular Diels-Alder reactions were monitored at ambient temperature by 400-MHz ^{1}H NMR (JEOL JNM GX-400) in an aqueous cesium borate buffer (borate-*d*). Initial concentrations of substrate and host were assumed from their respective stock-solution concentrations as

determined by ^1H NMR integration versus DMG with the following typical parameters: ACQTM 4.096s; PD 16.0s; PW1 7.0μs; TI 32scans; FR 4000Hz. The reaction temperature was maintained in a silicone oil bath monitored by an I^2R Thermowatch (±1°C).

Furoylallylamide (114)

To a solution of furoyl chloride (500μL, 4.82mmol) and CH_2Cl_2 (5mL) was added carefully allylamine (Aldrich, 99+%, 1000μL, 13mmol). After stirring at ambient temperature for 15min, 15% aqueous NaOH (3mL) was added. The phases were separated and the aqueous layer was extracted with CH_2Cl_2 (2x5mL). The combined organic layers were dried ($MgSO_4$), then filtered through a short pad of silica and washed with 4:1 (v/v) CH_2Cl_2/ethyl acetate. The filtrate was concentrated *in vacuo* to afford **114** as a yellow oil (R_f=0.5, 5:1 (v/v) CH_2Cl_2/ethyl acetate, 635mg, 87%); ^1H NMR (400 MHz, $CDCl_3$) δ 4.04 (t, 2H, *J*=6Hz, N-C*H*$_2$), 5.17 (d, 1H, *J*=10Hz, *cis*-vinyl-C*H*), 5.24 (d, 1H, *J*=17Hz, *trans*-vinyl-C*H*), 5.90 (ddt, 1H, *J*=10, 17, 6Hz, olefinic-C*H*), 6.40 (br s, 1H, N*H*), 6.48 (dd, 1H, *J*=2, 3Hz, H_4), 7.10 (dd, 1H, *J*=1, 3Hz, H_3), 7.42 (dd, 1H, *J*=1, 2Hz, H_5).

Furoyldimethylamide (115)

To a solution of furoyl chloride (Aldrich, 95%, 1000μL, 9.64mmol) and CH_2Cl_2 (10mL) was added carefully a solution of 40% dimethylamine in H_2O (Aldrich, 3mL). After stirring at ambient temperature for 10min, 15% aqueous NaOH (5mL) was added. The phases were separated and the aqueous layer was extracted with CH_2Cl_2 (2x5mL). The combined organic layers were dried ($MgSO_4$), then filtered through a short pad of silica and washed with 5:1 (v/v) CH_2Cl_2/ethyl acetate. The filtrate was concentrated

via rotary evaporation and allowed to air-dry overnight to give **115** as a yellow liquid (R_f=0.3, 5:1 (v/v) CH_2Cl_2/ethyl acetate, 1.467g, 109%). (The product was too volatile to concentrate *in vacuo*.); ^{1}H NMR (400 MHz, $CDCl_3$) δ 3.07 and 3.25 (br s, 3H each, Δν=71Hz, N(CH_3)$_2$), 6.45 (dd, 1H, J=2, 3Hz, H_4), 6.96 (dd, 1H, J=1, 3Hz, H_3), 7.47 (dd, 1H, J=1, 2Hz, H_5).

Furoylpyrrolidinylamide (116)

To a solution of furoyl chloride (Aldrich, 95%, 500μL, 4.82mmol) and CH_2Cl_2 (5mL) was added carefully pyrrolidine (Aldrich, 99%, 1000μL, 12mmol). After stirring at ambient temperature for 15min, 15% aqueous NaOH (3mL) was added. The phases were separated and the aqueous layer was extracted with CH_2Cl_2 (2x5mL). The combined organic layers were dried ($MgSO_4$), then filtered through a short pad of silica and washed with 4:1 (v/v) CH_2Cl_2/ethyl acetate. The filtrate was concentrated *in vacuo* to afford **116** as a yellow-white solid (R_f=0.25, 5:1 (v/v) CH_2Cl_2/ethyl acetate, 835mg, 105%); ^{1}H NMR (400 MHz, $CDCl_3$) δ 1.88 and 1.98 (quintet, 2H each, J=7Hz, Δν=40Hz, β-CH_2), 3.63 and 3.81 (t, 2H each, J=7Hz, Δν=71Hz, α-CH_2), 6.46 (dd, 1H, J=2, 3Hz, H_4), 7.04 (dd, 1H, J=1, 3Hz, H_3), 7.48 (dd, 1H, J=1, 2Hz, H_5).

Furoylpiperidinylamide (117)

A solution of piperidine (Aldrich, 98%, 1000μL, 9.9mmol) and CH_2Cl_2 (10mL), to which was added carefully furoyl chloride (500μL, 4.82mmol), afforded a white precipitate. After stirring at ambient temperature for 10min, H_2O (3mL) was added. The phases were separated and the aqueous layer was extracted with CH_2Cl_2 (2x5mL). The combined organic layers were dried ($MgSO_4$) and concentrated *in vacuo*. The golden brown sludge

was purified via flash chromatography on silica eluted with a gradient of 8% to 15% ethyl acetate/CH_2Cl_2 to afford **117** as a golden brown liquid (R_f=0.4, 5:1 (v/v) CH_2Cl_2/ethyl acetate, 884mg, 102%); ^{1}H NMR (400 MHz, $CDCl_3$) δ 1.60 (m, 4H, γ-CH_2 and one-half β-CH_2), 1.65 (m, 2H, one-half β-CH_2), 3.66 (br, 4H, α-CH_2), 6.42 (dd, 1H, J=2, 3Hz, H_4), 6.88 (d, 1H, J=3Hz, H_3), 7.43 (d, 1H, J=2Hz, H_5).

Furoylmorpholinylamide (118)

A solution of morpholine (Aldrich, 99+%, 1000μL, 11mmol) and CH_2Cl_2 (10mL), to which was added carefully furoyl chloride (500μL, 4.82mmol), afforded a white precipitate. After stirring at ambient temperature for 10min, H_2O (3mL) was added. The phases were separated and the aqueous layer was extracted with CH_2Cl_2 (2x5mL). The combined organic layers were dried ($MgSO_4$) and concentrated *in vacuo*. The yellow oil was purified via flash chromatography on silica eluted with a gradient of 25% to 30% ethyl acetate/CH_2Cl_2 to afford **118** as a white solid (R_f=0.2, 5:1 (v/v) CH_2Cl_2/ethyl acetate, 956mg, 110%). Alternatively, **118** could be crystallized as white needles via the slow evaporation of a CH_2Cl_2 solution; mp 58-59°C; ^{1}H NMR (400 MHz, $CDCl_3$) δ 3.70 (t, 4H, J=5Hz, α-CH_2), 3.78 (br, 4H, β-CH_2), 6.45 (dd, 1H, J=2, 3Hz, H_4), 6.99 (d, 1H, J=3Hz, H_3), 7.44 (d, 1H, J=2Hz, H_5).

Furanyldimethylamine (119)

To a suspension of lithium aluminum hydride (LAH, Alfa, 871mg, 22.9mmol) in tetrahydrofuran (THF, 20mL) was added dropwise over 10min a solution of furoyldimethylamide (**115**, 1.56g, 11.3mmol) in THF (10mL). The mixture was heated under argon at reflux for 18h. Upon cooling to

ambient temperature, excess LAH was destroyed by the careful successive addition of H_2O (900μL), 15% aqueous NaOH (900μL), and H_2O (2700μL). The clumps of lithium salts were broken up by the addition of ether; the salts were then removed via filtration and washed well with ether. The filtrate was dried ($MgSO_4$) and concentrated via rotary evaporation. (The product was too volatile to concentrate *in vacuo*.) The orange-yellow oil was allowed to air-dry overnight (1.07g, 76%); ^{1}H NMR (400 MHz, $CDCl_3$) δ 2.23 (s, 6H, $N(CH_3)_2$), 3.44 (s, 2H, CH_2), 6.17 (d, 1H, J=3Hz, H_3), 6.29 (dd, 1H, J=2, 3Hz, H_4), 7.35 (dd, 1H, J=1, 2Hz, H_5).

Furanylpyrrolidine (120)

To a suspension of LAH (392mg, 10.3mmol) in THF (5mL) was added dropwise over 10min a solution of furoylpyrrolidinylamide (**117**, 835mg, 5.06mmol) in THF (5mL). The mixture was heated under argon at reflux for 15h. Upon cooling to ambient temperature, excess LAH was destroyed by the careful successive addition of H_2O (400μL), 15% aqueous NaOH (400μL), and H_2O (1200μL). The lithium salts were removed via filtration and washed well with ether. The filtrate was dried ($MgSO_4$) and concentrated via rotary evaporation. The orange oil was allowed to air-dry for several days (460mg, 60%); ^{1}H NMR (400 MHz, $CDCl_3$) δ 1.77 (m, 4H, β-CH_2), 2.52 (m, 4H, α-CH_2), 3.61 (s, 2H, CH_2), 6.16 (dd, 1H, J=1, 3Hz, H_3), 6.28 (dd, 1H, J=2, 3Hz, H_4), 7.34 (dd, 1H, J=1, 2Hz, H_5).

Furanylpiperidine (121)

To a suspension of LAH (393mg, 10.3mmol) in THF (5mL) was added dropwise over 10min a solution of furoylpiperidinylamide (**117**, 884mg, 4.94mmol) in THF (5mL). The mixture was heated under argon at 50°C for

23h. Upon cooling to ambient temperature, excess LAH was destroyed by the careful successive addition of H_2O (400μL), 15% aqueous NaOH (400μL), and H_2O (1200μL). The gray-white clumps of lithium salts were broken up via the addition of ether; the lithium salts were then removed via filtration and washed well with ether. The filtrate was dried ($MgSO_4$) and concentrated via rotary evaporation. The orange oil was allowed to air-dry overnight (770mg, 94%); ^{1}H NMR (400 MHz, $CDCl_3$) δ 1.39 (m, 2H, γ-CH_2), 1.57 (quintet, 4H, J=6Hz, β-CH_2), 2.37 (br s, 4H, α-CH_2), 3.48 (s, 2H, CH_2), 6.15 (d, 1H, J=3Hz, H_3), 6.28 (dd, 1H, J=2, 3Hz, H_4), 7.35 (d, 1H, J=2Hz, H_5).

Furanylmorpholine (122)

To a suspension of LAH (406mg, 10.7mmol) in THF (5mL) was added dropwise over 10min a mixture of furoylmorpholinylamide (**118**, 956mg, 5.28mmol) in THF (5mL). The mixture was heated under argon at 50°C for 14h. Upon cooling to ambient temperature, excess LAH was destroyed by the careful successive addition of H_2O (400μL), 15% aqueous NaOH (400μL), and H_2O (1200μL). The gray-white clumps of lithium salts were broken up via the addition of ether; the lithium salts were then removed via filtration and washed well with ether. The filtrate was dried ($MgSO_4$) and concentrated via rotary evaporation. The golden-yellow liquid was allowed to air-dry overnight (821mg, 93%); ^{1}H NMR (400 MHz, $CDCl_3$) δ 2.45 (t, 4H, J=5Hz, α-CH_2), 3.51 (s, 2H, CH_2), 3.70 (t, 4H, J=5Hz, β-CH_2), 6.19 (d, 1H, J=3Hz, H_3), 6.29 (dd, 1H, J=2, 3Hz, H_4), 7.36 (d, 1H, J=2Hz, H_5).

Allylfuranyldimethylammonium bromide (98)

To a solution of furanyldimethylamine (**119**, 131mg, 1.05mmol) in CH_2Cl_2 (1mL) under argon was added excess allyl bromide (Aldrich,

1000μL, 11.6mmol). The brown solution was stirred at ambient temperature for 18h. An additional 1000μL of allyl bromide was added and the solution was stirred 24h. The reaction mixture was concentrated *in vacuo*, and **98** was isolated as a dark brown oil (212mg, 82%); ^{1}H NMR (400 MHz, $CDCl_3$) δ 3.30 (s, 6H, N(CH_3)$_2$), 4.31 (d, 2H, J=7Hz, $H_{6,7}$), 5.05 (s, 2H, $H_{1,2}$), 5.76 (d, 1H, J=10Hz, H_9), 5.86 (d, 1H, J=17Hz, H_{10}), 6.03 (ddt, 1H, J=10, 17, 7Hz, H_8), 6.46 (dd, 1H, J=2, 3Hz, H_4), 6.98 (d, 1H, J=3Hz, H_3), 7.52 (d, 1H, J=2Hz, H_5).

N,N-Dimethyl-3-aza-10-oxatricyclo[5.2.1.0^{1,5}]dec-8-ene bromide (101)

A solution of allylfuranyldimethylammonium bromide (**98**, 2.86mM) in borate-*d* was converted quantitatively to **101** via heating at 60°C for 3d; ^{1}H NMR (400 MHz, borate-*d*) δ 1.64 (dd, 1H, J=8, 12Hz, H_9), 1.95 (ddd, 1H, J=3, 5, 12Hz, H_{10}), 2.72 (dddd, 1H, J=3, 7, 8, 12Hz, H_8), 3.328 (s, 3H, N(CH_3)), 3.332 (s, 3H, N(CH_3)), 3.40 (t, 1H, J=12Hz, H_6), 4.00 (d, 1H, J=14Hz, H_1), 4.06 dd, 1H, J=7, 12Hz, H_7), 4.37 (d, 1H, J=14Hz, H_2), 5.27 (d, 1H, J=5Hz, H_5), 6.56 (AB, 1H, J=6Hz, Δν=11Hz, $H_{3,4}$), from ^{1}H-^{1}H decoupling.

Allylfuranylpiperidinium bromide (99)

To a solution of furanylpiperidine (**121**, 115mg, 0.697mmol) in $CHCl_3$ (1mL) under argon was added excess allyl bromide (1000μL, 11.6mmol). The reaction mixture was stirred at ambient temperature for 18h, then concentrated *in vacuo*; **99** was isolated as an orange oil (238mg, 119%); ^{1}H NMR (400 MHz, $CDCl_3$) δ 1.80-2.01 (m, 6H, β– and γ-CH_2), 3.61 (m, 2H, α-CH_2), 3.85 (m, 2H, α'-CH_2), 4.17 (d, 2H, J=7Hz, $H_{6,7}$), 5.00 (s, 2H, $H_{1,2}$), 5.78 (dd, 1H, J=1, 11Hz, H_9), 5.85 (dd, 1H, J=1, 17Hz, H_{10}), 6.02 (ddt, 1H, J=11, 17,

7Hz, H_8), 6.47 (dd, 1H, J=2, 3Hz, H_4), 6.98 (d, 1H, J=3Hz, H_3), 7.51 (d, 1H, J=2Hz, H_5).

Allylfuranylmorpholinium bromide (100)

To a solution of furanylmorpholine (**122**, 156mg, 0.934mmol) in $CHCl_3$ (1mL) under argon was added excess allyl bromide (1000μL, 11.6mmol). The reaction mixture was stirred at ambient temperature for 14h, then concentrated *in vacuo*; **100** was isolated as an orange oil (310mg, 115%); ^{1}H NMR (400 MHz, $CDCl_3$) δ 3.71 (AB m, 4H, β–CH_2), 4.10 (AB m, 4H, α-CH_2), 4.53 (d, 2H, J=7Hz, $H_{6,7}$), 5.30 (s, 2H, $H_{1,2}$), 5.80 (d, 1H, J=11Hz, H_9), 5.89 (d, 1H, J=17Hz, H_{10}), 6.01 (ddt, 1H, J=11, 17, 7Hz, H_8), 6.49 (dd, 1H, J=2, 3Hz, H_4), 7.06 (d, 1H, J=3Hz, H_3), 7.53 (d, 1H, J=2Hz, H_5).

Furanyldimethyl(2-methylallyl)ammonium chloride (105)

To a solution of furanyldimethylamine (**119**, 131mg, 1.05mmol) in $CHCl_3$ (1mL) under argon was added excess 3-chloro-2-methylpropene (Aldrich, 98%, 1000μL, 9.9mmol). The reaction mixture was stirred at ambient temperature for 14h, then concentrated *in vacuo*; **105** was isolated as a yellow oil (50mg, 96%); ^{1}H NMR (400 MHz, $CDCl_3$) δ 1.95 (s, 3H, C-CH_3), 3.19 (s, 6H, N(CH_3)$_2$), 4.27 (s, 2H, $H_{6,7}$), 5.06 (s, 2H, $H_{1,2}$), 5.45 (s, 1H, H_9), 5.49 (s, 1H, H_{10}), 6.36 (dd, 1H, J=2, 3Hz, H_4), 6.89 (d, 1H, J=3Hz, H_3), 7.45 (d, 1H, J=2Hz, H_5).

Furanyldimethyl(3,3-dimethylallyl)ammonium bromide (112) and furanyldimethyl(1,1-dimethylallyl)ammonium bromide (113)

To a solution of furanyldimethylamine (**119**, 30mg, 0.24mmol) in $CHCl_3$ (1mL) under argon was added excess 4-bromo-2-methyl-2-butene

(Aldrich, 97%, 500μL, 3.4mmol). The reaction mixture was stirred at ambient temperature for 18h, then concentrated *in vacuo*; **112** and **113** were isolated as a viscous black oil (50mg, 76%); ^{1}H NMR (400 MHz, $CDCl_3$) showed 2 sets of furanyl peaks and apparent doubling of remaining resonances, consistent with both S_N2 (**112**) and S_N2' (**113**) products.

References to Appendix 1

(1) (a) Breslow, R.; Rideout, D. *J. Am. Chem. Soc.* **1980**, *102*, 7816-7818; (b) Sternbach, D. D.; Rossana, D. M. *J. Am. Chem. Soc.* **1982**, *104*, 5853-5854.

(2) Menger, F. M. *Acc. Chem. Res.* **1985**, *18*, 128-134.

(3) Ciganek, E. *Org. Reactions* **1984**, *32*, 1-373.

(4) Tagmazyan, K. T.; Mkrtchyan, R. S.; Babayan, A. T., trans. from *Zh. Org. Khim.* **1974**, *10*, 1642-1648.

(5) (a) van Keulen, B.; Kellogg, R. M.; Piepers, O. *J. Chem. Soc., Chem. Commun.* **1979**, 285-286; (b) Dijkstra, G.; Kruizinga, W. H.; Kellogg, R. M. *J. Org. Chem.* **1987**, *52*, 4230-4234.

(6) According to nmr analysis of the mixture of enantiomerically pure **126** and alleged trimer, the earlier assignment of meso/*d l* diastereomers (made by Shepodd according to hplc elution order) was incorrect: Shepodd, T. J. Ph. D. Thesis, California Institute of Technology, 1988.

(7) Petti, M. A. Ph. D. Thesis, California Institute of Technology, 1988.

Appendix 2

Attempted Application of ESR Spectroscopy to Molecular Recognition

Throughout most of our work in molecular recognition in aqueous media, we have employed ^{1}H NMR spectroscopy to characterize host-guest interactions. However, nmr has failed to separately identify "free" and "bound" guest species: only time-averaged signals are observed because both "on" and "off" rates are fast on the nmr timescale (~10^3Hz). We therefore evaluate association constants with the non-linear, least-squares fitting program called MULTIFIT.[1]

Kotake and Janzen recently reported[2] the use of electron spin resonance (ESR) spectroscopy[3] with nitroxide radical spin label **127** to detect bimodal inclusion with β-cyclodextrin in water.[4] This paper rekindled our interest in using ESR, with its shorter timescale (~10^6Hz), to study host-guest complexation in our systems. The prospect of obtaining on-off rates led to the collaborative effort described (briefly) herein between Frank Coms and myself wherein we could take advantage of our separate areas of expertise.

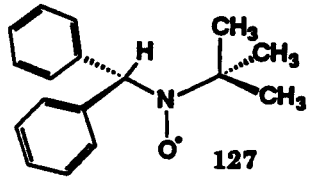

127

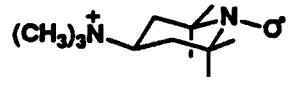

128

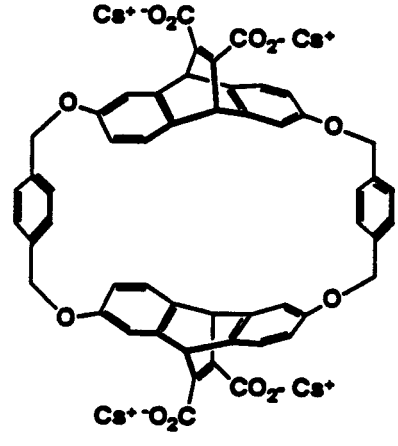

1

Spin label **128** was designed to potentially probe the structural and dynamic properties as a guest with host **1**: **128** features a nitroxide radical

to facilitate ESR detection and a quaternary ammonium group to deliver the spin label to the host. Compound **128** was synthesized from 4-amino-TEMPO[5] with Cs_2CO_3/DMF and excess iodomethane. An aqueous stock solution of **128** was readily prepared in borate-*d*.

With spin label **128** in hand, preliminary ESR experiments were performed to determine if any qualitative spectral changes occurred to reflect complexation with host **1**. The ESR spectrum of **128** in borate-*d* (Figure **A2.1a**) shows the expected three-line pattern for an isolated spin.[6] Upon addition of increasing amounts of host **1**, almost no change in the appearance of the ESR spectrum was observed. We noted only a slight decrease in the magnitude of the high field signal of the three-line pattern (Figure **A2.1b**).

We therefore returned to nmr spectroscopy: a competitive binding study between host **1** and guest **20** (ATMA, $-\Delta G°_{295}$ = 6.7kcal/mol) with **128** as an inhibitor provided K_a (**1**·**128**) ~700M^{-1}. This disappointingly low affinity may be the result of unfavorable steric interactions between the methyl groups of the TEMPO moiety that prevent optimal recognition of the quaternary ammonium group of **128**. This small K_a spelled the end of our investigation of **128** as an ESR probe for binding studies.

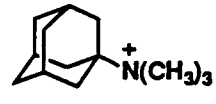

20

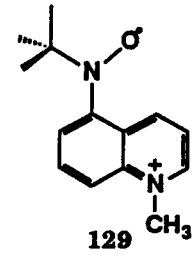

129

In the aftermath of this work, Coms has suggested that **129** (or a related compound) might be well-suited for EPR studies, given the affinity of host **1** for quinolinium guests (Chapter 1).

(a)

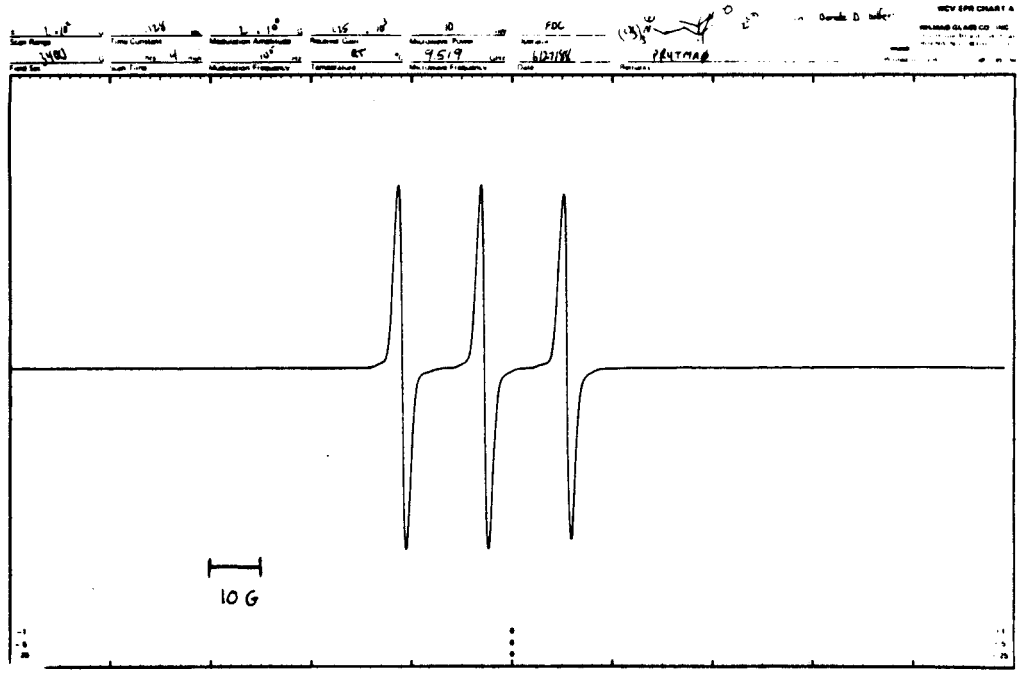

(b)

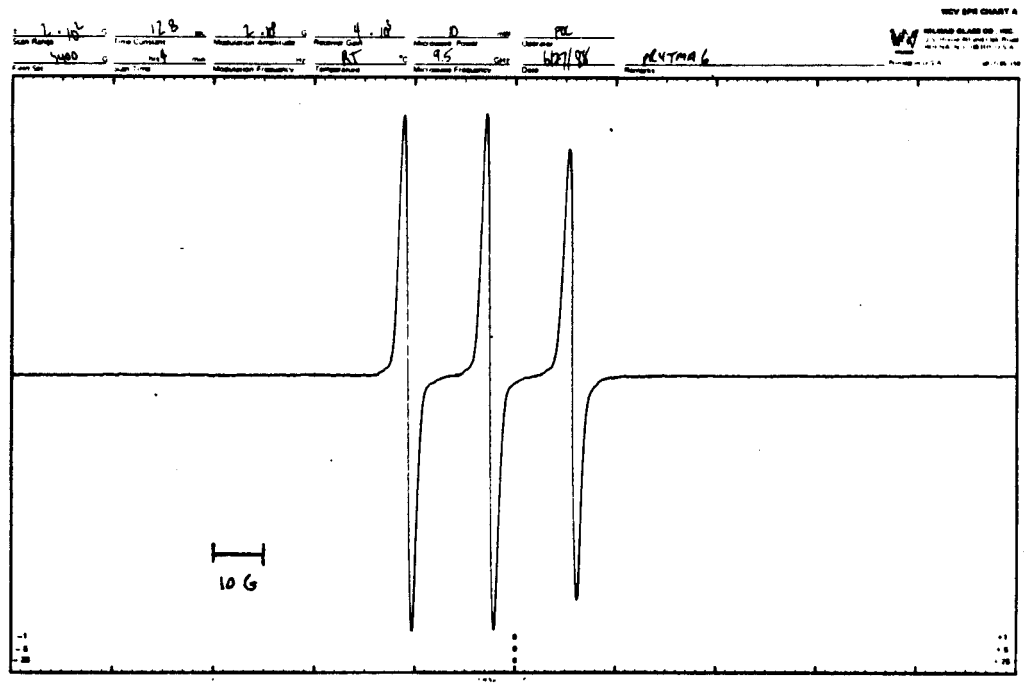

Figure A2.1. EPR spectroscopy used to probe host-guest complexation in borate-*d*: (a) guest only ([**128**]$_0$=316mM); (b) with added host ([**128**]$_0$=226mM, [**1**]$_0$=207mM).

Experimental for Appendix 2

NMR spectra were recorded on a JEOL JNM GX-400 spectrometer. Routine spectra were referenced to the residual proton and carbon signals of the solvents and are reported (ppm) downfield of 0.0 as δ values. Electron-impact (EI), fast-atom bombardment (FAB), and high-resolution mass spectrometry (HRMS) were performed by the staff of the University of California, Riverside. Reagent-grade solvents were obtained from commercial sources and were used without further purification.

Aqueous ESR experiments were performed on a Varian E-line Century Series X-band spectrometer at ambient temperature. Samples were drawn into 150mm x 0.5mm i.d. capillaries, then sealed with a flame.

Host and guest stock solutions for the aqueous NMR binding experiments were prepared with a standard 10mM deuterated cesium borate buffer at pD~9 (borate-*d*). The buffer was prepared as described in Chapter 1. The concentrations of the solutions were quantified via nmr integrations against a stock solution of DMG (4.20-4.23mM, vs potassium hydrogen phthalate, KHP) in borate-*d*. All volumetric measurements of aqueous solutions were made using adjustable volumetric pipets. All pulse delays for the aqueous stock-solution-integration experiments (15-20s) were at least 5 times the measured T_1 for the species involved.

4-Trimethylammonium-2,2,6,6-tetramethyl-1-piperidinyloxyl (128)

To a mixture of 4-amino-2,2,6,6-tetramethyl-1-piperidinyloxyl (4-amino-TEMPO, Aldrich, 97%, 116mg, 0.658mmol) and cesium carbonate (Aldrich, 99%, 1.06g, 3.25mmol) in dry DMF (5mL) under argon was added iodomethane (Aldrich, 99%, 320μL, 5.1mmol). After stirring *in the dark* at

ambient temperature for 16h, cesium salts were removed via filtration and washed well with acetonitrile. The filtrate was concentrated *in vacuo*, and **128** was crystallized from methanol as maroon-red plates (180mg, 80%); ^{1}H NMR (400 MHz, borate-*d*) δ 3.0 (br s, due to paramagnetic broadening), 3.2 (s, 9H, N(C*H*$_3$)$_3$), 3.35 (s, C*H*$_3$OH); HRMS 215.2131, calcd for $C_{12}H_{27}N_2O$ 215.2123.

References to Appendix 2

(1) Petti, M. A.; Shepodd, T. J.; Barrans, R. E., Jr.; Dougherty, D. A. *J. Am. Chem. Soc.* **1988**, *110*, 6825-6840.

(2) Kotake, Y.; Janzen, E. G. *J. Am. Chem. Soc.* **1988**, *110*, 3699-3701, and references therein.

(3) Wertz, J. E.; Bolton, J. R. *Electron Spin Resonance: Elementary Theory and Practical Applications*; McGraw-Hill: New York, 1972.

(4) To be technically correct, we point out that one could attribute the bimodal inclusion of **127** to binding of each of the phenyl rings, which are enantiotopic: β-cyclodextrin is chiral, so that inclusion will differentiate the phenyl groups.

(5) TEMPO = 2,2,6,6-tetramethyl-1-piperidinyloxyl.

(6) TEMPO was sufficiently water-soluble to observe by ESR spectroscopy, and exhibited a nearly identical "free" EPR spectrum in comparison to **128**.

Appendix 3

Attempted Resolution of 1,5-DEA Units

Two approaches were taken in an effort to obtain enantiomerically pure 1,5-DEA units (**52**). The first approach involved attaching chiral auxiliaries to diol-DEA **63** to give diastereomeric bis(esters). The second approach employed the asymmetric Diels-Alder methodology successfully applied to the 2,6-DEA units (**29**).[1]

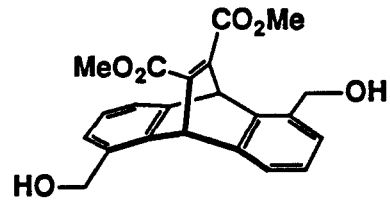

63

Six different chiral auxiliaries were attached to diol-DEA **63** to afford six pairs of diastereomeric esters (Figure **A3.1**). The pendant chiral auxiliaries included Mosher's (MTPA) esters[2] (**130**), esters of pyroglutamic acid (SPCA, **131**), Cbz-L-Pro esters (**132**), *l*-menthoxyformyl esters (**133**), *O*-methylmandelate esters (**134**), and *l*-menthoxyacetate esters (**135**). All diastereomeric pairs were distinguishable (to varying degrees) by 400MHz ^{1}H NMR spectroscopy. In our hands, none of the six pairs of diastereomers could be separated by crystallization or by tlc, although the MTPA esters **130** were separated by analytical hplc.

SPCA esters **131** were separated painstakingly via preparative-scale tlc or hplc (Figure **A3.2**). The resolved SPCA esters (**136** and **137**) so obtained were hydrolyzed to give enantiomerically pure diols **138** and **139**. The alcohols were oxidized to the bis(aldehydes) **140** and **141**; only bis(aldehyde) **142** was oxidized to the bis(carboxylic acid) **143**. Further efforts awaited results of binding studies using racemic 1,5-DEA units.

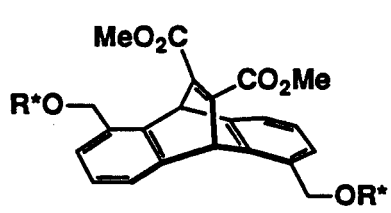

and

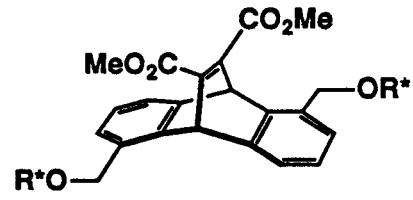

R*

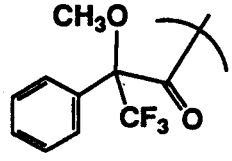

130

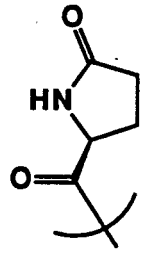

131

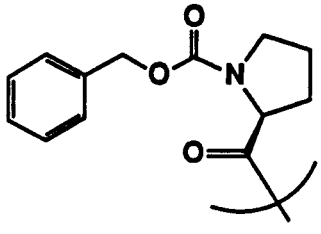

132

R*

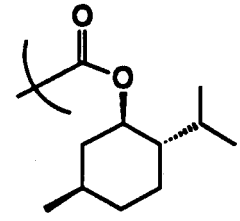

133

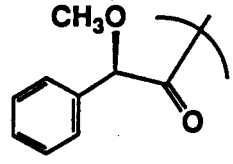

134

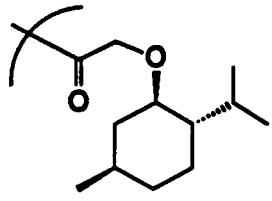

135

Figure A3.1: Diastereomeric bis(esters) from **63**.

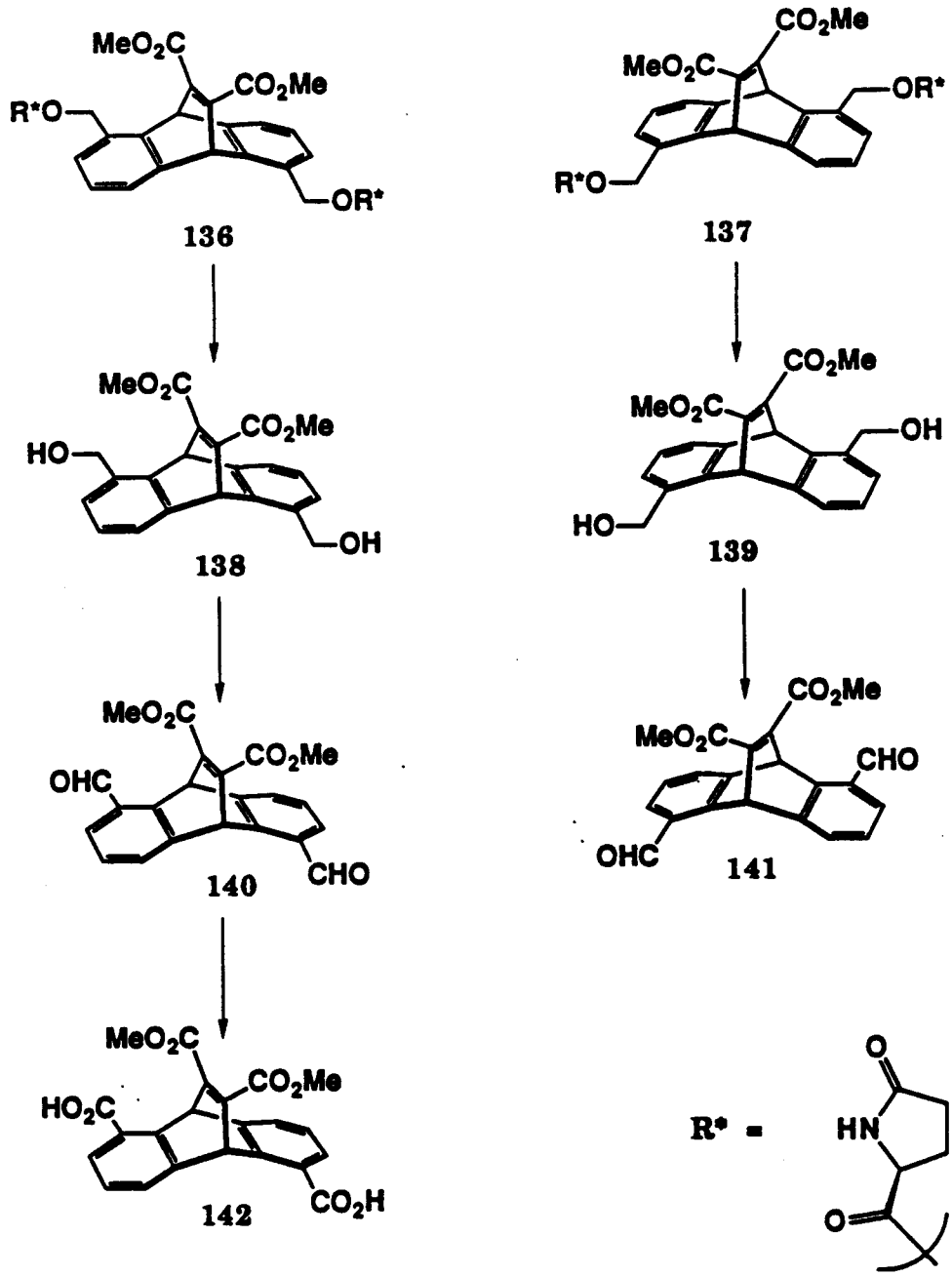

Figure A3.2: Chromatographically separated esters carried forth to give enantiomerically pure 1,5-DEAs.

Application of the asymmetric Diels-Alder reaction methodology[1] was attempted for the 1,5-DEA systems. The thermal, uncatalyzed reaction of anthracene **33** and dimenthyl fumarate in refluxing toluene afforded a mixture of all four possible diastereomeric adducts (**143-146**, Figure **A3.3**) as expected. Evidence for selectivity was found from ^{1}H NMR integration of peaks for the ethano-bridge protons (all singlets, δ 3.2-3.4; 2:20:40:5). The diethylaluminum chloride-catalyzed reaction (-45°C to +10°C) afforded a mixture of all four diastereomeric adducts, although the ratio of adducts reflected different selectivity compared to the uncatalyzed reaction.[3] In our hands, the four diastereomeric adducts could not be separated by crystallization or by tlc.

We can only speculate as to the reasons for incomplete olefin facial selectivity. Qualitatively, it appeared that 1,5-anthracene **33** was much less soluble in toluene (-45°C) than was 2,6-anthracene **32**. Also, the orientation of 1,5-CH_2OTBS groups may be unfavorable for the Lewis acid to control olefin facial selectivity.[4] It is the intuitive sense of the author that this problem should be surmountable with more careful attention to solvent, temperature, and concentration for ensuring solubility of **33** to achieve the desired selectivity.

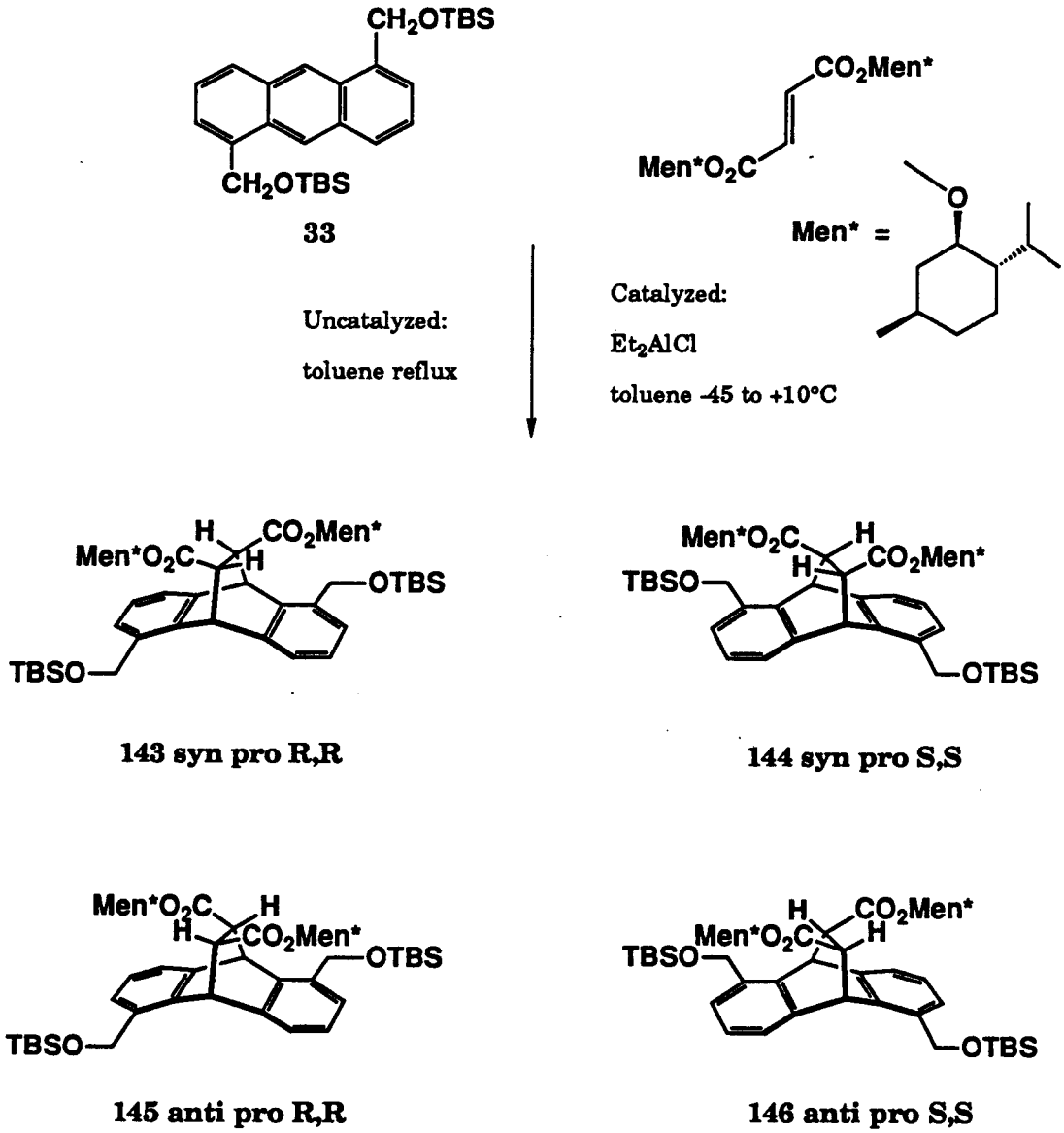

Figure A3.3: Asymmetric Diels-Alder reaction scheme for 1,5-DEAs.

Experimental for Appendix 3

Melting points (corrected) were recorded on a Thomas-Hoover melting point apparatus. NMR spectra were recorded on a JEOL JNM GX-400 spectrometer. Routine spectra were referenced to the residual proton and carbon signals of the solvents and are reported (ppm) downfield of 0.0 as δ values. Optical rotations were recorded on a Jasco DIP-181 digital polarimeter at 293±2K. Flash chromatography was performed according to the method of Still *et al.*[5] HPLC and reverse-phase HPLC (RPHPLC) were performed on a Perkin-Elmer Series 2 liquid chromatograph. Preparative HPLC used a 1" X 25cm Vydac 101HS1022 silica column; analytical RPHPLC used a 5mm X 25cm Whatman Partisil ODS-3 C_{18} column.

Solvents were distilled from drying agents as noted: dichloromethane, CaH_2; toluene, sodium metal; carbon tetrachloride, P_2O_5; tetrahydrofuran (THF), sodium benzophenone ketyl. Reagent-grade solvents were obtained from commercial sources and were used without further purification.

Mosher's (MTPA) esters. 1,5-Bis[(-)-methoxytrifluoromethylphenylcarbonyloxymethyl]-9,10-dihydro-9,10-(1,2-dicarbomethoxy)ethenoanthracene (130)

A mixture of 1,5-bis[hydroxymethyl]-9,10-dihydro-9,10-(1,2-dicarbomethoxy)ethenoanthracene (**63**, 38mg, 0.10mmol), dry pyridine (0.1mL), (-)-methoxytrifluoromethylphenylcarbonyl chloride[2] (550μL, 0.4*M* in CCl_4), and CCl_4 (5mL) was stirred under N_2 at ambient temperature for 2d, and monitored by tlc. The resulting milky white suspension was diluted

with ether (25mL), then washed successively with saturated aqueous NaCl (5mL), 5% HCl (5mL), saturated aqueous $NaHCO_3$ (5mL), and H_2O (10mL). The organic layer was dried ($MgSO_4$) and concentrated *in vacuo*. The product was purified via flash chromatography on silica eluted with 2:1 (v/v) petroleum ether/ether to afford **130** (both diastereomers) as a colorless oil (81mg, 100%); ^1H NMR (400 MHz, $CDCl_3$) δ 3.38 and 3.41 (dd, 6H, J<1Hz, OCH_3 of MTPA), 3.80 and 3.81 (s, 6H, CO_2CH_3), 5.58 and 5.59 (d AB, 4H, J=2, 12Hz, Δν=34 and 94Hz, respectively, CH_2), 5.84 and 5.95 (s, 2H, $H_{9,10}$), 6.95 and 6.98 (t, 2H, J=8Hz, $H_{3,7}$), 7.09-7.14 (m, 4H, $H_{2,6}$ and $H_{4,8}$), 7.24-7.30 and 7.32-7.39 (m, 10H, C_6H_5 of MTPA); ^{19}F NMR (470 MHz, 30%TFA/$CDCl_3$) δ -72.65, -72.78.

SPCA esters. 1,5-Bis[(*S*)-(-)-pyrrolidone-5-carbonyloxymethyl]-9,10-dihydro-9*S*,10*S*-(1,2-dicarbomethoxy)ethenoanthracene (136) and 1,5-bis[(*S*)-(-)-pyrrolidone-5-carbonyloxymethyl]-9*R*,10*R*-dihydro-9,10-(1,2-dicarbomethoxy)ethenoanthracene (137)

To a mixture of 1,5-bis[hydroxymethyl]-9,10-dihydro-9,10-(1,2-dicarbomethoxy)ethenoanthracene (**63**, 3.68g, 9.68mmol), (*S*)-(-)-pyrrolidone-5-carboxylic acid (3.60g, 27.1mmol), 4-dimethylaminopyridine (DMAP, Aldrich, 99%, 109mg, 0.893mmol), in CH_2Cl_2 (75mL) stirred under N_2 at ambient temperature was added a solution of *N,N*-dicyclohexylcarbodiimide (DCC, 6.09g, 29.3mmol) in CH_2Cl_2 (50mL). *N,N*-Dicyclohexylurea (DCU) precipitated immediately as a white solid. The mixture was stirred for 90min. The DCU was removed via filtration and washed with CH_2Cl_2. The filtrate was concentrated and the product was purified via flash chromatography on silica eluted with a gradient of 5% to 20% methanol in 1:1 (v/v) CH_2Cl_2/ether to afford **136** and **137** (both

diastereomers) as a white foam (R_f=0.1 in 6:6:1 (v/v/v) CH_2Cl_2/ether/methanol, 5.59g, 96%). A sample (214mg) was subjected to preparative scale tlc eluted with 10-15% isopropanol/benzene to separate the diastereomers (26 elutions). (Alternatively, preparative scale hplc (silica column, 6-8% isopropanol in 1:1 (v/v) hexane/$CHCl_3$, 25mL/min) was used to isolate the faster eluting (higher R_f) isomer (360mg).) Higher R_f isomer **136** (92mg): $[\alpha]_D$ (c=4.6) +7.1°; ^{1}H NMR (400 MHz, $CDCl_3$) δ 2.09-2.41 (m, 8H, SPCA CH_2 groups), 3.74 (s, 6H, CO_2CH_3), 4.20 (dd, 2H, J=5, 8Hz, SPCA CH), 5.32 (AB, 4H, J=12Hz, Δν=105Hz, DIOLAD CH_2), 5.79 (s, 2H, $H_{9,10}$), 6.89 (s, 2H, SPCA NH), 6.99 (d, 2H, J=7Hz, $H_{2,6}$), 7.02 (t, 2H, J=7Hz, $H_{3,7}$), 7.37 (d, 2H, J=7Hz, $H_{4,8}$); lower R_f isomer **137** (55mg): $[\alpha]_D$ (c=2.8) +55°; ^{1}H NMR (400 MHz, $CDCl_3$) δ 2.15-2.45 (m, 8H, SPCA CH_2 groups), 3.74 (s, 6H, CO_2CH_3), 4.28 (dd, 2H, J=5, 9Hz, SPCA CH), 5.31 (AB, 4H, J=12Hz, Δν=55Hz, DIOLAD CH_2), 5.79 (s, 2H, $H_{9,10}$), 6.62 (s, 2H, SPCA NH), 7.00 (t, 2H, J=7Hz, $H_{3,7}$), 7.03 (dd, 2H, J=2, 8Hz, $H_{2,6}$), 7.39 (dd, 2H, J=2, 7Hz, $H_{4,8}$).

Resolved 1,5-bis[hydroxymethyl]-9*S*,10*S*-dihydro-9,10-(1,2-dicarbomethoxy)-ethenoanthracene (138) and 1,5-bis[hydroxymethyl]-9*R*,10*R*-dihydro-9,10-(1,2-dicarbomethoxy)ethenoanthracene (139)

Separate solutions of resolved 1,5-bis[(*S*)-(-)-pyrrolidone-5-carbonyl-oxymethyl]-9,10-dihydro-9,10-(1,2-dicarbomethoxy)ethenoanthracenes (**138**, 75.6mg, 0.126mmol; **139**, 43.3mg, 0.072mmol) in 10% methanolic HCl (5mL) were stirred under nitrogen at ambient temperature for 24h and monitored by tlc (6:6:1 (v/v/v) CH_2Cl_2/ether/methanol). Each reaction mixture was neutralized carefully with solid sodium bicarbonate. Excess bicarbonate was removed via filtration, and the filtrates were concentrated. The products were each purified via flash chromatography on silica eluted with

a gradient of 5% to 10% methanol in 1:1 (v/v) CH_2Cl_2/ether to afford **138** (44.2mg, 93%) and **139** (25.9mg, 95%) as yellow oils; **138**: $[\alpha]_D$ -19° (*c*=2.24, CH_3OH), $[\alpha]_D$ -39° (*c*=7.5, CH_3OH); **139**: $[\alpha]_D$ +11° (*c*=1.30, CH_3OH).

Resolved 1,5-diformyl-9*S*,10*S*-dihydro-9,10-(1,2-dicarbomethoxy)ethenoanthracene (140) and 1,5-diformyl-9*R*,10*R*-dihydro-9,10-(1,2-dicarbomethoxy)-ethenoanthracene (141)

Resolved bis(aldehydes) were synthesized according to the procedure for racemic material (Chapter 4) using resolved 1,5-bis[hydroxymethyl]-9,10-dihydro-9,10-(1,2-dicarbomethoxy)ethenoanthracenes (**138**, 39.2mg, 0.103mmol; **139**, 25.2mg, 0.066mmol); **140** was isolated as a white solid (25.2mg, 65%): $[\alpha]_D$ -170° (*c*=1.26, $CHCl_3$), $[\alpha]_D$ -106° (*c*=6.7, $CHCl_3$); **141** was isolated as a yellow oil (20.6mg, 83%): $[\alpha]_D$ +156° (*c*=1.03, $CHCl_3$).

Resolved 1,5-dicarboxy-9*S*,10*S*-dihydro-9,10-(1,2-dicarbomethoxy)ethenoanthracene (142)

Resolved bis(carboxylic acid) was synthesized according to the procedure for racemic material (Chapter 4) using 1,5-diformyl-9*S*,10*S*-dihydro-9,10-(1,2-dicarbomethoxy)ethenoanthracene (**140**, 134mg, 0.356mmol); **142** was isolated as a white solid (0.14g, 97%): $[\alpha]_D$ -113° (*c*=0.34, CH_3OH).

Cbz-L-Pro esters. 1,5-Bis[(*N*-benzyloxycarbonyl)-L-prolinyloxymethyl]-9,10-dihydro-9,10-(1,2-dicarbomethoxy)ethenoanthracene (132)

To a mixture of 1,5-bis[hydroxymethyl]-9,10-dihydro-9,10-(1,2-dicarbomethoxy)ethenoanthracene (**63**, 0.191g, 0.503mmol), *N*-benzylxoxycarbonyl-L-proline (0.377g, 1.50mmol), and a trace amount of

DMAP (ca. 30mg) in dry CH_2Cl_2 (3mL) stirred under argon at ambient temperature was added a solution of DCC in CH_2Cl_2 (1.4mL, 1.11*M*). After stirring overnight, the precipitated DCU was removed via filtration and washed with CH_2Cl_2. The yellowish-white filtrate was concentrated and the product was partially purified via flash chromatography on silica eluted with a gradient of 4% to 20% methanol in 4:1 (v/v) petroleum ether/$CHCl_3$ to afford **132** (both diastereomers) as a white foam (R_f=0.4 in 8:2:1 (v/v/v) petroleum ether/$CHCl_3$/methanol, 472mg, 112%). The foam was recrystallized from $CHCl_3$ to afford a 1:1 mixture of diastereomers (115mg, 27%). Variable temperature ^{1}H NMR (90 MHz, $CDCl_3$, 25-60°C) experiments revealed a dynamic process consistent with slow rotation about each of two C-N bonds of the carbamate groups: peaks for $H_{9,10}$, Cbz-CH_2, and N-αCH_2 began to coalesce as the temperature increased.

***l*-Menthoxyformyl esters. 1,5-Bis[*l*-menthoxycarbonyloxymethyl]-9,10-dihydro-9,10-(1,2-dicarbomethoxy)ethenoanthracene (133)**

To a mixture of 1,5-bis[hydroxymethyl]-9,10-dihydro-9,10-(1,2-dicarbomethoxy)ethenoanthracene (**63**, 43mg, 0.11mmol) in dry CH_2Cl_2 (1.5mL) stirred under argon at ambient temperature was added *l*-menthylchloroformate (65μL, 0.30mmol) and dry pyridine (0.2mL). After stirring 7h, the mixture was concentrated *in vacuo*. The product was purified via flash chromatography on silica eluted with a gradient of 20% to 50% ethyl acetate/isooctane to afford **133** (both diastereomers) as a colorless oil (R_f=0.15 in 5:1 (v/v) ethyl acetate/isooctane, 81mg, 96%). (The oil did not yield to crystallization.) ^{1}H NMR (400 MHz, $CDCl_3$) δ 0.7-2.1 (2x, m, menthyl peaks), 3.77 (2x, s, 6H, CO_2CH_3), 4.51 (2x, m, 2H, OCO_2-CH), 5.30 and 5.31 (AB, 4H, J=12Hz, Δν=50 and 94Hz, respectively, DIOLAD CH_2), 5.85

and 5.87 (s, 2H, $H_{9,10}$), 6.97 and 6.98 (t, 2H, J=8Hz, $H_{3,7}$), 7.05 (2x, dd, 2H, J=1, 8Hz, $H_{2,6}$), 7.37 and 7.39 (d, 2H, J=8Hz, $H_{4,8}$).

***O*-Methylmandelate esters. 1,5-Bis[(*R*)-(-)-α-methoxyphenylacetyloxymethyl]-9,10-dihydro-9,10-(1,2-dicarbomethoxy)ethenoanthracene (134)**

To a mixture of 1,5-bis[hydroxymethyl]-9,10-dihydro-9,10-(1,2-dicarbomethoxy)ethenoanthracene (**63**, 38mg, 0.10mmol), (*R*)-(-)-α-methoxyphenylacetic acid (54mg, 0.32mmol), and a trace amount of DMAP (ca. 5mg) in dry CH_2Cl_2 (1.5mL) stirred under argon at ambient temperature was added a solution of DCC in CH_2Cl_2 (0.3mL, 1.11*M*). After stirring overnight, the precipitated DCU was removed via filtration and washed with CH_2Cl_2. The filtrate was concentrated and the brownish yellow residue was purified via flash chromatography on silica eluted with a gradient of 0% to 10% methanol/$CHCl_3$ to afford **134** (both diastereomers) as a colorless oil (R_f=0.1 in 1:1 (v/v) petroleum ether/$CHCl_3$, 83mg, 122%). (The oil did not yield to crystallization.) ^{1}H NMR (400 MHz, $CDCl_3$) δ 3.33 and 3.35 (s, 6H, OCH_3), 3.76 (2x, s, 6H, CO_2CH_3), 4.78 (2x, s, 2H, CH), 5.30 and 5.34 (AB, 4H, J=12Hz, Δν=57 and 153Hz, respectively, DIOLAD CH_2), 5.69 and 5.82 (s, 2H, $H_{9,10}$), 6.91-6.96 (2x, m, 4H, $H_{3,7}$ and $H_{2,6}$), 7.29-7.42 (2x, m, 12H, phenyl group and $H_{4,8}$).

***l*-Menthoxyacetate esters. 1,5-Bis[(*l*)-menthoxyacetyloxymethyl]-9,10-dihydro-9,10-(1,2-dicarbomethoxy)ethenoanthracene (135)**

To a mixture of 1,5-bis[hydroxymethyl]-9,10-dihydro-9,10-(1,2-dicarbomethoxy)ethenoanthracene (**63**, 39mg, 0.10mmol), (*l*)-menthoxyacetic acid (80mg, 0.37mmol), and a trace amount of DMAP (ca. 5mg) in dry CH_2Cl_2 (1.5mL) stirred under argon at ambient temperature

was added a solution of DCC in CH_2Cl_2 (0.3mL, 1.11*M*). After stirring overnight, the precipitated DCU was removed via filtration and washed with CH_2Cl_2. The filtrate was concentrated and the white oily residue was purified via flash chromatography on silica eluted with a gradient of 20% to 50% ethyl acetate/isooctane to afford **135** (both diastereomers) as a colorless oil (R_f=0.1 in 5:1 (v/v) ethyl acetate/isooctane, 76mg, 96%). (The oil did not yield to crystallization.) ^{1}H NMR (400 MHz, $CDCl_3$) δ 0.7-2.2 (2x, m, menthyl peaks), 3.77 (2x, s, 6H, CO_2CH_3), 4.11 and 4.12 (AB, 4H, *J*=16Hz, Δν=7 and 26Hz, respectively, O-CH_2-CO_2), 5.34 (2x, AB, 4H, *J*=14Hz, Δν=6Hz, DIOLAD CH_2), 5.81 (2x, s, 2H, $H_{9,10}$), 6.99 (2x, t, 2H, *J*=7Hz, $H_{3,7}$), 7.05 (2x, d, 2H, *J*=8Hz, $H_{2,6}$), 7.37 (2x, m, 2H, $H_{4,8}$).

Uncatalyzed, thermally induced asymmetric Diels-Alder reaction between 1,5-bis[*tert*-butyldimethylsilyloxymethyl]anthracene and dimenthyl fumarate (143-146)

To a solution of 1,5-bis[*tert*-butyldimethylsilyloxymethyl]anthracene (**33**, 119mg, 0.255mmol) in dry toluene (2mL) under argon was added a solution of di-(-)-menthyl fumarate in toluene (0.5mL, 1.32M, 0.66mmol, with trace BHT). The golden brown solution was heated at reflux 9d. After cooling, the reaction mixture was concentrated *in vacuo*. The resulting brownish orange oil was subjected to flash chromatography on silica eluted with a gradient of 50% to 0% CCl_4 in 1:1 (v/v) benzene/isooctane. All four diastereomeric adducts **143-146** were isolated together as a colorless oil (125mg, 57%); ^{1}H NMR (400 MHz, $CDCl_3$) integration of ethano-bridge protons at 3.3ppm indicated that the four adducts were isolated as a 2:20:40:5 mixture: δ 0.05 ($Si(CH_3)_2$), 1.0 ($SiC(CH_3)_3$), 0.6-2.0 (menthyl peaks), 3.3 (ethano-*H*), 4.6 (menthyl O-C*H*), 4.9 (diastereotopic 1,5-CH_2-O), 5.1

($H_{9,10}$), 7.0-7.2 (aromatics). Efforts to separate the diastereomers via tlc or crystallization as per the 2,6-adducts were unsuccessful.

Attempted Lewis-acid-catalyzed asymmetric Diels-Alder reaction between 1,5-bis[*tert*-butyldimethylsilyloxymethyl]anthracene and dimenthyl fumarate (143-146)

To a solution of di-(+)-menthyl fumarate in toluene (1.0mL, 1M, 1.0mmol) under argon cooled in a dry ice/acetonitrile bath (-50 to -45°C) was added a solution of diethylaluminum chloride in toluene (1.6mL, 1.8M, 2.9mmol). After 5min, to the reddish orange solution was added a solution of 1,5-bis[*tert*-butyldimethylsilyloxymethyl]anthracene (**33**, 476mg, 1.02mmol) in dry toluene (8.0mL). The anthracene appeared to precipitate from the cold mixture, which was maintained in a bath of not greater than -20°C for 12h then allowed to warm to 10°C overnight. Following workup as per the 2,6-adducts[1] (**34** and **35**, see Chapter 1), nmr analysis of the crude mixture indicated the presence of all four diastereomeric adducts **143-146**, albeit in a different ratio (ca. 10:2:8:1) from the uncatalyzed reaction.

References to Appendix 3

(1) Petti, M. A.; Shepodd, T. J.; Barrans, R. E., Jr.; Dougherty, D. A. *J. Am. Chem. Soc.* **1988**, *110*, 6825-6840.

(2) Dale, J. A.; Dull, D. L.; Mosher, H. S. *J. Org. Chem.* **1969**, *34*, 2543-2549.

(3) The selectivity observed in the uncatalyzed reaction may result from a strong preference for the *anti* diastereomers due to unfavorable steric interactions when the substituents are *syn*. The change in selectivity for the catalyzed reaction may reflect *partial* selectivity for the olefin diastereoface.

(4) Shepodd, T. J. Ph. D. Thesis, California Institute of Technology, 1988.

(5) Still, W. C.; Kahn, M.; Mitra, A. *J. Org. Chem.* **1978**, *43*, 2923-2925.

Appendix 4

Miscellaneous Compounds

This appendix covers the synthesis of miscellaneous compounds not related directly to any of the other sections of this thesis. A brief description ot the intended purpose of each compound is given below.

The quinolinium and isoquinolinium salts **147-150**, and the neutral compounds from which they were synthesized, will be used by McCurdy to probe the scope of the ion-dipole effect as a force for binding (Chapter 1) and catalysis (Chapter 3).

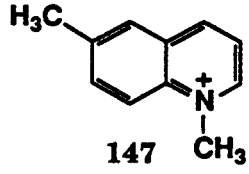

147

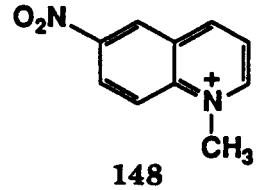

148

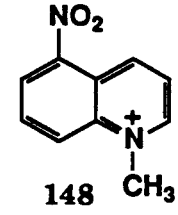

148

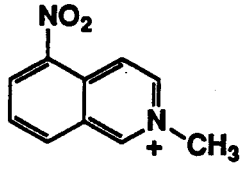

150

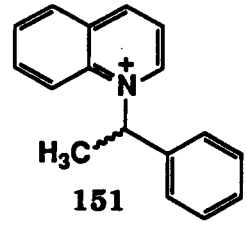

151

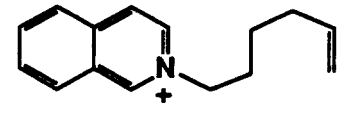

152

The synthesis of **151** was attempted in order to address enantioselectivity in the host-catalyzed alkylation reactions (Chapter 3). The purification of racemic **151** was left incomplete when it was discovered that benzyl bromide undergoes solvolysis in pD~9 buffer faster that it reacts with quinoline (**3**) or isoquinoline (**6**).

Compound **152** was an alternate candidate as an intramolecular Diels-Alder substrate (Appendix 1) based upon literature precedent[1] for the uncatalyzed reaction. CPK models spelled the termination of this approach, as both olefin and isoquinolinium moieties could not be encapsulated within the rhomboid-host conformation.

The preparation of the aminolysis reagent **153**[2] is included to facilitate future efforts toward the synthesis of hosts solubilized with quaternary ammonium groups. Below is shown the successful application of dimethylaluminum dimethylamide to this problem by Warner.

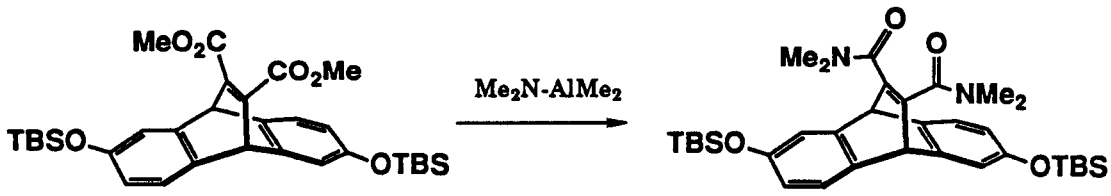

62 **154**

Experimental for Appendix 4

Melting points (corrected) were recorded on a Thomas-Hoover melting point apparatus. NMR spectra were recorded on Varian EM-390 or JEOL JNM GX-400 spectrometers. Routine spectra were referenced to the residual proton and carbon signals of the solvents and are reported (ppm) downfield of 0.0 as δ values. Flash chromatography was performed according to the method of Still *et al.*[3] Electron-impact (EI), fast-atom bombardment (FAB), and high-resolution mass spectrometry (HRMS) were performed by the staff of the University of California, Riverside.

Solvents were distilled from drying agents as noted: dichloromethane, CaH_2; toluene, sodium metal; and ethereal solvents, sodium benzophenone ketyl. Dimethylformamide (DMF) was distilled *in vacuo* at ambient temperature from calcined CaO onto freshly activated 4Å sieves and stored over at least two successive batches of freshly activated 4Å sieves. Reagent-grade solvents were obtained from commercial sources and were used without further purification.

6,*N*-Dimethylquinolinium iodide (147)

A mixture of 6-methylquinoline (Aldrich, 700μL, 5.20mmol) and iodomethane (Aldrich, 99%, 500μL, 7.87mmol) stirred at ambient temperature under argon for 4h deposited a yellow precipitate within 30min. The product was recrystallized from methanol/$CHCl_3$ as yellow plates (unrecorded yield); ^{1}H NMR (400 MHz, $CDCl_3$) δ 2.66 (s, 3H, CH_3), 4.89 (s, 3H, *N*-CH_3), 8.00 (br s, 1H, H_5), 8.03 (dd, 1H, J=2,9Hz, H_7), 8.08 (dd, 1H, J=6,8Hz, H_3), 8.26 (d, 1H, J=9Hz, H_8), 8.86 (d, 1H, J=8Hz, H_4), 10.25 (d, 1H, J=6Hz, H_2); HRMS 158.0979, calcd for $C_{11}H_{12}N$ 158.0970.

N-Methyl-6-nitroquinolinium iodide (148)

A mixture of 6-nitroquinoline (Aldrich, 98%, 860mg, 4.84mmol) and iodomethane (Aldrich, 99%, 500μL, 7.87mmol) in $CHCl_3$ (1mL) and methanol (0.5mL), which was briefly sonicated, then stirred at ambient temperature under argon for 8h, deposited a precipitate. The product was recrystallized from methanol/$CHCl_3$ as golden brown needles (unrecorded yield); ^1H NMR (400 MHz, $CDCl_3$) δ 1.92 (s, 3H, *N*-C*H*$_3$), 7.55 (dd, 1H, *J*=4, 8Hz, *H*$_3$), 8.20 (d, 1H, *J*=9Hz, *H*$_8$), 8.33 (dd, 1H, *J*=1, 8Hz, *H*$_4$), 8.44 (dd, 1H, *J*=2, 9Hz, *H*$_7$), 8.77 (d, 1H, *J*=2Hz, *H*$_5$), 9.07 (dd, 1H, *J*=1, 4Hz, *H*$_2$); HRMS 189.0664, calcd for $C_{10}H_9N_2O_2$ 189.0664.

N-Methyl-5-nitroquinolinium iodide (149)

A mixture of 5-nitroquinoline (Aldrich, 99%, 848mg, 4.85mmol) and iodomethane (Aldrich, 99%, 500μL, 7.87mmol) in $CHCl_3$ (1mL), which was briefly sonicated, then stirred at ambient temperature under argon for 5h, deposited a precipitate within 1h. The product was triturated with benzene and collected via filtration as red needles; HRMS 189.0670, calcd for $C_{10}H_9N_2O_2$ 189.0664.

N-Methyl-5-nitroisoquinolinium iodide (150)

A suspension of 5-nitroisoquinoline (Aldrich, 98%, 849mg, 4.78mmol) and iodomethane (Aldrich, 99%, 500μL, 7.87mmol) in $CHCl_3$ (1mL) and methanol (1mL), which was briefly sonicated, then stirred at ambient temperature under argon for 5h, deposited a precipitate. The product was recrystallized from methanol/$CHCl_3$ as reddish white needles; HRMS 189.0691, calcd for $C_{10}H_9N_2O_2$ 189.0664.

N-(1-Phenethyl)quinolinium iodide (151)

A solution of quinoline (Aldrich, 96%, 600μL, 4.89mmol) and 1-phenethyl bromide (Aldrich, 97%, 720μL, 5.12mmol) in acetonitrile (3mL) was heated at reflux under argon overnight. Attempted recrystallization from methanol/$CHCl_3$ was unsuccessful; the product was partially purified via flash chromatography on silica eluted with a gradient of 5% to 20% methanol/$CHCl_3$ to afford a brown solid that was contaminated with both starting materials, according to tlc and nmr.

N-(5-Hexenyl)isoquinolinium bromide (152)

A solution of isoquinoline (Aldrich, 97%, 570μL, 4.71mmol) and 6-bromo-1-hexene (Aldrich, 95%, 680μL, 4.82mmol) in DMF (3mL) under argon was heated at 60°C for 2h. The reaction mixture was concentrated via rotary evaporation *in vacuo* to afford a dark orange oil, which was purified via flash chromatography on silica eluted with a gradient of 10% to 40% methanol/$CHCl_3$; **152** was isolated as an oily tan solid (R_f=0.2, 10:1 (v/v) $CHCl_3$/methanol, 786mg, 57%); ^1H NMR (400 MHz, borate-*d*) δ 1.48 (quintet, 2H, *J*=7Hz, γ-CH_2), 2.12 (m, 4H, β- and δ-CH_2), 4.74 (t, 2H, *J*=7Hz, vinyl-CH_2), 5.03 (m, 2H, α-CH_2), 5.85 (m, 1H, olefinic-C*H*), 8.03 (t, 1H, *J*=7Hz), 8.19 (d, 1H, *J*=8Hz, H_3), 8.23 (s, 1H, H_1), 8.24 (t, 1H, *J*=7Hz), 8.39 (d, 1H, *J*=8Hz, H_2), 8.41 (d, 1H, *J*=7Hz), 8.50 (d, 1H, *J*=7Hz); ^{13}C NMR (100MHz, borate-*d*) δ 18.57, 23.87, 26.26, 55.54, 109.05, 120.50, 121.25, 121.70, 123.99, 124.05, 125.43, 128.00, 131.09, 132.78, 142.79.

Dimethylaluminum dimethylamide (153)[2]

To an oven-dried flask cooled in a dry ice/acetone bath (-78°C) was introduced dry CH_2Cl_2 (10mL) and condensed anhydrous dimethylamine (Aldrich, bp +7°C, ca. 6mL) from a gas cylinder. To this stirred solution was added carefully a solution of trimethylaluminum in hexanes (10mL, 2.0M), with concommitant evolution of CH_4 gas. (**Caution!!** Trimethylaluminum is **pyrophoric**; residual reagent in the syringe was destroyed safely by careful treatment with isopropanol.) The -78°C bath was removed and the mixture was allowed to warm to room temperature (excess dimethylamine "boiled off"). The colorless solution (ca. 1.0M **153**, in 1:1 (v/v) hexane/CH_2Cl_2) was transferred via Teflon tubing to a dry, argon-filled flask and stored at 4°C. (The mild reagent solution was used several times without incident.)

References to Appendix 4

(1) Gupta, R. B.; Franck, R. W. *J. Am. Chem. Soc.* **1987**, *109*, 5393-5403.

(2) Basha, A.; Lipton, M.; Weinreb, S. M. *Tetrahedron Lett.* **1977**, 4171-4174.

(3) Still, W. C.; Kahn, M.; Mitra, A. *J. Org. Chem.* **1978**, *43*, 2923-2925.

Appendix 5

D Values

Reported on the following pages are *D* values (positive = upfield shifts; negative = downfield shifts) for new host/guest pairs described in this thesis. Below are the proton numbering schemes for the 2,6- and 1,5-*p*-xylyl-linked hosts.

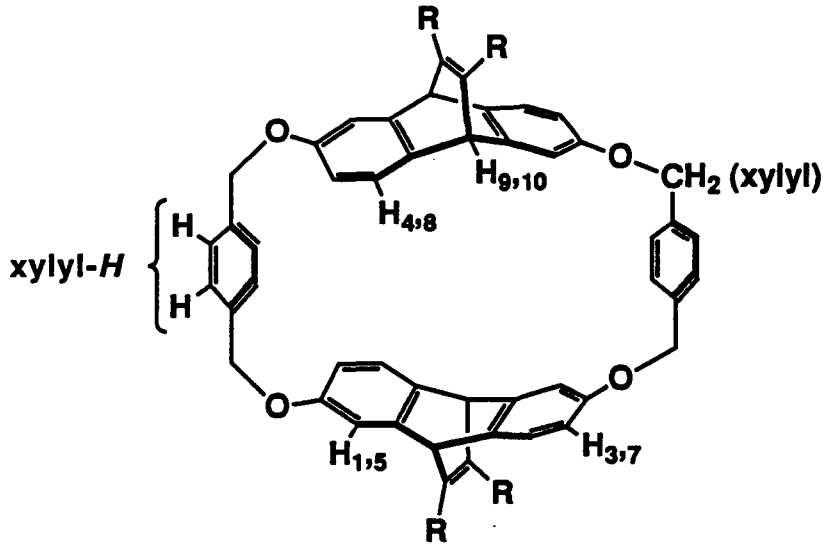

1: R = CO_2^- Cs^+
27: R = CO_2Me

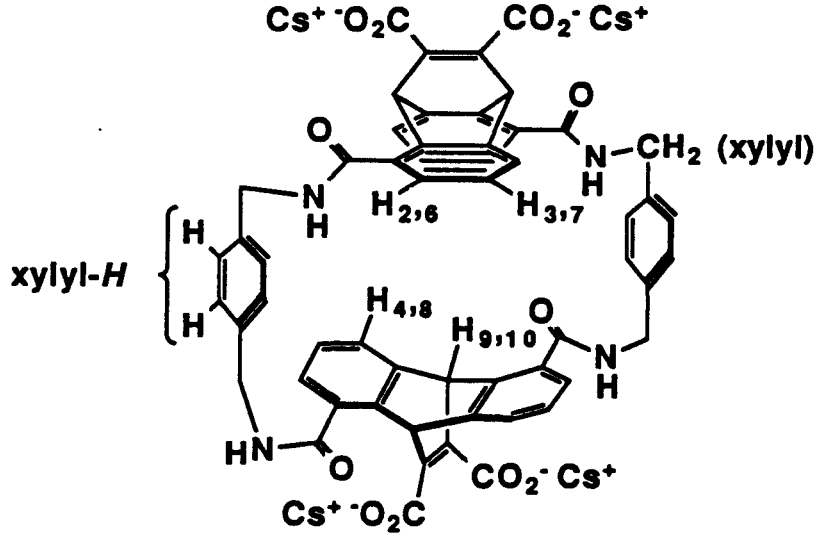

71

Host **27** and guests in $CDCl_3$

(Chapter 1)

guest **10**

H_2	3.06
N-CH_3	2.65

guest **11**

H_1	2.42
N-CH_3	1.92
H_3	2.24
H_4	2.99
H_5	2.56
H_6	1.93
H_7	3.11
H_8	3.01

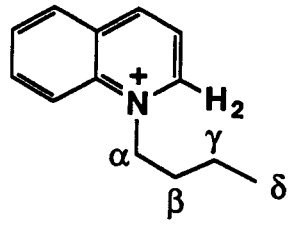

guest **15**		host **27**	
α-CH_2	0.21	xylyl-H	0.09
β-CH_2	0.12	xylyl-CH_2	0.30
δ-CH_3	-0.01	$H_{1,5}$	0.13
H_2	0.42	$H_{3,7}$	0.11

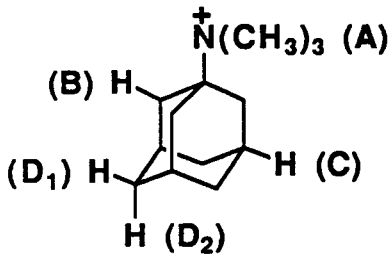

guest **20**	
A	2.99
B	2.92
C	1.11
D_1	1.07
D_2	0.67

Host **1** and guests in borate-*d*

(Chapter 1)

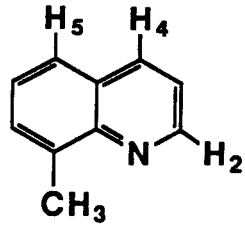

guest **12**		host **1**	
H_2	2.26	xylyl-*H*	0.29
H_4	3.48	$H_{1,5}$	0.14
H_5	1.98	$H_{4,8}$	-0.07
C8-C*H*$_3$	2.08		

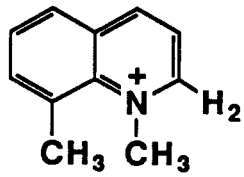

guest **13**		host **1**	
N-C*H*$_3$	1.77	xylyl-*H*	0.03
H_2	1.58	$H_{1,5}$	0.10
C8-C*H*$_3$	2.08	$H_{3,7}$	0.22
		$H_{4,8}$	-0.03

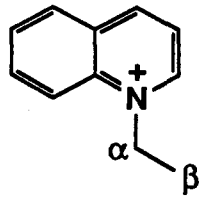

guest 14

α-CH_2	1.35
β-CH_2	0.62

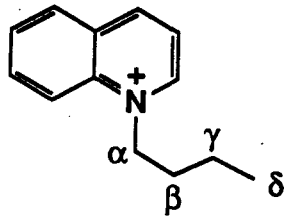

guest 15

α-CH_2	1.07
β-CH_2	0.76
γ-CH_2	0.20
δ-CH_3	-0.12

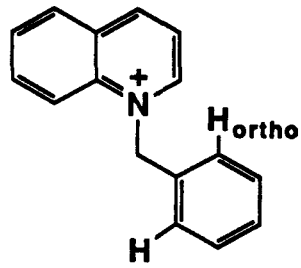

guest 16

N-CH_2	1.21
ortho-H	-0.38

host 1

xylyl-H	0.16
$H_{1,5}$	0.21
$H_{3,7}$	0.20
$H_{4,8}$	0.04

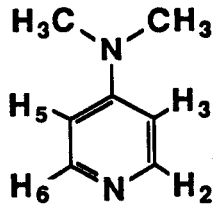

guest **17**		host **1**	
$H_{2,6}$	3.34	xylyl-*H*	-0.06
$H_{3,5}$	2.32	$H_{1,5}$	0.02
$N(CH_3)_2$	2.60	$H_{3,7}$	0.02
		$H_{4,8}$	-0.03

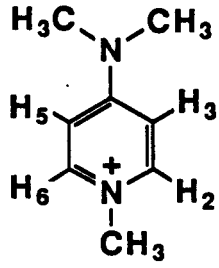

guest **18**		host **1**	
N^+-CH_3	1.07	xylyl-*H*	-0.10
$H_{2,6}$	3.02	$H_{1,5}$	0.01
$H_{3,5}$	2.18	$H_{3,7}$	0.02
$N(CH_3)_2$	2.24	$H_{4,8}$	-0.06

guest **19**

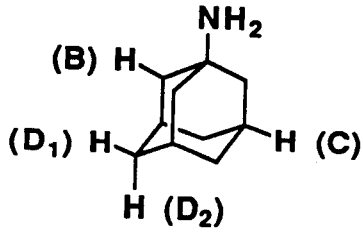

B	0.45
C	0.63
D_1	0.62
D_2	0.64

guest **21**

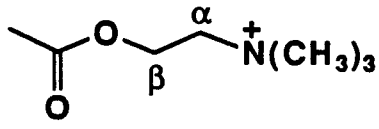

$N(CH_3)_3$	1.37
α-CH_2	1.82
β-CH_2	1.30
CH_3	0.16

guest **21** with host **40**

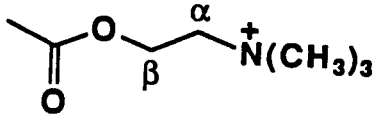

$N(CH_3)_3$	0.20
α-CH_2	0.21
β-CH_2	0.16
CH_3	0.04

Host **71** and guests in borate-*d*

(Chapter 4)

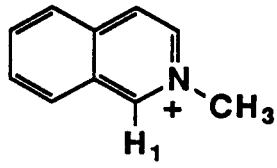

guest **11**		host **71**	
H_1	2.35	xylyl-*H*	-0.02
N-C*H*$_3$	0.84	xylyl-C*H*$_2$	0.09
		$H_{2,6/3,7}$	-0.34
		$H_{4,8}$	-0.06
		$H_{9,10}$	-0.21

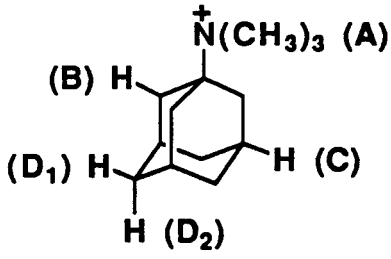

guest **20**		host **71**	
A	1.34	xylyl-*H*	0.19
B	2.18	xylyl-C*H*$_2$	0.12
C	2.58	$H_{2,6/3,7}$	-0.67
D_1	2.56	$H_{4,8}$	-0.50
D_2	2.46	$H_{9,10}$	-0.50

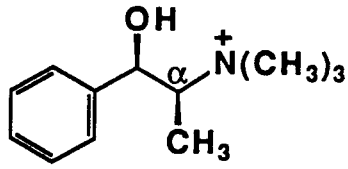

guest **81**		host **71**	
N(CH_3)$_3$	3.84	xylyl-*H*	0.22
Cα-CH_3	2.70	xylyl-CH_2	0.18
		$H_{2,6/3,7}$	-0.81
		$H_{4,8}$	-0.53
		$H_{9,10}$	-0.43

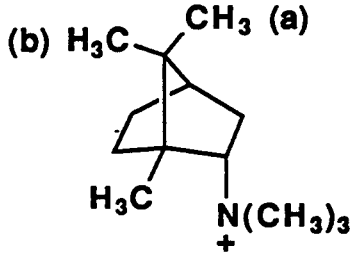

guest **83**		host **71**	
C1-CH_3	0.93	xylyl-*H*	0.11
N(CH_3)$_3$	0.63	xylyl-CH_2	0.10
C7-CH_3(a)	0.99	$H_{2,6/3,7}$	-0.46
C7-CH_3(b)	0.98	$H_{4,8}$	-0.34
		$H_{9,10}$	-0.34

Host **1** and iDA substrates/products in borate-*d*

(Appendix 1)

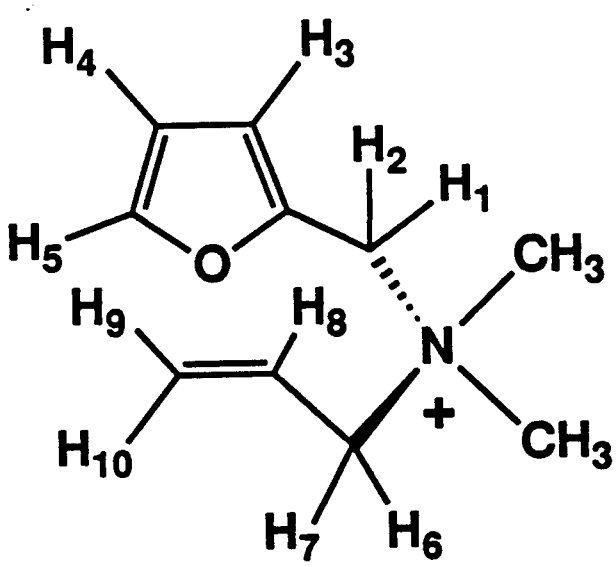

substrate 98

H_5	0.49
H_4	1.46
H_3	1.20
$H_{1/2}$	3.37
$H_{2/1}$	3.83
$N(CH_3)_2$	3.18
$H_{6,7}$	3.01
H_8	2.32
H_9	0.78
H_{10}	1.52

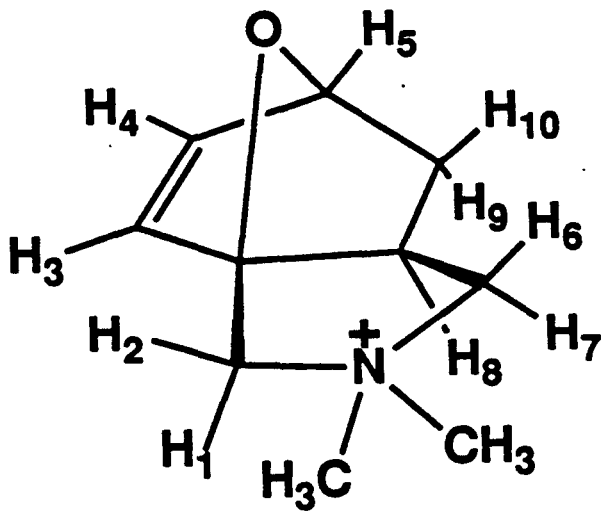

product 101

H_4	0.78
H_{10}	1.84
H_9	1.42
H_8	2.52
$H_{6,7}$	1.72
$N(CH_3)_a$	1.87
$N(CH_3)_b$	1.88
$N(CH_3)_c$	1.94
$N(CH_3)_d$	2.07
$H_{1/2}$	2.61
$H_{2/1}$	2.44